

**Screening of antimicrobial effects of selected fungi and studies on
antibiotic constituents of**

***Bulgaria inquinans* (Pers.) Fr. (Bulgariaceae)
and *Meripilus giganteus* (Pers.:Fr.) P. Karst. (Meripilaceae)**

DISSERTATION

In fulfilment of the requirements for the degree of *Dr. rer. nat*
At the Institute of Pharmacy, University of Hamburg

by
Natalia Osmanova

Hamburg 2011

1. Referee: Priv.-Doz. Dr. W. Schultze
Institute of Pharmacy, University of Hamburg

2. Referee: Prof. Dr. rer. nat. Sascha Rohn
Institute of Food Chemistry, University of Hamburg

The present work was performed from March 2005 to June 2009 under the supervision of Priv.-Doz. Dr. W. Schultze at the Institute of Pharmacy, University of Hamburg, Germany

Dedicated to my family

Acknowledgements

I am very grateful to Priv.-Doz. Dr. Wulf Schultze for the opportunity to conduct this research under his supervision, for his invaluable support and inspiring discussions.

I am grateful to Professor Dr. Dr. h.c. mult. W. Francke, Prof. Dr. J. Thiem and Prof. Dr. C. Meier (Institute of Organic Chemistry) for their kind permission to utilise the laboratory facilities provided by Organic Chemistry.

Support from the following people is gratefully acknowledged: Dr. Volker Sinnwel and his team and Dr. Thomas Hackl (Institute of Organic Chemistry) for NMR measurements and help in spectra interpretation; Dr. Stephan Franke, Manfred Preuße, Cristina Christ, Gaby Graak and Annegret Meiners (Institute of Organic Chemistry) for HREIMS, direct inlet EIMS and FAB-MS measurements; Dr. Stephan Franke for useful consultations; Professor Dr. Dr. h.c. mult. Wittko Francke, Stephan von Reuß and Armin Troeger for providing *R*(-)-1-octenol and useful advice about enantioselective GC; Professor Dr. Peter Heisig, Tatjana Claußen and Antje Schnasse (Institute of Pharmacy) for the help in microbiological experiments; Professor Dr. Ulrike Lindequist and Dr. Kristian Wende (Institute of Pharmacy, Ernst-Moritz-Arndt University, Greifswald, Germany) for providing cytotoxic investigations; Professor Dr. Bernward Bisping (Institute of Food Chemistry) for his support; Prof. Dr. C. S. Leopold (Institute of Pharmacy) for permission to finish experiments using HPLC.

Special thanks are also due to the members of my working group: Kai Haacker and Frank Meyer for their ever-present help and support.

I am most grateful to Dr. Ed Bradburn for his invaluable assistance and unstinting support, which was instrumental in seeing this dissertation to fruition.

List of Abbreviations

<i>br</i>	broad
COSY	Correlation Spectroscopy
¹³ C NMR	Carbon-13 Nuclear Magnetic Resonance Spectroscopy
δ	chemical shift (ppm)
<i>d</i>	doublet
<i>dd</i>	double doublet
DMSO	dimethyl sulfoxide
EI	Electron Impact
EIMS	Electron Impact Mass Spectrometry
FID	Flame Ionization Detector
GC-MS	Gas chromatography-mass spectrometry
¹ H NMR	Proton Nuclear Magnetic Resonance Spectroscopy
HMBC	Heteronuclear Multiple Bond Correlation
HSQC	Heteronuclear Single Quantum Coherence
HPLC	High Performance Liquid Chromatography
Hz	Hertz
¹ <i>J</i>	direct coupling constant (Hz)
² <i>J</i>	germinal coupling constant (Hz)
³ <i>J</i>	vicinal coupling constant (Hz)
⁴ <i>J</i>	allylic coupling (Hz)
λ_{\max}	maximum absorption (nm)
[M]	molecular ion
MS	Mass Spectrometry
<i>m/z</i>	mass charge ratio
NMR	Nuclear Magnetic Resonance
NOESY	Nuclear Overhauser Effect Spectroscopy
pH	$-\log (c\text{H}_3\text{O}^+)$
ppm	parts per million
RI	Kováts retention indices
R _f	retention factor (TLC)
<i>s</i>	singlet
<i>t</i>	triplet
TIC	Total Ion Chromatogram
TFA	trifluoroacetic anhydride
TLC	Thin Layer Chromatography
TMS	Tetramethylsilane
TOF	Time-of-flight (mass spectrometry)
v/v	volume per volume

Table of Contents

<u>1. Aim of the study</u>	1
<u>2. Introduction</u>	1
2.1 Natural sources of remedies	4
2.2 Fungi	5
2.2.1 Definition and properties.....	5
2.2.2 Fungal secondary metabolites.....	8
2.2.3 Importance of fungi.....	8
2.2.4 Medical use of fungi.....	10
<u>3. Experimental part</u>	16
3.1 Preliminary screening tests for determination of biological activity	16
3.1.1 Agar diffusion tests of fungi extracts.....	16
3.1.2 Agar overlay technique on TLC plates.....	19
3.2 Investigations of <i>Bulgaria inquinans</i>	24
3.2.1 Taxonomy of <i>Bulgaria</i>	24
3.2.2 Biological characteristics of <i>B. inquinans</i>	25
3.2.3 Chemical composition and bioactivity – an overview.....	29
3.2.4 Detection of bioactive compounds in <i>Bulgaria</i> extracts.....	37
3.2.4.1 Determination of haemolytic TLC zones in ether extract.....	37
3.2.4.2 TLC zones with antibacterial activity.....	38
3.2.5 Isolation of antibacterial substances from <i>Bulgaria</i> extracts.....	41
3.2.5.1 Isolation of antibacterial azaphilones from preparative TLC plates.....	41
3.2.5.2 Optimisation of azaphilones separation using analytical HPLC.....	45
3.2.5.3 Formation of azaphilones in acetonitrile extract.....	46
3.2.5.4 Isolation of azaphilones by preparative HPLC.....	48
3.2.5.5 Structure elucidation of bulgarialactone B (HPLC Peak 2).....	50
3.2.5.6 Structure elucidation of bulgarialactone D (HPLC Peak 1).....	62
3.2.6 Antibacterial activity of <i>Bulgaria</i> hydrodistillate.....	74
3.2.6.1 Detection of bioactive TLC zones.....	74
3.2.6.2 Isolation of antibacterial compounds from preparative TLC plates.....	74
3.2.6.3 Structure elucidation of bulgariafuran.....	79
3.2.7 Volatiles of <i>Bulgaria</i> fruit bodies.....	89
3.2.7.1 GC-MS analysis of the hydrodistillate.....	89
3.2.7.2 Determination of the enantiomeric ratio for 1-octen-3-ol	92
3.2.8 Cytotoxicity of <i>Bulgaria</i> extracts.....	97
3.3 Investigations of <i>Meripilus giganteus</i>	101
3.3.1 Taxonomy of <i>Meripilus</i>	101
3.3.2 Biological characteristics of <i>M. giganteus</i>	101
3.3.3 Chemical composition and bioactivity – an overview.....	103

3.3.4	Detection of bioactive compounds in <i>Meripilus</i> extracts.....	105
3.3.4.1	Determination of haemolytic TLC zones in ether extract.....	105
3.3.4.2	TLC zones with antibacterial activity.....	106
3.3.5	Isolation of antibacterial substances from <i>Meripilus</i> extract	109
3.3.5.1	Structure elucidation of meripiluslactone.....	109
3.3.6	Volatiles of <i>Meripilus</i> fruit bodies.....	123
3.3.7	Antibacterial activity of <i>Meripilus</i> hydrodistillate.....	125
3.3.8	Cytotoxicity of <i>M. giganteus</i> extracts.....	129
4.	<u>Summary and outlook</u>	133
5.	<u>Materials and Methods</u>	145
5.1	Fungi material.....	145
5.2	Origin of fungi.....	146
5.3	Microscopy.....	146
5.4	Methods of Extraction.....	146
5.4.1	Preparation of extracts.....	146
5.4.2	Hydrodistillation.....	147
5.5	Chromatography.....	147
5.5.1	Thin layer chromatography (TLC)	147
5.5.2	Preparative and semi-preparative chromatography.....	147
5.5.3	Biological <i>in situ</i> tests on TLC.....	147
5.5.4	Solvent systems for thin layer chromatography.....	148
5.5.5	Detection on TLC plates.....	148
5.5.6	Analytical High Performance Liquid Chromatography (HPLC).....	149
5.5.7	Preparative High Performance Liquid Chromatography (Preparative HPLC).....	149
5.5.8	Gas chromatography (GC).....	150
5.6.8.1	Determination of the absolute configuration of 1-octen-3-ol	150
5.6	Spectroscopic methods.....	152
5.6.1	Mass spectroscopy in ESI mode.....	152
5.6.2	GC-MS Coupling.....	152
5.6.3	Nuclear Magnetic Resonance spectroscopy (NMR).....	154
5.7	Bioassays.....	154
5.7.1	Determination of antimicrobial activity (agar diffusion test).....	154
5.7.2	<i>In-situ</i> bioassays on thin layer plates (agar overlay technique).....	155
5.7.3	Haemolytic activity assay (blood gelatine test).....	156
5.7.4	Cytotoxicity test.....	157
6.	<u>Hazardous chemicals</u>	159
7.	<u>Appendix I</u> (NMR spectra).....	160
8.	<u>Appendix II</u> (Azaphilones: a class of fungal metabolites with diverse biological activities. Review)	172
9.	<u>References</u>	230

1. Aim of the study

The present study investigates macrofungi native to Germany for their antimicrobial potential. Two principles were applied to the selection of study subjects. Firstly, the chemical composition and bioactivity of many native fungi has not yet been studied in detail. Secondly, fungi lack a protective outer layer (such as epidermis or bark) and are forced to rely solely on their chemical defensive mechanisms. It is precisely these defensive chemicals that constitute a potential source of antimicrobial substances. The investigation procedure was structured as follows:

- Preparation of extracts from about 30 macromycetes utilising a variety of solvents
- Testing the above extracts using standard antimicrobial bioassays to determine antimicrobial bioactivity
- Developing and optimising specific antimicrobial *in situ* bioassays for testing fungi extracts on thin layer chromatography plates in order to obtain rapid and direct information about active compounds and compound groups
- Isolating the most interesting biologically active compounds and elucidating their structures using modern MS and NMR techniques

2. Introduction

Even in the early 21st century, infectious disease persists as one of the leading causes of illness and death, second only to cardiovascular disorders. Figures from the World Health Organization reveal that infectious diseases account for about 15 million cases annually and thus 26% of all global mortality. Microbial infections account for 85-90% of all cases of infectious disease [1].

The commonest and most effective treatment of infectious disease to date has been the application of drugs with antimicrobial activity. While these drugs are termed "antibiotics" in common parlance and this usage refers generally to substances that kill or inhibit the growth of (disease-causing) bacteria, the term antibiotic is more precisely defined by the scientific community. Coined in 1942 by Selman Waksman, an antibiotic (from the Greek *anti* against and *biosis* way of life) was defined as "any

substance produced by a microorganism that is antagonistic to the growth of other microorganisms in high dilution" [2]. Since then, the term has been expanded to include naturally occurring antimicrobial substances not produced by microorganisms – including those produced by plants, fungi and marine organisms – as well as purely synthetic antibacterial compounds such as the sulfonamides, quinolones and oxazolidinones [3]. As such, antibiotics belong to the broader group of antimicrobial compounds used to treat infections caused by any microorganisms, including fungi and protozoa [4]. Some antibiotics, such as the aminoglycosides, are still produced and isolated from bacteria (in this case, the *Streptomyces* genus), but with advances in medicinal chemistry, most antibiotics are now semi-synthetic, *i.e.* modified chemically from original compounds found in nature [2, 3].

The success of a particular antibiotic depends on the microorganism's ability to withstand its effect: if this ability rises significantly, the microorganism is said to have developed antibiotic resistance (with microorganisms carrying several resistance being termed multi-resistant). Antibiotic resistance may evolve via natural selection acting upon random mutations or may also be engineered by applying an evolutionary stress to a population. Significantly, once the required gene is available, bacteria may prove capable of transferring this genetic information in the population horizontally (*i.e.* between individuals) by plasmid exchange.

The complex threat presented by antibiotic resistance is well illustrated by the present situation concerning vancomycin. Vancomycin, a macrolide glycopeptide, is a distinct class of antibiotics unrelated to any other group of antibiotics used routinely in medical practice such as penicillins, streptomycins, cephalosporins, quinolones, sulfonamides or erythromycins. Although medical use of vancomycin had been reserved for the specific treatment of multi-resistant, life-threatening staphylococcal infections, a number of studies then revealed resistance in enterococcal strains, termed Vancomycin-Resistant *Enterococci* (VRE). During 2004, VRE was responsible for nearly a third of all hospital infections in intensive care units, according to the Centers for Disease Control and Prevention (CDC). Three years later, the United States then reported seven cases of a Vancomycin-resistant

Staphylococcus aureus strain, termed VRSA. In one of the VRSA cases, scientists confirmed the transfer of a key antibiotic resistance gene from *Enterococcus* to *Staphylococcus* [5, 6].

Whether or not it is the case that the overprescription and misuse of antibiotics promoted the evolution of the VRE and VRSA strains, the fact remains that new strains of harmful bacteria able to resist targeted treatments are appearing at an alarming rate [7, 8]. In this environment, the effective life of existing antibiotics is clearly very limited and the pressure to discover new antibiotics is one of the most acute problems facing medical science. Significantly, while new antibiotics may be derived from microorganisms (figures indicate the launch of around three such products ever year), the localisation of naturally derived compounds with antibiotic properties presents scientists with an additional strategy for achieving this objective [9].

Indeed, the therapeutic use of natural products has a long and distinguished history: if we look at phytochemicals, for example, we find that from prehistoric to early modern times, the treatment of ailments often involved the application of poultices or infusions sourced from hundreds – if not thousands – of indigenous plants [10]. Interestingly, the same holds true for mushrooms (*i.e.* macrofungi with a distinctive fruiting body large enough to be seen with the naked eye and to be picked by hand): the use of mushrooms in folk medicine has a particularly long and sophisticated tradition in Asia, for example [11, 12, 13, 14]. However, since the introduction of antibiotics into modern medicine in the 1950s, the therapeutic use of chemicals derived from natural products has been virtually nonexistent – notwithstanding the fact that successful early antibiotics such as penicillin are in fact derived from microscopic fungi. Indeed, the fungi kingdom defines a group of organisms in which one can reliably expect to identify a huge range of antibiotic constituents. The reason for this stems from one particular characteristic shared by all fungi, namely their lack of a protective outer layer such as a cuticle, epidermis, bark or cork, thereby depriving fungi of the opportunity to defend against microbial attack using the same mechanisms available to plants. Lacking protective barriers, fungi are

forced to rely solely on their chemical defensive mechanisms – and it is precisely these defensive chemicals that constitute a rich source of antimicrobial substances. Accordingly, the topic of antimicrobial fungal extracts presents clinical microbiologists with a promising field of investigation, not least because compounds from natural sources achieve comparable levels of efficiency to synthetic substances and "classical" antibiotics with demonstrably fewer (and less severe) side effects [7, 8, 13].

2.1 Natural sources of remedies

Natural sources have been used as an inexhaustible source of medicaments for hundreds of years: the first scientific experiments on the antimicrobial properties of plants, for example, have been documented from as early as the 14th century [15]. Until the 1970s, new drug compounds were almost exclusively of plant-based origin [16]. Even in more recent times, this proportion has fallen only moderately: a major review published in 2007 and covering the period 1981-2006 showed that 63% of the 974 new small-molecule drug compounds were derived wholly or partially from natural (included plant-based) sources. For antimicrobials, plus anti-cancer, anti-hypertensive and anti-inflammatory drugs, the numbers were even higher: approximately 75% of these classes of compounds were derived from natural sources [17].

If we consider phytochemicals – i.e. compounds naturally occurring in plants – as one example of naturally derived compounds, we find that most of the biologically active compounds are secondary metabolites with complex structures: phenolic acids, quinones, flavonoids, flavones, flavonols, tannins and coumarins, terpenoids and “essential oils”, polyacetylenes, alkaloids and pectins. Significantly, not only are a proportion of these compounds entirely novel substances, but many are the result of the plant's response to evolutionary pressure and therefore confer selective advantage against microbial attack and form a response to particular pathogens in the plant's environment [18, 19].

Nor are plants alone in possessing this characteristic: this specificity of response has been discovered in many other classes of organisms and is a key factor in the particular success of naturally derived compounds as lead structures for antibacterial therapies [3]. One of these other classes is the kingdom of fungi, and, as we will see, it presents us with one of the most interesting natural sources of antimicrobial compounds.

2.2 Fungi

2.2.1 Definition and properties

The term "fungi" refers to a group of eukaryotic organisms whose members include microorganisms such as yeasts and moulds as well as the more familiar (macroscopic) mushrooms¹. The group is considered sufficiently distinct from other groups of organisms – such as plants, animals or bacteria – to be described as a separate kingdom (see Figure 1) [20]. While between 80 000 and 100 000 species of fungi are known to date, some estimates of total numbers suggest that as many as 1.5 million species may exist [21]. Recent work has seen around 1800 new species described annually [22].

Fungi possess a cell wall and vacuoles [23]. They reproduce by both sexual and asexual means, and are spore-producing like lower plants (such as ferns and mosses). However, fungi differ from plants in several key aspects:

- Since fungi lack stems, leaves and root (“cormus”) they belong to the Thallophyta
- Fungi totally lack chloroplasts, do not photosynthesize and are heterotrophic organisms, requiring preformed organic compounds as energy sources. While most fungi are C–heterotrophs, some are N–heterotrophs.

¹ A “mushroom” is any macrofungus with a distinctive fruiting body which can be hypogeous or epigeous, large enough to be seen with the naked eye and to be picked by hand. This latter definition is an official standard given by Dictionary of the Fungi, 10th Edition [24].

- Unlike the cell walls of plants which consist of cellulose, cell walls of some fungi – e.g. those belonging to the subphylum Mycobionta (chitin fungi) – contain chitin

As with other eukaryotes, fungal cells contain membrane-bound nuclei with chromosomes that contain DNA with non-coding regions called introns and coding regions called exons. Fungi possess membrane-bound cytoplasmic organelles such as mitochondria, sterol-containing membranes, and ribosomes of the 80S type. Most fungi possess a generally undifferentiated mycelium, which is formed by hyphae. Hyphae are cylindrical, thread-like structures 0.5–100 μm in diameter, up to several centimetres in length and nearly always coenocytic. Under certain circumstances, fungi are able to create secondary fruiting bodies formed by pseudotissues (plektenchyma or pseudo-parenchyma). The fruiting bodies (Asci for Ascomycetes and Basidia for Basidiomycetes) produce spores [24]. Many fungi are parasites on plants, animals (including humans), and other fungi. Other species of fungi are saprotrophic, or obtain nutrients in a symbiotic relationship with plant species. Nutrition is always absorptive (osmotrophic) and never phagotrophic. Fungi have a characteristic range of soluble carbohydrates and storage compounds, including sugar alcohols such as mannitol, disaccharides and polysaccharides – especially glycogen, which is also found in animals. Fungi never produce starch.

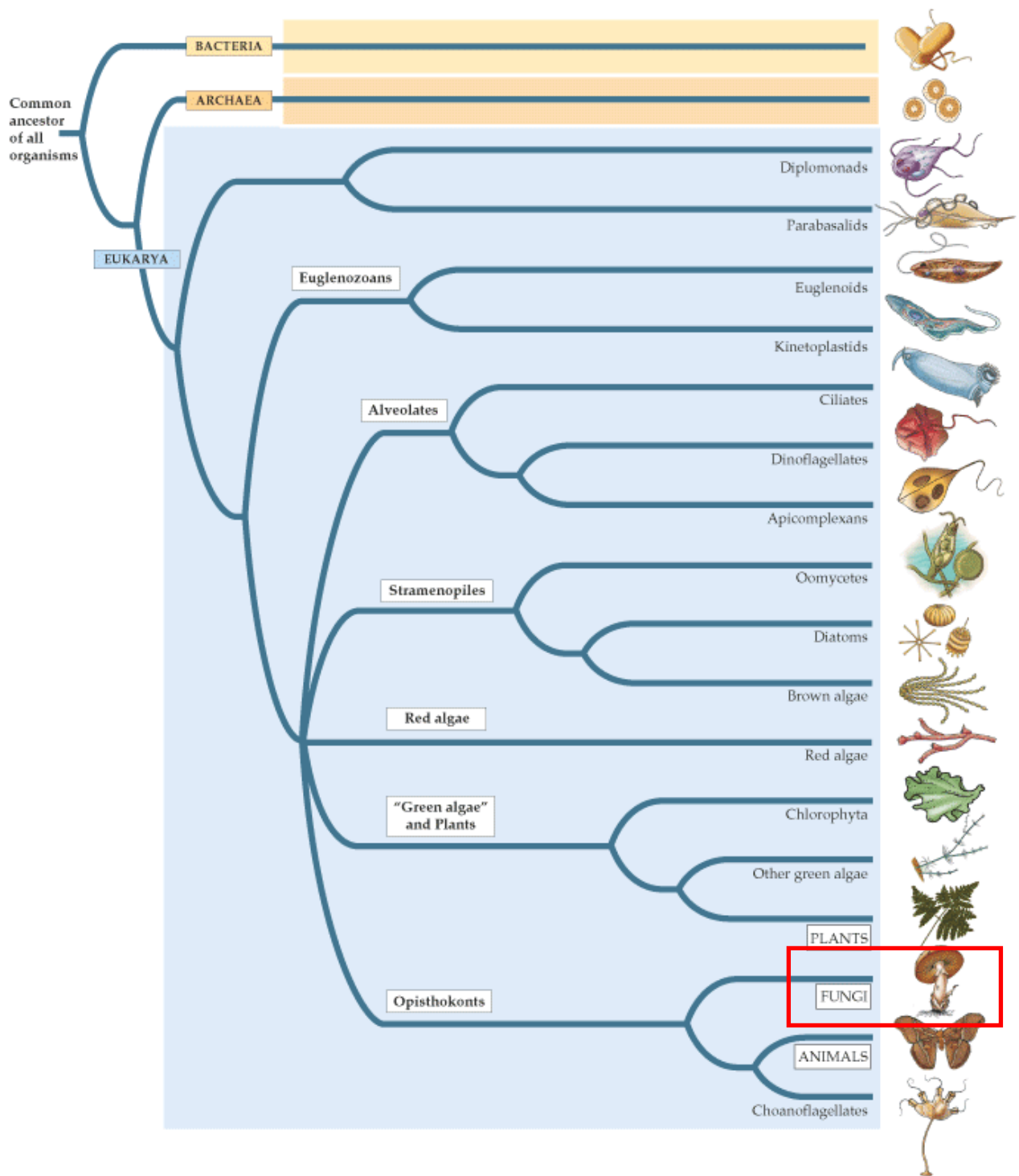


Figure 1: Protist diversity. The diagram clearly shows that fungi are more closely related to animals than to plants. This fact has not only been established by the incidence of chitin, glycogen and heterotrophic behaviour in fungi, but is also supported by molecular phylogenetics [20].

2.2.2 Fungal secondary metabolites

Fungi produce a variety of constituents belonging to numerous groups of chemical compounds, including organic acids, polyenes and polyynes, phenolic compounds (quinones, anthraquinones, xanthenes, etc.), mono- to triterpenes (including volatiles and steroids), bioactive polysaccharides, lipopolysaccharides, proteins, N- and S-containing compounds [25, 26, 27].

Some secondary constituents – such as penicillin and muscarin – are highly specific and confined to fungi. Flavonoids and tannins are almost completely absent.

Since many fungal metabolites have proven bioactive qualities, it is unsurprising that past research has focused on the screening and reviewing of new active principles from fungi [10, 28, 29, 30].

2.2.3 Importance of fungi

Two of the most significant areas to consider for fungi are their interaction with the earth's ecology – particularly including their interrelationships with other organisms – and their exploitation by humankind to produce food or chemical compounds.

In ecological terms, fungi can be found thriving in a huge number of different environments all over the planet and play very important roles in most ecosystems. Along with bacteria, fungi are the major decomposers in most terrestrial (and some aquatic) ecosystems and therefore play an important role in biogeochemical cycles and in many food webs [31]. As decomposers, fungi play an essential role in nutrient cycling, especially as saprotrophs and symbionts, degrading organic matter to inorganic molecules that can then re-enter anabolic metabolic pathways in plants or other organisms [32, 33].

Many fungi have important symbiotic relationships with organisms from most if not all Kingdoms. Mycorrhizal symbiosis between plants and fungi is one of the best-known plant-fungus associations and is of significant importance for plant growth and persistence in many ecosystems (such as deciduous or coniferous forests). The other key symbiotic complex involves lichens: lichens are formed by a symbiotic relationship between algae or cyanobacteria and fungi, in which individual

photobiont cells are embedded in a tissue formed by the fungus [34, 35]. Notwithstanding these many symbiotic relationships, a great many fungi are also parasitic on plants, animals (including humans) or other fungi and can cause their hosts considerable distress or damage. Plant diseases are a common occurrence and can impact agriculture, e.g. the stem rusts caused by the fungus *Puccinia graminis* is a severe disease affecting cereal crops. Some fungi can cause serious diseases such as mycotoxicoses (caused by toxic constituents such as aflatoxin, citrinin, fusarium, muscarin, ochratoxin or patulin), mycoses and allergoses in humans and animals, several of which may be fatal if untreated. These latter include aspergillosis, candidosis, coccidioidomycosis, cryptococcosis, histoplasmosis, mycetoma and paracoccidioidomycosis. Finally, many fungal species are poisonous to humans, with toxicities ranging from slight digestive problems, allergic reactions or hallucinations to critical organ failure and death (e.g. *Amanita phalloides*).

In terms of commercial exploitation, fungi are either used as a food source or processed for their constituents. Many fungi used for food products are either grown for direct consumption – such as *Agaricus bisporus*, *Pleurotus ostreatus* and *Lentinula edodes* – or applied to the process of food preparation or preservation. Certain types of cheeses require the inoculation of milk curds with fungal species that impart a unique flavour and texture to the cheese: the blue colouration of Roquefort cheese is achieved by inoculation with *Penicillium roqueforti*, for example. Other food applications include the industrial production of beer and yeast, as well as the manufacture of several organic acids (citric, gluconic, lactic and malic acids). Fungi are also sources of industrial enzymes, including amylases, cellulases, invertases, proteases, xylanases and the lipases used in biological detergents.

Finally, and most relevant for the present work, many species of fungus produce metabolites that are major sources of pharmacologically active drugs, including antibiotics (*Penicillium sp.*), ergot alkaloids (*Claviceps purpurea*), HMG-CoA reductase inhibitors (Lovastatin from *Aspergillus terreus*) and immunostimulators (glucans from *Schizophyllum commune* and *Lentinula edodes*).

2.2.4 Medical use of fungi

The medicinal use of mushrooms has a very long tradition in the Asia and Africa, whereas their use in the Western countries has been increasing only moderately in recent decades [14, 36, 37]. In recent years, a number of pharmacological actions have been intensively investigated, including cytotoxic/antitumor, immunosuppressive, antipruritic, antierythema, antifungal, antioxidant and free-radical scavenging activities. The recently-founded scientific publication *International Journal of Medicinal Mushrooms* (Begell House, Editor-in-Chief S. P. Wasser) and international conferences on this topic have confirmed this trend, as have several books and reviews concerning medicinal mushrooms and biologically active compounds from fungi [10, 28, 29, 30, 40].

Table 1 provides a concise overview of the key biological activities of selected fungal species:

	Antibacterial		Antifungal	Antiviral	Antitumor	Immunosuppressive and Antiallergics	Immunomodulators	Free-radical scavenging	Antiatherogenic	Hypoglycaemic	Hepatoprotective	Anti-inflammatory	CNS
	Gram-positive	Gram-negative											
Agaricaceae													
<i>Agaricus blazei</i> Murrill [10,30]				+	+			+	+	+			
Auriculariaceae													
<i>Auricularia auricula-judae</i> (Bull. ex Fr.) [38]					+								
Bulgariaceae													
<i>Bulgaria inquinans</i> (Pers.) Fr. [39, 40]	+	+	+		+			+					
Cortinariaceae													
<i>Rozites caperata</i> (Pers.: Fr.) P. Karst. [38]				+									
Entolomataceae													
<i>Pleurotus mutilus</i> (Fr.) Gillet [30]	+	+											
Fomitopsidaceae													
<i>Piptoporus betulinus</i> (Bull.: Fr.) P. Karst.[41]			+										

	Antibacterial		Antifungal	Antiviral	Antitumor	Immunosuppressive and Antiallergics	Immunomodulators	Free-radical scavenging	Antiatherogenic	Hypoglycaemic	Hepatoprotective	Anti-Inflammatory	CNS
	Gram-positive	Gram-negative											
Ganodermaceae													
<i>Ganoderma applanatum</i> (Pers.) Pat [41]	+	+			+							+	
<i>Ganoderma lucidum</i> (Curtis) P. Karst. [10, 30, 41, 42]	+			+	+		+	+	+	+	+	+	+
<i>Ganoderma pfeifferi</i> Bres. [10]	+			+	+								
Hericiaceae													
<i>Hydnum caput-medusae</i> (Bull.) Pers. [10]							+						
<i>Hericium erinaceus</i> (Bull.) Pers. [10, 30, 41]							+					+	
Hygrophoraceae													
<i>Hygrophorus sp.</i> [40, 43]	+		+										
Hymenochaetaceae													
<i>Inonotus obliquus</i> (Ach. ex Pers.) Pilát [10, 30, 41]	+			+	+		+				+	+	
<i>Inonotus hispidus</i> (Bull.: Fr.) P. Karst. [10]				+									
<i>Phellinus linteus</i> (Berk. & M.A. Curtis) Teng [10, 41]	+			+	+		+					+	

	Antibacterial		Antifungal	Antiviral	Antitumor	Immunosuppressive and Antiallergics	Immunomodulators	Free-radical scavenging	Antiatherogenic	Hypoglycaemic	Hepatoprotective	Anti-Inflammatory	CNS
	Gram-positive	Gram-negative											
Marasmiaceae													
<i>Collybia maculata</i> (Alb. & Schwein.: Fr.) P. Kumm. [10]				+									
<i>Flammulina velutipes</i> (M. A. Curtis: Fr.) P. Karst.[10, 41]	+	+		+			+						
<i>Lentinula edodes</i> (Berk.) Pegler [10, 30, 41]			+	+	+		+	+	+	+	+		
Micromonosporaceae													
<i>Actinoplanes brasiliensis</i> Thiemann (1969) [44]	+						+						
Meripiliaceae													
<i>Grifola frondosa</i> (Dicks.) Gray [10, 30, 41]	+		+	+	+		+		+	+			
<i>Meripilus giganteus</i> (Pers.) P. Karst. [30, 40, 45]	+		+										
Ophiocordycipitaceae													
<i>Cordyceps sinensis</i> (Berk.) Sacc. [41]	+	+			+		+	+	+	+	+	+	+
Pleurotaceae													
<i>Pleurotus eryngii</i> (DC.: Fr.) Quél. [10]					+								
<i>Pleurotus ostreatus</i> (Jacq.) P. Kumm. [10, 30, 41, 46]	+			+						+			+

	Antibacterial		Antifungal	Antiviral	Antitumor	Immunosuppressive and Antiallergics	Immunomodulators	Free-radical scavenging	Antiatherogenic	Hypoglycaemic	Hepatoprotective	Anti-Inflammatory	CNS
	Gram-positive	Gram-negative											
Polyporaceae													
<i>Cryptoporus volvatus</i> (Peck) Shear [10]	+	+					+						
<i>Fomes fomentarius</i> (L.) J.J. Kickx [30, 41]	+			+			+						
<i>Lentinus strigellus</i> Berk. [10]	+		+	+	+	+	+						
<i>Trametes versicolor</i> (L.) Lloyd [10, 30, 41]				+	+		+				+	+	
<i>Polyporus umbellatus</i> (Pers.) [10]							+				+	+	
Schizophyllaceae													
<i>Schizophyllum commune</i> Fr. [10, 30, 41]	+		+	+	+		+						
Sparassidaceae													
<i>Sparassis crispa</i> (Wulfen) Fr. [30]	+						+						
Strophariaceae													
<i>Pholiota nameko</i> (T. Ito) S. Ito [30]	+		+	+	+		+			+	+	+	
<i>Kuehneromyces mutabilis</i> (Schaeff.) Singer & A.H [10]				+									

	Antibacterial		Antifungal	Antiviral	Antitumor	Immunosuppressive and Antiallergics	Immunomodulators	Free-radical scavenging	Antiatherogenic	Hypoglycaemic	Hepatoprotective	Anti-Inflammatory	CNS
	Gram-positive	Gram-negative											
Tremellaceae													
<i>Tremella fuciformis</i> Berk. [30, 47]							+						
<i>Tremella mesenterica</i> Retz. [10, 47]							+						
Tricholomataceae													
<i>Tricholoma lobayense</i> R. Heim [10, 42]					+		+						
<i>Tricholoma mongolicum</i> S. Imai [10]							+						

Table 1: Biological activities of selected fungal species

3. Experimental part

3.1. Preliminary screening tests for the determination of biological activity

In order to single out fungal species with the most marked antimicrobial activity, the investigation of fungi material commenced with preliminary bioactivity screening tests. The test encompassed about thirty different fungal species. Research subjects were pre-selected based on the observation of their ecological behaviour in the field and as a result of data supplied from the literature about their activities. Important criteria included any or all of the following: never known to be consumed by animals, very rarely colonised by invertebrates and resistant to mould (or at least rarely contaminated with mould).

3.1.1 Agar diffusion test of fungi extracts

The first group of subjects tested included eight fungi species whose antimicrobial activity was already known [48]: *Bulgaria inquinans*, *Ischnoderma benzoinum*, *Langermannia gigantea*, *Lycoperdon perlatum*, *Meripilus giganteus*, *Scleroderma citrinum*, *Stereum hirsutum* and *Trametes gibbosa*.

An agar diffusion test of methanol and ether extracts was used to determine antimicrobial bioactivity in this group. Since ethyl acetate is known to be difficult to remove from test discs, ether was used as a mid-polar solvent (with a few exceptions, e.g. *B. inquinans*). Extracts with pentane as an apolar solvent were included only rarely in the tests, since experience had indicated that strong antibacterial activity was more likely to be found in more polar extracts. To establish minimum active volume, four different amounts of each extract were tested, namely 25 µl, 50 µl, 100 µl and 200 µl. Test microorganisms were *S. aureus* and *E. coli*. To determine the quantity of dry substance in applied extracts, test discs were weighed before and after the application of the extract. The approximate average value for 25 µl of ether extract was found to be about 6 mg of dry substance, which thus provided a rough estimate of the extract concentration. However, since it was difficult to determine the exact amount of bioactive compound, the weight of the dry substance in the extracts is not an indicative value, although it was not neglected when considering the biological

activity of the extracts. Results from the antimicrobial investigations of *B. inquinans* extracts will be given as an illustration of the agar diffusion test.

Methanol and ether extracts from *B. inquinans* were found to be the most active extracts (Figure 2 and Figure 3). The activity of the ether extract against *S. aureus* was evident and congruent with the control in all tested amounts. The activity of the methanol and ethyl acetate extracts, however, was low-grade. Further, it was ascertained that the methanol and ethyl acetate extracts from *B. inquinans* were not active against *E. coli*.

The ether and methanol extracts from *B. inquinans* were also tested with regard to their antifungal potential (test culture of *C. albicans*, Figure 4): a weak antifungal effect was shown by the ether extract, dosage 200 μ l; the methanol extract exhibited activity against *C. albicans* at discs with 25 μ l, 50 μ l and 100 μ l.

Although the agar diffusion technique is simple, it necessitates labour-intensive and time-consuming ancillary work such as preparing Petri dishes (agar application), an inoculum application for numerous Petri dishes and the extract application itself. Furthermore, this method is non-specific, since it does not permit the experimenter to assign biological activity to a single compound or compound group respectively but only to the extract in total.

Further tests were therefore performed using the agar overlay technique on TLC plates. This elegant, simple and rapid method is highly sensitive and permits immediate detection of active compounds in the extracts, coupled with an accurate localisation of active substances.

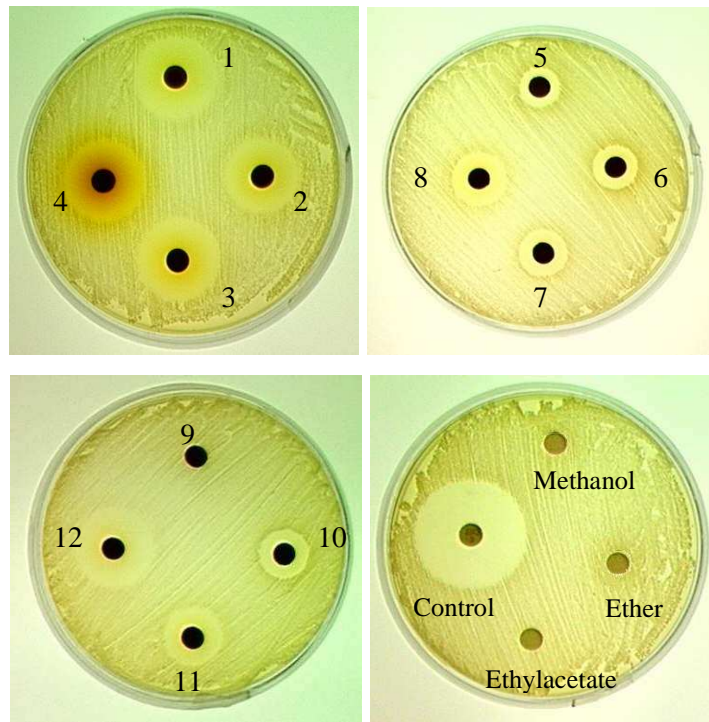


Figure 2: Antimicrobial activity (agar diffusion test) of *B. inquinans* extracts against *S. aureus*
 Ether extract: 1) 25 μ l, 2) 50 μ l, 3) 100 μ l, 4) 200 μ l
 Methanol extract: 5) 25 μ l, 6) 50 μ l, 7) 100 μ l, 8) 200 μ l
 Ethyl acetate extract: 9) 25 μ l, 10) 50 μ l, 11) 100 μ l, 12) 200 μ l
 Control – gemifloxacin 5 μ g

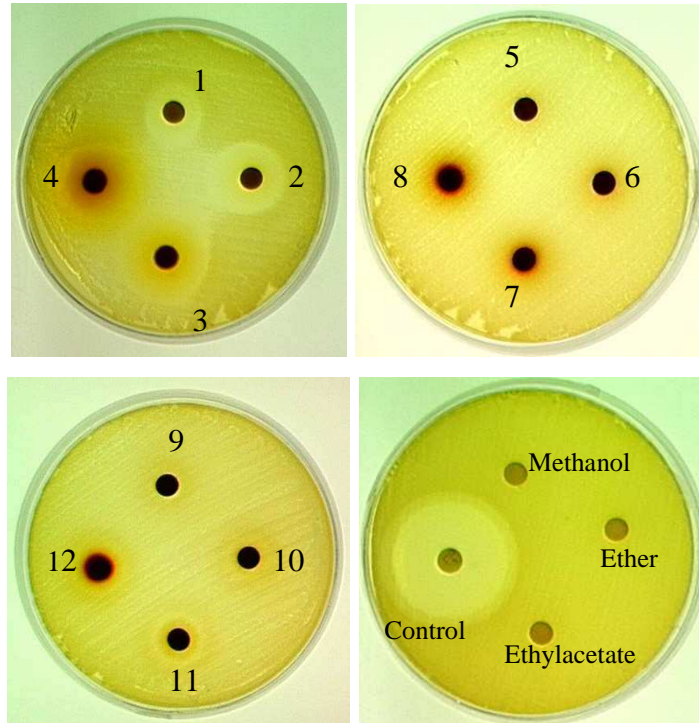


Figure 3: Antimicrobial activity (agar diffusion test) of *B. inquinans* extracts against *E. coli*
 Ether extract: 1) 25 μ l, 2) 50 μ l, 3) 100 μ l, 4) 200 μ l
 Methanol extract: 5) 25 μ l, 6) 50 μ l, 7) 100 μ l, 8) 200 μ l
 Ethyl acetate extract: 9) 25 μ l, 10) 50 μ l, 11) 100 μ l, 12) 200 μ l
 Control – gemifloxacin 5 μ g

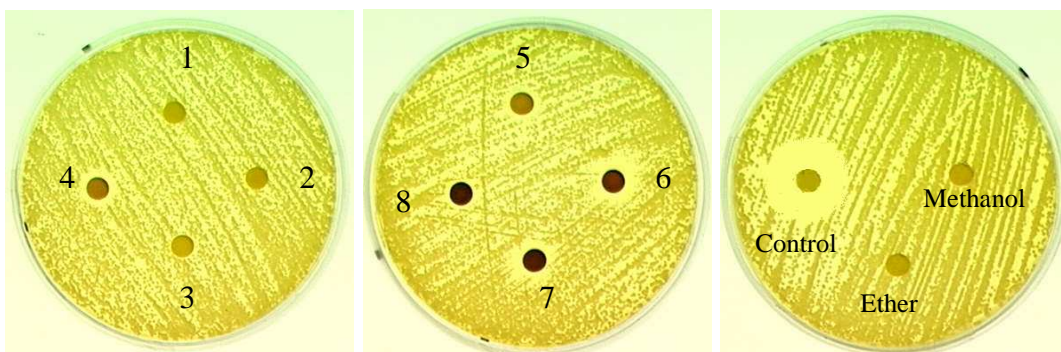


Figure 4: Antifungal activity of *B. inquinans* extracts against *C. albicans*

Ether extract: 1) 25 μ l, 2) 50 μ l, 3) 100 μ l, 4) 200 μ l

Methanol extract: 5) 25 μ l, 6) 50 μ l, 7) 100 μ l, 8) 200 μ l

Control – clotrimazole 10 μ g

3.1.2 Agar overlay technique on TLC plates

The second group included 22 species of fungi (see unmarked species in Table 2 and Table 3) and was tested for antimicrobial activity using a modified agar overlay technique.

The agar overlay method is a modification of the bioautographic agar overlay method developed by Rahalison *et al* for the detection of antifungal compounds in higher plants. In the original test, inhibition of fungal growth was assessed by detecting dehydrogenase activity with thiazolyl blue (methylthiazolyltetrazolium chloride; MTT by Fluka). In this test, chromatograms were placed on a hot plate maintained at 35 °C. Approximately 10 ml of the inoculum was rapidly distributed over the TLC plate (10 x 10 cm) with a sterile pipette. After solidification of the medium, TLC plates were incubated overnight at 30 °C in polyethylene boxes lined with moist chromatography paper. The bioautograms were sprayed with an aqueous solution (2.5 mg/ml) of MMT and incubated for 4 h at 30 °C. Clear inhibition zones were observed against a purple background [49].

For the proposed modified agar overlay method, both normal TLC plates and reversed-face plates (RP-18) may be used. The modified technique also avoids the stage of spraying with thiazolyl blue and accelerates the test, while nonetheless producing very clear results: inhibition zones around active bands can be detected easily in visible light.

For the modified agar overlay method as used, china blue lactose agar was also tested, but the results obtained were not as expressive and clear as results with normal agar: specifically, the inhibition zones were difficult to detect. Examples of tests with china blue lactose agar will not be given in this work.

In order to optimise the agar overlay method, efforts were made to identify the universal solvent systems suited to most of the extracts. Experimentation identified the optimal solvent compositions as trichloromethane/toluene/methanol (8:1:1) and dichloromethane/toluene/methanol (8:2:2).

The agar overlay technique may also be applied to both developed and undeveloped TLC plates. Undeveloped plates may be used as an alternative to the standard agar diffusion test: here, extracts or substances can be spotted directly on the TLC plate and overlaid with agar. In this case, the test provides information about the extract in total and not about active substances.

It was also discovered that certain types of plates were not suited to the agar overlay technique, such as TLC plates silica gel 60 F₂₅₄ by Merck (the coating was not stable when covered with warm agar). The best results were obtained using pre-coated Adamant UV₂₅₄ plates by Macherey-Nagel.

Broad-spectrum antibiotic ciprofloxacin (3.5 µg) aquatic solution, active against both gram-positive and gram-negative bacteria, was used as a reference compound: it was spotted onto the developed TLC surface just before the inoculum application.

Figure 5 presents the results of using the agar overlay technique to detect zones with antimicrobial activity in the methanol extracts of selected fungi species.

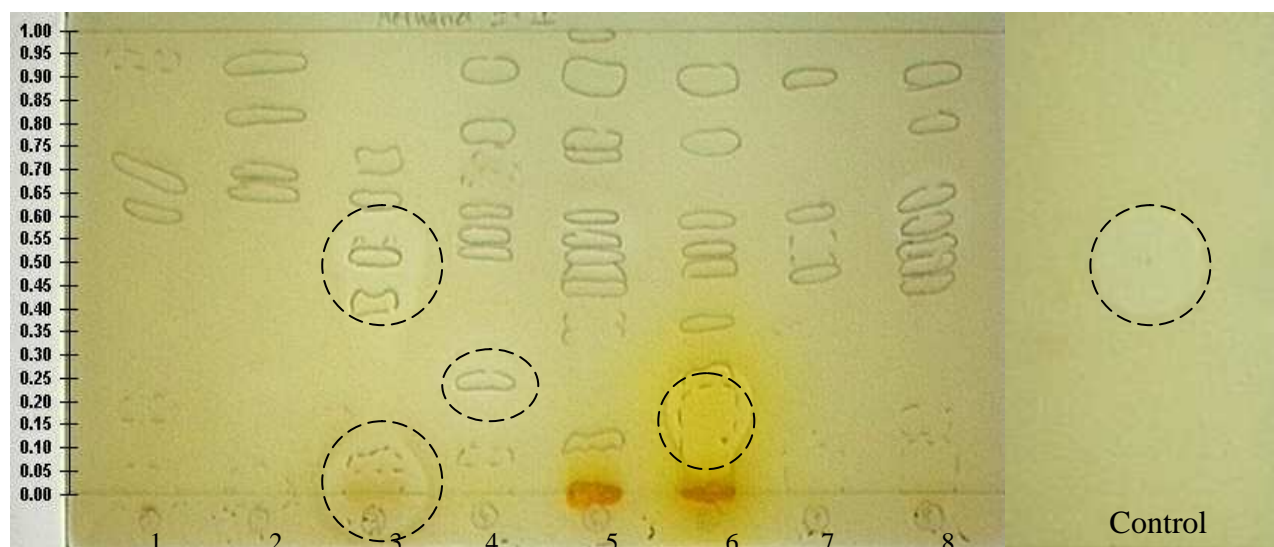


Figure 5: Testing methanol extracts of selected species of fungi (agar overlay technique) for antimicrobial activity against *S. aureus*. Inhibition zones are marked.

Solvent system: trichloromethane/toluene/methanol (8:1:1)

1) *Armillaria ostoyae* 20 μ l; 2) *Stropharia aeruginosa* 20 μ l; 3) *Fistulina hepatica* 20 μ l;

4) *Laetiporus sulphureus* 10 μ l; 5) *Ganoderma lipsiense* 20 μ l; 6) *Phaeolus spadiceus* 7 μ l;

7) *Gyromitra esculenta* 20 μ l; 8) *Stropharia rugosoannulata* 20 μ l

Control – ciprofloxacin 3.5 μ g

Data summarising the antimicrobial activity of tested extracts are presented in tables 5 and 6. Each table includes results obtained by testing different species of fungi using both the agar diffusion and agar overlay techniques.

Based on data obtained, *B. inquinans* and *M. giganteus* were chosen as research objects for further bioactivity tests and the isolation of active compounds, owing to their strong antimicrobial activity.

Species Name	Extract type			Additional investigations
	Methanol	Ether	Pentane	
<i>Amanita phalloides</i> (Vaill. ex Fr.) Link	–	–	+	HD –
<i>Armillaria mellea</i> (Vahl) P. Kumm.	–	±	not tested	
<i>Armillaria ostoyae</i> (Romagn.) Herink	–	++	+	HD –
<i>Ascocoryne sarcoides</i> (Jacq.) J.W. Groves & D.E. Wilson	+	++	+	
<i>Bulgaria inquinans</i> (Pers.) Fr.	++	+++	not tested	Ethyl acetate ++ HD +
<i>Chondrostereum purpureum</i> (Pers.) Pouzar	–	+	+	
<i>Rhodocollybia maculata</i> (Alb. & Schwein.) Singer = <i>Collybia maculata</i> (Alb. & Schwein.) P. Kumm.	+	+	++	
<i>Coprinus atramentarius</i> (Bull.) Fr.	–	+	–	
<i>Fistulina hepatica</i> (Schaeff.) With.	++	–	–	
<i>Ganoderma lipsiense</i> (Batsch) G.F. Atk.	+	+	–	
<i>Geastrum triplex</i> Jungh.	–	–	–	
<i>Gyromitra esculenta</i> (Pers.) Fr.	–	–	–	
<i>Hypholoma capnoides</i> (Fr.) P. Kumm.	+	–	–	
<i>Hypholoma fasciculare</i> (Huds.) P. Kumm.	++	+	+	HD –
<i>Inonotus obliquus</i> (Ach. ex Pers.) Pilát	±	Not tested	not tested	Ethyl acetate – HD ±
<i>Ischnoderma benzoinum</i> (Wahlenb.) P. Karst.	±	+	not tested	
<i>Laetiporus sulphureus</i> (Bull.) Murrill	+	–	–	
<i>Langermannia gigantea</i> (Batsch) Rostk.	±	+	not tested	
<i>Lycoperdon perlatum</i> Pers.	±	+	not tested	
<i>Lyophyllum connatum</i> (Schumach.) Singer	not tested	not tested	not tested	Ethyl acetate (Lyophyllin) +
<i>Meripilus giganteus</i> (Pers.) P. Karst.	++	++	not tested	HD +
<i>Paxillus atrotomentosus</i> (Batsch) Fr.	+	±	not tested	
<i>Paxillus involutus</i> (Batsch) Fr.	±	+	not tested	
<i>Phaeolus spadiceus</i> (Pers.: Fr.) Rauschert = <i>P. schweinitzii</i> (Fr.) Pat.	++	–	–	
<i>Scleroderma citrinum</i> Pers.	±	±	not tested	
<i>Stereum hirsutum</i> (Willd.) Pers.	±	±	not tested	
<i>Stropharia aeruginosa</i> (Curtis) Quéf.	+	–	–	
<i>Stropharia rugosoannulata</i> Farl. Ex Murrill	+	–	–	
<i>Trametes gibbosa</i> (Pers.) Fr.	±	+	not tested	

Table 2: Summary of antimicrobial tests for selected fungi species. Test microorganism: *S. aureus*. The highlighted lines show the fungi with the strongest antibiotic properties. Fungi shown in bold type were selected for detailed investigation.

Species Name	Extract type		Additional investigations
	Methanol	Ether	
<i>Amanita phalloides</i> (Vaill. ex Fr.) Link	–	–	
<i>Armillaria mellea</i> (Vahl) P. Kumm.	–	–	
<i>Armillaria ostoyae</i> (Romagn.) Herink	±	±	
<i>Ascocoryne sarcoides</i> (Jacq.) J.W. Groves & D.E. Wilson	±	+	
<i>Bulgaria inquinans</i> (Pers.) Fr.	–	++	Ethyl acetate –
<i>Chondrostereum purpureum</i> (Pers.) Pouzar	–	+	
<i>Rhodocollybia maculata</i> (Alb. & Schwein.) Singer = <i>Collybia maculata</i> (Alb. & Schwein.) P. Kumm.	+	+	
<i>Coprinus atramentarius</i> (Bull.) Fr.	–	+	
<i>Fistulina hepatica</i> (Schaeff.) With.	++	–	
<i>Ganoderma lipsiense</i> (Batsch) G.F. Atk.	+	+	
<i>Geastrum triplex</i> Jungh.	–	–	
<i>Gyromitra esculenta</i> (Pers.) Fr.	–	–	
<i>Hypholoma capnoides</i> (Fr.) P. Kumm.	+	–	
<i>Hypholoma fasciculare</i> (Huds.) P. Kumm.	–	–	
<i>Inonotus obliquus</i> (Ach. ex Pers.) Pilát	–	–	
<i>Ischnoderma benzoinum</i> (Wahlenb.) P. Karst.	–	–	
<i>Laetiporus sulphureus</i> (Bull.) Murrill	–	–	
<i>Langermannia gigantea</i> (Batsch) Rostk.	–	–	
<i>Lycoperdon perlatum</i> Pers.	–	±	
<i>Lyophyllum connatum</i> (Schumach.) Singer	not tested	not tested	Ethyl acetate (Lyophyllin) +
<i>Meripilus giganteus</i> (Pers.) P. Karst.	+	+	
<i>Paxillus atrotomentosus</i> (Batsch) Fr.	++	–	
<i>Paxillus involutus</i> (Batsch) Fr.	+	+	
<i>Phaeolus spadiceus</i> (Pers.: Fr.) Rauschert = <i>P. schweinitzii</i> (Fr.) Pat.	+	+	
<i>Scleroderma citrinum</i> Pers.	–	–	
<i>Stereum hirsutum</i> (Willd.) Pers.	–	–	
<i>Stropharia aeruginosa</i> (Curtis) Quéf.	+	±	
<i>Stropharia rugosoannulata</i> Farl. Ex Murrill	–	–	
<i>Trametes gibbosa</i> (Pers.) Fr.	–	–	

Table 3: Summary of antimicrobial tests for selected fungi species. Test microorganism: *E. coli*. The highlighted lines show the fungi with the strongest antibiotic properties. Fungi shown in bold type were selected for detailed investigation.

3.2. Investigations of *Bulgaria inquinans*

3.2.1 Taxonomy of *Bulgaria*

According to the Dictionary of the Fungi [24], *B. inquinans* is grouped into the phylum *Ascomycota*, class *Leotiomycetes* O. E. Erikss. u. Wink. (1997), order *Leotiales* Korf u. Lizoň (2001) and family *Bulgariaceae* Fr. (1849). It must be mentioned that the former taxon *Leotiales* Carpenter (1988) is regarded as synonymous with *Helotiales* Nannf. (1932) [50]. Thus, *B. inquinans* was also placed in the *Helotiales*.

The concept of the taxon *Bulgariaceae* is not accepted by all authors; e.g. Dennis did not use this term and grouped *Bulgaria* into the *Helotiaceae* (order *Helotiales*) [51]. In contrast, in the Nordic Macromycetes [52] one finds *Bulgaria* inserted into the *Leotiaceae* Corda (1842), a family that is much more restricted in extent in the new edition of the Dictionary of the Fungi. The *Bulgariaceae* family comprises 4 genera and seven species [24].

Concerning the genus *Bulgaria*, only one species exists for which 10 synonyms can be found in the Index Fungorum database [53].

The genus *Bulgaria* (anamorph: *Endomelanconium*) is represented by only one species, namely *B. inquinans* (Pers.) Fr. [24].

For this ascomycete, the Index Fungorum provides ten synonyms, including *B. polymorphy* Oeder ex Wettst., *Phaeobulgaria inquinans* (Pers.) Nannf. and *Phaeobulgaria polymorpha* (Oeder) Ferd. & Jørgensen [53]. According to the Index Fungorum, two varieties are accepted for *B. inquinans*: *B. inquinans* var. *inquinans* (Pers.) Fr. and *B. inquinans* var. *chalybea* Berk. (= *B. chalybea* (Berk.) Cooke & Masee).

B. inquinans is also known as “black jelly drops”, “poor man's liquorice”, “black bulgar”, “rubber buttons” and “Schmutzbecherling” (German, “dirty mushroom”): “inquinans” means “polluting” or “staining” in Latin, in reference to the dark marks this fungus leaves when rubbed with fingers. This can be one useful distinguishing feature for *B. inquinans*, since no marks are left when touching the

similar-looking and equally gelatinous black basidiomycete *Exidia glandulosa* (former name *E. truncate*), which has hyaline spores only.

Phylum: Ascomycota

Order: Leotiales

Family: Bulgariaceae

3.2.2 Biological characteristics of *B. inquinans*

Fruit body: Globose with a tightly inrolled margin when young and having a scurfy brownish exterior, later expanding then flattened, with a smooth black disc with no stalk. Its flat-topped cap is black and shiny on the inside, while rough and dark brown on the outside, its flesh is tough but gelatinous and rubbery.

Flat-topped at first but becoming slightly cup shaped, *B. inquinans* is easily overlooked because it is almost black. The fertile surface is shiny, and the sides (the outsides of the cup) are felt-like and dark brown (Figure 6).

The flesh of the fruit body is dark ochre-brown. It is soft and rubbery in wet weather but in dry conditions, it becomes tougher and more elastic.



Figure 6: Fruit bodies of *B. inquinans* growing on three different substrates: a) *Carpinus betulus*; b) *Betula pendula*; c) *Quercus robur*.

Taste/odour: Not distinctive [54].

Microscopy and spore print: Microscopic investigations of mature fruit bodies showed large asci (up to $200 \times 10 \mu\text{m}$) in accordance with the literature (Figure 7). The ascus pore is amyloid and turns blue with iodine (Melzer's reagent) as can be seen in Figure 8. The asci are cylindric-clavate and 8-spored. Ascospores of two kinds are found: one is dark brown-green and opaque, with a kidney-shaped, oval or round form; the other is hyaline and smaller, containing several oil drops (Figure 7 and Figure 9). The dimensions of the dark spores are $\sim 10\text{--}14 \times 6\text{--}7 \mu\text{m}$. The dimensions of the hyaline spores are $\sim 5\text{--}9 \times 3\text{--}5 \mu\text{m}$. During the microscopic investigation, it was discovered that only some asci bear both kinds of spores as described in the literature [51] and that the hyaline spores are not always located in the lower part of asci: investigation revealed spores at the upper tip of ascus or alternated with dark brown spores. Asci were also observed bearing only hyaline spores, some of which were partly or completely disintegrated (Figure 7).

Paraphyses were very slender ($\sim 100\text{--}125 \times 2\text{--}2.5 \mu\text{m}$); slightly swollen brown tips as described in the literature could not always be observed. Only some paraphyses showed characteristic branching and curling (Figure 8).



Figure 7: Microscopic preparation of *B. inquinans*: asci with different spores and parts of paraphyses. For details, see text.



Figure 8: Characteristic paraphysis with branching and curling. For details, see text.



Figure 9: Microscopic detection of amyloid structures in the hymenium of *B. inquinans* by dyeing with Melzer's reagent (iodine reaction). Ascus pores and thick spore walls stain blue – more clearly visible in magnification (a). For details, see text.

During the microscopic process, the contents of the asci, spore cells and paraphyses acquired a red colouration. The process of staining, starting from the edges of the cover slips and spreading slowly over the preparation, was apparent after about 15 minutes and well-developed after a further 15 minutes (Figure 10). This interesting phenomenon has not yet been described in literature and may be explained by the presence of azaphilones and their reaction with nitrogen-containing substances, such as amino acids released from broken cells. This kind of reaction causes the formation of vinylogous γ -pyridones, which have very strong non-selective biological activity (especially antibacterial and antifungal) and could be considered as a possible defence mechanism triggered by mechanical damage to the fungus (for details see Section 3.2.3).

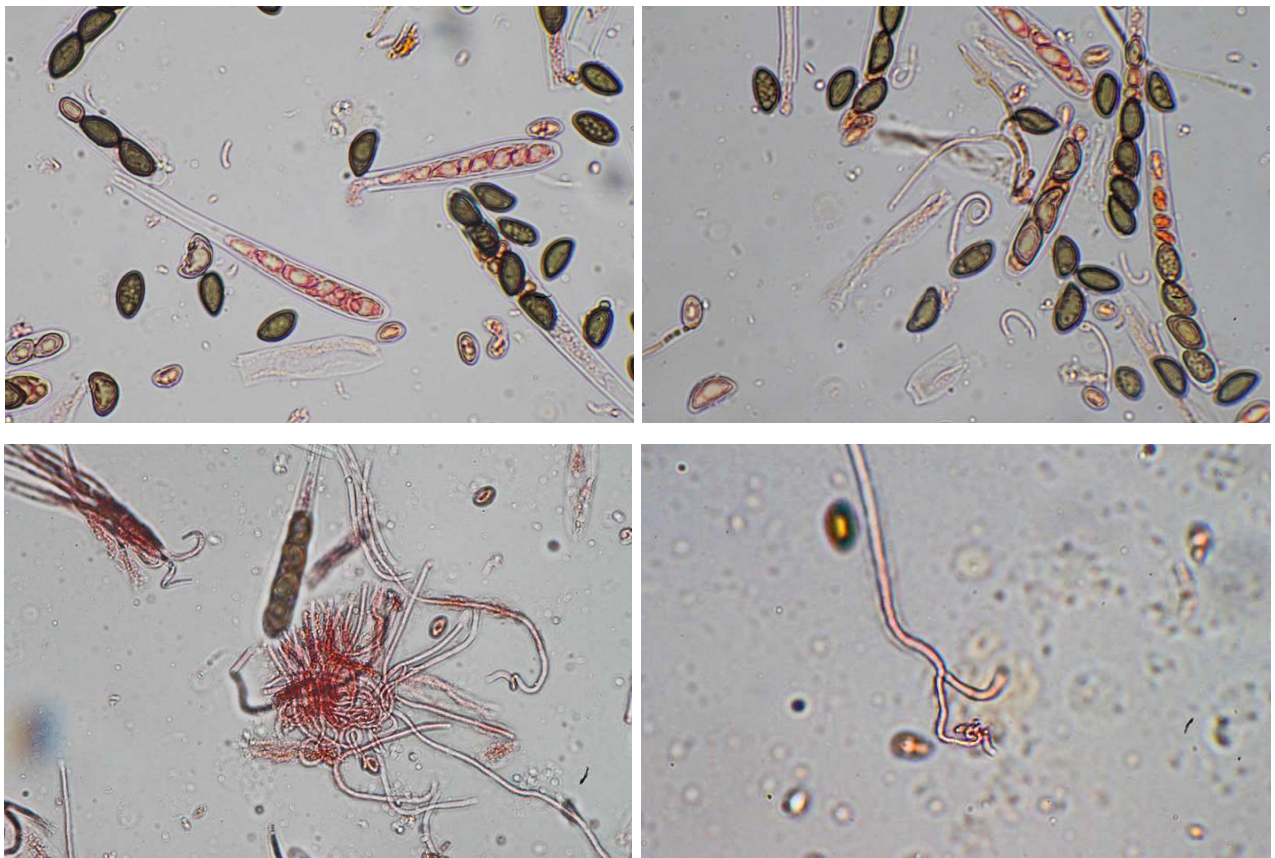


Figure 10: Microscopic preparation (aqueous medium) of hymenial elements of *B. inquinans*. After 30 minutes, a distinct red staining of asci, spores and paraphyses can be observed. For details, see text.

Ecology and habitat: *Bulgaria* is found in clustered groups on dead hardwood trees, especially oaks and maples. It grows in groups only on freshly fallen trunks and branches, especially of *Quercus*, occasionally also of *Betula*, *Castanea*, *Carpinus* and *Ulmus* (Figure 6). Often growing in dense masses, but not confluent, individual fruit bodies are between 0.5 cm and 4 cm across and typically 1 cm tall. Saprobic, sometimes also parasitic.

Season: It is a winter fungus, sometimes persisting through to March, mainly from October to February.

Occurrence: Frequent [55, 56]

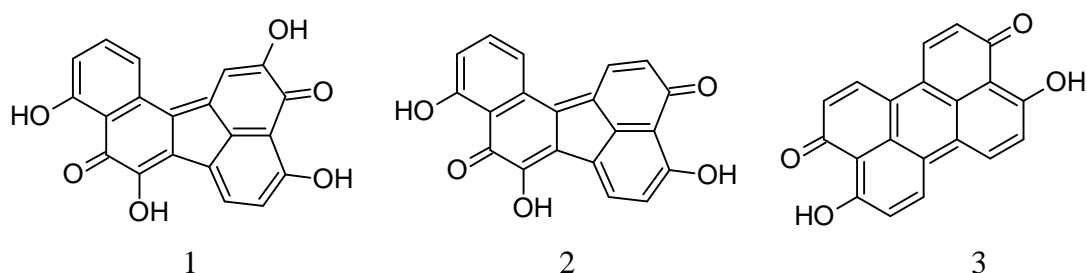
3.2.3 Chemical composition and bioactivity – an overview

A number of researchers have investigated the chemical constituents and bioactivity of *B. inquinans*.

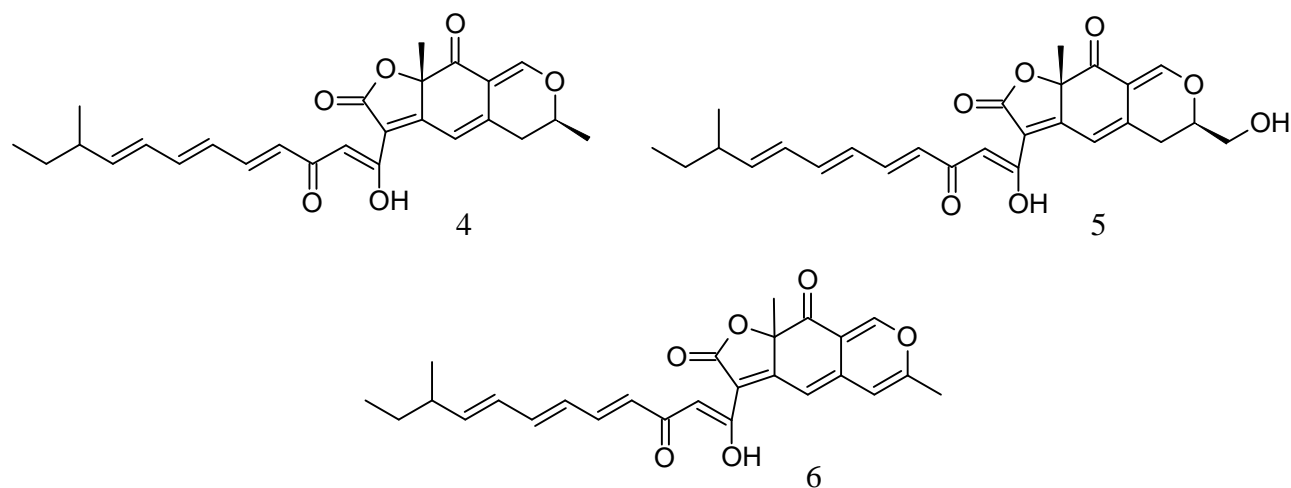
Edwards and Lockett isolated three crystalline quinones from dried fruit bodies of *B. inquinans* [57]. Two of these quinones were identified as derivatives of benzo[*j*]fluoranthene (bulgarhodin and bulgarein), while the third was characterised as 4,9-dihydroxyperylene-3,10-quinone. This was the first recorded isolation of a natural product with a structure based on the benzofluoranthene nucleus. Bulgarhodin (1), C₂₀H₁₀O₆ (M^+ 346), consists of purple hair-like needles. The pigment is sparingly soluble in common organic solvents, where it yields pale red solutions. In sulphuric acid, it dissolves to yield a solution with an intense green colouration. Absorption in visible and UV light is broad and not very characteristic for such solutions. In aqueous sodium hydroxide, bulgarhodin dissolves to yield a green solution that quickly deposits a green sodium salt. This property is characteristic of extended quinones. On exposing the alkaline solution to the air, the sodium salt slowly dissolves, producing a solution with a purple colouration. Bulgarein (2), C₂₀H₁₀O₅ (M^+ 330), is more soluble in organic solvents than bulgarhodin. Saturated ethanol solutions are purple, with more dilute solutions being intensely blue. In UV and visible light, the relatively sharp band at 375 nm is accompanied by broad absorption at 570 and 630 nm; on dilution, the 375 nm band becomes broader and the 570 nm

absorption disappears. As with bulgarhodin, solutions of the pigment in sulphuric acid are green, but alkaline solutions possess a stable blue colour unlike those of the former pigment [57].

4,9-Dihydroxyperylene-3,10-quinone (3), the third and least abundant constituent of the mixture, can be readily distinguished from bulgarhodin and bulgarein by the red colouration produced in sulphuric acid [57].



Stadler *et al* isolated three azaphilones (bulgarialactones A (4), B (5) and C (6)) from mycelial culture, which was obtained from fruit bodies and supplied a sufficient quantity of metabolites [58]. Bulgarialactones were acquired as dark red oils with molecular masses of 436, 452 and 434 Da respectively.

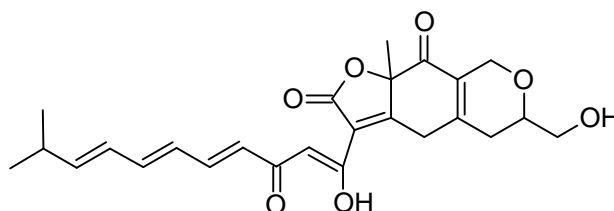


Bulgarialactones can be detected easily on silica gel TLC plates developed with toluene/acetone (7:3): $R_f = 0.86$ – bulgarialactone A; $R_f = 0.42$ – bulgarialactone B; and $R_f = 0.88$ – bulgarialactone C. Methanol solutions of bulgarialactones absorb UV light at the following wavelengths (λ_{max}): bulgarialactone A – 260 nm, 275 nm,

281 nm, 290 nm, 324 nm, 341 nm; bulgarialactone B – 307 nm, 394 nm, 438 nm; bulgarialactone C – 270 nm, 305 nm, 392 nm, 416 nm, 504 nm.

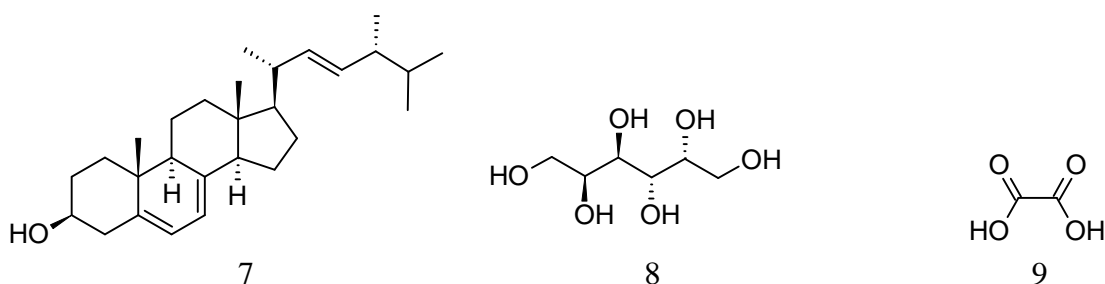
Bulgarialactones A and B possess antimicrobial (*Bacillus brevis*, *B. subtilis* and *Micrococcus luteus*), cytotoxic and nematicidal activities (*Caenorhabditis elegans*) and inhibit the binding of 3H-SCH 23390 to the dopamine D1 receptor *in vitro*. No growth inhibition of the filamentous fungi *Mucor miehei*, *Penicillium notatum* and *Paecilomyces variotii*, the yeast *Nematospora coryli* or the gram-negative bacterium *Enterobacter dissolvens* was noted with either compound. Due to its instability and the limited amounts available, bulgarialactone C was not tested [58].

Musso *et al* also isolated bulgarialactones A-C from a mycelial culture of *B. inquinans* [83]. In addition, a new bulgarialactone – an inhibitor of Hsp90 (heat shock protein 90, belonging to a class of proteins upregulated in response to stress) – was isolated:



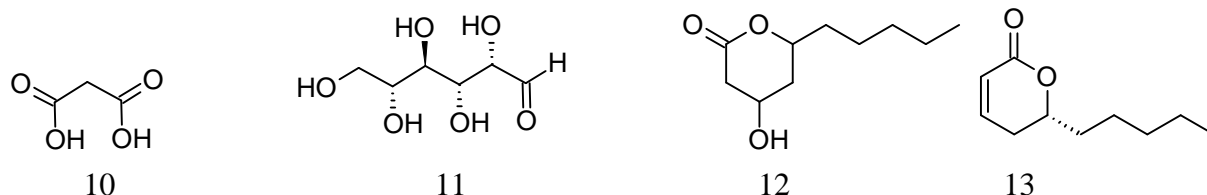
While Musso *et al* name this new bulgarialactone “bulgarialactone D”, their data were published after the appearance of the article “Azaphilones: a class of fungal metabolites with diverse biological activities” by Osmanova *et al*, which first makes mention of a bulgarialactone D – a natural constituent, isolated from fruit bodies of *Bulgaria* [130]. Since the chemical structures of these substances are different (and to avoid potential confusion), we have chosen to refer to the bulgarialactone isolated by Musso *et al* as bulgarialactone D_(Musso) in the present work. The isolation and structure elucidation of bulgarialactone D is described in sections 3.2.5.4 and 3.2.5.6, respectively.

Ergosterol (7), galactitol (8) and ethandioic acid (9) were isolated from fruit bodies of *B. inquinans* [59].



Dichloromethane extract of *B. inquinans* exhibited activity against *B. subtilis*, *Escherichia coli*, *Cladosporium cucumerinum* and *Biomphalaria glabrata*. A dosage of 100 µg spotted and developed on a TLC plate has also shown antioxidant and free radical scavenging activity. A methanol extract displayed activity only against *B. subtilis* and *E. coli* [40].

A group of researchers from the Institute of Mycology in China identified propanedioic acid (10), glucose (11) and two kinds of fragrance components: 2H-pyran-2-one, 5,6-dihydro-6-pentyl (12) and 2H-pyran-2-one, tetrahydro-4-hydroxy-6-pentyl (massoia lactone) (13) [60].

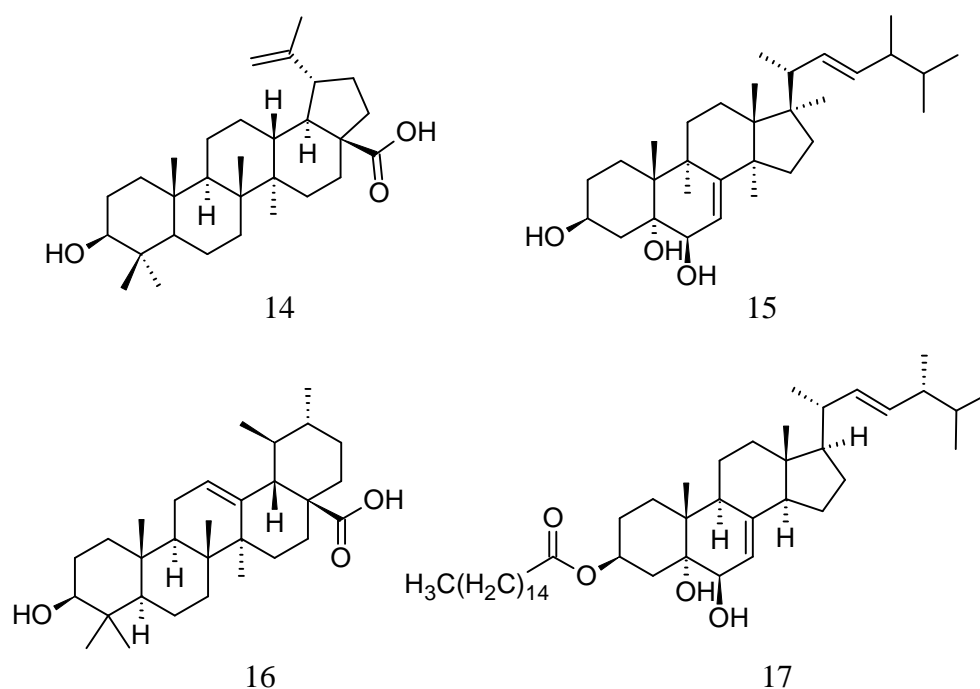


It was confirmed that *B. inquinans* also contains simple saturated hydrocarbon compounds with 13, 14, 15, 16, 17, 20, 21, 36 and 44 carbon atoms [60].

Extracting pulverised *B. inquinans* or its mycelium with 3-6 times its volume of 40-95% ethanol for 1-2 h, filtering the extracted solution and concentrating to an extract containing 0.2-0.8% ergosterol yields an extract termed “Jiaotuoluoyinxie” by the researchers (the name possibly being derived from the Chinese name for *B. inquinans*, “Jiaotuoluo”). The end product may be supplied in capsule, tablet, granule, or powder form: it is effective for removing toxic materials, promoting blood circulation, and countering blood stagnation. It can be used for the treatment of dermatoses such as blood stasis type psoriasis, vitiligo and dermatitis [61].

Colloidal polysaccharides were obtained by Ling: these can be used as a medicine in their own right or as a part of prescription together with other drugs for countering tumours, sores and hepatitis, increasing white cell count, boosting the immune system and reducing blood fat [62].

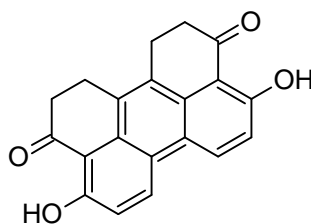
According to Peng Zhang and others, betuinic acid (14), cerevisterol (15), ursolic acid (16) and (24R)ergosta-7,22E-diene-3beta,5alpha,6beta-triol-3-O-palmitate (17) are responsible for antimicrobial activity in *B. inquinans*. Isolation was carried out using 70% ethanol on air-dried fruit bodies of *B. inquinans* [63].



The effects of *B. inquinans* ethanol extracts were tested on ICR mice. The scratching behaviour and vascular permeability changes induced by compound 48/80, histamine and serotonin levels were studied by Shuishi Jiang and others.² Ethanol extracts dose-dependently inhibited the scratching behaviour induced by compound 48/80 and serotonin. The results obtained would suggest that *B. inquinans* extract is effective against cutaneous pruritus and erythema, which are probably mediated by inhibiting the release of histamine from mast cells and antagonizing the effect of serotonin [64].

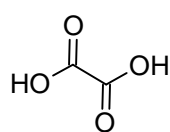
² Compound 40/80 is a polymer formed from the condensation of N-methyl-p-methoxyphenethylamine with formaldehyde. It promotes histamine release and is used in biochemical research to force mast cell degranulation.

4,9-dihydroxy-1,2,11,12-tetrahydroperylene-3, 10-quinone(1) (18) was isolated from an ethanol extract of *B. inquinans* fruit bodies [65].

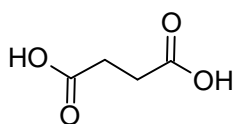


18

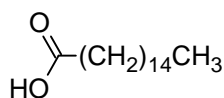
In addition, several organic acids were isolated from *B. inquinans* by column chromatography on silica gel and identified on the basis of physical/chemical constants and spectral analysis. Their structures were identified as oxalic acid (ethanedioic) (19), succinic acid (butanedioic acid) (20), palmitic acid (hexadecanoic acid) (21), cinnamic acid (22), 4-hydroxybenzoic acid (benzoic acid, 4-hydroxy) (23), 2,4-dihydroxybenzoic acid (24), isovanillic acid (benzoic acid,3-hydroxy-4-methoxy) (25), caffeic acid (26), coumaric acid (27), protocatechuic acid (benzoic acid, 3,4-dihydroxy) (28) [66].



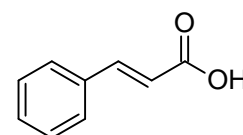
19



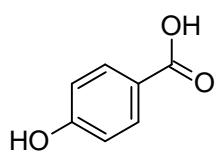
20



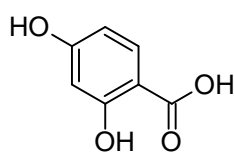
21



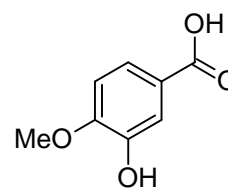
22



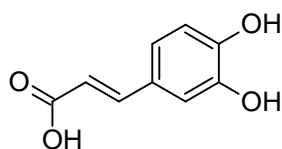
23



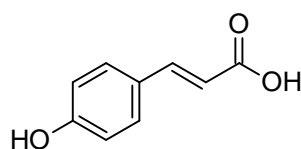
24



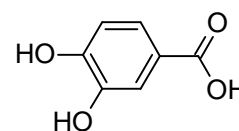
25



26



27

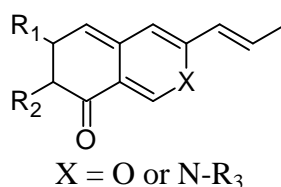


28

The chemical composition of *B. inquinans* is highly complex. The most interesting compounds isolated from fruit bodies and cell cultures of this ascomycete

are bulgarialactones – members of a large group of yellow fungal pigments known as azaphilones.

Azaphilones, a structurally diverse family of fungal secondary metabolites, have mainly been isolated from perfect and imperfect stages of ascomycetes such as *Aspergillus deflectus*, *Penicillium*, *Hypoxylon* and *Monascus spp.* Azaphilones are pigments with a pyrone-quinone structure containing a highly oxygenated bicyclic core and a quaternary centre. Their name references their affinity for ammonia, yielding vinylogous γ -pyridones. Such exchange of the pyrane oxygen for nitrogen causes a colour change from yellow to red [58, 67, 68].



This appears to be a characteristic reaction. It can take place both with ammonia alone [69, 70] and the side chain of a macrocyclic polypeptide [71, 72].

The potent non-selective biological activities of azaphilones may be related to their production of vinylogous γ -pyridones [73]. Their most remarkable properties include their natural occurrence, yellow-red spectra, relative thermostability (compared with other natural red pigments) and easy derivation.

Azaphilones exhibit a wide range of interesting biological activities, such as antimicrobial, antifungal, antiviral, antioxidant, cytotoxic, nematocidal and anti-inflammatory activities.

Fungi containing azaphilones have been used as colorants in foodstuffs and alcoholic beverages in certain Asian countries.

The present state of knowledge on azaphilone-containing species of fungi, structures and activities has recently been summarised in the article “Azaphilones: a class of fungal metabolites with diverse biological activities” [130]. The complete text of this article is given in Appendix II.

Based on a review of the literature data and the strong antibacterial effects alluded to above, *Bulgaria inquinans* proved to be a challenging subject and was chosen for further investigations.

A further key aspect was the fact that certain experiments had been conducted on dried fruit bodies [57, 63] or mycelial cultures [58]. It was therefore of interest to implement biological tests and isolation of bioactive compounds from fresh fruit bodies of *B. inquinans*.

Although many substances and bioactivities had already been identified, no information on volatile compounds from *B. inquinans* or their bioactivity had been presented. One requirement was therefore to determine the composition and biological activity of *B. inquinans* volatiles.

3.2.4 Detection of bioactive compounds in *Bulgaria* extracts

3.2.4.1 Determination of haemolytic TLC zones in ether extract

Haemolysis is a breakdown of red blood cells (RBCs) either in the blood vessels (intravascular haemolysis) or elsewhere in the body (extravascular). It causes haemolytic anaemia, whose characteristic signs include pallor, fatigue and shortness of breath, and is capable of causing heart failure.

Haemolysis can be either intrinsic or extrinsic. Extrinsic haemolysis as caused by fungi is not uncommon: it may be induced by fungal antigens and toxins or can appear after repeated ingestion of some species of edible mushrooms such as *Paxillus involutus*, *Hygrophorus pustulatus*, *Hypholoma capnoides*, *Collybia butyraceae*, *Coprinus atramentarius*, *Flammulina velutipes*, *Hygrocybe virgineus* and others [74, 75]. Fungi-induced hemolysis may also be caused by haemolysins, in particular: lectins (*Laetiporus sulphureus*) [76]; cytolysin (*Pleurotus ostreatus*) [77, 78]; and flammutoxin (*Flammulina velutipes*) [79].

Since no information had been identified concerning the haemolytic activity of *B. inquinans*, the investigation of biological activities in *Bulgaria* ether extracts started by addressing this topic. A test was carried out on developed TLC plates in order to locate a band or bands responsible for haemolytic activity. First, 20 μ l of ether extract was developed in the solvent system trichloromethane/toluene/methanol (8:1:1). The TLC plate was then carefully dried and covered with blood gelatine (see Section 5.7.3). Results were obtained after 12 hours exposure.

Two clear haemolytic zones were detected: their R_f values were found to be 0.05 and 0.45, respectively (Figure 11, mode 1). On comparing results of a blood gelatine test plate with the TLC plates acquired in UV light (254 and 366 nm), a plate sprayed with anisaldehyde reagent (Figure 11, mode 4) and a plate observed in ammonia vapour under visible light (Figure 11, mode 5), it was possible to establish the exact position of the upper active band ($R_f = 0.45$). This band exhibited yellow fluorescence in UV light (366 nm), a specific red colour after reaction with ammonia vapour (Figure 11, modes 3 and 5) and proved to be an azaphilone (see Section 3.2.3).

The position of the second haemolytic zone ($R_f = 0.05$) could not be determined clearly on the parallel TLC plate (modes 2–5). Thus, no reliable isolation was possible.

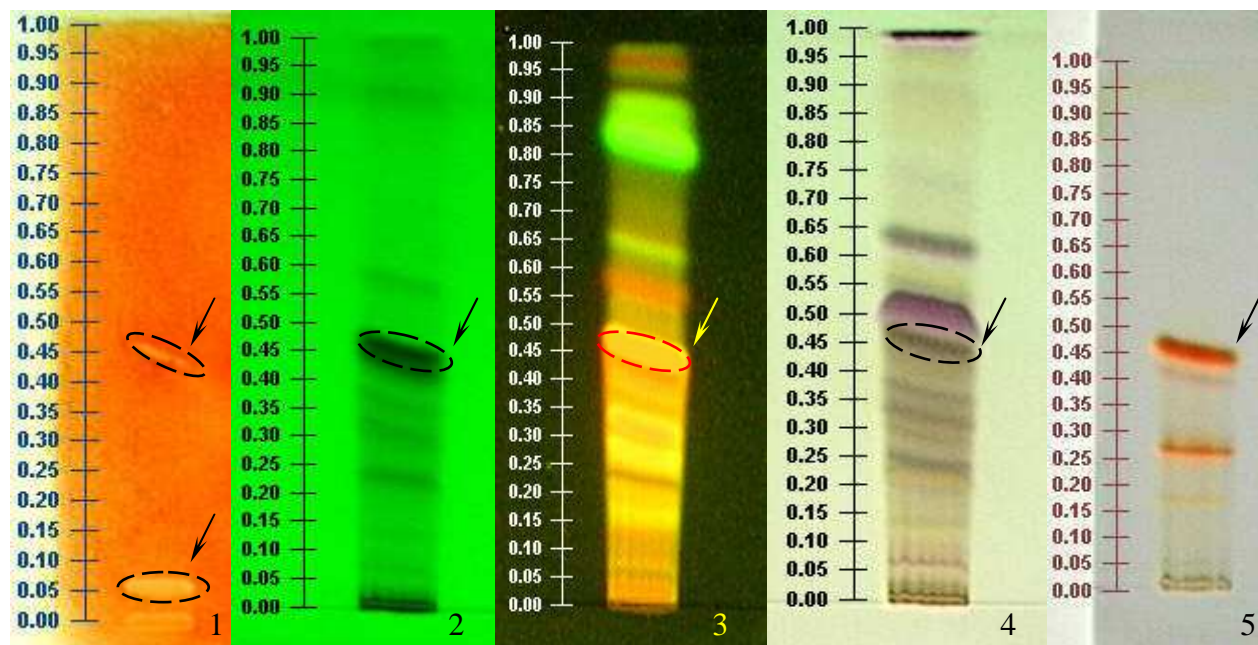


Figure 11: Haemolytic activity of *B. inquinans* ether extract in a blood gelatine test
 Solvent system: trichloromethane/toluene/methanol (8:1:1)
 Detection mode: (1) Visible light (blood-gelatin plate); (2) UV light 254 nm; (3) UV light 366 nm; (4) Visible light (spraying with anisaldehyde reagent); (5) Visible light (reaction with ammonia vapour). Arrows on modes 2–5 indicate the position of the haemolytic azaphilone band (for details, see text).

3.2.4.2 TLC zones with antibacterial activity

An agar overlaying method was used for the identification of bands with antibiotic properties in the *Bulgaria* ether extract (see Section 5.7.2).

TLC plates were developed in the trichloromethane/toluene/methanol (8:1:1) solvent system, dried and then covered with a thin layer of warm agar containing an inoculum of *S. aureus*. On evaluation of the results, it was found that two zones had become bright red following contact with agar media. Such properties belong to azaphilones: these change their colour from yellow to red in the presence of proteins, amino acids and nucleic acids [80, 81] (see Section 3.2.3).

Although the separation of the ether extract on TLC plate was quite good, the sizeable inhibition zone made it difficult to assign antimicrobial activity to a certain band (Figure 12).

Stadler *et al* [58] reported on the separation and isolation of three azaphilones from an acetone extract of *B. inquinans*. A silica gel TLC plate was used, plus a 7:3 toluene/acetone solvent system. Isolated azaphilones were named bulgarialactones and possessed the following R_f values: bulgarialactone A ($R_f = 0.86$), bulgarialactone B ($R_f = 0.42$) and bulgarialactone C ($R_f = 0.88$).

It was therefore decided to test this toluene/acetone mixture for ether extract separation, followed by the application of the agar overlaying technique to detect azaphilone bands. There were three inhibition zones of bacterial growth visible on the agar-overlaid plate (Figure 13): their good separation and optical intensity permitted the assignment of antimicrobial activity to specific bands. Two of the bioactive bands pertained to azaphilones (see Section 3.2.3): the band with $R_f = 0.20$ and the band with $R_f = 0.38$ (Figure 13, detection mode 1). However, one must also note that bands marked by arrows are identical in spite of their R_f values differing slightly between detection modes (Figure 13): this behaviour depends on the type of TLC plate used for bioassays and chromatography (see Section 5.5.3). The strong fluorescence of azaphilones (Figure 13 detection mode: 3) also makes it difficult to estimate exact R_f values. No bands with azaphilone properties were detected at $R_f = 0.42$, $R_f = 0.86$ or $R_f = 0.88$ as described in [58].

Accordingly, the discovery of two new biologically active azaphilones in the ether extract of *B. inquinans* was postulated. The activity of both was comparable with that of the control antibiotic (Figure 13, control). Consequently, the solvent system toluene/acetone (7:3) was chosen as an optimal system for further azaphilone separation and isolation from TLC plates. The third active zone ($R_f = 0.05$) contained several small adjacent bands and reliable detection of the active compound was therefore not possible.

An agar overlay method with china blue lactose agar (CM0209) was also used for determination of antimicrobial activity in the *B. inquinans* ether extract. It was envisaged that the presence of dye in agar media would improve the visibility of the inhibition zones and facilitate evaluation of the results. Unfortunately, the results obtained were ambiguous and will therefore not be illustrated in the present work.

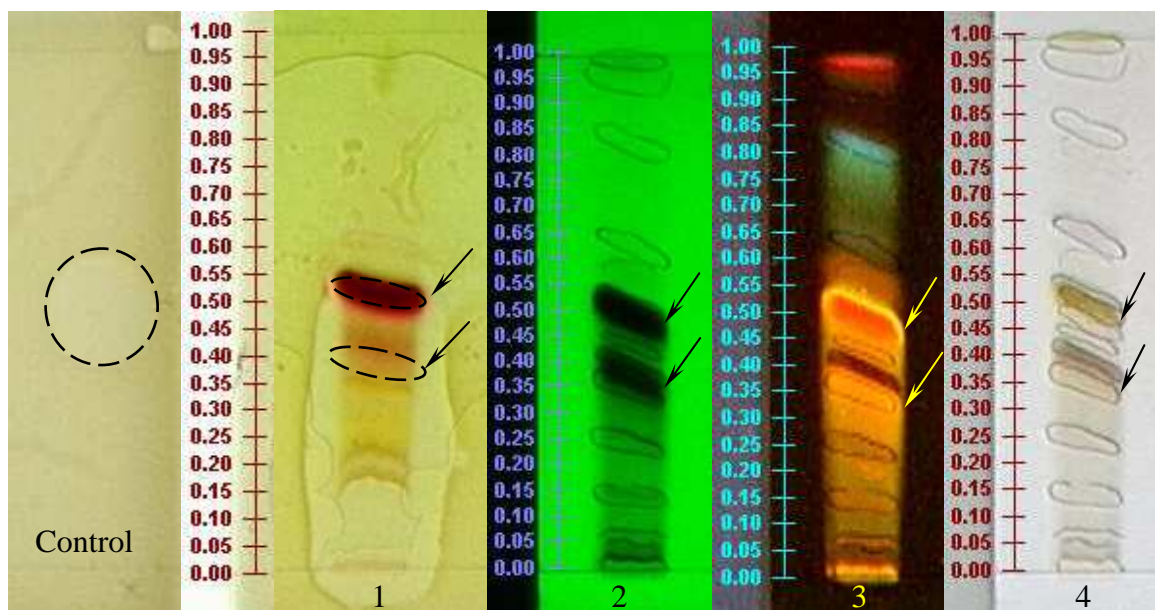


Figure 12: Detection of bacterial growth inhibition zones on TLC plates (agar overlay technique) in *B. inquinans* ether extract (for details, see text)
 Solvent system: trichloromethane/toluene/methanol (8:1:1); control: ciprofloxacin 3.5 μg .
 Detection mode: (1) Visible light (agar overlaid extract); (2) UV light 254 nm; (3) UV light 366 nm; (4) Visible light (anisaldehyde reagent). Azaphilone bands are indicated by arrows.

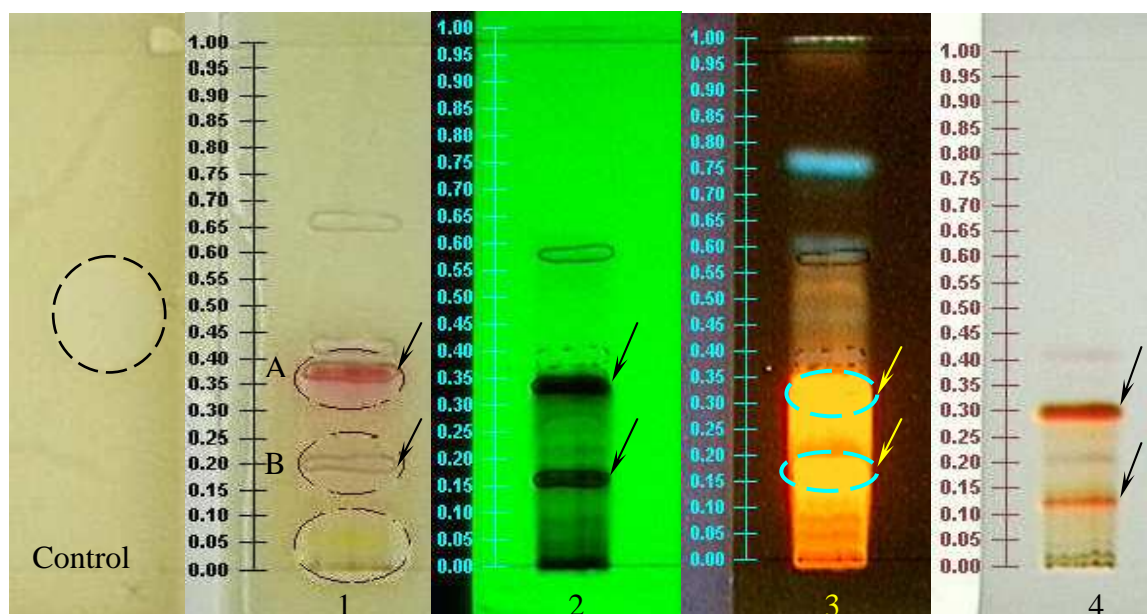


Figure 13: Detection of bacterial growth inhibition zones on TLC plates (agar overlay technique) in *B. inquinans* ether extract (for details, see text)
 Solvent system: toluene/acetone (7:3); control: ciprofloxacin 3.5 μg .
 Detection mode: (1) Visible light (agar overlaid extract); (2) UV light 254 nm; (3) UV light 366 nm; (4) Visible light (anisaldehyde reagent). Azaphilone bands (A and B) are marked by arrows.
 For the R_f value differences, see text.

3.2.5 Isolation of antibacterial substances from *Bulgaria* extracts

3.2.5.1 Isolation of antibacterial azaphilones from preparative TLC plates

Isolation of two antimicrobial zones from an ether extract was carried out on preparative TLC plates developed in the solvent system toluene/acetone (7:3). Both bands, band B ($R_f = 0.20$) and band A ($R_f = 0.38$) in Figure 13 (detection mode: 4), were eluted from the plates with pure ether.

As already mentioned, the active constituents were assumed to be azaphilones because of their characteristic dyeing on contact with agar and ammonia vapour (Figure 13, detection modes 1 and 4, respectively).

Isolation from preparative TLC plates presented a number of significant problems. Employing ether for desorbing the active compounds from TLC plates had not shown any indications of decomposition or chemical rearrangement. However, the disadvantage of this apolar solvent was its low elution capacity, i.e. only a portion of the compound was regained from the plate, while a considerable part remained adsorbed on the silica gel. The amounts gained in this way were insufficient for any structure elucidation techniques.

In order to test the stability of the *Bulgaria* ether extract during storage, the TLC pattern of a freshly prepared extract was compared with one left at room temperature for approximately a week. It was found that the active substance A is a dominant band in the extract kept for one week, whereas substance B dominates in a freshly prepared extract (Figure 14); however, this interesting phenomenon does not explain desorption problems.

When testing alternative polar solvents such as acetone and methanol for the elution of active bands, a colour change in the solution was observed: from yellow to red and yellow to blue, respectively. Moreover, within a short period, these solutions turned to colourless. One was therefore able to conclude that these supposed azaphilones are unstable and decompose under the experimental conditions chosen. It was further concluded that ether is also a sub-optimal solvent for extract preparation, since it proved incapable of providing a good desorption rate from TLC.

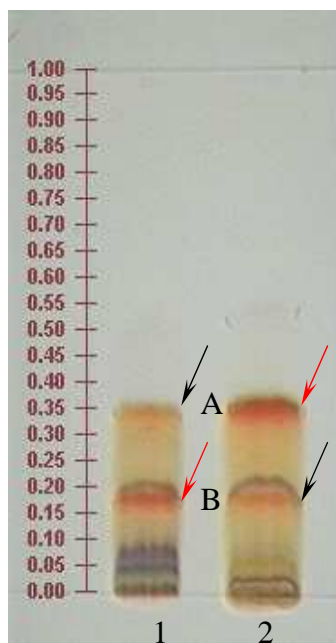


Figure 14: *B. inquinans* ether extracts. Solvent system: toluene/acetone (7:3)
 Detection: visible light (ammonia vapour); 10 μ l applied
 (1) Freshly prepared extract; (2) Extract stored for one week at room temperature.
 Red arrow marks the dominating azaphilone.

Two further organic solvents were therefore tested as extractants: acetone and acetonitrile. Acetone was chosen because Stadler *et al* reported the extraction of fresh *B. inquinans* fruit bodies with acetone and the isolation of bulgariolactones B in a quantity sufficient for structure elucidation [58]. A further reason for testing acetone as an extractant was the decomposition observed when using acetone for TLC desorption (see previous page), since it was still unclear whether this was attributable to the acetone or to the catalytic properties of the silica gel.

All three extracts (ether, acetone and acetonitrile) were prepared under similar conditions (fungus quantity, extraction temperature, extractant volume and extraction time). After concentration, extracts were applied to a silica gel TLC plate and developed in a toluene/acetone (7:3) solvent system. The results are shown in Figure 15.

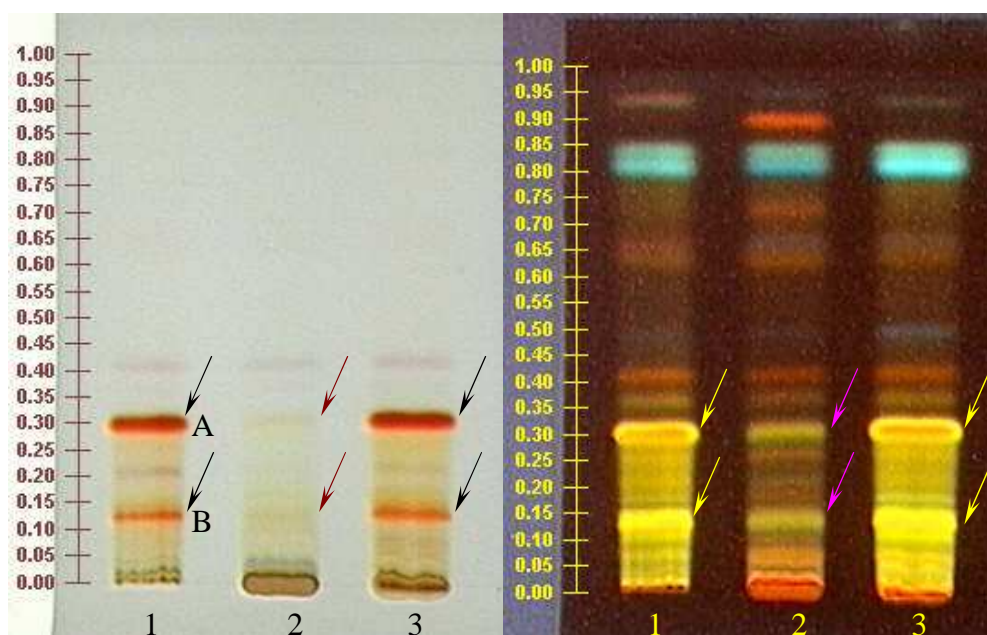


Figure 15: Comparison of *B. inquinans* extracts. Solvent system: toluene/acetone (7:3)
 Detection: Visible light (ammonia vapour) and UV light 366 nm. Quantity applied: 10 μ l.
 (1) ether extract; (2) acetone extract; (3) acetonitrile extract. For details, see text.

The smallest quantities of azaphilones were detected in the acetone extract, while the ether and acetonitrile extracts contained sufficient amounts of both active bands (A and B). Evaluated by degree of fluorescence, the concentration of the active substance B in the acetonitrile extract proved greater than in the ether extract (Figure 15, (3), detection mode UV light 366 nm).

The results indubitably show that acetone is sub-optimal both for extraction of active compounds from *Bulgaria* and for elution of these substances from TLC plates.

The acetonitrile extract seemed to offer the greatest potential for further experiments: taking into account the phenomenon obtained when comparing fresh ether extract with the extract kept for a week at room temperature (Figure 14), it was natural next step to perform experiments for optimising the extraction temperature.

Extraction was carried out at a low temperature ($-18\text{ }^{\circ}\text{C}$) and at room temperature ($18\text{ }^{\circ}\text{C}$); the extractant was acetonitrile. Conducting the experiment at sub-zero temperatures confers obvious advantages in terms of the resulting quantities of azaphilones (Figure 16). It became clear that the quantities of the two azaphilones

and their stability in extracts depend on several factors: the extractant, the extraction temperature and the conditions under which the extract is stored.

Additionally, extraction at sub-zero temperatures helps to avoid problems in relation to the extract's water content: normally, the presence of water strongly retards the process of concentration while also requiring heat treatment.

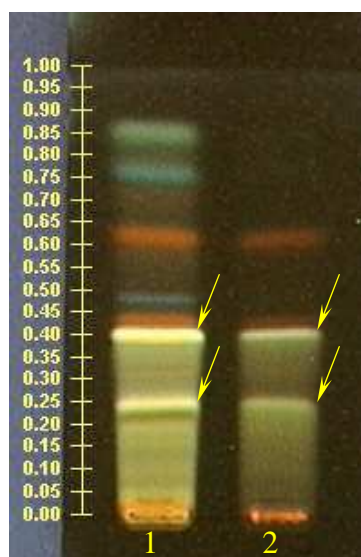


Figure 16: Comparison of *B. inquinans* acetonitrile extracts. Solvent system: toluene/acetone (7:3). Detection: UV light 366 nm; quantity applied: 10 μ l. (1) low-temperature extract; (2) room temperature extract. Arrows indicate azaphilone substances. For details, see text.

Although the experiments demonstrated that acetonitrile is an optimal extractant and provides better desorption from the TLC plate, the resulting active compounds isolated still contained admixtures: both MS and NMR revealed the presence of impurities. Accordingly, an attempt was made to optimise the separation of active substances on TLC plates by using different solvent systems and phases: these experiments showed that RP-18 HPTLC plates yield the best separation, while a 7:3 acetonitrile/water solvent system turned out to be optimal. Interestingly, Stadler *et al.* reported this solvent system as system for final purification (by HPLC) of bulgarialactones isolated from silica gel [58].

As can be seen in Figure 17, the band at $R_f = 0.20$ on the HPTLC plate corresponds to substance A ($R_f = 0.33$ on the silica gel plate), while the band with $R_f = 0.54$ on the HPTLC plate corresponds to substance B ($R_f = 0.15$ on the silica gel plate).

Since the best separation of active substances was obtained on RP-18 HPTLC plates, it was reasonable to employ HPLC for further isolation in order to reduce impurity levels and achieve a greater sample throughput (preparative scale). This method also avoids the problem of active compound desorption. Moreover, the acetonitrile extract is perfectly suited for HPLC separation and isolation.

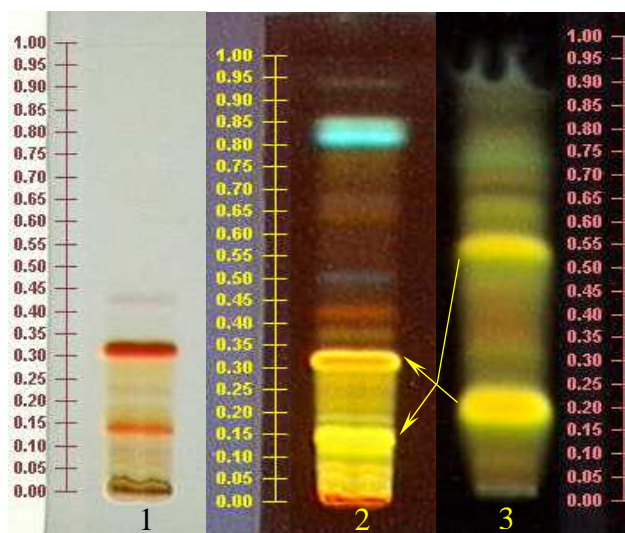


Figure 17: *B. inquinans* acetonitrile extracts on different TLC-plates. Quantity applied: 5 μ l.
 (1) silica gel phase: solvent system toluene/acetone (7:3); visible light (ammonia vapour reaction).
 (2) silica gel phase: solvent system toluene/acetone (7:3); UV light 366 nm.
 (3) RP-18 HPTLC phase: solvent system acetonitrile/water (7:3); UV light 366 nm.

3.2.5.2 Optimisation of azaphilones separation using analytical HPLC

For further experiments, a cold acetonitrile extract ($-18\text{ }^{\circ}\text{C}$) of *Bulgaria* was used. In order to create a HPLC method for optimal isolation of active substances from this acetonitrile extract, an analytical column LiChrospher[®] 100 RP-18e (5 μ m) was used. A wavelength of 450 nm proved to be the optimal monitoring wavelength. Only two main peaks were detected on the HPLC chromatogram: a 7-minute peak corresponded to band (B) with $R_f = 0.15$ on a silica gel TLC plate; a 22.5-minute corresponded to band (A) with $R_f = 0.33$ (Figure 17 and Figure 18). A 35-minute run with a constant flow of 0.25 ml/min was sufficient for separation of both azaphilones.

3.2.5.3 Formation of azaphilones in acetonitrile extract

Section 3.2.5.1 has already presented the results of comparing an extract freshly prepared at 20 °C with an extract left at room temperature for one week (Figure 14). In order to study the influence of different parameters on the composition of acetonitrile extracts prepared at –18 °C, the following experiments were conducted:

- a) After filtration, the extract was immediately subjected to HPLC
- b) The extract was then stored at room temperature for a week and again subjected to HPLC

The results of these experiments are presented in Figure 18. Compared to the first analysis, the second HPLC experiment revealed a reduction in the intensity of Peak 1, plus a considerable enlargement of Peak 2 and the appearance of a new additional peak (Peak 3) at the 8.5-minute mark.

The same experiment was then performed with extracts concentrated *in vacuo* at 40 °C (the temperature recommended by the manufacture of the vacuum evaporator). Results are given in Figure 19: while similar to those of the previous experiment, including the new peak (Peak 3) at the 8.5-minute mark, Peak 2 is now the strongest peak and an additional peak (Peak 4) has now emerged at the 24-minute mark.

Although both additional peaks (at 8.5 and 24 minutes, respectively) possess UV spectra identical to those of Peak 1 and Peak 2, the different retention time indicates a difference in their structure. It was therefore presumed that these peaks were the products of partial decomposition or a rearrangement of the original azaphilone structure. However, an attempt to isolate these additional peaks in order to establish their structure was unsuccessful: their colour changed from yellow to pink almost immediately, indicating a rapid rate of decomposition.

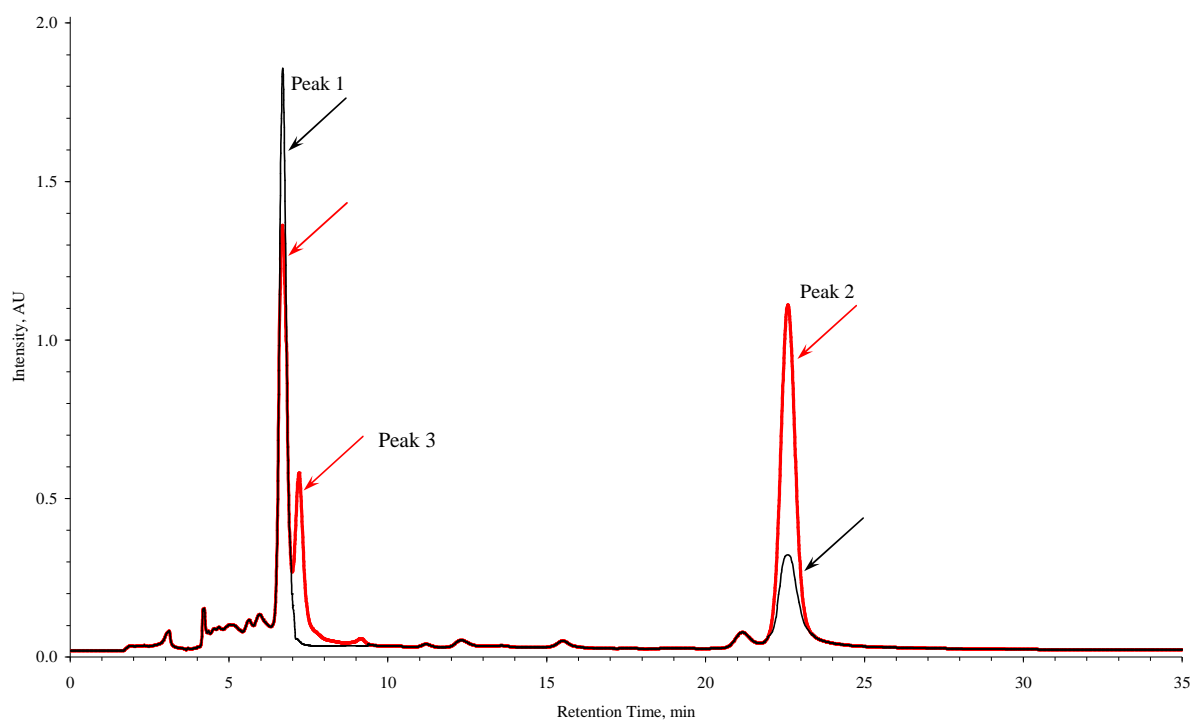


Figure 18: HPLC chromatogram of *B. inquinans* acetonitrile extracts ($-18\text{ }^{\circ}\text{C}$). Solvent system: acetonitrile/water (7:3). Monitoring wavelength: 450 nm. For details, see text.

— Fresh extract
 — Extract stored for one week at room temperature

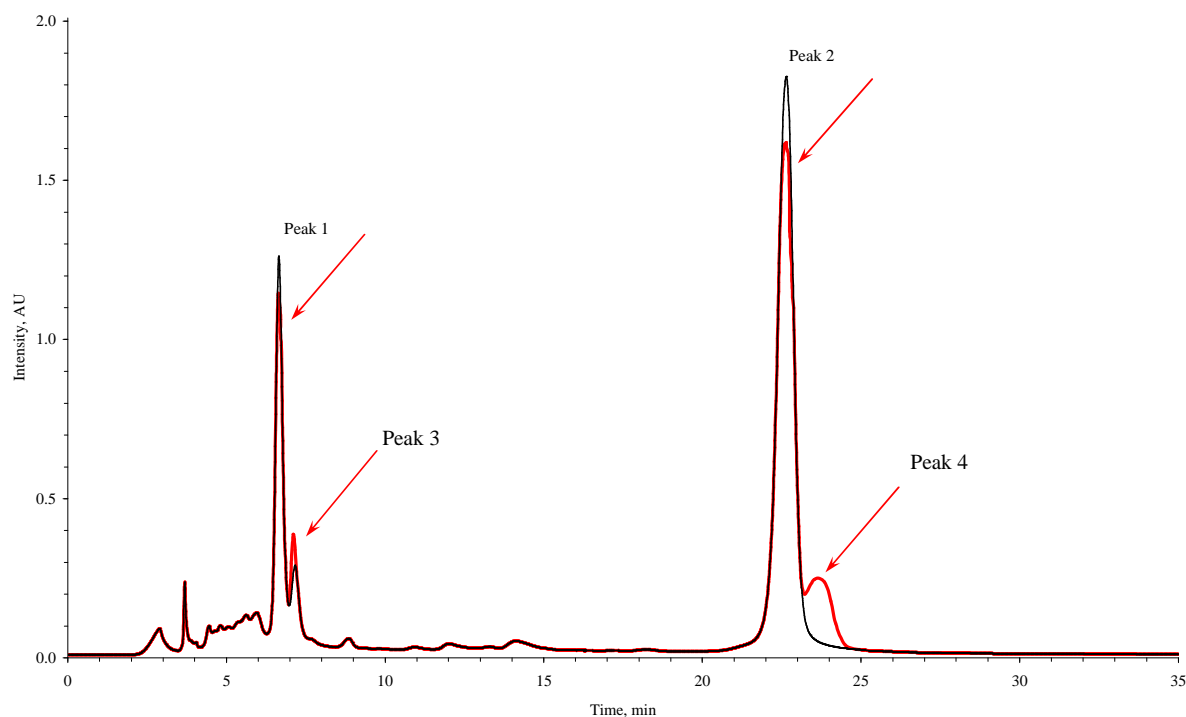


Figure 19: HPLC chromatogram of *B. inquinans* acetonitrile extracts ($-18\text{ }^{\circ}\text{C}$, concentrated *in vacuo* at $40\text{ }^{\circ}\text{C}$). Solvent system: acetonitrile/water (7:3); monitoring wavelength: 450 nm. For details, see text.

— Concentrated fresh extract
 — Concentrated extract stored for one week at room temperature.

3.2.5.4 Isolation of azaphilones by preparative HPLC

Azaphilone isolation was realized by using a LiChrospher® 250-10 RP-18 (10 µm) preparative column. The programme developed was transferred successfully from analytical HPLC: a 7:3 acetonitrile/water solvent system with a monitoring wavelength of 450 nm. The flow was increased to 3 ml/min.

Both peaks (1 and 2) (Figure 20) were collected and concentrated under nitrogen flow to reduce the risk of decomposition connected with heat treatment (concentration).

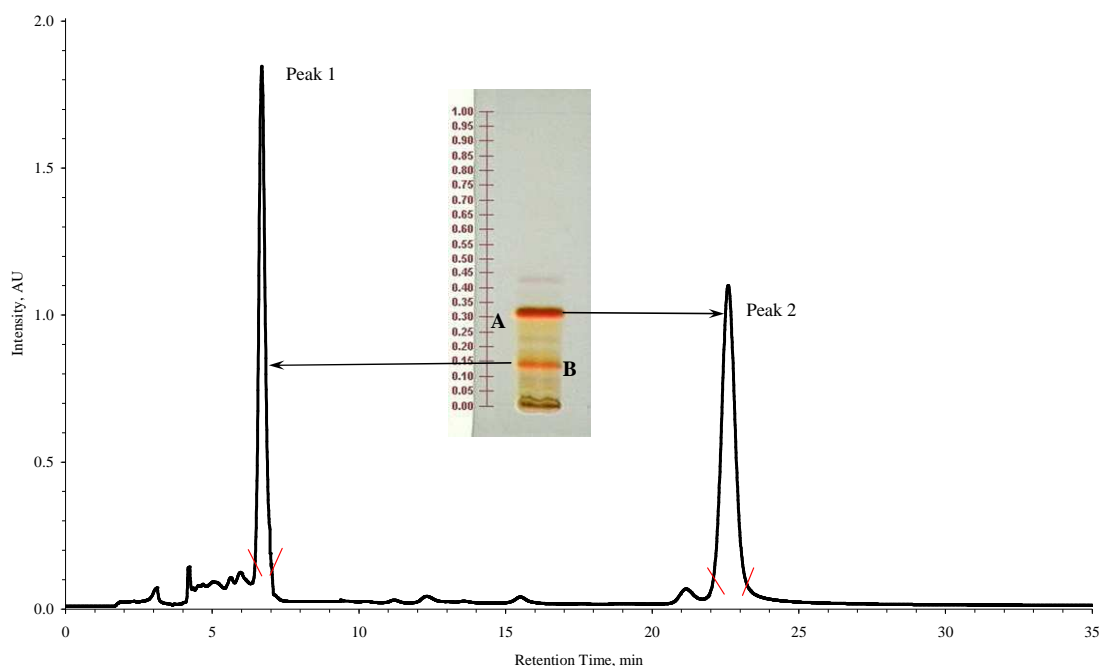


Figure 20: HPLC chromatogram of *B. inquinans* acetonitrile extract
Solvent system: acetonitrile/water (7:3); monitoring wavelength 450 nm.

It was possible to isolate about 5 mg of each substance: isolated substances were re-subjected into analytical HPLC to check their purity. The compounds separated had identical UV spectra in acetonitrile, exhibiting absorption maxima (λ) at 226, 296, 327 and 452 nm (Figure 21 and Figure 22). The purity and quantity of isolated azaphilones was sufficient for further NMR and MS experiments.

MS (ESI in negative mode) and several NMR techniques (^1H , ^{13}C , H,H-COSY, HMBC, HSQC and NOESY) were used for the structure elucidation of both constituents (HPLC: Peak 1 and 2 in Figure 20). For NMR, deuterated

trichloromethane proved unsuitable: it forms traces of hydrochloric acid that lead to relatively rapid substance decomposition (as indicated by a colour change). Substance decomposition was also observed in deuterated acetone. Accordingly, deuterated acetonitrile was chosen as a solvent for NMR.

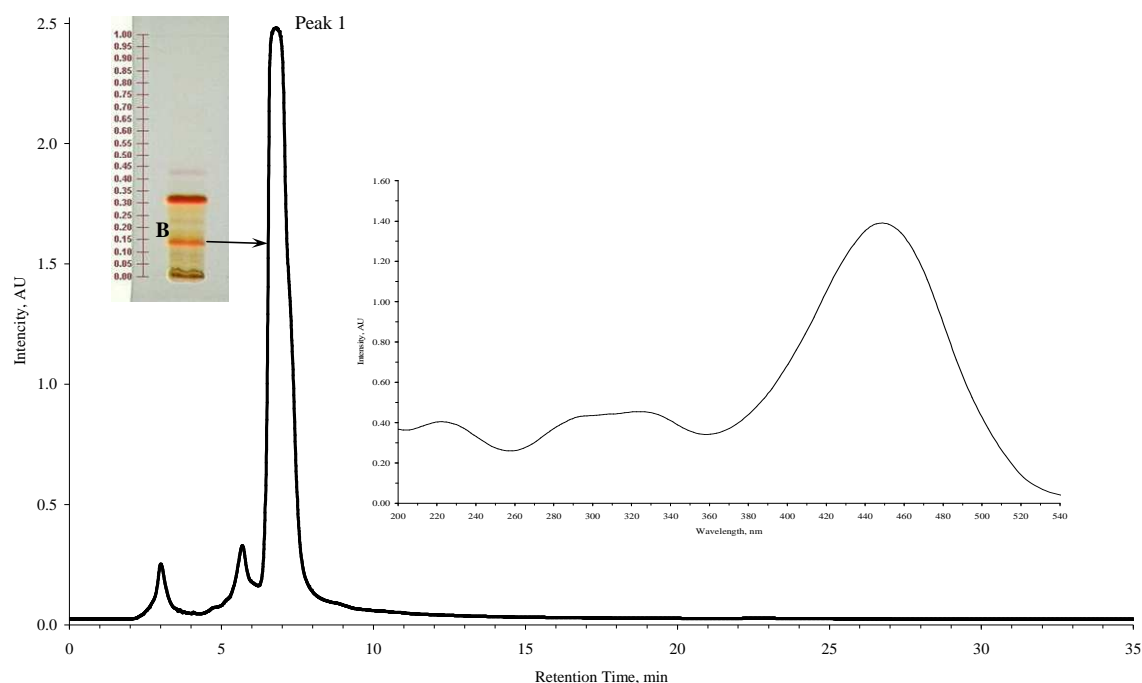


Figure 21: HPLC chromatogram and UV spectrum of Peak 1 isolated from *B. inquinans* acetonitrile extract. Solvent system: acetonitrile/water (7:3); monitoring wavelength: 450 nm.

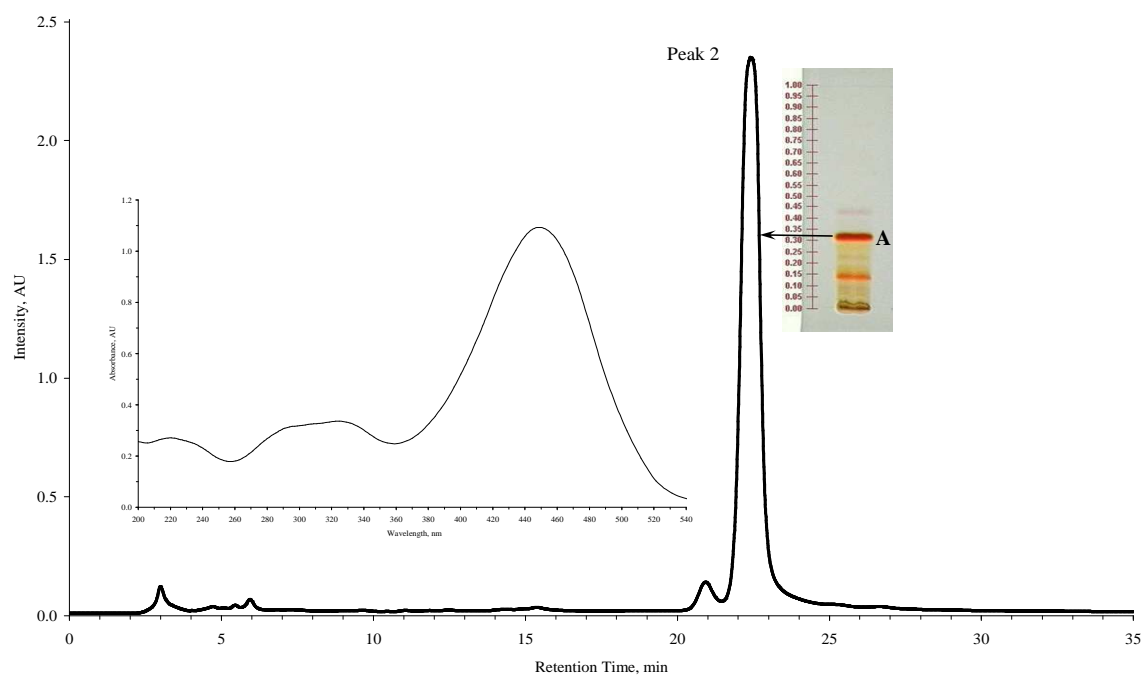
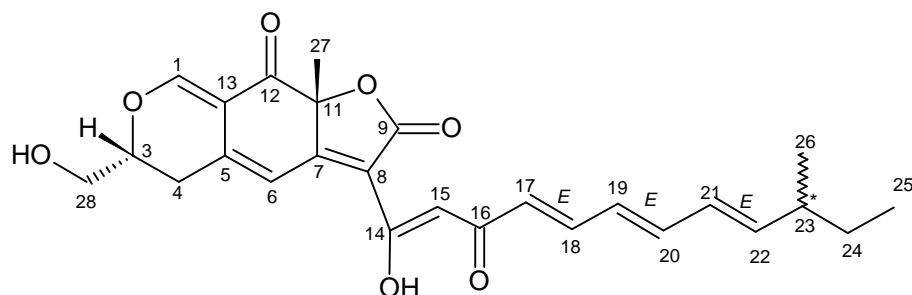


Figure 22: HPLC chromatogram and UV spectrum of Peak 2 isolated from *B. inquinans* acetonitrile extract. Solvent system: acetonitrile/water (7:3); monitoring wavelength: 450 nm.

3.2.5.5 Structure elucidation of bulgarialactone B (HPLC Peak 2)

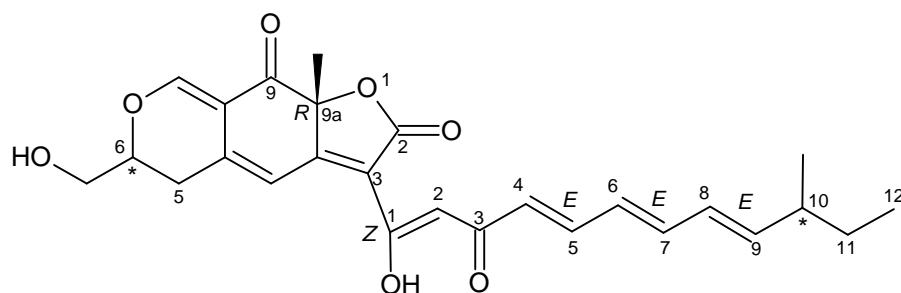


One should note that two numbering systems exist for this compound: Stadler, who first isolated this compound from *B. inquinans*, termed the compound bulgarialactone B and used the numbering given above.

However, the IUPAC name – as generated by ACD/Name – is:

(9aR)-6-(hydroxymethyl)-3-[(1Z,4E,6E,8E)-1-hydroxy-10-methyl-3-oxododeca-1,4,6,8-tetraen-1-yl]-9a-methyl-5,6-dihydro-2H-furo[3,2-g]isochromene-2,9(9aH)-dione

According to this name, the numbering is as follows:



The CAS name as given by SciFinder is:

2H-Furo[3,2-g][2]benzopyran-2,9(9aH)-dione, 5,6-dihydro-6-(hydroxymethyl)-3-[(1Z,4E,6E,8E)-1-hydroxy-10-methyl-3-oxo-1,4,6,8-dodecatetraenyl]-9a-methyl-, (6R,9aR)-rel-(+)- (9CI)

The numbering is identical to IUPAC numbering. The bulgarialactone B CAS number is 180786-03-2.

This compound was isolated from a cold acetonitrile extract of fresh *B. inquinans* fruit bodies by preparative HPLC as described above (Figure 22). About 5 mg of pure substance was gained from 1.5 kg of fungi material. As mentioned above (Section 3.2.3), some specific properties revealed the azaphilone character of this compound. Its chemical composition was determined by high-resolution MS analysis. For ionisation, electrospray (ESI) was used in negative mode with *i*-propanol as the solvent.

As can be seen from Figure 23, this high-resolution negative ESI spectrum shows a characteristic ion series. The mass peak m/z 451 ($C_{26}H_{27}O_7$) represents the quasi-molecular ion $(M-H)^-$, i.e. the molecular mass of this compound is one mass unit larger, namely 452 ($C_{26}H_{28}O_7$). The addition of one methanol molecule gives rise to the association complex $[(M-H)+CH_3OH]^-$ with the formula $C_{27}H_{31}O_8$ and the nominal mass 483 Da. The base peak m/z 497 ($C_{28}H_{33}O_8$) is generated by the addition of one ethanol molecule to the quasi-molecular ion, yielding the association complex $[(M-H)+C_2H_5OH]^-$. Finally, the ion-molecule reaction between the $(M-H)^-$ ion and *i*-propanol leads to the adduct ion $[(M-H)+i-C_3H_7OH]^-$ with the nominal mass 511 Da ($C_{29}H_{36}O_8$).

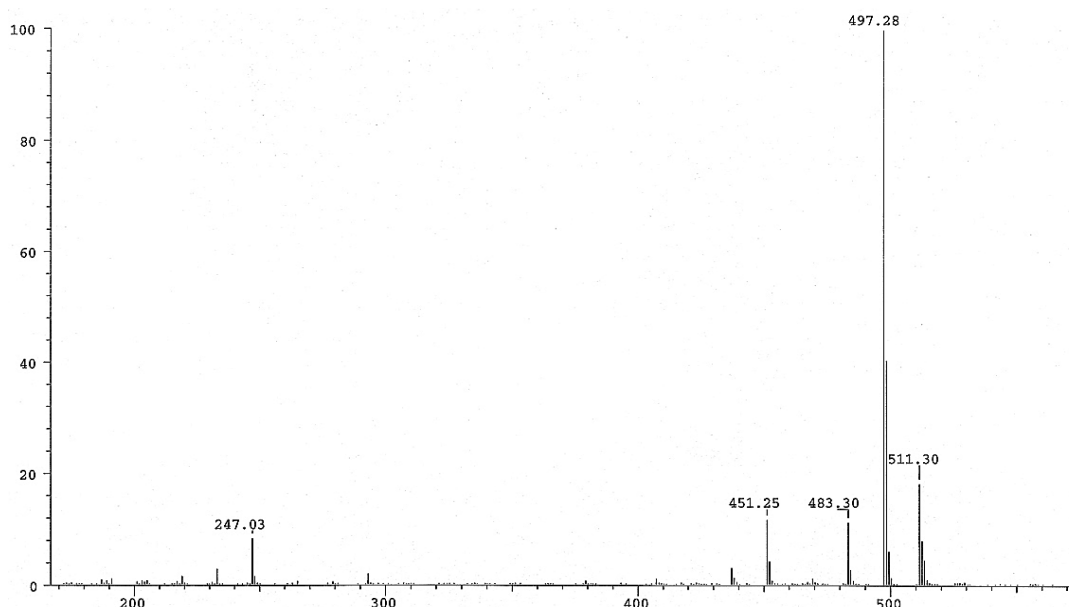


Figure 23: Negative ESI spectrum of HPLC Peak 2 isolated from *B. inquinans* acetonitrile extract. Solvent: *i*-propanol.

When testing the stability of this azaphilone compound in *i*-propanol, it was found to be stable for several hours. However, a repeated MS measurement 16 hours later revealed one new peak at m/z 469 (56% intensity – Figure 24). While an interpretation of this effect is non-trivial, this ion may be explained by the association of water with the quasi-molecular ion, giving rise to the species $[(M-H)+H_2O]^-$ as a result of a slight change in the molecular structure (e.g. rearrangement).

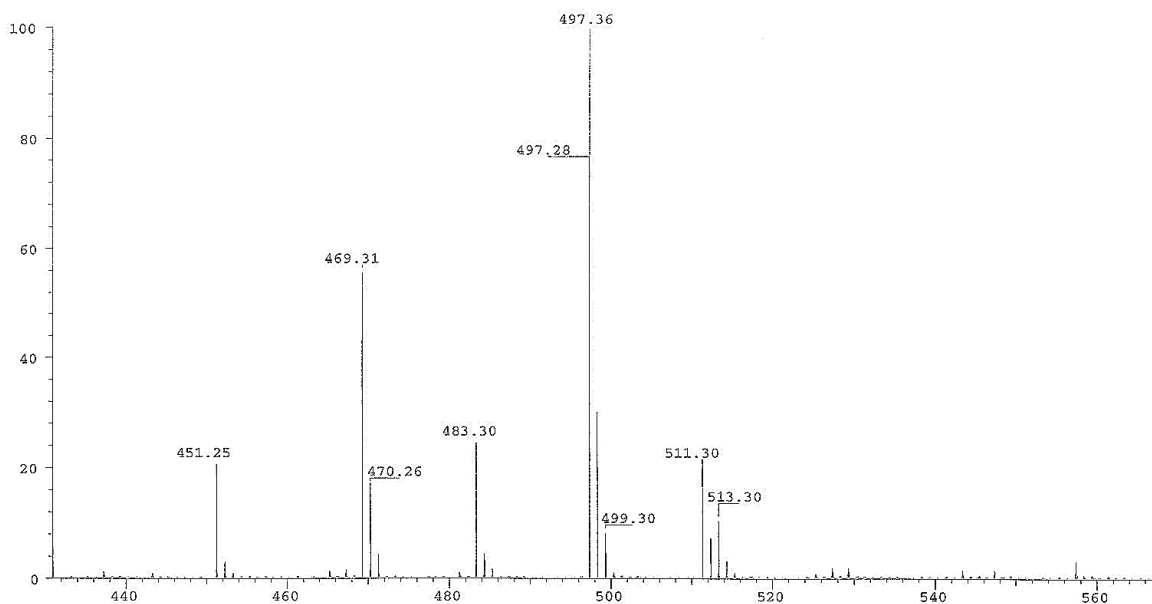


Figure 24: Negative ESI spectrum of HPLC Peak 2 isolated from *B. inquinans* acetonitrile extract measured 16 h later. Solvent: *i*-propanol.

Alternatively, a decomposition process may have started, leading to the formation of a second molecule (quasi-molecular ion $(M_2-H)^-$) showing the base peak m/z 469. This theory is supported by the MS experiment (Figure 25): the preferred solvent for this type of MS experiment is methanol (acetonitrile is unsuited).

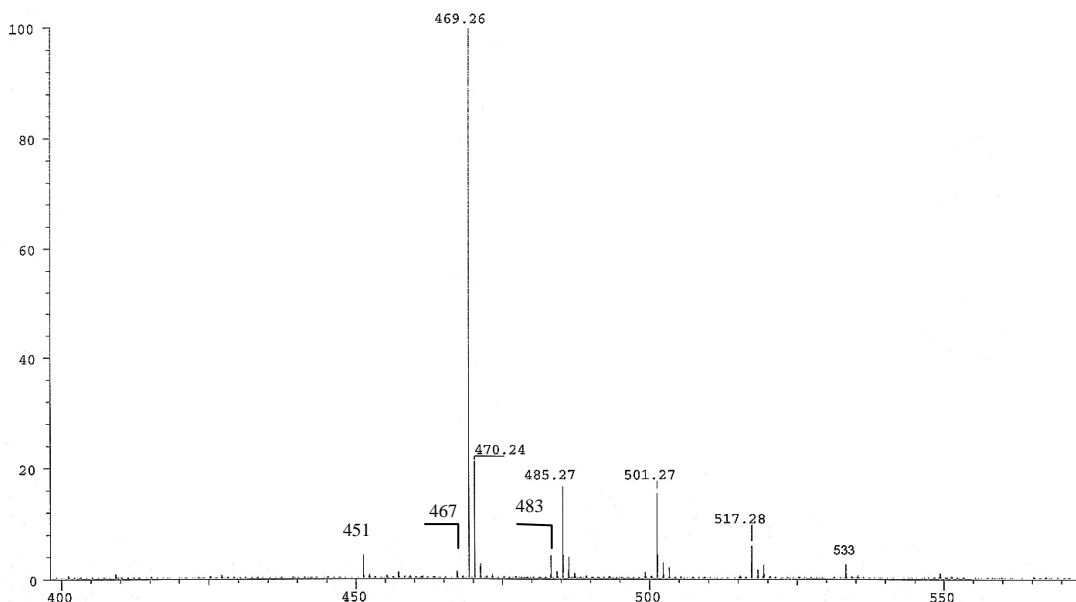


Figure 25: Negative ESI spectrum of HPLC Peak 2 isolated from *B. inquinans* acetonitrile extract. Solvent: methanol.

This negative ESI spectrum not only shows the quasi-molecular ion m/z 451 $[(M-H)]^-$ mentioned above, plus several additional ions (m/z 469 (+H₂O), m/z 483 (+CH₃OH), m/z 501 (+H₂O+CH₃OH) and m/z 533 (+H₂O+2×CH₃OH)), but also a series of ions that could well belong to a second molecule. This theory is also supported by the HPLC measurements, which show the formation of a decomposition product (Figure 19, Peak 4). This second molecule is suspected to possess a quasi-molecular ion at m/z 467 $[(M_2-H)]^-$, which forms the association complexes +H₂O (m/z 485) and +H₂O+CH₃OH (m/z 517). It may therefore be possible that the original azaphilone undergoes a decomposition process, forming a molecule that possesses an additional oxygen function (m/z 467).

As shown above, high-resolution mass spectrometry in negative ion mode (Figure 23) established the chemical formula of compound A (HPLC Peak 2) as C₂₆H₂₈O₇ with a molecular ion $[M-H]^- = 451$. This in turn permits the estimation of the double-bond/ring equivalent (DBE) as equal to 13. NMR data analysis reveals the presence of seven double bonds (C=C) and three C=O groups (Table 4), yielding the simple conclusion that the molecule must contain three rings. Moreover, it is clear that the molecule bears one quaternary olefinic carbon and lacks a terminal olefinic methylene group. Table 4 presents the results of ¹H and ¹³C NMR spectroscopy.

The ¹³C spectrum revealed only 17 C-atoms (Appendix I, Figure 63). However, ten of the 11 missing signals (C-1, C-5, C-7, C-8, C-11, C-12, C-13, C-14, C-16 and C-25) were detected by applying the two-dimensional techniques: HSQC (Figure 27) and HMBC (Appendix I, Figure 64 and Figure 65). Only one C-signal (C-9 at $\delta = 168.1$ ppm) could not be traced; however, its existence was deduced from other data (see text below). From the HSQC spectrum obtained, it was possible to assign associated protons to 14 C-atoms and thus discover their multiplicity.

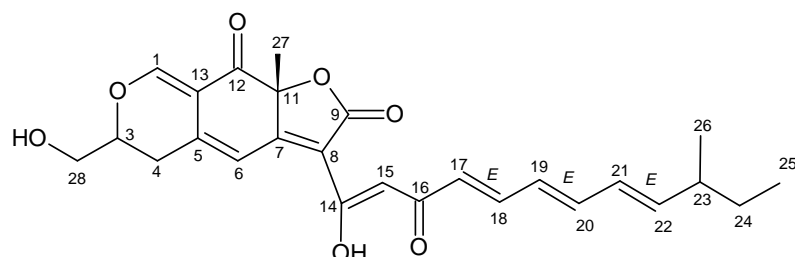
The complete ¹H spectrum (Figure 26) shows the presence of nine protons in the aromatic ($\delta = 6-8$ ppm) and olefinic ($\delta = 4.5-6.5$ ppm) regions; this accords with the ¹³C NMR data. Eleven protons were detected in the aliphatic region ($\delta = 0-2$ ppm). Six protons were found in the range from $\delta = 2.5$ ppm to $\delta = 4.3$ ppm, indicating adjacent heteroatoms or double bonds. The region from $\delta = 0.5$ ppm to $\delta =$

2.5 ppm comprises three methyl groups (H-25, H-26 and H-27) and a CH₂- group (H-24) (see expansions in Figure 26). Overall, 26 protons were identified in the ¹H NMR spectrum, i.e. two protons are missing with respect to the molecular formula. While one proton was indirectly detectable with H,H-COSY, the other was outside the measured range. At this stage, the NMR data obtained for compound A (HPLC Peak 2) were compared to the literature and were found to be congruent with the results published by Stadler *et al* [58] for a compound named bulgarialactone B, isolated from both fruiting bodies and cell cultures of *B. inquinans*.

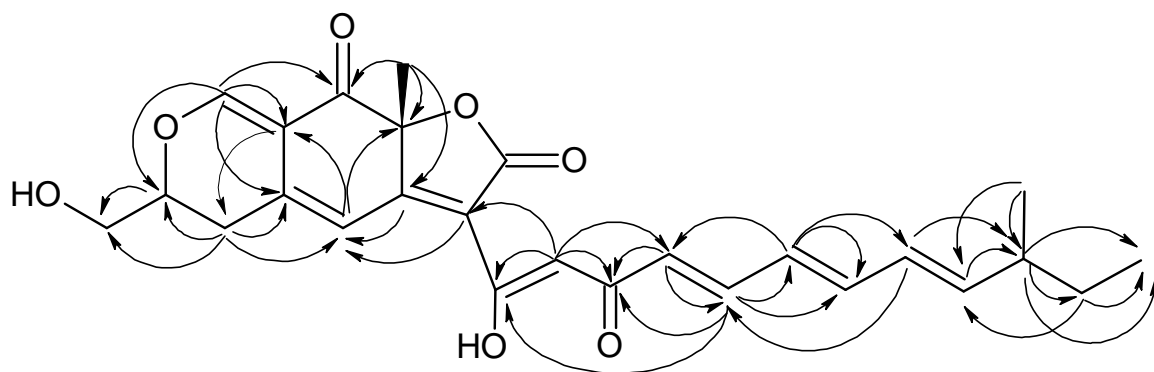
C-atom	Structural element	¹³ C NMR (CD ₃ CN) 100.13 MHz, ppm	Stadler ¹³ C NMR (CDCl ₃), ppm	¹ H NMR (CD ₃ CN) by 400.13 MHz, ppm	H,H coupling constants, Hz	Stadler ¹ H NMR (CDCl ₃), ppm	Stadler H,H coupling constants, Hz
25	—CH ₃	11.1 <i>q</i>	11.7	3H, 0.86 <i>t</i>	³ J _{H-25, H-24} = 7.43	0.88 <i>t</i>	7.3
26	—CH ₃	18.7 <i>q</i>	19.7	3H, 1.01 <i>d</i>	³ J _{H-26, H-23} = 6.75	1.03 <i>d</i>	6.6
27	—CH ₃	26.9 <i>q</i>	27.8	3H, 1.71 <i>s</i>		1.75 <i>s</i>	
4	—CH ₂ —	28.6 <i>t</i>	29.3	Ha, 2.80 <i>ddd</i>	² J _{H-4a, H-4b} = 17.2 ³ J _{H-4a, H-3} = 10.9 ⁴ J _{H-4a, H-6} = 1.5	2.89 <i>ddd</i>	1.5, 11.5, 17.2
				Hb, 2.86 <i>dd</i>	² J _{H-4b, H-4a} = 17.2 ³ J _{H-4b, H-3} = 3.7	2.81 <i>dd</i>	3.5, 17.2
24	—CH ₂ —	28.9 <i>t</i>	29.5	2H, 1.36 <i>m</i> *		1.37 <i>dq</i>	7.3, 7.3
23	>CH—	38.3 <i>d</i>	38.8	1H, 2.15 <i>s</i> *		2.16 <i>dtq</i>	7.8, 7.3, 6.6
28	—CH ₂ —	62.0 <i>t</i>	63.8	H _a , 3.69 <i>m</i> *		3.97 <i>dd</i>	3.5, 12.2
				H _b , 3.78 <i>m</i> *		3.85 <i>dd</i>	5.4, 12.2
	—OH			1H, 3.18 <i>t</i>	³ J _{OH-28, H-28} = 5.9	3.5 <i>s</i>	
3	>CH—	79.3 <i>d</i>	79.0	1H, 4.41 <i>m</i>		4.39 <i>m</i>	
11	>C<	86.3 <i>s</i>	86.3	—			
15	=CH—	99.9 <i>d</i>	100.9	1H, 6.75 <i>s</i>		6.80 <i>s</i>	
6	=CH—	111.7 <i>d</i>	113.4	1H, 7.07 <i>s</i>		7.17 <i>brs</i>	
13	=C<	111.9 <i>s</i>	112.3	—			
8	=C<	113.4 <i>s</i>	115.2	—			
17	=CH—	126.1 <i>d</i>	126.5	1H, 6.23 <i>d</i>	³ J _{H-17, H-18} = 15.0	6.11 <i>d</i>	15.1
21	=CH—	128.5 <i>d</i>	128.5	1H, 6.23 <i>dd</i> *	³ J _{H-21, H-20} = 11.4 ³ J _{H-21, H-22} = 15.1	6.14 <i>dd</i>	10.7 15.2
19	=CH—	128.8 <i>d</i>	128.8	1H, 6.36 <i>dd</i>	³ J _{H-19, H-18} = 11.4 ³ J _{H-19, H-20} = 15.1	6.27 <i>dd</i>	11.3 14.8
20	=CH—	141.5 <i>d</i>	142.3	1H, 7.33 <i>dd</i>	³ J _{H-20, H-21} = 11.4 ³ J _{H-20, H-19} = 15.1	6.59 <i>dd</i>	10.7 14.8
18	=CH—	141.9 <i>d</i>	142.4	1H, 6.69 <i>dd</i> *	³ J _{H-18, H-19} = 11.4 ³ J _{H-18, H-17} = 15.0	7.34 <i>dd</i>	11.3 15.1
5	=C<	143.9 <i>s</i>	140.8	—			
22	=CH—	146.3 <i>d</i>	146.9	1H, 5.91 <i>dd</i>	³ J _{H-22, H-23} = 8.0 ³ J _{H-22, H-21} = 15.1	5.87 <i>dd</i>	7.8 15.2
1	=CH—	159.9 <i>d</i>	158.9	1H, 7.86 <i>s</i>		7.85 <i>s</i>	
9	>C=O	—	168.1				
7	=C<	170.2 <i>s</i>	168.2	—			
14	=C<	180.1 <i>s</i>	177.5	—			
	—OH			—		16.0 <i>brs</i>	
16	>C=O	183.3 <i>s</i>	185.0	—			
12	>C=O	190.3 <i>s</i>	190.0	—			

Table 4: NMR data (¹³C and ¹H NMR) of the azaphilone (HPLC Peak 2) isolated from a cold acetonitrile extract of *Bulgaria*, compared with bulgarialactone B data from Stadler *et al* [58]. For details, see text (* indicates overlaid signals or multiplets that could not be analysed).

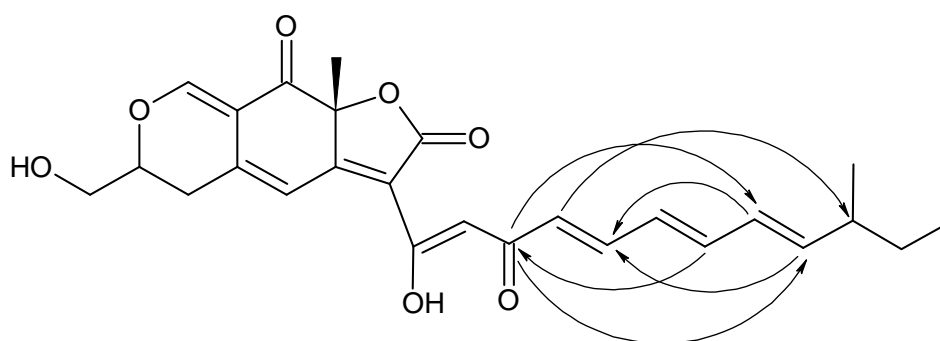
This fact of congruence, together with the azaphilone characteristics shown by compound A, its MS data and the matching R_f value (TLC plates), presented strong evidence for the equivalence of this compound with bulgarialactone B. This equivalence was confirmed by a detailed analysis of the couplings in H,H-COSY and HMBC, as shown below:



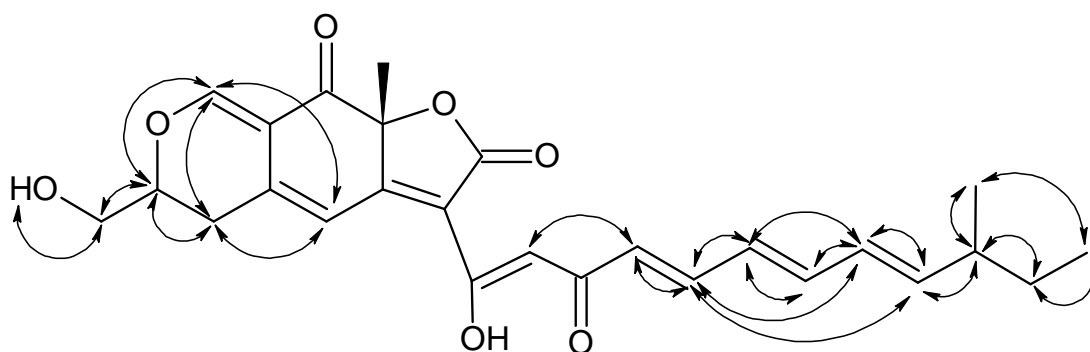
HMBC (1):



HMBC (2):



H,H-COSY:



Furthermore, a number of interesting aspects deserve mention.

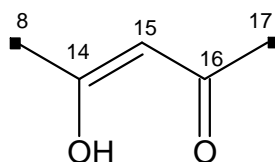
The chemical shifts for C-1 (159.8 ppm) and C-3 (79.3 ppm), together with their respective J_{CH} coupling constants 7.87 ppm and 4.41 ppm, made it possible to configure the partial structure to include a heteroatom (oxygen) between C-1 and C-3 [82].

The presence of a free hydroxyl group at C-28 is proved by its representative chemical shift, namely $\delta = 62.0$ ppm [82]. The presence of this OH- group is further confirmed by the couplings observed in H,H-COSY between proton H-28 ($\delta = 3.73$ ppm) and the proton at $\delta = 3.18$ ppm (OH- group).

The relative stereochemistry of the CH₃- group (C-27 at 26.9 ppm) was established by NOESY correlation with proton H-3.

It was impossible to trace the C-9 atom and any of its couplings. However, evidence for the existence and position of this carbonyl function received strong support from a consideration of its molecular formula, since only one C-atom and two O-atoms remained. It was therefore possible to determine the partial structure of lactone by the characteristic chemical shifts of C-8 (113.4 ppm) and C-11 (86.3 ppm) atoms: the single remaining possibility was to draw a lactone carbonyl group with C-9 between C-8 and C-11 [82].

In contrast to Stadler, direct detection of the C-14 hydroxyl group's proton was not possible, but its existence was nonetheless proven indirectly by applying the molecular formula and considering the C-14 chemical shift (180.01 ppm). Typical chemical shift values of C-15 (99.9 ppm) and C-16 (183.3 ppm) also suggested the partial structure [82]:



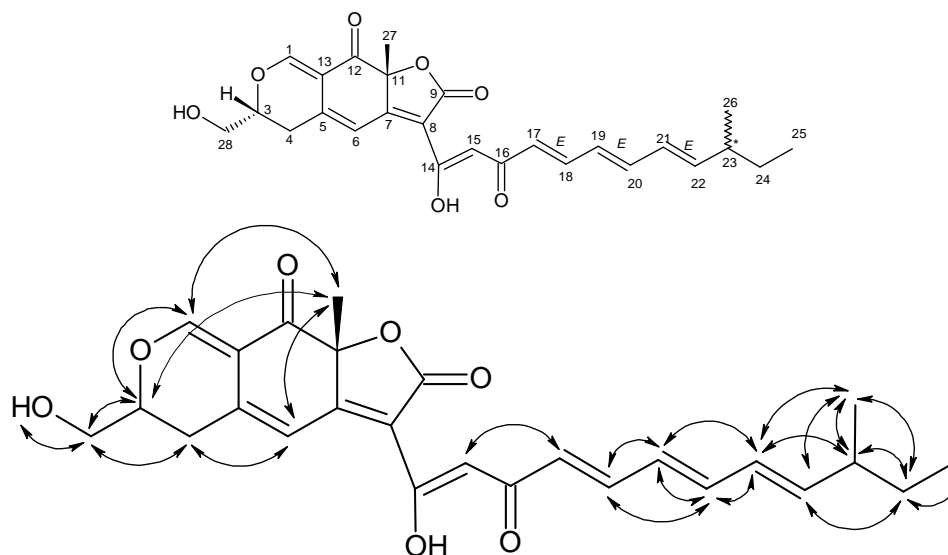
Since the current measurements did not detect the C-14 hydroxyl function's proton, it proved difficult to distinguish between two possible tautomeric structures:



However, since it had been proven that the isolated constituent is also bulgarialactone B, whose structure had been elucidated by Stadler [58], it proved possible to apply these data in order to confirm the structure, i.e. to unequivocally assign the δ -values 183.3 ppm and 180.1 ppm to C-16 and C-14, respectively. A comparison of the HMBC couplings and their intensity also supported the presence of the tautomeric form 1) above.

HSQC was also unable to assign the C-23 proton directly (Figure 27). The position of proton H-23 ($\delta = 2.15$ ppm) in the molecule was established from its coupling with the following protons: H-26 ($\delta = 1.01$ ppm), H-24 ($\delta = 1.36$ ppm) and H-22 ($\delta = 5.90$ ppm) in H,H-COSY. However, it was not possible to determine the relative configuration of C-23 by spectroscopic methods and the limited amount of the substance available excluded the preparation of suitable derivatives; the same holds true for the C-3 atom, whose configuration remained undetermined.

By considering the NOESY spectrum analysis and characteristic coupling constant values of ${}^3J_{\text{H-17, H-18}} = 15.0$ Hz, ${}^3J_{\text{H-19, H-20}} = 15.1$ Hz and ${}^3J_{\text{H-21, H-22}} = 15.1$ Hz, it proved possible to establish a trans-configuration for double bonds between the C-17/C-18, C-19/C-20 and C-21/C-22 protons:



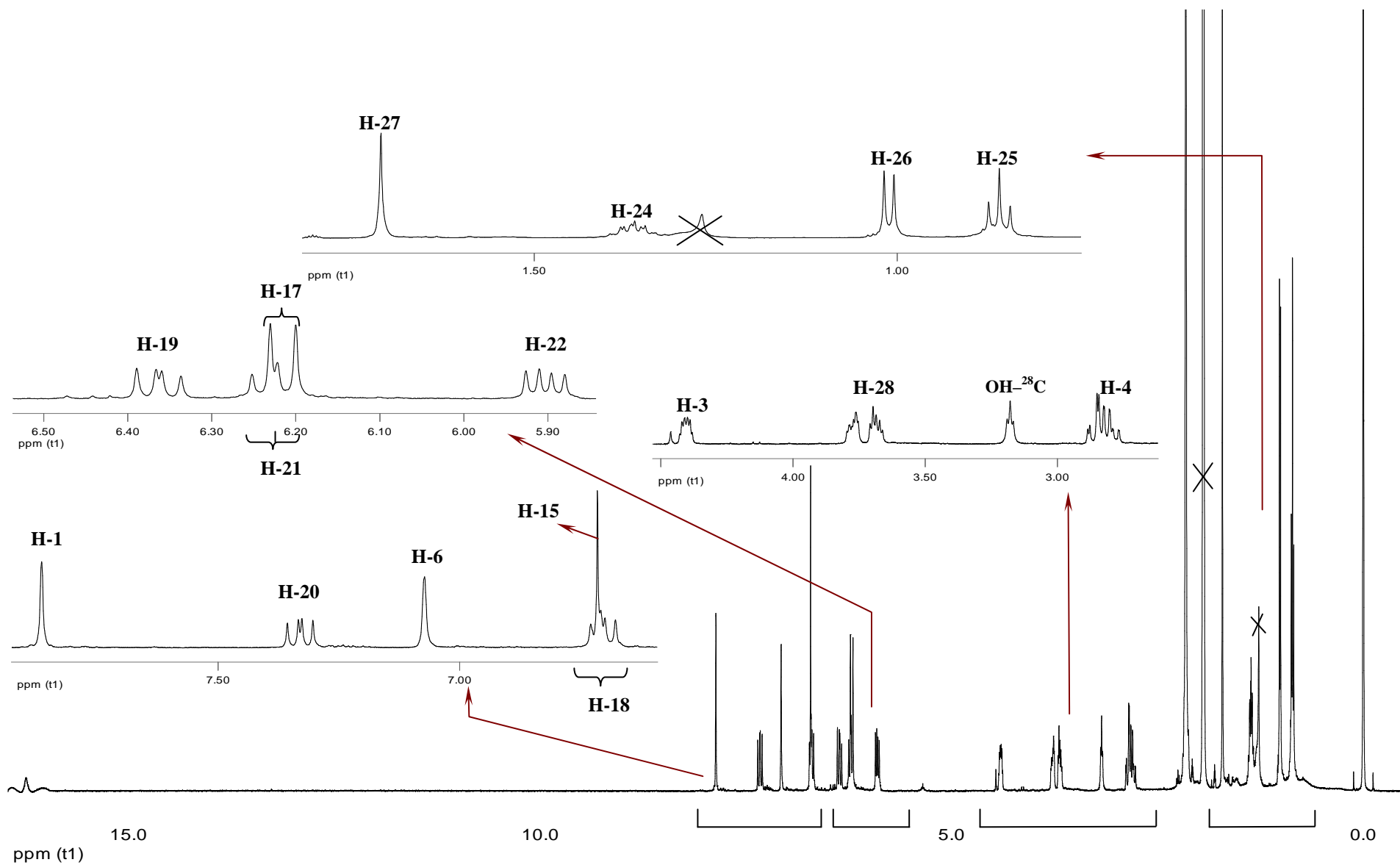


Figure 26: ^1H NMR spectrum of bulgarialactone B (HPLC Peak 2). Impurity signals are struck through.

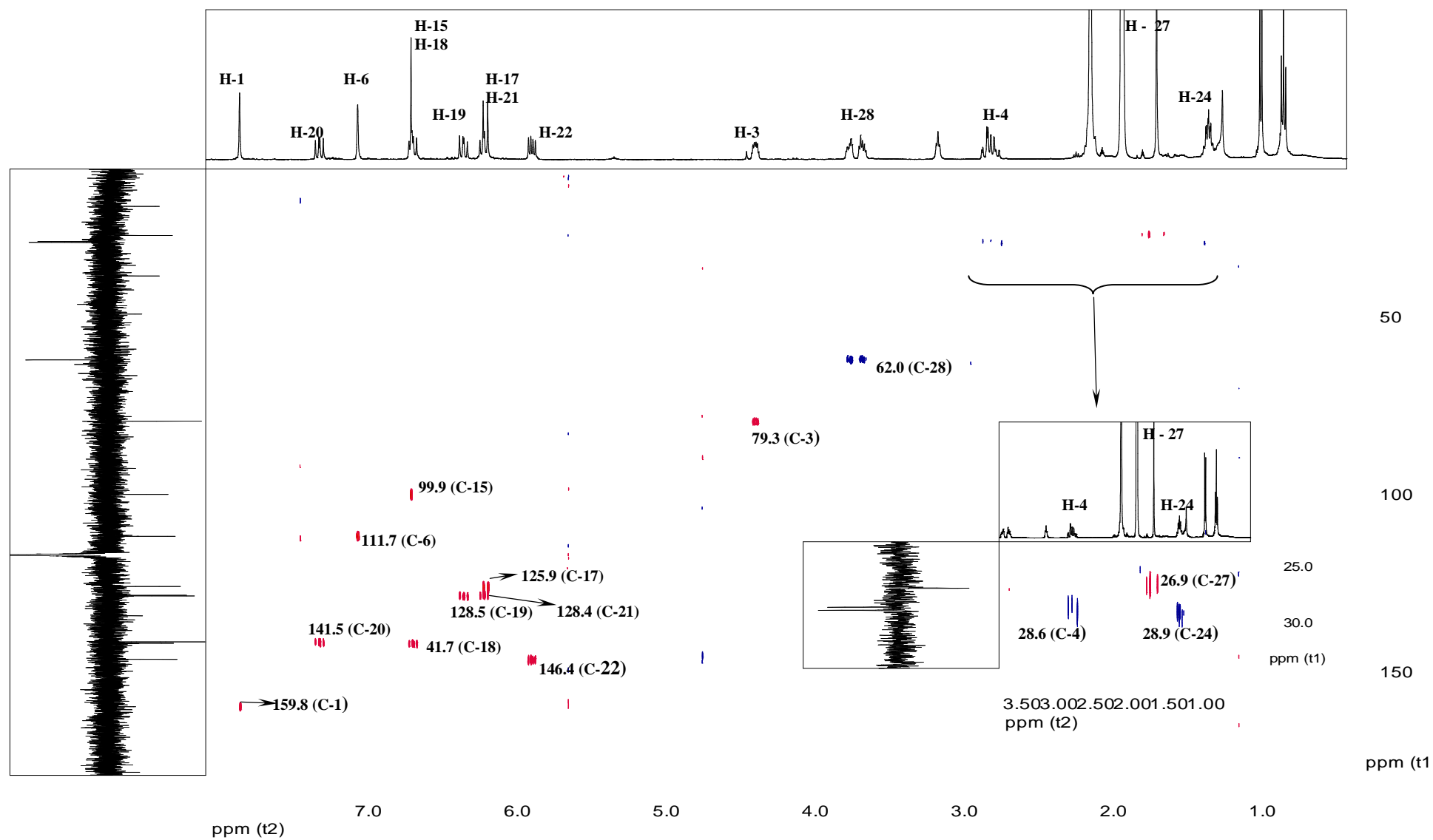
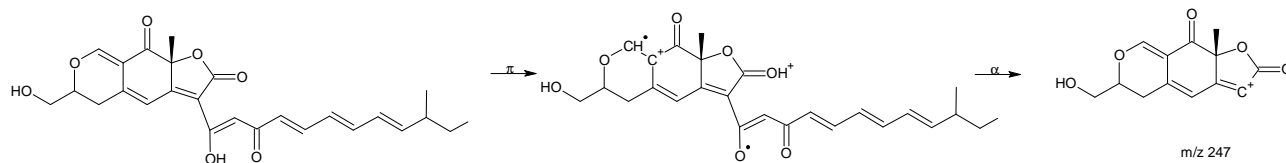


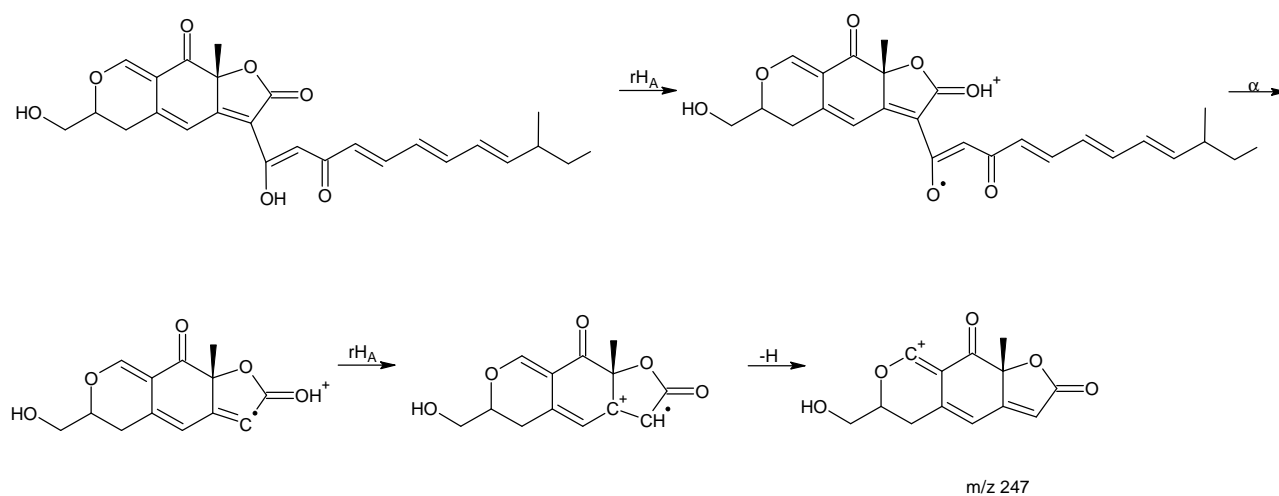
Figure 27: HSQC NMR spectrum of bulgarialactone B (HPLC Peak 2).

Lastly, considering the fragmentation pathway of the interesting small peak m/z 247 (see EI mass spectrum, Figure 23), which is in good accordance with the structure of bulgarialactone B, several suggestions were offered by the Mass Frontier spectral interpretation software application. Below, two plausible suggestions are selected:

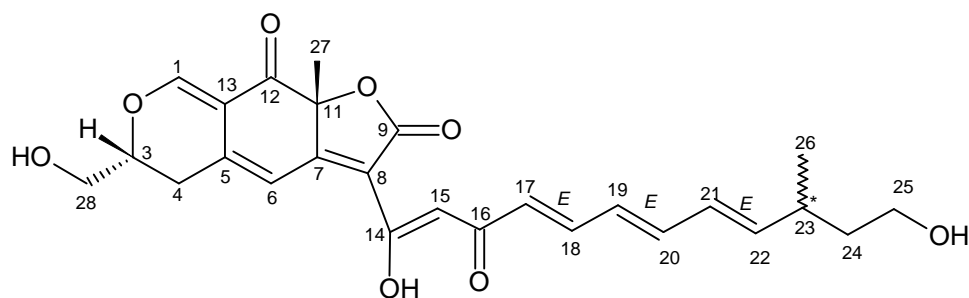
1)



2)



3.2.5.6 Structure elucidation of bulgarialactone D (HPLC Peak 1)

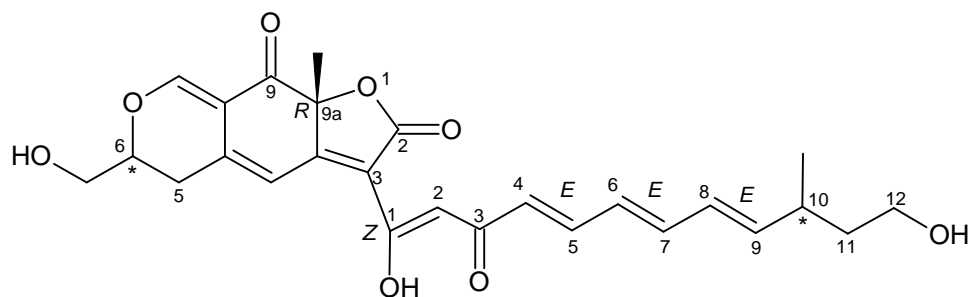


The trivial name bulgarialactone D³ is suggested for this new constituent, isolated from *Bulgaria* fruit bodies: the same approach is taken to the enumeration of atoms as for bulgarialactone B.

The IUPAC name as generated by ACD/Name is:

(9a*R*)-3-[(1*Z*,4*E*,6*E*,8*E*)-1,12-dihydroxy-10-methyl-3-oxododeca-1,4,6,8-tetraen-1-yl]-6-(hydroxymethyl)-9a-methyl-5,6-dihydro-2*H*-furo[3,2-*g*]isochromene-2,9(9a*H*)-dione

The suggested numbering is as follows:



As with bulgarialactone B (HPLC Peak 2, Figure 20), this compound was isolated from a cold acetonitrile extract of fresh *B. inquinans* fruit bodies by preparative HPLC (Peak 1), as previously described. About 5 mg of pure substance was gained from 1.5 kg of fungi material.

As mentioned above (Section 3.2.3), some specific properties indicated the azaphilone character of this compound. Its elemental composition was determined by high-resolution MS analysis. For ionisation, electrospray (ESI) was used in negative mode with *i*-propanol as the solvent. High-resolution MS of negative ions established the chemical formula of this substance as C₂₆H₂₈O₈ with a molecular ion [M-H]⁻ = 467 Da.

³ As mentioned in Chapter 3.2.3, since the literature names two different substances as “bulgarialactone D”, the present work will refer to the bulgarialactone isolated by Musso *et al* [83] as bulgarialactone D_(Musso).

The ESI spectrum presented in Figure 28 shows a characteristic ion series, which can be interpreted as follows: the mass peak m/z 467 ($C_{26}H_{27}O_8$) represents the quasi-molecular ion $(M-H)^-$, i.e. the molecular mass of this compound is one mass unit larger, namely 468 Da ($C_{26}H_{28}O_8$). The ion with a nominal mass m/z 499 can be explained by the addition of one methanol molecule, forming the association complex $[(M-H)+CH_3OH]^-$ with the molecular formula $C_{27}H_{31}O_9$. Analogously, the addition of one ethanol molecule $[(M-H)+C_2H_5OH]^-$ leads to the base peak (m/z 513) with the molecular formula $C_{28}H_{33}O_9$. Finally, the ion-molecule reaction between the $(M-H)^-$ ion and *i*-propanol leads to the adduct ion $[(M-H)+i-C_3H_7OH]^-$ with the nominal mass 527 Da ($C_{29}H_{36}O_9$).

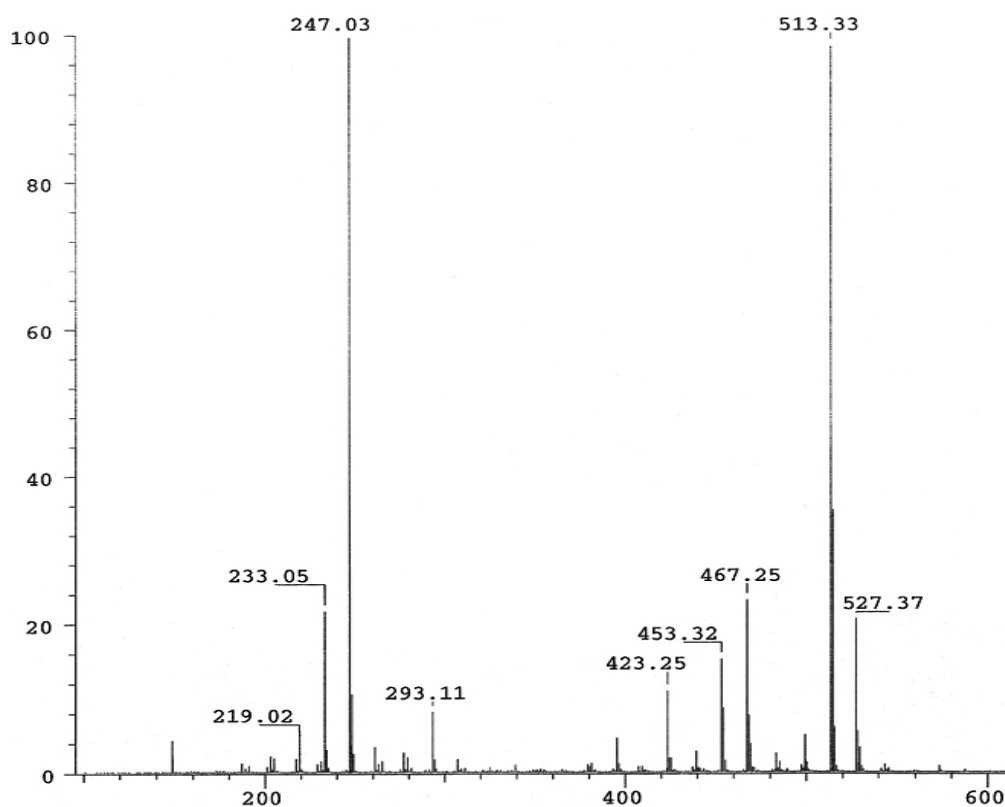


Figure 28: Negative ESI spectrum of HPLC Peak 1 isolated from *B. inquinans* acetonitrile extract. Solvent: *i*-propanol. For details, see text.

The chemical formula suggested for the molecular ion $C_{26}H_{28}O_8$ permitted the estimation of the double-bond/ring equivalent (DBE) as equal to 13. Analysis of ^{13}C NMR and HSQC data revealed the presence of seven double bonds ($C=C$) and three $C=O$ groups. The molecule was therefore proven to have three rings.

The results of NMR analysis are summarised in Table 5 overleaf.

C-atom	Structural element	¹³ C-NMR (CD ₃ CN) 100.13 MHz, ppm	Bulgarialactone B	¹ H-NMR (CD ₃ CN) by 400.13 MHz, ppm	H,H-coupling constants, Hz	Bulgarialactone B	H,H-coupling constants, Hz
26	—CH ₃	19.3 <i>q</i>	18.7 <i>q</i>	3H, 1.02 <i>d</i>	³ J _{H-26, H-23} = 6.7	3H, 1.01 <i>d</i>	³ J _{H-26, H-23} = 6.75
27	—CH ₃	27.1 <i>q</i>	26.9 <i>q</i>	3H, 1.71 <i>s</i>		3H, 1.71 <i>s</i>	
4	—CH ₂ —	28.7 <i>t</i>	28.6 <i>t</i>	Ha, 2.79 <i>ddd</i>	² J _{H-4a, H-4b} = 17.3 ³ J _{H-4a, H-3} = 10.9 ⁴ J _{H-4a, H-6} = 1.4	Ha, 2.80 <i>ddd</i>	² J _{H-4a, H-4b} = 17.2 ³ J _{H-4a, H-3} = 10.9 ⁴ J _{H-4a, H-6} = 1.5
				Hb, 2.85 <i>dd</i>	² J _{H-4b, H-4a} = 17.3 ³ J _{H-4b, H-3} = 3.9	Hb, 2.86 <i>dd</i>	² J _{H-4b, H-4a} = 17.2 ³ J _{H-4b, H-3} = 3.7
23	>CH—	33.5 <i>d</i>	38.3 <i>d</i>	1H, 2.41 <i>m</i>*	³ J _{H-23, H-22} = 7.9 ³ J _{H-23, H-24} = 13.7 ³ J _{H-23, H-26} = 6.7	1H, 2.15 <i>s</i> *	
24	—CH ₂ —	39.1 <i>t</i>	28.9 <i>t</i>	2H, 1.52 <i>dd</i>	³ J _{H-24, H-23} = 13.7 ³ J _{H-24, H-25} = 6.8	2H, 1.36 <i>m</i> *	
25	—CH ₂ —	59.4 <i>t</i>	11.1 <i>q</i>	2H, 3.48 <i>m</i>*	³ J _{H-25, H-24} = 6.8	3H, 0.86 <i>t</i>	³ J _{H-25, H-24} = 7.43
28	—CH ₂ —	62.1 <i>t</i>	62.0 <i>t</i>	Ha, 3.69 <i>dd</i>	² J _{H-28a, H-28b} = 12.4 ³ J _{H-28a, H-3} = 3.4	Ha, 3.69 <i>m</i> *	
				Hb, 3.77 <i>dd</i>	² J _{H-28b, H-28a} = 12.4 ³ J _{H-4b, H-3} = 5.3	Hb, 3.78 <i>m</i> *	
	—OH			—		1H, 3.18 <i>t</i>	³ J _{OH-28, H-28} = 5.9
3	>CH—	79.4 <i>d</i>	79.3 <i>d</i>	1H, 4.40 <i>m</i>		1H, 4.41 <i>m</i>	
11	>C<	86.6 <i>s</i>	86.3 <i>s</i>	—		—	
15	=CH—	100.1 <i>d</i>	99.9 <i>d</i>	1H, 6.71 <i>s</i>		1H 6.75 <i>s</i>	
6	=CH—	111.7 <i>s</i>	111.7 <i>d</i>	1H, 7.07 <i>s</i>		1H, 7.07 <i>s</i>	
13	=C<	111.9 <i>d</i>	111.9 <i>s</i>	—		—	
8	=C<	113.7 <i>s</i>	113.4 <i>s</i>	—		—	
17	=CH—	125.9 <i>d</i>	126.1 <i>d</i>	1H, 6.21 <i>d</i>	³ J _{H-17, H-18} = 15.0	1H, 6.23 <i>d</i>	³ J _{H-17, H-18} = 15.0
21	=CH—	128.4 <i>d</i>	128.5 <i>d</i>	1H, 6.22 <i>dd</i>*	³ J _{H-21, H-20} = 11.0 ³ J _{H-21, H-22} = 15.1	1H, 6.23 <i>dd</i> *	³ J _{H-21, H-20} = 11.4 ³ J _{H-21, H-22} = 15.1
19	=CH—	128.5 <i>d</i>	128.8 <i>d</i>	1H, 6.36 <i>dd</i>	³ J _{H-19, H-18} = 10.7 ³ J _{H-19, H-20} = 15.1	1H, 6.36 <i>dd</i>	³ J _{H-19, H-18} = 11.4 ³ J _{H-19, H-20} = 15.1
20	=CH—	141.5 <i>d</i>	141.5 <i>d</i>	1H, 7.33 <i>dd</i>	³ J _{H-20, H-21} = 11.4 ³ J _{H-20, H-19} = 15.1	1H, 7.33 <i>dd</i>	³ J _{H-20, H-21} = 11.4 ³ J _{H-20, H-19} = 15.1
18	=CH—	141.7 <i>d</i>	141.9 <i>d</i>	1H, 6.69 <i>dd</i>*	³ J _{H-18, H-19} = 10.7 ³ J _{H-18, H-17} = 15.0	1H, 6.69 <i>dd</i> *	³ J _{H-18, H-19} = 11.4 ³ J _{H-18, H-17} = 15.0
5	=C<	143.9 <i>d</i>	143.9 <i>s</i>	—		—	
22	=CH—	146.4 <i>d</i>	146.3 <i>d</i>	1H, 5.90 <i>dd</i>	³ J _{H-22, H-23} = 7.9 ³ J _{H-22, H-21} = 15.1	1H, 5.91 <i>dd</i>	³ J _{H-22, H-23} = 8.0 ³ J _{H-22, H-21} = 15.1
1	=CH—	159.80 <i>d</i>	159.9 <i>d</i>	1H, 7.87 <i>s</i>		1H, 7.86 <i>s</i>	
7	=C<	170.0 <i>s</i>	170.2 <i>s</i>	—		—	
14	=C<	181.5 <i>s</i>	180.1 <i>s</i>	—		—	
	—OH			—		—	
16	>C=O	183.3 <i>s</i>	183.3 <i>s</i>	—		—	
12	>C=O	190.3 <i>s</i>	190.3 <i>s</i>	—		—	

Table 5: NMR data (¹³C and ¹H-NMR) of the azaphilone (HPLC Peak 1) isolated from a cold acetonitrile extract of *Bulgaria*, compared with Bulgarialactone B data. For details, see text (* indicates overlaid signals or multiplets which could not be analysed; signals with strong deviations are highlighted in light blue.)

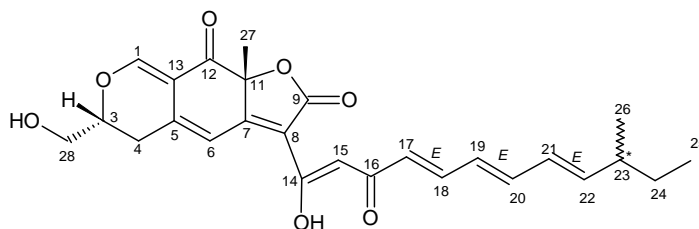
The ^{13}C NMR spectrum revealed 21 carbon signals (Appendix I, Figure 66): their multiplicity was established from HSQC spectrum data (Figure 31). Five C atoms were therefore absent: the positions of four atoms (C-8, C-11, C-12 and C-14) were identifiable from HMBC spectrum data (Figure 67 and Figure 68). Only one carbon atom (C-9) remained undetected.

The complete ^1H spectrum (Figure 29) shows the presence of nine protons in the aromatic ($\delta = 6\text{--}8$ ppm) and olefinic ($\delta = 4.5\text{--}6.5$ ppm) regions. Eight protons were found in the aliphatic region ($\delta = 0\text{--}2$ ppm). A further eight protons were located in the region between $\delta = 2.2$ and 4.5 ppm. The proton of the hydroxyl group at C-28 remained hidden. The proton of the hydroxyl function (H-14) remained undetected since it was out of the measuring range. The region from $\delta = 0.8$ to 2.2 ppm includes two methyl groups (H-26 and H-27) and a $\text{CH}_2\text{—}$ group (H-23).

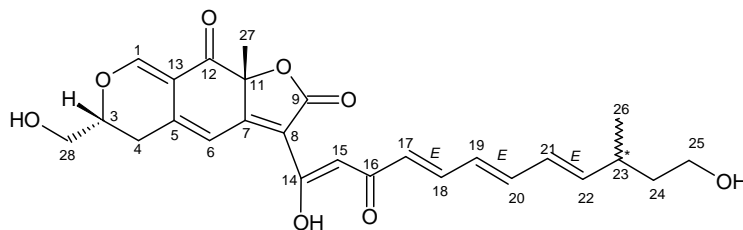
A comparison of the NMR data of this compound with those of bulgarialactone B (Table 4 and Table 5) reveals a strong structural similarity between these two constituents, indicated by a high degree of congruence in the ^{13}C and ^1H NMR spectra. However, on evaluating the results obtained, it became clear that this azaphilone must be a new bulgarialactone, since its mass did not match the masses of any bulgarialactones described in the literature to date, namely: bulgarialactone A (436 Da), bulgarialactone B (452 Da) and bulgarialactone C (434 Da) [58]. It was therefore decided to name this new compound bulgarialactone D.

Strong deviations from bulgarialactone B can only be observed in the ^{13}C NMR spectrum, namely for the signals C-23 (33.5 ppm for bulgarialactone D and 38.3 ppm for bulgarialactone B), C-25 (39.1 for bulgarialactone D and 28.9 ppm for bulgarialactone B) and C-25 (59.4 for bulgarialactone D and 11.1 ppm for bulgarialactone B; for data, see highlighted region in Table 5).

Concerning the proton spectrum, distinct changes were registered in comparison with bulgarialactone B in the pattern of H-23 ($\delta = 2.41$ ppm), H-24 ($\delta = 1.52$ ppm) and H-25 ($\delta = 3.48$ ppm; for data, see Figure 30 and highlighted region in Table 5):



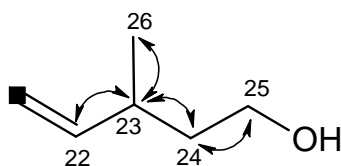
bulgarialactone B



bulgarialactone D

The great similarity between the NMR spectra of these compounds means the ensuing detailed discussion can be restricted to only those signal groups that show deviation.

The chemical shift value of the C-25 atom ($\delta = 59.4$ ppm) indicates the presence of oxygen, which NMR data places within a hydroxyl group. The C-25 methylene group indicates the absence of branching, which reveals a lack of further CH_3 — groups at C-25. The carbon C-25 atom possesses two protons (H-25, $\delta = 3.48$ ppm), which appear as a symmetric multiplet in the ^1H NMR spectrum (Figure 29). These protons show a coupling in the H,H-COSY spectrum with the protons H-24 (1.52 ppm) and H-23 (2.41 ppm). The latter shifts also confirm the presence of oxygen. The same holds true for the C-24 atom ($\delta = 39.1$ ppm). The protons of this C-atom (H-24) show a double doublet ($^3J_{\text{H-24, H-25}} = 6.8$ Hz; $^3J_{\text{H-24, H-23}} = 13.7$ Hz). The signal of the adjacent proton H-23 is split into a complex multiplet, the coupling of which could be analysed by considering the splitting of the adjacent proton signals H-22 and H-26. The following coupling constants were determined: $^3J_{\text{H-23, H-22}} = 7.9$ Hz and $^3J_{\text{H-23, H-26}} = 6.7$ Hz. These couplings, together with $^3J_{\text{H-23, H-24}} = 13.7$ Hz, were approximately confirmed by the automated coupling constants analyser provided by the MestRec software application.



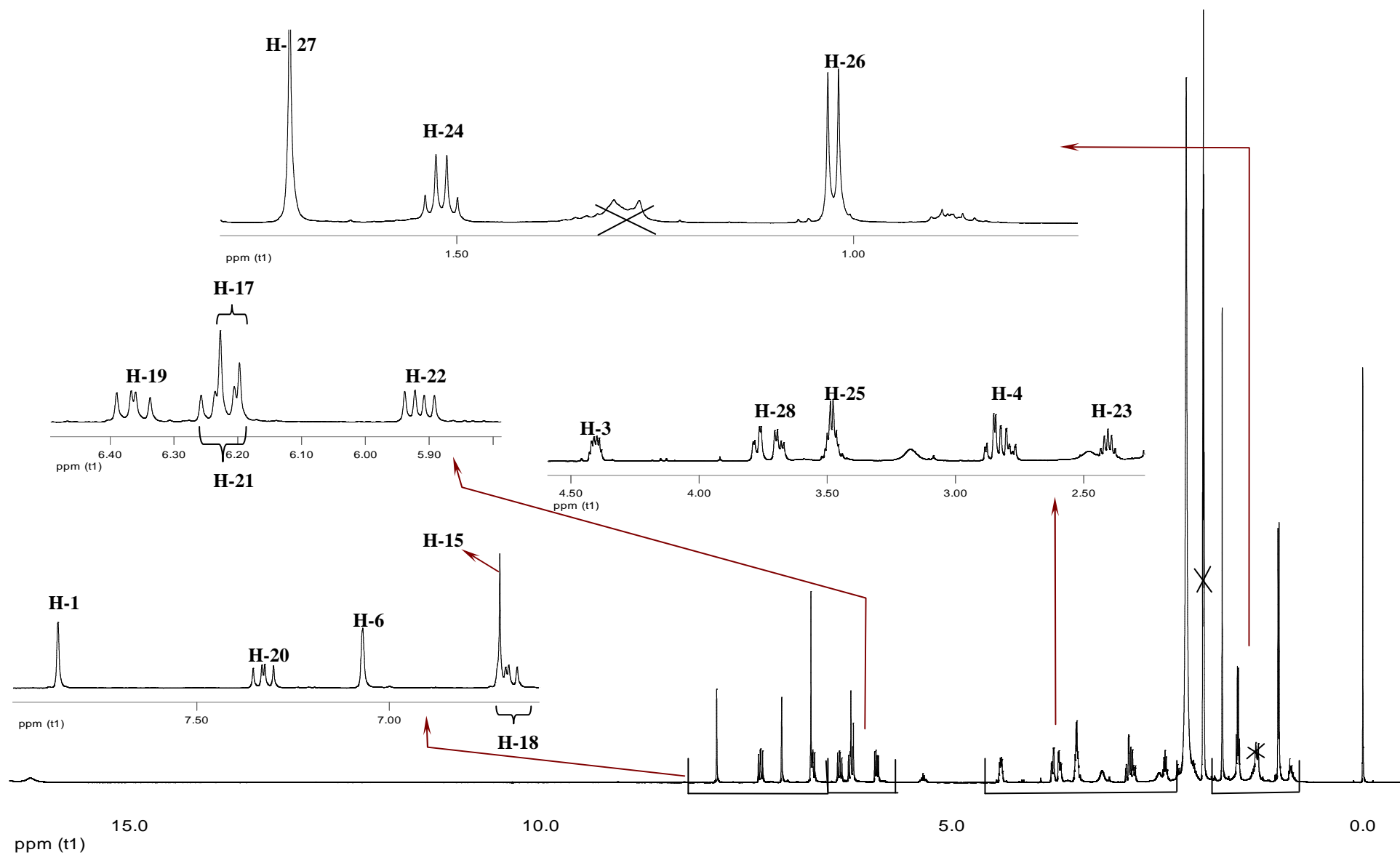


Figure 29: ^1H NMR spectrum of bulgariolactone D (Peak 1) isolated by HPLC. Impurity signals are struck through.

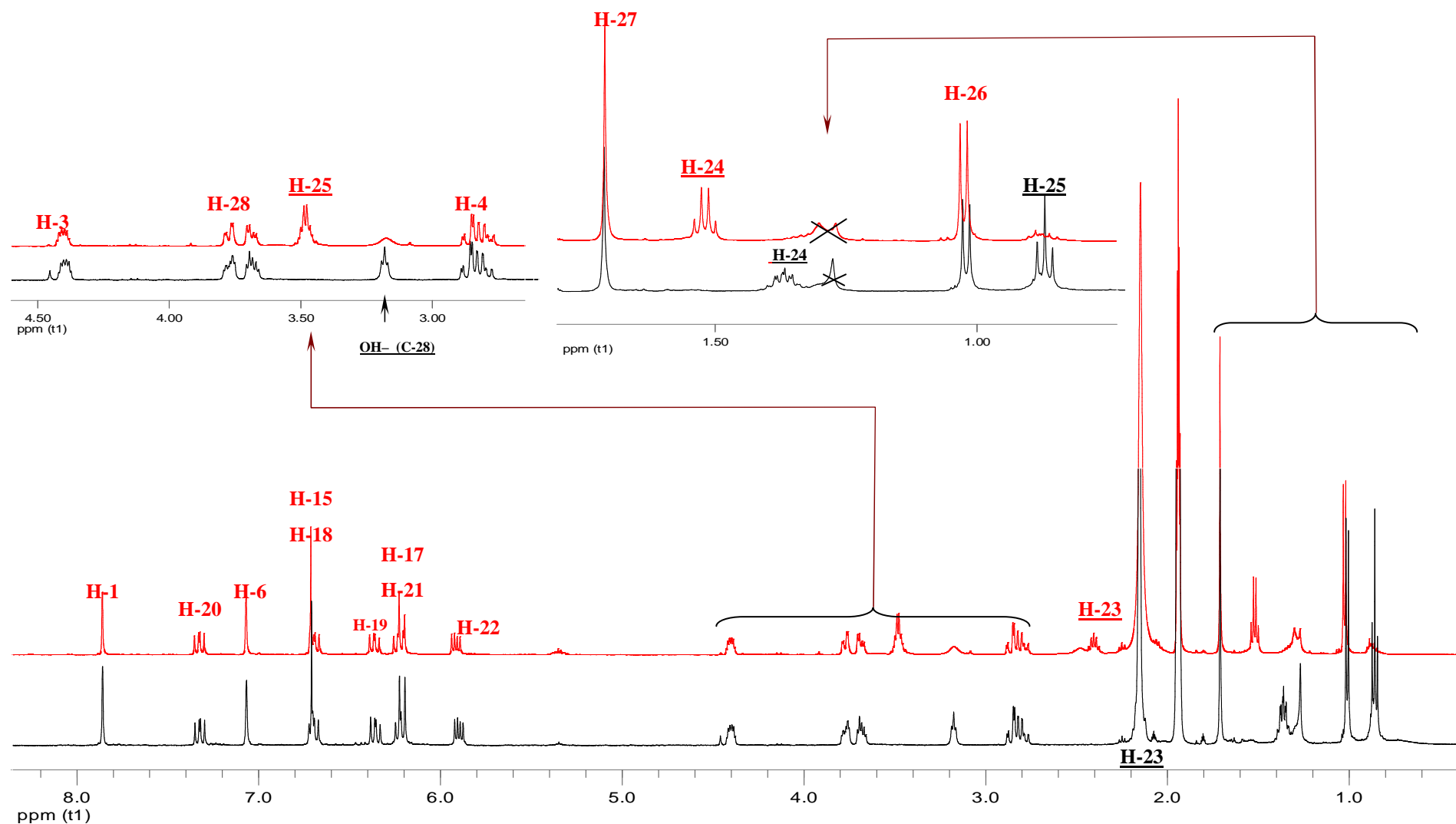
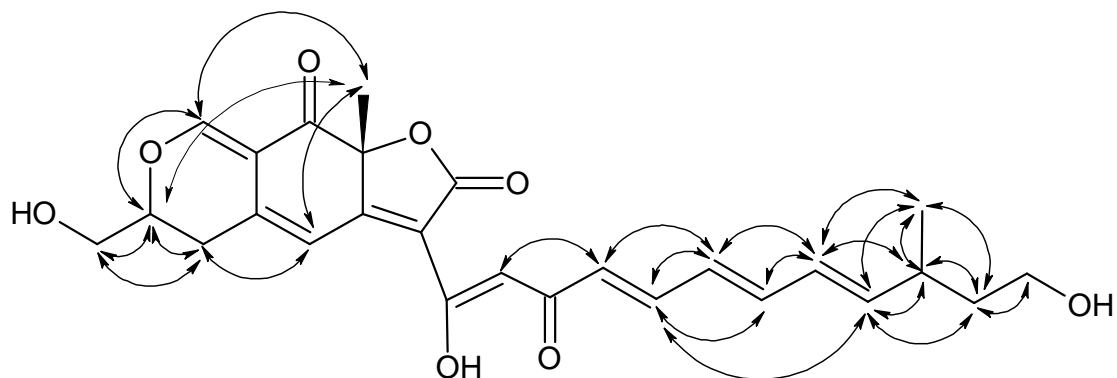


Figure 30: Comparison of ^1H NMR spectra of two azaphilones isolated from *B. inquinans* by HPLC (for details see text):
 — Proton spectrum of bulgarialactone B (H-23 is masked by the signal at 2.15 ppm).
 — Proton spectrum of bulgarialactone D. Deviating protons are underlined.

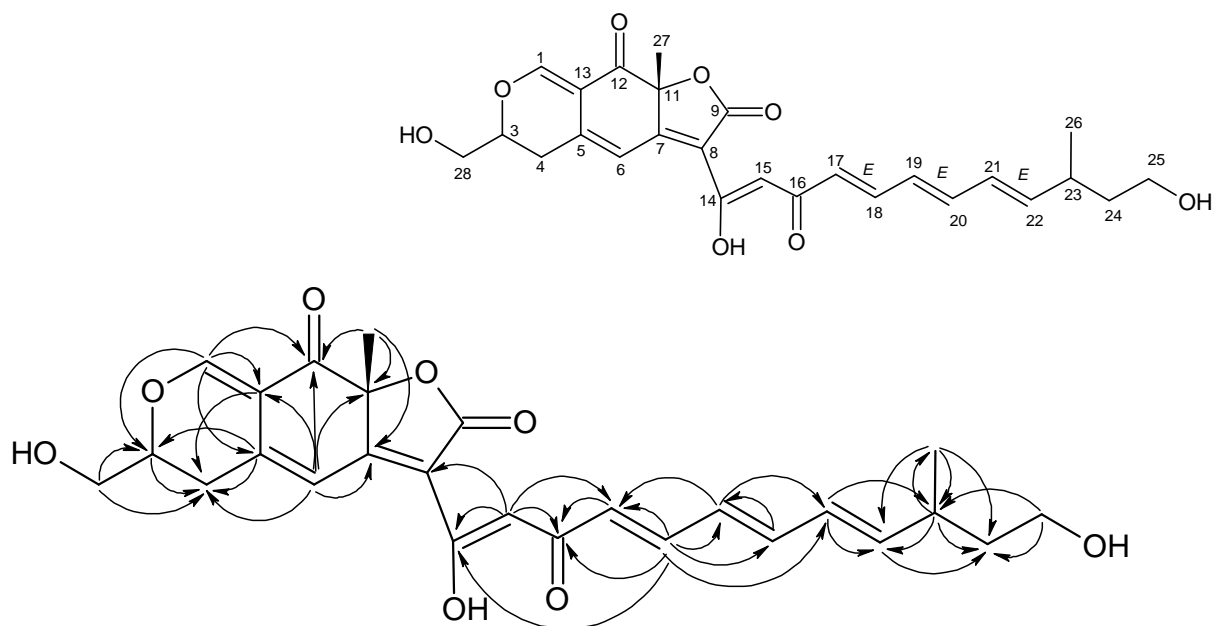
The partial structure analysed so far includes one chiral C-atom (C-23); it was not possible to establish the exact configuration of this atom.

NOESY determined relative stereochemistry at C-11, as previously demonstrated for bulgarialactone B (see Section 3.2.5.5). Further analysis of NOESY data, combined with characteristic coupling constant values ($^3J_{\text{H-17, H-18}} = 15.0 \text{ Hz}$, $^3J_{\text{H-19, H-20}} = 15.1 \text{ Hz}$ and $^3J_{\text{H-21, H-22}} = 15.1 \text{ Hz}$) established a trans-configuration for the double bonds C-17/C-18, C-19/C-20 and C-21/C-22:

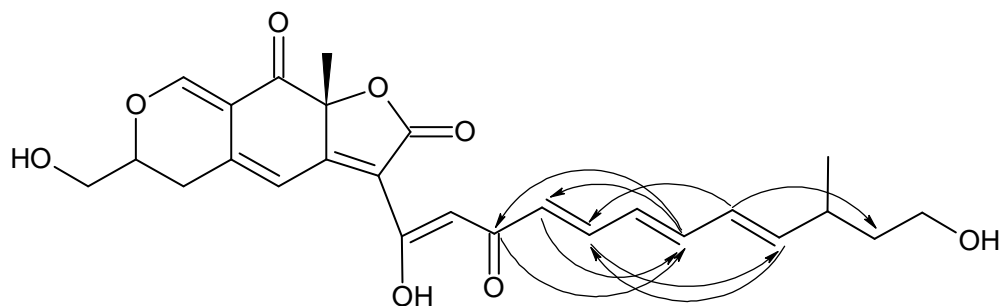


Detailed analysis of HMBC and H,H-COSY spectra established the following atomic correlations:

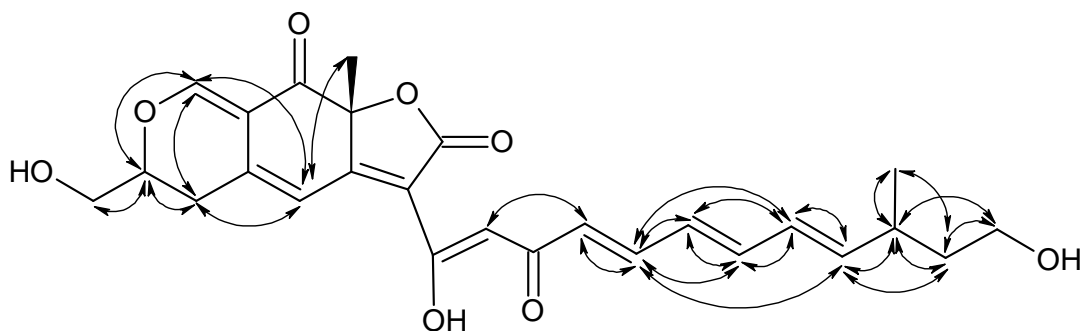
HMBC (1):



HMBC (2):



H,H-COSY:



As can be seen from Table 5 and Figure 30, the remainder of the molecule must be identical with the bulgariolactone B structure previously analysed.

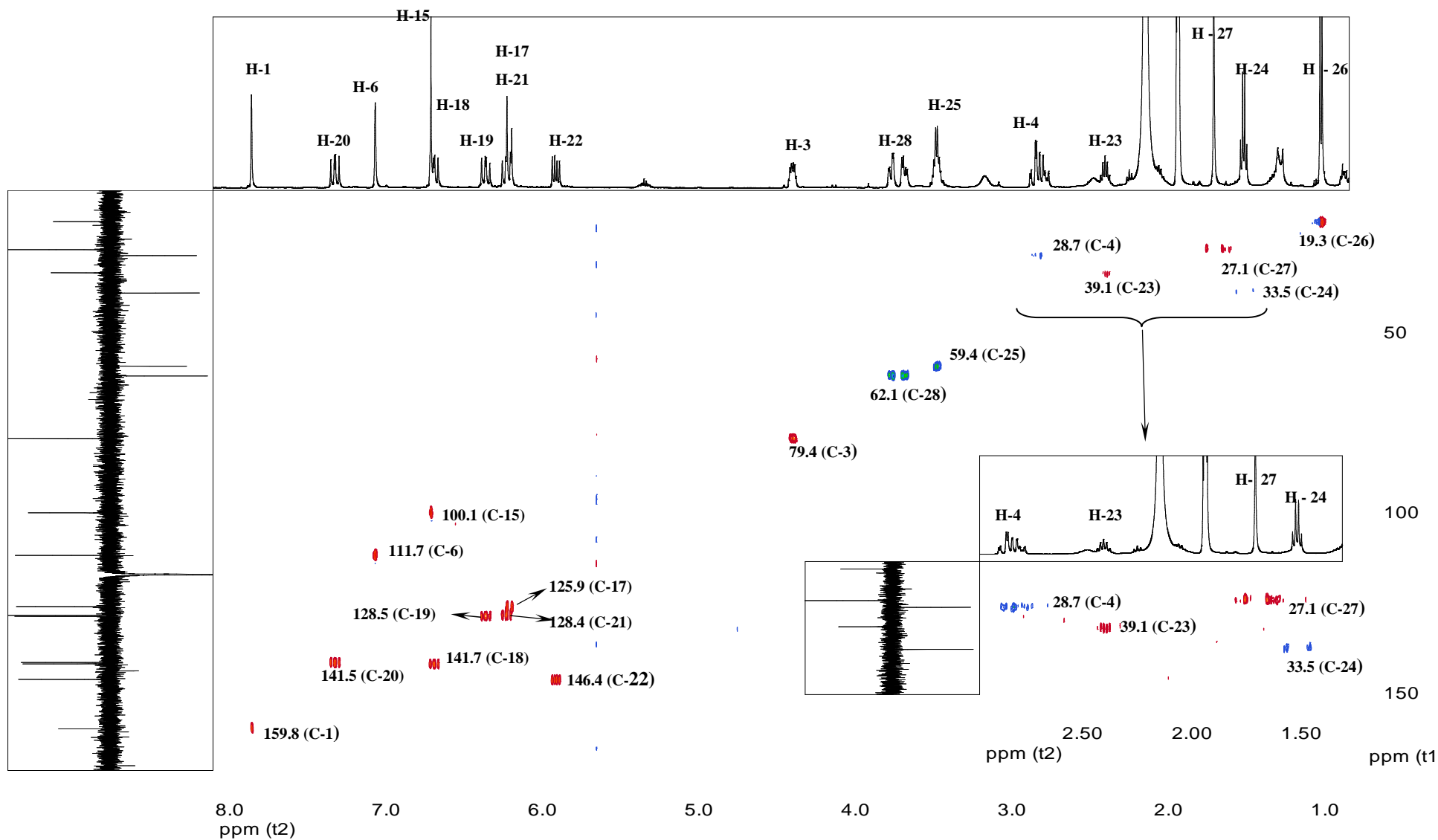
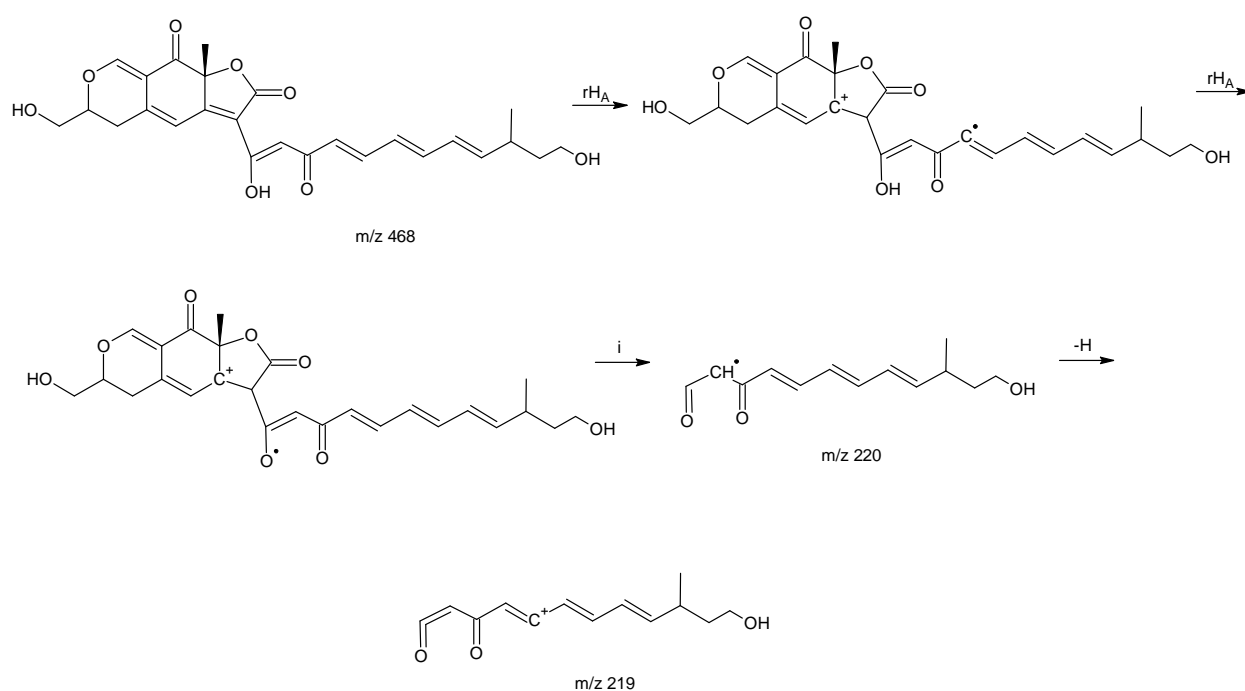


Figure 31: HSQC NMR spectrum of bulgarialactone D (Peak 1) isolated by HPLC

One final analysis re-considers the mass spectrum of bulgarialactone D (see Figure 28). The spectrum reveals the characteristic fragment m/z 247, the genesis of which has previously been discussed in detail (Section 3.2.5.5) and whose presence also confirms a part of the bulgarialactone D structure. Secondly, although not especially abundant, the fragment m/z 219 is also of interest since its fragmentation pathway supports the established structure to a certain degree. One possible fragmentation pathway for generating this ion is given by Mass Frontier as follows:



The research on *Bulgaria* azaphilones may be summarised as follows:

- A series of HPLC experiments have shown that fresh fruit bodies of *B. inquinans* contain just two azaphilones: bulgarialactone B, the structure of which was already known, and bulgarialactone D.
- It has been shown that the bulgarialactone D isolated by HPLC is not only a new azaphilone derived from *B. inquinans* but a new naturally-occurring compound
- Both azaphilones display strong antibacterial activity against *S. aureus*, comparable with the activity of the reference antibiotic ciprofloxacin (3.5-5 μg).
- Bulgarialactone D is relatively instable and partially decomposes to bulgarialactone B at room temperature. It was therefore only possible to isolate sufficient quantities from ether or acetonitrile extracts freshly prepared at sub-zero temperatures ($-18\text{ }^{\circ}\text{C}$).

3.2.6 Antibacterial activity of *Bulgaria hydrodistillate*

3.2.6.1 Detection of bioactive TLC zones

Agar diffusion tests have shown that volatiles of *B. inquinans* are active against *S. aureus* (see Section 3.1.1, “Agar diffusion test of fungi extracts”). It was therefore decided to apply an agar overlay technique to a hydrodistillate (HD) in order to identify the zones responsible for this effect. TLC plates with applied HD were developed in the solvent system toluene/ethyl acetate (95:5). Two zones of bacterial growth inhibition were discovered: one matched a band with $R_f = 0.98$, while the other growth inhibition covered a large area from $R_f = 0.0$ to $R_f = 0.25$, including several very faint bands visible only in UV light (Figure 32, mode 1 and 2). However, spraying with anisaldehyde reagent revealed the lower band responsible for antimicrobial activity (Figure 32, mode 4); activity of this band was comparable with the control (Figure 32, control). Both active bands were well separated on the TLC plate and easily detectable either in visible light (band with $R_f = 0.15$ after spraying with anisaldehyde reagent) or in both visible and UV light (band with $R_f = 0.98$). The decision was therefore made to isolate the bands from TLC plates. Before the isolation experiment commenced, GC measurements were taken to confirm the purity of both active bands: these measurements demonstrated that both active bands were relatively pure and were viable for isolation from preparative TLC plates. According to the literature, this experiment constituted the first application of the agar overlay technique on TLC plates to a hydrodistillate of *B. inquinans*.

3.2.6.2 Isolation of antibacterial compounds from preparative TLC plates

After confirming purity with GC, isolation of bioactive substances from *B. inquinans* hydrodistillate was performed using preparative TLC plates developed in the solvent system toluene/ethyl acetate (95:5). The two bands possessing antimicrobial activity ($R_f = 0.98$ and a large band with $R_f = 0.10-0.25$; Figure 32) were subsequently eluted from silica gel with ether.

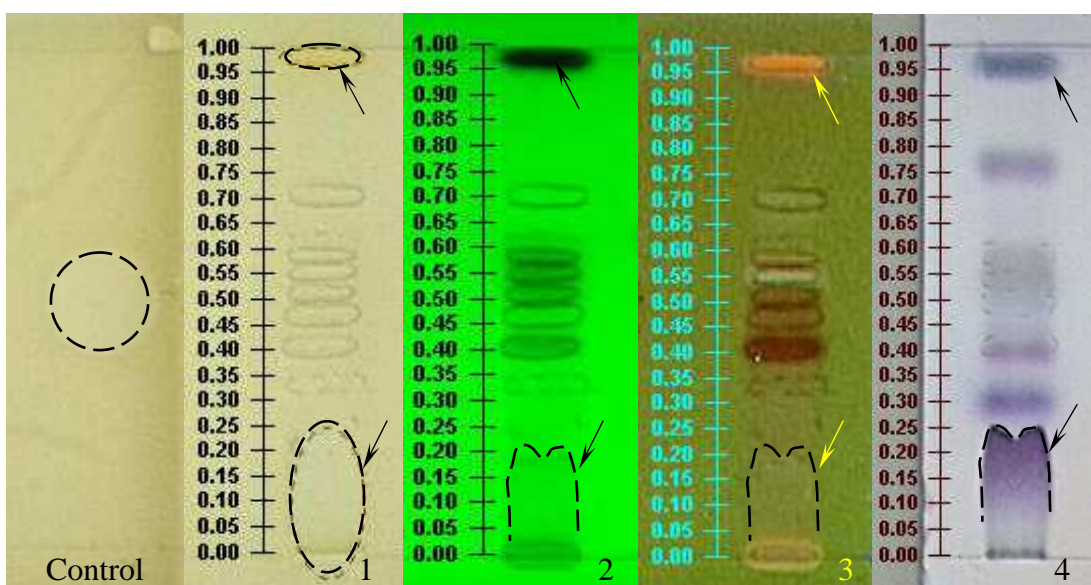


Figure 32: Antimicrobial activity of *B. inquinans* hydrodistillate against *S. aureus*. Solvent system: toluene/ethyl acetate (95:5); control: ciprofloxacin 3.5 μg
 Detection mode: (1) Visible light (agar overlaid HD); (2) UV light 254 nm; (3) UV light 366 nm; (4) Visible light (anisaldehyde reagent). For details, see text.

GC and GC-MS analysis revealed that the isolated band with $R_f = 0.10\text{--}0.25$ contained hexadecanoic, pentadecanoic and linoleic acids. Thus, the antibacterial activity of this zone may be explained by the presence of linoleic acid, whose antimicrobial properties are well known [84, 85]. The presence of linoleic acid was also confirmed by TLC, as can be seen in Figure 33.

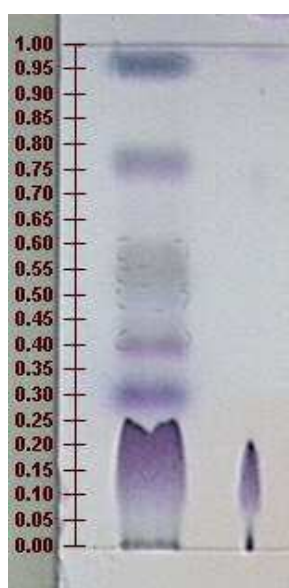


Figure 33: Hydrodistillate of *B. inquinans* with the reference substance linoleic acid. Solvent system: toluene/ethyl acetate (95:5). Detection mode: visible light (anisaldehyde reagent).

GC-MS analysis revealed the presence of a molecular ion $[M^+]$ 202 in the active band with $R_f = 0.98$ (Figure 38). Unfortunately, the eluate from this zone contained several other compounds as impurities. Furthermore, insufficient quantities of pure substance ($M = 202$ Da) were obtained for structure elucidation as a result of losses during the purification procedure. As can be deduced from the high R_f value (0.98) of the substance on the TLC plate, this unknown compound is apolar, i.e. it lacks functional groups. An attempt was therefore made to obtain sufficient quantities of this substance for NMR analysis from pentane and ether extracts (Figure 34). However, none of the extracts obtained contained the target compound.

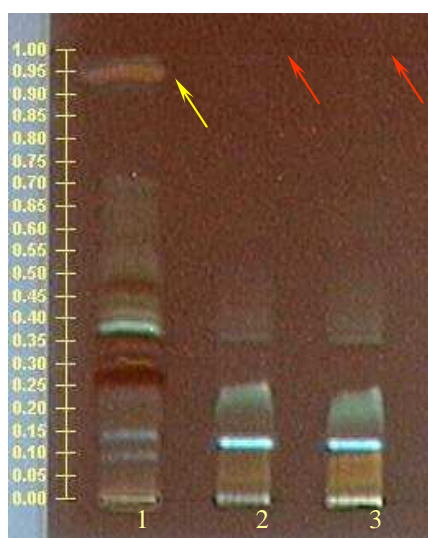


Figure 34: *B. inquinans* extracts developed on silica gel TLC plates. Solvent system: toluene/ethyl acetate (95:5). Detection mode: UV light 366 nm. (1) hydrodistillate; (2) pentane extract; (3) ether extract. Red arrows indicate the absence of antibacterial band. For details, see text.

The absence of the $[M^+]$ 202 compound in the pentane extract was also proven by GC-MS, as can be seen from the total ion chromatogram (TIC) in Figure 35.

The fact that this active substance exhibits strong antibacterial activity and was detectable only in the hydrodistillate suggests that this unknown $[M^+]$ 202 compound is not a genuine constituent, but is possibly formed by the fungus as a defensive response to injury or calefaction.

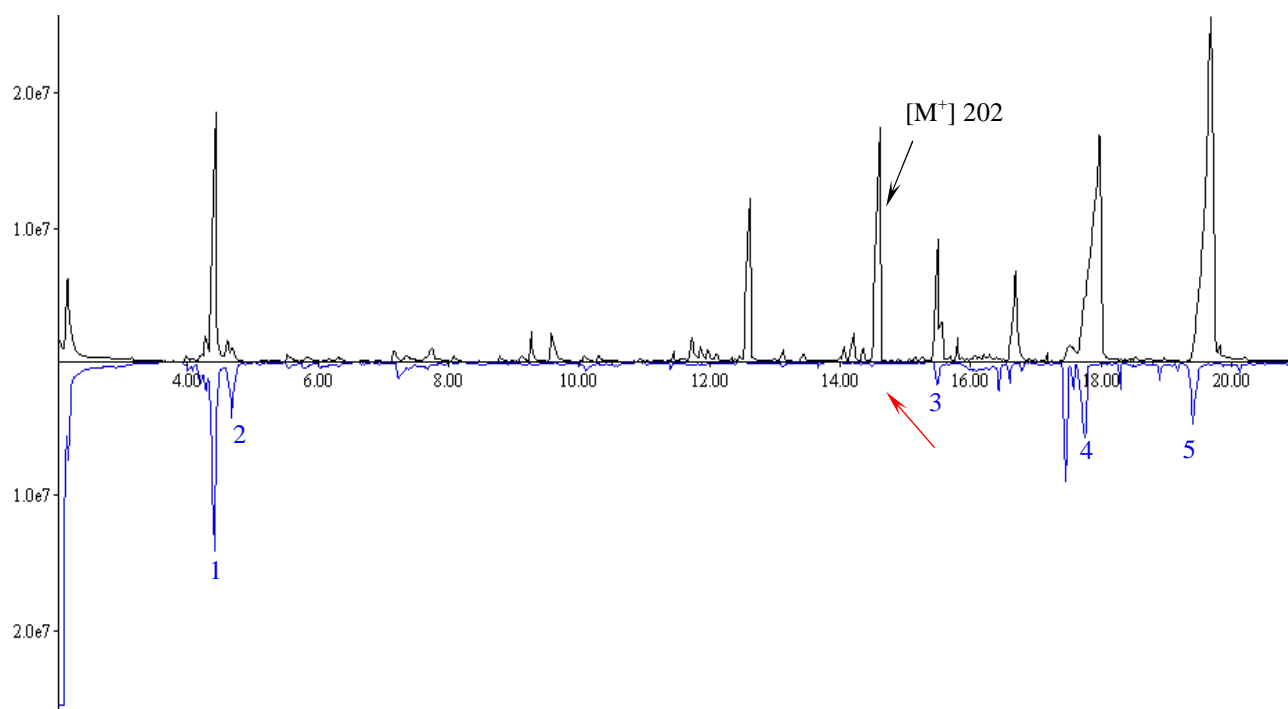


Figure 35: GC-MS of *B. inquinans* hydrodistillate (top trace) and pentane extract. Peaks identified from *B. inquinans* pentane extract: (1) 1-octen-3-ol; (2) furan, 2-pentyl-; (3) 1,3-diphenyl-2-one; (4) n-hexadecanoic acid; (5) linoleic acid. Arrow marks the missing peak for the antibacterial compound.

Since attempts to isolate this compound from the TLC plate proved unsuccessful with the standard solvent system (toluene/ethyl acetate (95:5)) at room temperature, a further attempt at isolation was made using semi-preparative silica gel TLC plates developed in pure pentane at sub-zero temperatures ($-18\text{ }^{\circ}\text{C}$). This technique is suitable for terpenes and permits not only the separation of hydrocarbons from oxygenated constituents but also the separation of compounds within the terpene hydrocarbon group [86, 87]. Guaiazulene was chosen as a reference (Figure 36) since this polar hydrocarbon (and dye) normally permits the differentiation of hydrocarbon and oxygenated compound groups on the TLC plate.

After development, the plates were immediately sprayed with distilled water to prevent rapid drying and as a precaution against the catalytic activity of the silica gel. The target substance was easy to detect in UV light at 254 and 366 nm ($R_f = 0.28$). On exposure to room temperature, this colourless band turned yellow-red in visible light, thus indicating decomposition. This method resulted in the

successful isolation of 3.8 mg of the antibacterial constituent from *B. inquinans* hydrodistillate. The compound's purity was examined via GC-MS (Figure 37), which confirmed the isolated substance to be sufficiently pure for further NMR analysis.

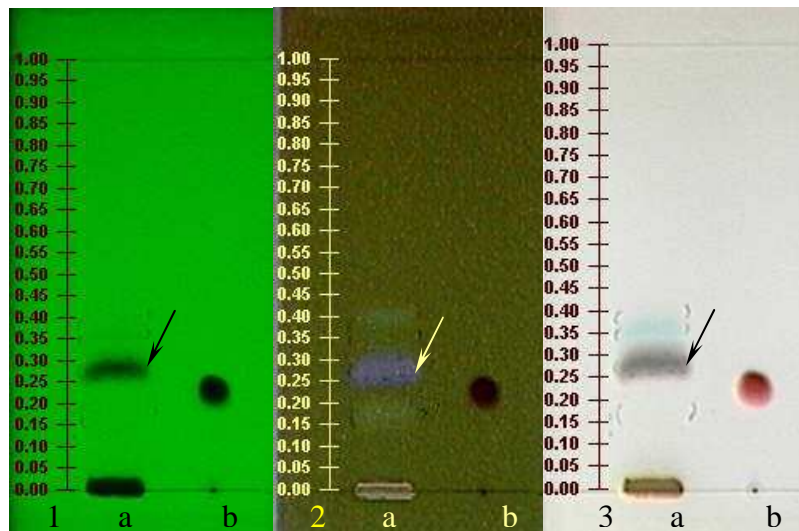


Figure 36: *B. inquinans* hydrodistillate (HD) developed on silica gel TLC plates at sub-zero temperatures ($-18\text{ }^{\circ}\text{C}$) in pure pentane: (a) *B. inquinans* HD; (b) reference substance guaiazulene. Detection modes: (1) UV light 254 nm; (2) UV light 366 nm; (3) visible light (anisaldehyde reagent). An arrow marks the antibacterial compound ($[\text{M}^+] 202$).

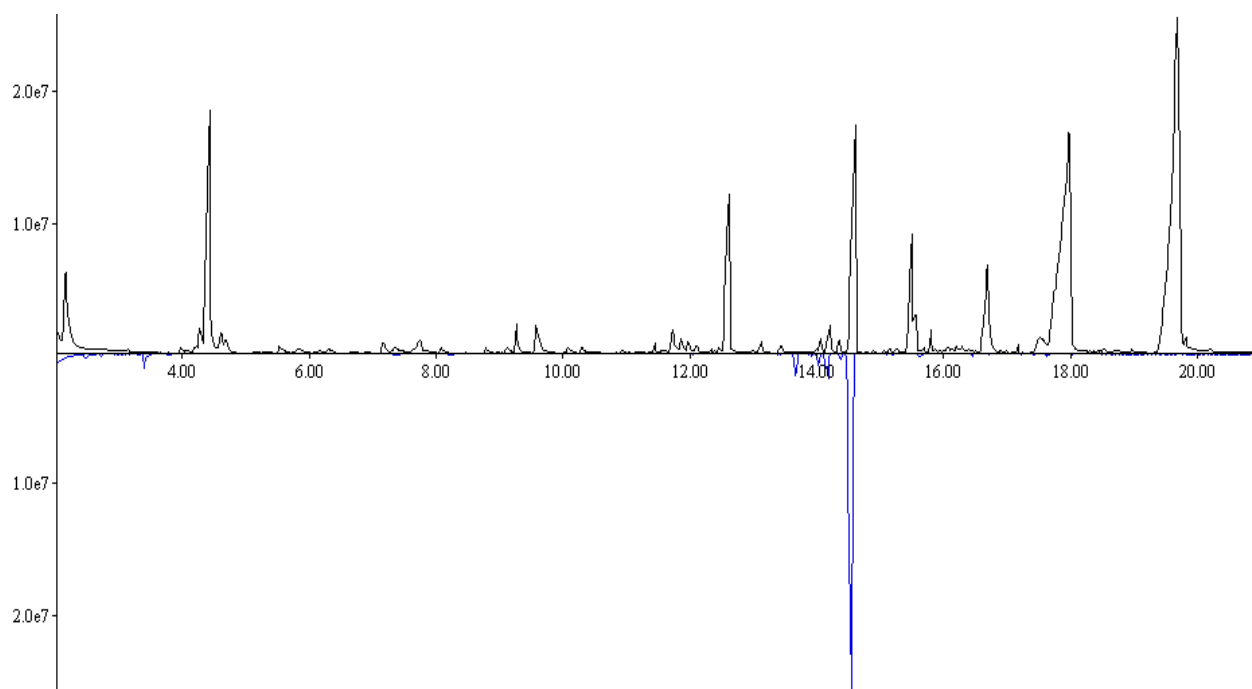
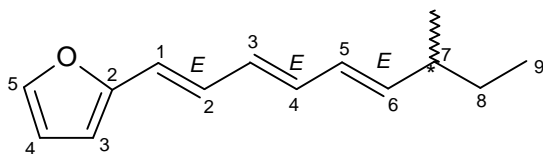


Figure 37: Comparison of the total ion chromatograms of *B. inquinans* hydrodistillate (upper trace) and the isolated bioactive compound ($R_f = 0.28$, $[\text{M}^+] 202$)

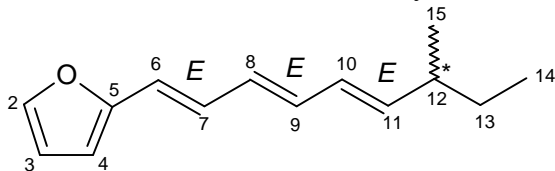
— *B. inquinans* HD

— Antibacterial compound isolated from *B. inquinans* HD

3.2.6.3 Structure elucidation of bulgariafuran



IUPAC: 2-[(1E,3E,5E)-7-methylnona-1,3,5-trienyl]furan



Note: the numbering shown here follows the same system as used for bulgrialactones; this system will also be used in the subsequent discussion

While investigations on TLC plates suggested this compound was a hydrocarbon (marked zone with $R_f = 0.28$, Figure 36), GC analysis nonetheless revealed a contrary result: the major deviation between Kováts retention indices (RI) on a polar Carbowax and on a non-polar CP-Sil phase ($2200-1680 = 520$ RI units) proved the existence of a functional group in this molecule. The MS spectrum (Figure 38) showed a base peak at m/z 202 (100%). Its molecular ion character is supported by the presence of following fragments: m/z 187 (M^+-15 , $-\text{CH}_3$), m/z 173 (M^+-29) and m/z 145 (M^+-57).

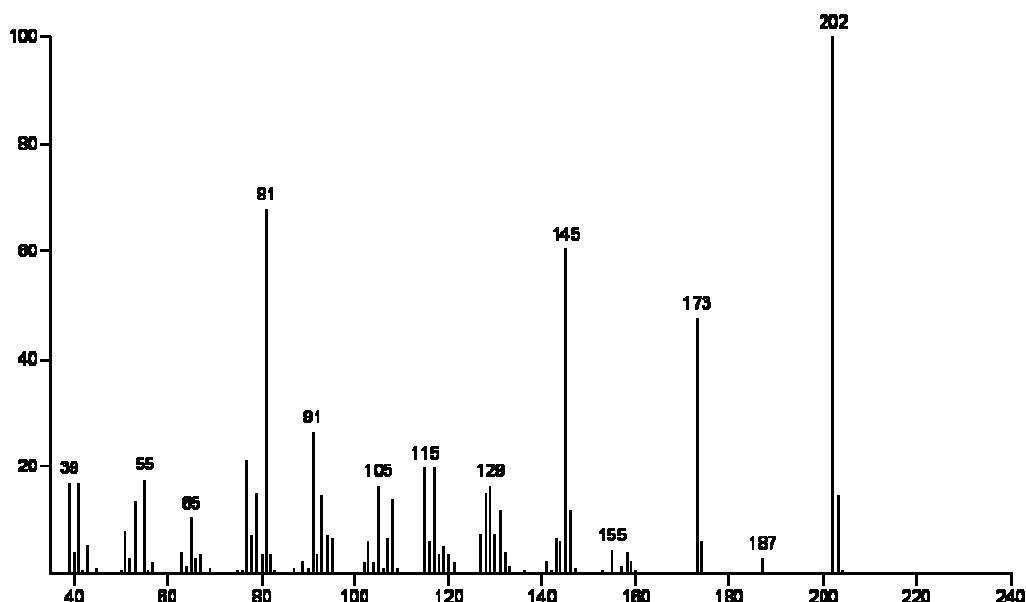


Figure 38: MS spectrum of bulgariafuran isolated from *B. inquinans* hydrodistillate ($R_f = 0.28$)

As regards the presence of heteroatoms, one was able to exclude sulphur, chlorine and bromine since the spectrum lacks their specific isotope patterns. The molecule

was therefore likely to contain oxygen: for a single oxygen, the formula would be C₁₄H₁₈O. This suggestion was confirmed by the ¹³C NMR data, which revealed 14 carbon signals. The exact positions of all C-atoms were detected directly from the ¹³C NMR spectrum (Appendix I, Figure 69). The multiplicity of carbon atoms and their corresponding protons was assigned from HSQC data (Figure 40). Two peaks ($\delta = 65.87$ ppm and 15.24 ppm) were assigned to a ionol impurity, a stabiliser of ether. Ten olefinic C-atoms were found in total, indicating the presence of five double bonds. Calculation of the double bond equivalent (DBE = 6) proved the existence of one ring in this molecule.

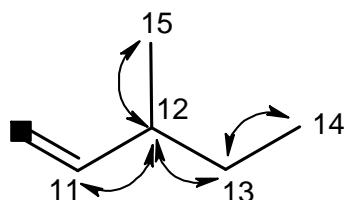
The results of ¹H NMR and ¹³C NMR analysis are summarised in Table 6. The complete ¹H spectrum (Figure 39) shows nine protons in the aromatic ($\delta = 6$ –8 ppm) and olefinic ($\delta = 4.5$ –6.5 ppm) regions. Nine protons were also found within the range of $\delta = 0$ –2 ppm (aliphatic region). Three signals belong to ionol ($\delta = 3.48$ ppm, $\delta = 1.56$ and $\delta = 1.21$ ppm), a fact demonstrated by measuring the ¹H NMR spectrum of pure ionol.

¹³ C NMR (CD ₃ CN) by 100.13 MHz, ppm	C-atom	Structural element	¹ H NMR (CD ₃ CN) by 400.13 MHz, ppm	H,H-coupling constants, Hz
11.8 <i>q</i>	14	–CH ₃	3H, 0.86 <i>t</i>	³ J _{H-14, H-13} = 7.5
20.1 <i>q</i>	15	–CH ₃	3H, 1.01 <i>d</i>	³ J _{H-15, H-12} = 6.7
29.8 <i>t</i>	13	–CH ₂ –	2H, 1.34 <i>m</i> *	
38.7 <i>d</i>	12	>CH–	1H, 2.11 <i>m</i> *	³ J _{H-12, H-15} = 6.7 ³ J _{H-12, H-11} = 7.8 ³ J _{H-12, H-13} = 13.8
107.9 <i>d</i>	4	=CH–	1H, 6.32 <i>d</i> *	³ J _{H-4, H-3} = 3.1
111.7 <i>d</i>	3	=CH–	1H, 6.37 <i>dd</i> *	³ J _{H-3, H-4} = 3.1 ³ J _{H-3, H-2} = 1.8
118.9 <i>d</i>	9	=CH–	1H, 6.30 <i>dd</i> *	³ J _{H-9, H-8} = 14.8
128.1 <i>d</i>	7	=CH–	1H, 6.71 <i>dd</i>	³ J _{H-7, H-8} = 10.7 ³ J _{H-7, H-6} = 14.5
128.8 <i>d</i>	10	=CH–	1H, 6.09 <i>dd</i>	³ J _{H-10, H-9} = 10.4 ³ J _{H-10, H-11} = 15.0
130.4 <i>d</i>	8	=CH–	1H, 6.31 <i>dd</i> *	³ J _{H-8, H-9} = 14.8 ³ J _{H-8, H-7} = 10.7
134.1 <i>d</i>	6	=CH–	1H, 6.31 <i>d</i> *	³ J _{H-6, H-7} = 14.5
141.7 <i>d</i>	11	=CH–	1H, 5.6 <i>dd</i>	³ J _{H-11, H-12} = 7.8 ³ J _{H-11, H-10} = 15.0
141.9 <i>d</i>	2	=CH–	1H, 7.35 <i>d</i>	³ J _{H-2, H-3} = 1.8
153.6 <i>s</i>	5	>C=	–	

Table 6: NMR characteristics of isolated bulgariafuran

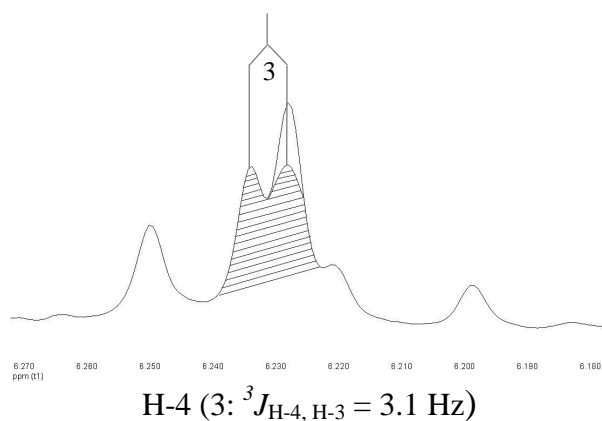
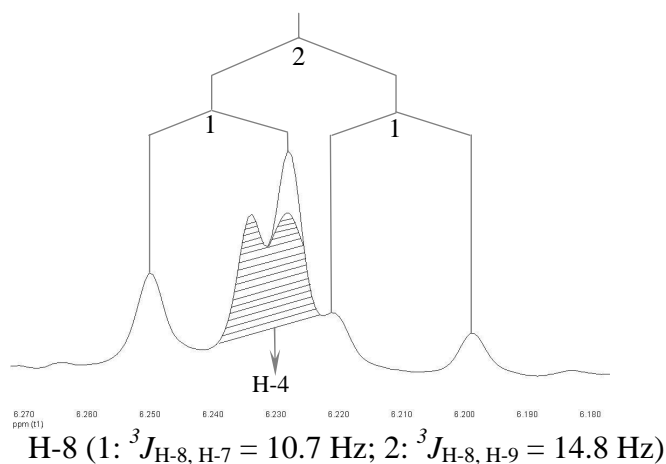
* Indicates overlaid signals or multiplets that could not be analysed.

Detailed NMR analysis was started on the methyl group C-14, whose signal was split into a triplet by the neighbouring methylene group CH₂— (H-13) (${}^3J_{\text{H-14, H-13}} = 7.5$ Hz), a fact confirmed by COSY measurements that further revealed the coupling of CH₂— (C-13) to the methine group CH— (H-12). Besides H-13, COSY analysis also discovered two further coupling partners of this methine group, namely CH₃— (H-15) and =CH— (H-11), which lead to the formation of a multiplet of the H-12 proton. The coupling constants of H-12 with H-15 and H-11 could be deduced directly from these partners, whereas the interaction with H-13 was an approximate calculation offered by the coupling constant analyser within the MestRec software application. Based on COSY analysis and coupling constant values, the following partial structure was therefore determined:



The chemical shifts values for C-14 (11.8 ppm), C-13 (29.8 ppm), C-12 (38.7 ppm), C-15 (20.1) and C-11 (141.7 ppm) offered further evidence in support of this partial structure [82].

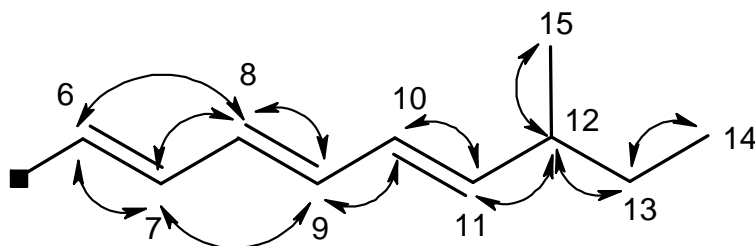
Further analysis of the COSY spectrum confirmed the second coupling partner of =CH— (H-11) as =CH— (H-10), whose signal appears in the ¹H NMR spectrum as a characteristic double doublet (Figure 39), generated by its couplings with two neighbouring protons: H-11 and H-9 (${}^3J_{\text{H-10, H-11}} = 15.0$ Hz and ${}^3J_{\text{H-10, H-9}} = 10.4$). The proton H-9 forms a double doublet overlaid by the single proton H-6. Two vicinal coupling constants were observed: ${}^3J_{\text{H-9, H-10}} = 10.4$ Hz and ${}^3J_{\text{H-9, H-8}} = 14.8$ Hz. The H-8 signal also appears as a double doublet, although partly overlaid with the H-4 signal:



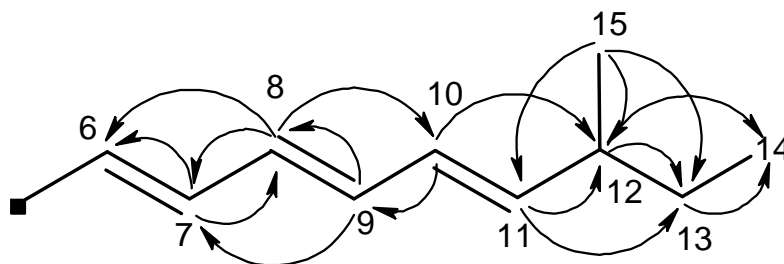
COSY analysis was also successful in identifying H-7 as the second coupling partner of H-8 (besides H-9). The signal of the H-7 methane group is represented as a double doublet with the coupling constants ${}^3J_{\text{H-7, H-8}} = 10.7$ Hz and ${}^3J_{\text{H-7, H-6}} = 14.5$ Hz. The H-6 proton was also found by analysing the COSY spectrum: it is a single proton, whose signal is overlaid by H-9 and must be split into a doublet, as could be deduced from the H-7 signal splitting at 6.71 ppm.

Thus, by combining the results of COSY analysis and the coupling constant analyser provided by MestRec, it was possible to establish the following substructure increment, which was also supported by the ${}^1\text{H}/{}^{13}\text{C}$ HMBC spectrum correlations (see also Appendix I, Figure 70 and Figure 71):

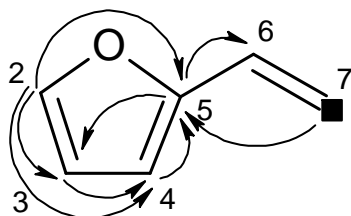
COSY:



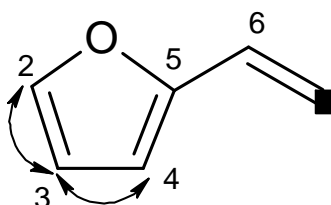
HMBC:



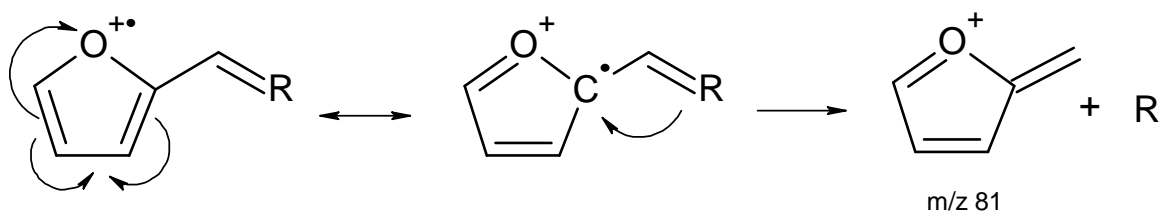
Since the single proton H-6 only shows a doublet, induced by the adjacent H-7 and no other major coupling constants, it was supposed that its neighbouring C-atom is quaternary, i.e. not possessing hydrogen. HMBC analysis permitted the identification of this atom as the olefinic C-atom C-5 ($\delta = 153.6$ ppm), possessing the following ^{13}C - ^1H correlations:



The C-6/C-5 connection is also supported by COSY spectrum data, which show an allylic coupling between H-6 and the olefinic H-4 ($\delta = 6.32$ ppm), and an HMBC correlation between H-4 and C-5. The correlation of H-7 to H-4 and to C-5 also accords well with the proposed structural element; the same holds true for the H-4/C-5 coupling (HMBC). The olefinic proton C-4 appears as a partly-resolved doublet with the coupling constant 3.1 Hz. As can be gathered from COSY spectrum data, the coupling partner is the adjacent olefinic proton H-3 ($^3J_{\text{H-4}, \text{H-3}} = 3.1$ Hz), which is recognised as a double doublet:

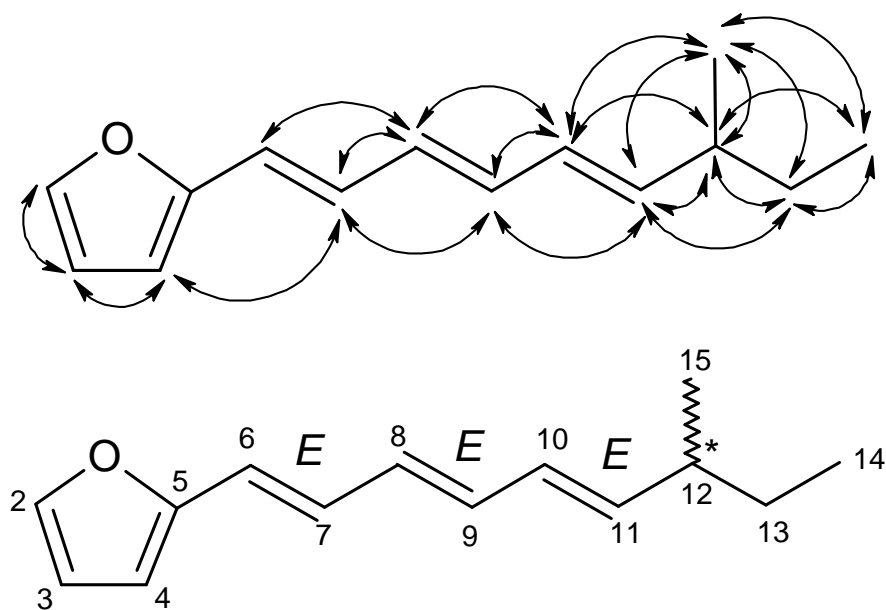


The second coupling partner of H-3 was identified as H-2 (see graphic above); its signal is split into a poorly-resolved broad doublet ($^3J_{\text{H-2, H-3}} = 1.8 \text{ Hz}$). This structural increment was in accordance with the COSY and HMBC correlations, as illustrated in the above graphic. H-2 is attached to the olefinic carbon C-2, which still had an open bond. An identical situation was discovered at C-5. According to the DBE (6), this molecule must contain one ring. Since no further C-atoms remain, but only a single oxygen, the structure of the molecule can only be completed by forming a furan ring, with oxygen inserted between C-2 and C-5. Several facts corroborate the furan ring structure: C-2 and C-3 chemical shifts accord well with the furan ring structure as given in the literature [82]; the same holds true for the coupling constants $^3J_{\text{H-2, H-3}}$ and $^3J_{\text{H-3, H-4}}$ [82]. In addition, the mass spectrometric fragmentation also agrees with the proposed furan structure, as it clearly shows the characteristic fragment m/z 81 of this compound in great abundance (Figure 38). This fragmentation can be explained as follows [88, 89]:



The last part of this analysis focuses on the configuration of the double bonds. In the furan ring, the situation is clear: as expected, proton H-3 shows interference with both H-2 and H-4 in the NOESY spectra. The olefinic proton coupling constants in the double-bond region of the side chain range between 14.5 and 15.0 Hz, which presents a strong argument for a trans-configuration.

This proposition was confirmed by the NOESY data: no correlation was observed between the protons of each double bond, as demonstrated by the following graphic (top graphic, the lower graphic provides a numbering reference):



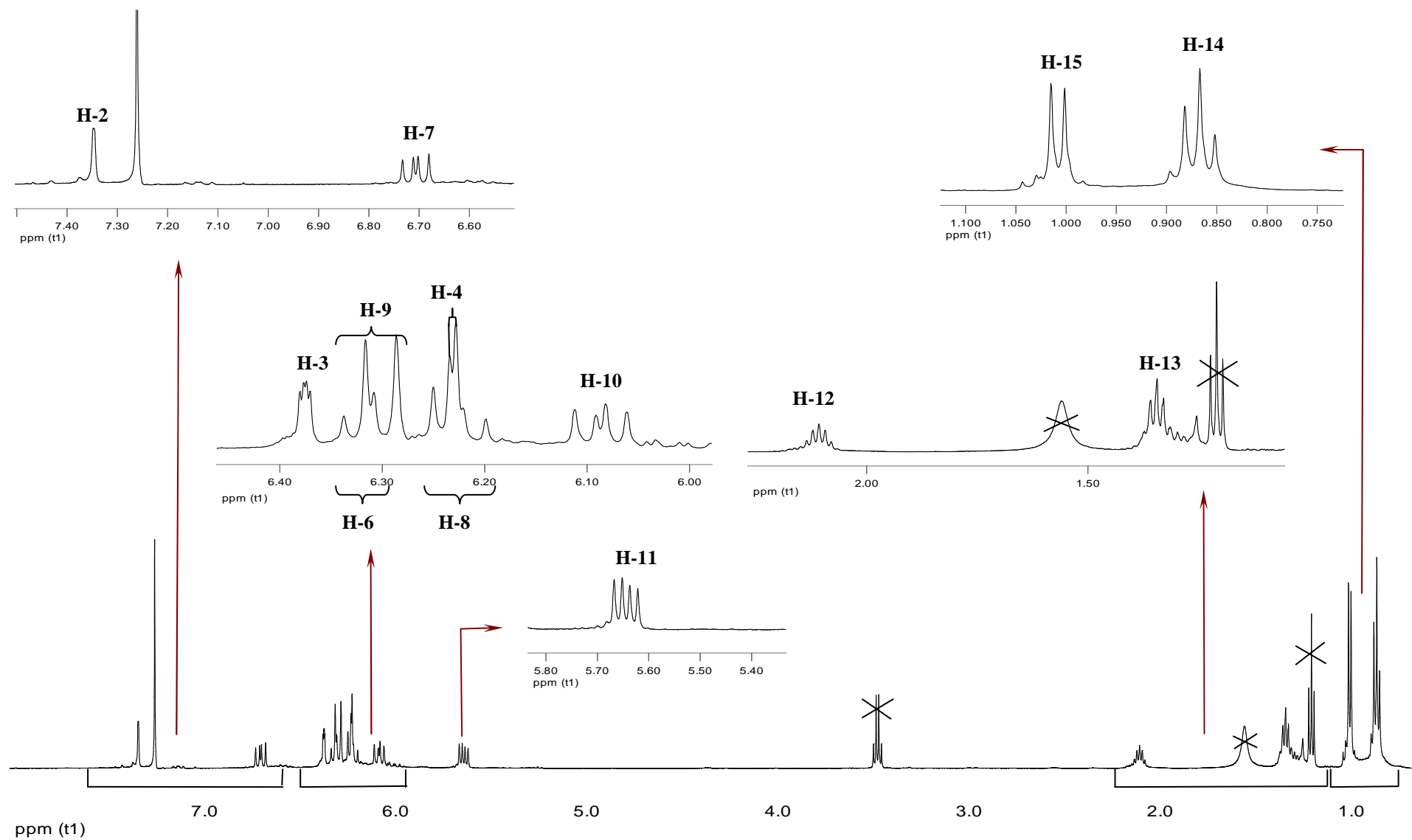


Figure 39: Proton NMR spectrum of bulgariafuran from *B. inquinans* hydrodistillate. For naming, see text.

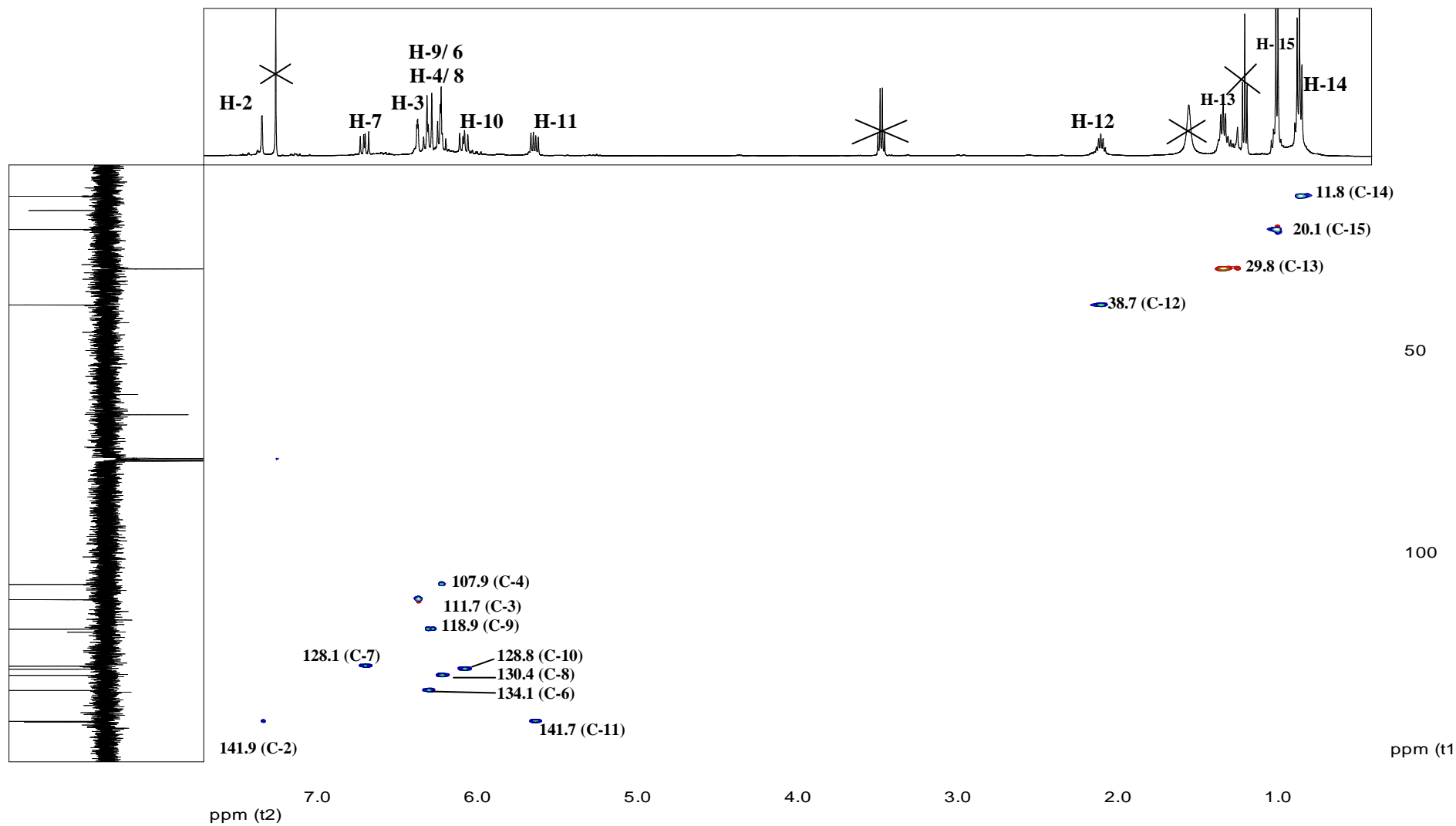


Figure 40: HSQC NMR spectrum of bulgariafuran isolated from *B. inquinans* hydrodistillate. For naming, see text.

For this new natural compound, the name bulgariafuran is suggested. As mentioned above (see Section 3.2.6.2), this bioactive substance was detected only in the hydrodistillate and was entirely absent (even as a trace constituent) from both pentane and ether extracts. This fact, together with the strong antibacterial activity (see Section 3.2.6.1) of bulgariafuran suggests that it may be formed from 1-octen-3-ol (a primary component of the pentane extract) or from bulgarialactone D as a defensive response to calefaction. However, further investigation is required to confirm the mechanism of the transformation pathway.

Structurally, bulgariafuran is similar to dendrolasin, dehydrodendrolasin, perillene and rosefuran: these substances are pheromones that belong to the class of furano-sesquiterpenes and have been isolated from insects, marine animals and plant species [90, 91, 92, 93]. Although further work is required to determine the biogenetic precursors of naturally occurring furan derivatives, some evidence suggests the suitability of α , β -unsaturated carbonyl compounds for this role [90].

3.2.7 Volatiles of *Bulgaria* fruit bodies

3.2.7.1 GC-MS analysis of the hydrodistillate

Identification of compounds was performed by comparing the mass spectra with those given by several electronic libraries. Additionally, retention indices of reference compounds were used, and co-injection of commercially-available standards was also performed.

The results of these GC-MS analyses are summarised in Figure 41 (TIC) and Table 7. Overall, a total of 16 constituents were identified, representing 78.76% of all volatiles. As can be seen from Table 7 (FID), the major components of this hydrodistillate are n-hexadecanoic acid (~16%), linoleic acid (~19%) and linoleic acid ethyl ester (~10%; all figures are proportions of the total hydrodistillate). As a result of strong peak overlaying in TIC, only FID permitted the determination of exact amounts of these substances. The antibacterial substance bulgariafuran yields a quantity of about 3% (FID); the proportion of *R*-(-)-1-octene-3-ol is ~4% (FID).

No typical volatiles of either the terpene or the phenylpropanoid group were encountered in this *B. inquinans* hydrodistillate. Instead, the majority of volatiles are those derived from fatty acid metabolism.

Dry column pre-fractionation on silica gel was performed to detect minor compounds and to separate overlaying peaks; this process resulted in two fractions. Fraction 1 was eluted with pure pentane in order to gain the apolar hydrocarbon group (Figure 42). This fraction contained some unidentified substances, possibly impurities from silica gel (region from 4 to 6 min), together with bulgariafuran. It is extremely interesting that the hydrocarbon fraction (Fraction 1) is represented only by a single compound bearing a furan ring, namely bulgariafuran (2.84% FID). The fact that this constituent appears in the hydrocarbon fraction indicates that it is highly apolar, despite the presence of a heteroatom.

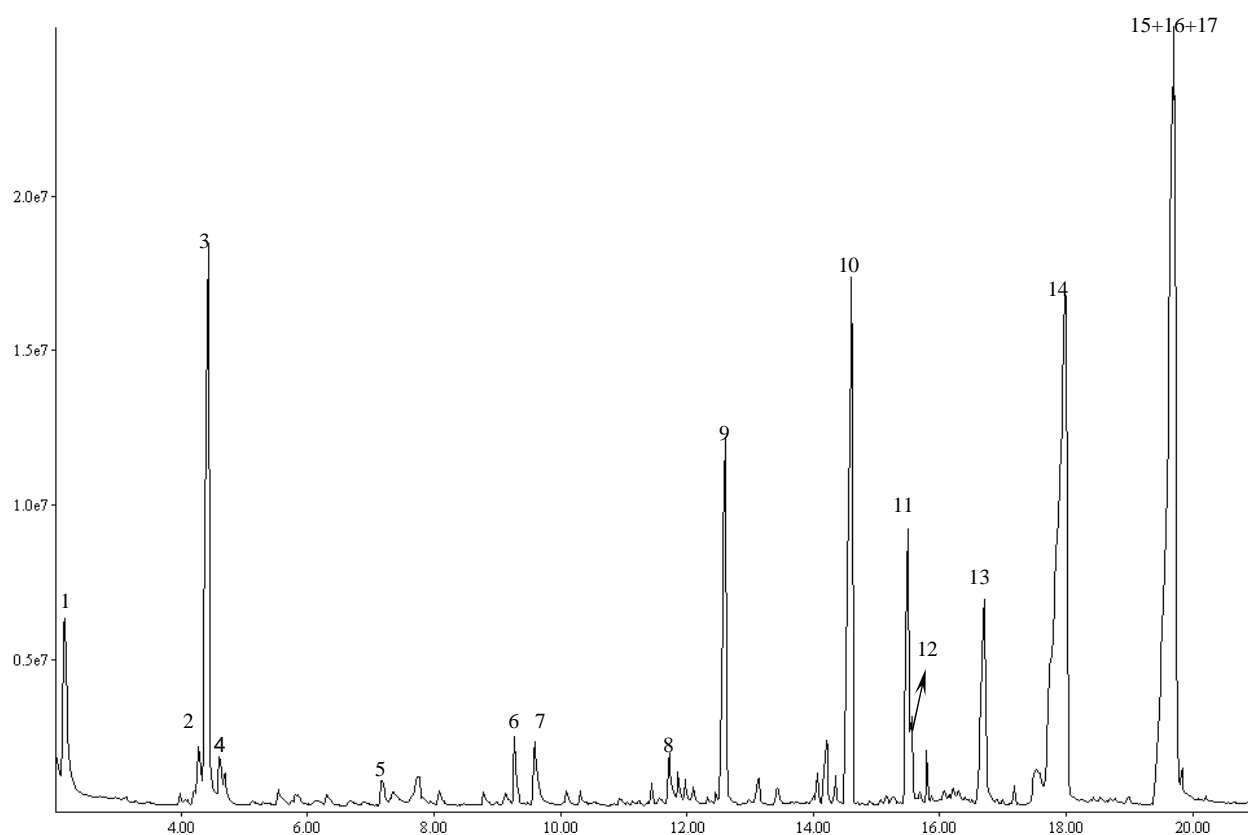


Figure 41: GC-MS chromatogram (TIC) of *B. inquinans* hydrodistillate

Peak Nr	Substance	GC-MS				Identified by	GC-FID	
		Retention Time	Kováts retention index	TIC, %	[M+]		Retention Time	%
1	Hexanal	2.16	—	3.21	100	EI-MS	6.33	2.30
2	1-octen-3-on	4.27	954	0.65	126	EI-MS/RI	18.34	0.29
3	<i>R</i> -(-)-1-octen-3-ol	4.43	963	9.53	128	EI-MS/RI/ Co-injection	19.30	4.23
4	Furan, 2-pentyl-	4.61	978	0.54	138	EI-MS/RI	21.56	0.23
5	2-Nonenal	7.16	1136	0.47	140	EI-MS/RI	22.43	0.27
6	2-Undecanone	9.27	1271	0.88	170	EI-MS/RI	30.77	0.20
7	2,4-Decadienal	9.58	1293	1.56	152	EI-MS//RI	32.34	0.48
8	Massoia Lactone	11.73	1441	0.82	168	EI-MS/RI/Co-injection	40.60	0.27
9	<i>Unknown</i>	12.62	1505	6.73	178	EI-MS	42.03	1.64
10	Bulgariafuran	14.61	1661	12.4	202	EI-MS/NMR	45.52	2.84
11	1,3-diphenyl-2-propanone	15.50	1739	1.21	210	EI-MS/RI/Co-injection	53.84	4.27
12	Tetradecanoic acid	15.55	1744	1.39	228	EI-MS/RI/Co-injection	57.47	0.82
13	Pentadecanoic acid	16.07	1846	4.73	242	EI-MS/RI/Co-injection	60.68	0.92
14	<i>n</i> -Hexadecanoic acid	17.98	1965	24.60	256	EI-MS/RI/Co-injection	63.18	15.66
15	Linoleic acid	19.60	2127	33.10	280	EI-MS/RI Co-injection	69.31	19.29
16	Linoleic acid ethyl ester	19.67	2134		308	EI-MS/RI	71.08	9.98
17	Oleic acid ethyl ester	19.76	2143		310	EI-MS/RI	71.08	2.74

Table 7: Chemical composition of *B. inquinans* hydrodistillate

Fraction 2 was refluxed with ether and contained a greater number of polar (oxygenated) compounds (Figure 43). In total, the compounds of Fraction 2 represent 75.92% (FID) of the total *Bulgaria* volatiles, a far higher proportion of volatiles than found in Fraction 1.

The present work constitutes the first investigation of the chemical composition of a hydrodistillate from *B. inquinans* fruit bodies. As can be seen from Table 7, two interesting and unusual compounds were identified in the *Bulgaria* hydrodistillate: massoia lactone (8) and 1,3-diphenyl-2-propanone (11).

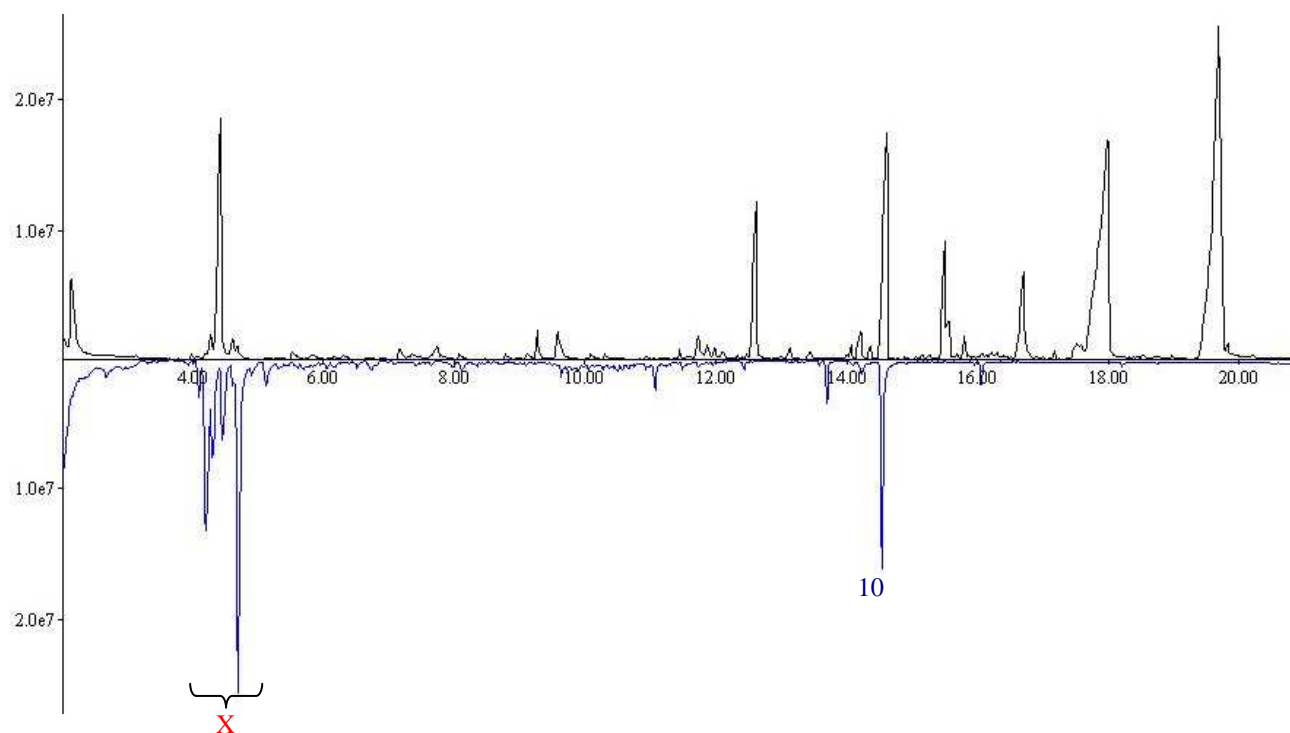


Figure 42: GC-MS chromatogram (TIC) of *Bulgaria* hydrodistillate (top trace) compared with that of Fraction 1 (for details, see text).

Peak numbers reference the corresponding substances from Table 7.

X = Impurities

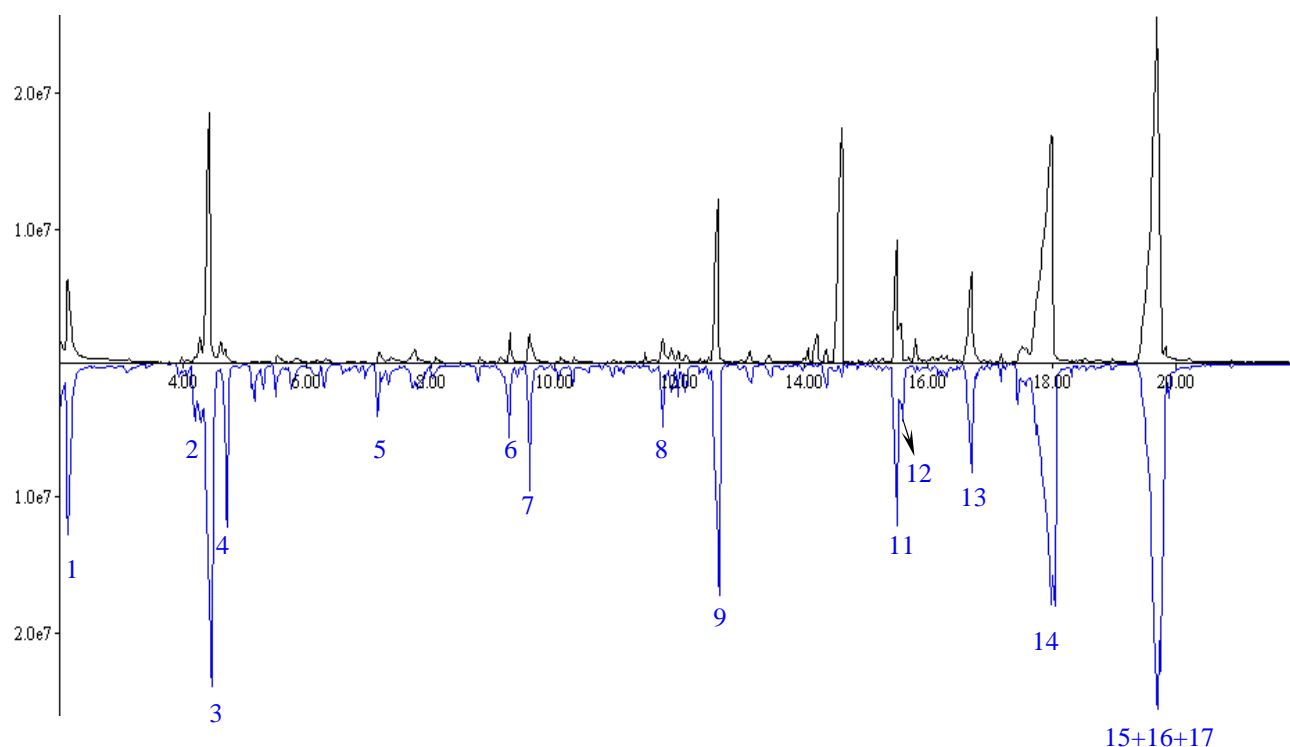


Figure 43: GC-MS chromatogram (TIC) of *Bulgaria* hydrodistillate (top trace) compared with that of Fraction 2 (for details, see text).

Peak numbers reference the corresponding substances from Table 7.

Massoia lactone was originally isolated from the bark of the Massoia tree (*Cryptocarya massoia*) [94]. This substance, which is used as a coconut flavouring, has also been identified in methanol extracts and the essential oil of *Baccharis magellanica* and *B. elaeoides* leaves. The essential oil obtained from both species contains about 9.2% massoia lactone and shows activity against *S. aureus* [95]. Massoia lactone also exerts a sedative effect; however, therapeutic use of this substance appears dubious since the effective dose is close to the toxic dose [96]. The second compound, 1,3-diphenyl-2-propanone (4.3% FID), is a chemical commonly used to add flavouring or fragrance by the food industry, but is not referred to in the literature as a naturally-occurring substance [97]. Since contamination of the hydrodistillate by the introduction of this substance can be excluded, the present work is the first research to demonstrate that 1,3-diphenyl-2-propanone is a natural compound.

3.2.7.2 Determination of the enantiomeric ratio for 1-octen-3-ol

As shown by the GC-MS chromatogram (Figure 35, lower trace, Peak 1), 1-octen-3-ol – also known as mushroom alcohol – is the dominant compound in *B. inquinans* pentane extracts. TLC analysis (Figure 44) also confirms that 1-octen-3-ol is a main component of *Bulgaria* ether extracts.

In order to estimate its enantiomeric composition, 1-octen-3-ol was isolated from a pentane extract on a preparative TLC plate developed in a toluene/ethyl acetate (95:5) solvent system and analysed by GC-MS (Figure 45). Following isolation, 1-octen-3-ol was transformed into a TFA (trifluoroacetic anhydride) derivative, which was then analysed by GC on a chiral stationary phase LIPODEX® E (octakis-(2,6-di-O-pentyl-3-O-butyryl)- γ -cyclodextrin). The derivatisation process is described in Section 5.6.8.1. Note: although König has published a standard method for the derivatisation of 1-octen-3-ol, certain useful simplifications were achieved in this process by the present research (see Section 5.6.8.1) [98, 99]. The derivatisation technique used also combines elements from a sample preparation method proposed by Tsutsumi *et al* [100].

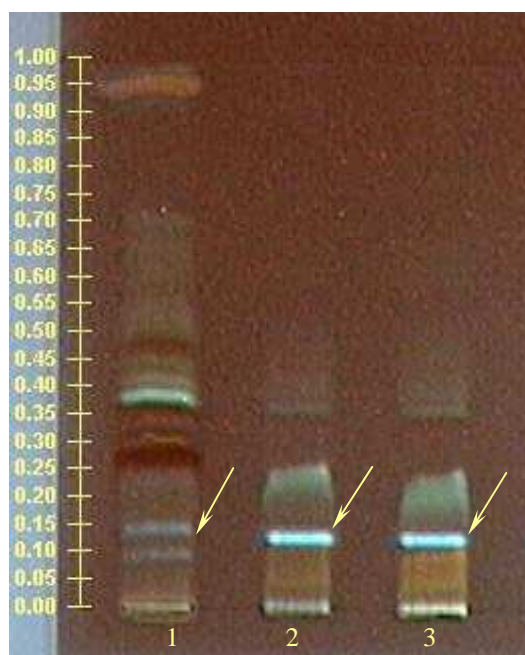


Figure 44: *B. inquinans* extracts developed on a silica gel TLC plate. Solvent system: toluene/ethyl acetate (95:5). Detection mode: UV light 366 nm. (1) hydrodistillate; (2) pentane extract; (3) ether extract. Yellow arrows indicate 1-octen-3-ol.

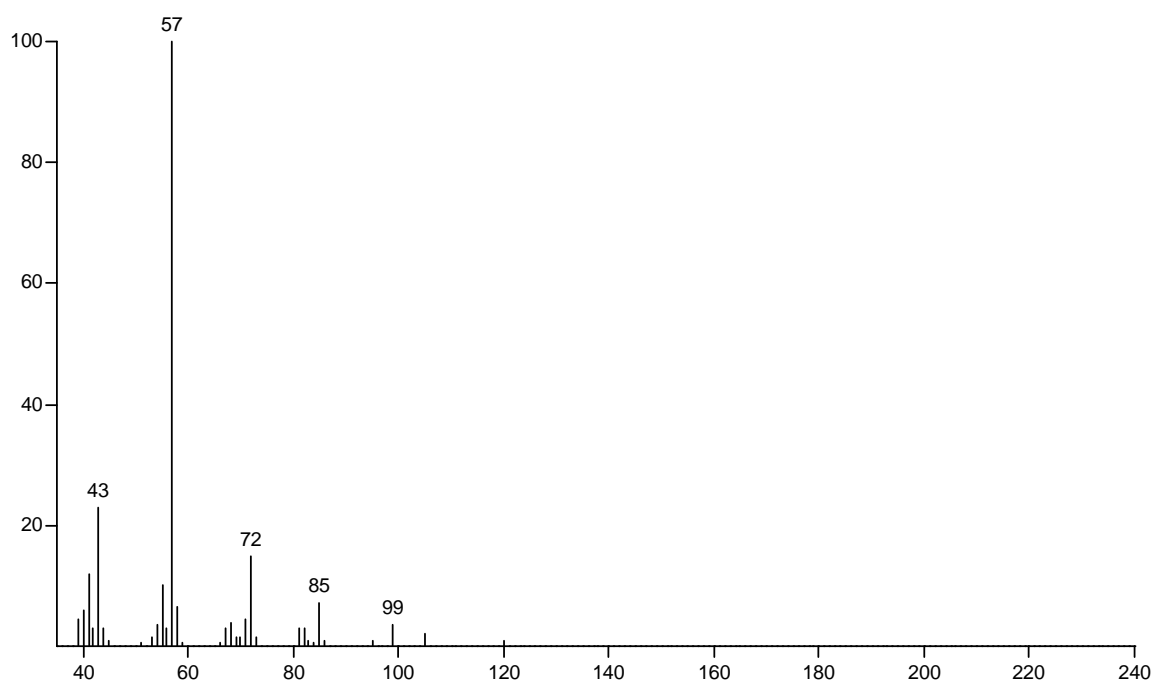


Figure 45: MS spectrum of 1-octen-3-ol, isolated from *B. inquinans* pentane extract (Figure 44, mode 2)

The first step was to use GC to analyse *S*-(+)- and *R*-(-)-1-octen-3-ol standards as TFA derivates, in order to establish their retention times (RT). The standards were injected both separately (Figure 46) and as a mixture (ratio 6:3) (Figure 47).

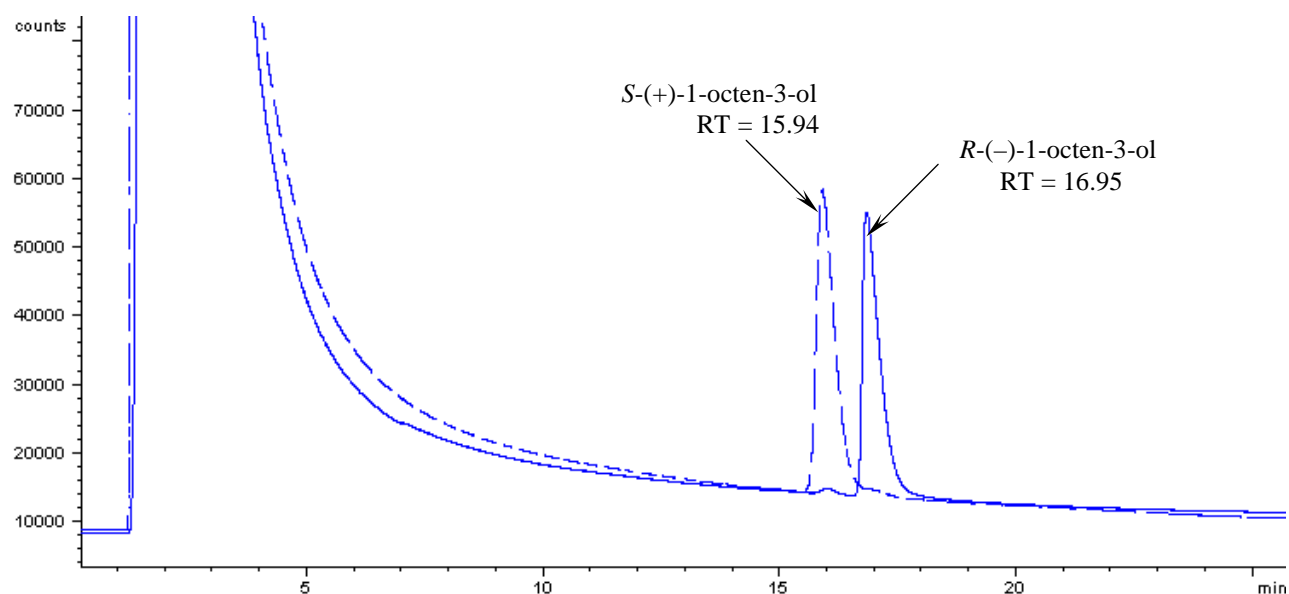


Figure 46: GC chromatogram of 1-octen-3-ol standards on a chiral stationary phase:

--- *S*-(+)-1-octen-3-ol
— *R*-(-)-1-octen-3-ol

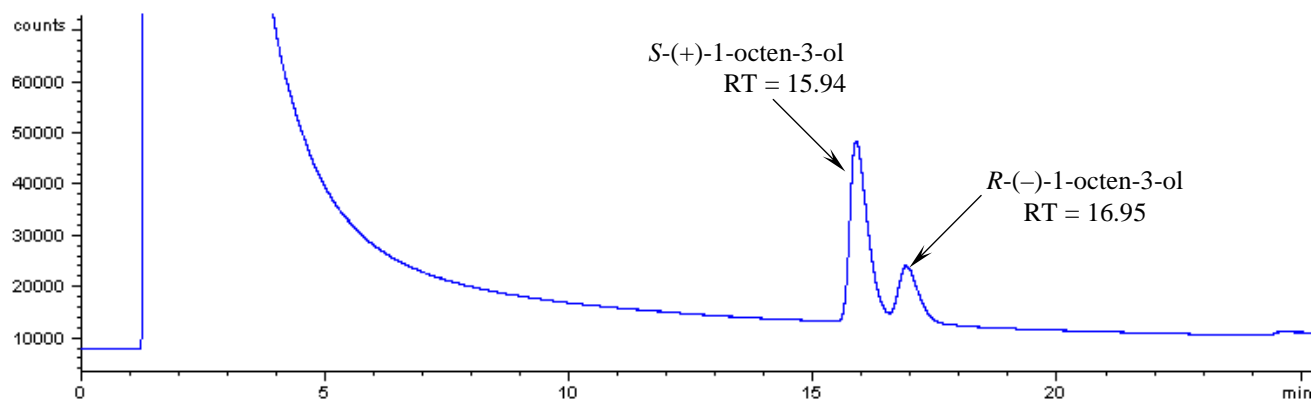


Figure 47: GC chromatogram of 1-octen-3-ol enantiomer mixture (*S*/*R*) (standards), ratio 6:3

For enantiomeric ratio determination of 1-octen-3-ol, experimentation showed that it was unnecessary to isolate this substance from the *Bulgaria* pentane extract: for derivatisation, the crude pentane extract was used and analysed in the same way using a chiral GC column. To confirm the results obtained, the pentane extract was co-injected with the *R*-(-)-1-octen-3-ol standard (Figure 48). No deviation was found. As is clearly shown by Figure 48, the result is identical to that found for the

hydrodistillate: both the hydrodistillate and pentane extract of *Bulgaria* contain 1-octen-3-ol enantiomers in an *R* to *S* ratio of 99:1.

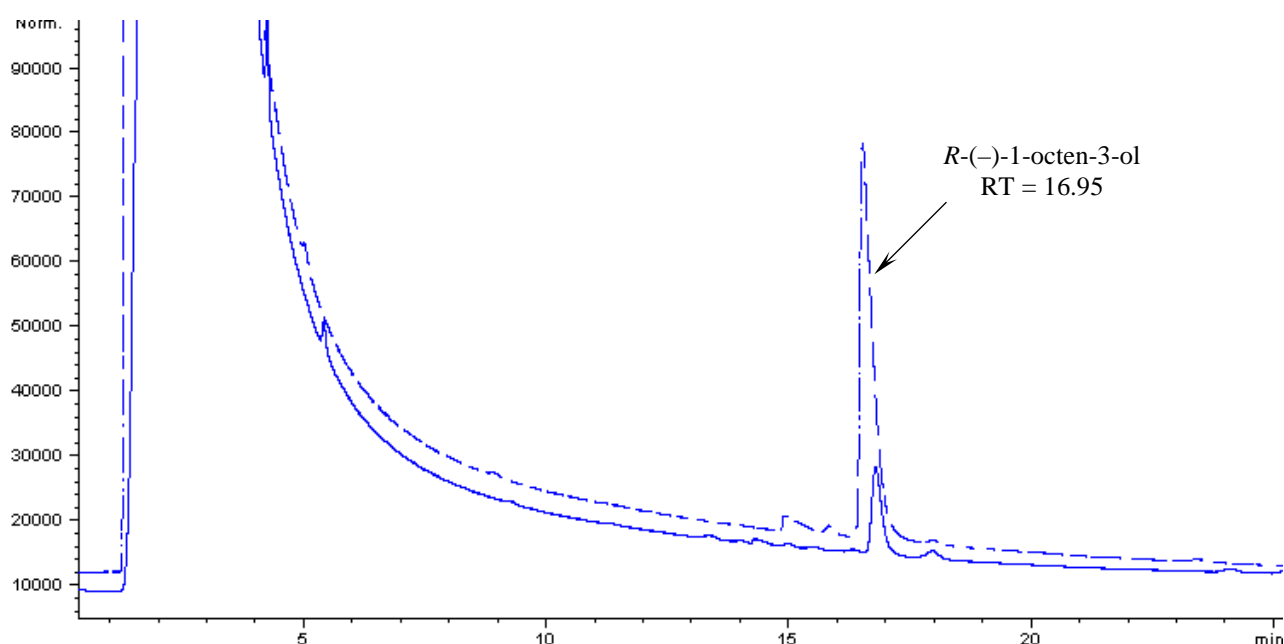


Figure 48: Detection of *R*-(-)-1-octen-3-ol in a *B. inquinans* pentane extract on a chiral phase
— *B. inquinans* pentane extract
- - - *B. inquinans* pentane extract co-injected with *R*-(-)-1-octen-3-ol (standard)

It was therefore established that *R*-(-)-1-octen-3-ol is both the dominant enantiomer within the *B. inquinans* hydrodistillate and the dominant substance in the pentane extract (Figure 35); this accords with the fact that *R*-octenol is a characteristic compound that has been isolated from many fungi species. The *S* enantiomer, on the other hand, is not so widespread in nature; it has been discovered in *Pycnoporus cinnabarinus* by Campos and apparently possesses a vegetable-like odour [101]. There may be a simple reason for the preponderance of *R*-octenol in nature, since *R*-octenol performs two highly contrasting yet very important biological tasks in fungi. First, in low concentrations, it attracts a greater variety of insect species than *S*-octenol; second, some fungi species produce high concentrations of *R*-octenol to defend against mycophagous insects [102, 103, 104], 105]. Moreover, the latter fact may explain why *B. inquinans* is apparently never colonised by any insect species.

The studies on *B. inquinans* volatiles may be summarised as follows:

- Fruit bodies of *B. inquinans* were found to produce traces of volatiles, the composition of which was investigated for the first time. A total of 16 substances were identified by GC-MS analysis combined with the co-injection of standards and the comparison of retention indices.
- Major volatile compounds are n-hexadecanoic acid (~16%), linoleic acid (~19%), linoleic acid ethyl ester and oleic acid ethyl ester (10%; all figures are proportions of the total hydrodistillate)
- A new antibacterial substance, bulgariafuran, was isolated from the hydrodistillate by preparative TLC (~3% FID). Bulgariafuran was detected only in the hydrodistillate (and not present in the pentane extract) and possessed strong antibacterial qualities. Accordingly, it is possible that the substance is not a genuine constituent, but is possibly formed by the fungus as a defensive response to damage or calefaction.
- Bulgariafuran and linoleic acid are the substances responsible for the antibacterial activity exhibited by the *Bulgaria* hydrodistillate
- *R*-(-)-1-Octene-3-ol (~4%) was determined as the dominant enantiomer by enantioselective GC; it was also the main component of the *B. inquinans* pentane extract and is a possible precursor of bulgariafuran.
- Finally, the present work is the first research to identify 1,3-diphenyl-2-propanone as a naturally-occurring substance

3.2.8 Cytotoxicity of *Bulgaria* extracts

The determination of cytotoxicity is a standard procedure and necessary in cases where a new substance with antibiotic properties is discovered. It is essential that cytotoxicity is very low. Experiments conducted by Stadler *et al* have described the cytotoxicity of bulgariolactones as moderate: the IC₉₀ towards murine L1210 cells (lymphocytic leukaemia) was found to be 10 µg/ml [58]. However, these experiments were conducted using bulgariolactones isolated from mycelial cultures and used a murine cell line (as noted above): the present research takes a different approach, utilising dried ether and methanol extracts, and testing cytotoxicity against human bladder cancer cells. Note that both extracts themselves exhibit strong antibiotic activity, with the ether extract also exhibiting haemolytic capability.

Cytotoxicity determination for *Bulgaria* extracts was carried out using a human bladder cancer test system (cell line 5637). For this experiment, dried methanol and ether extracts were used. Both extracts were diluted in DMSO. The first dilution was 200 mg/l and this solution was then successively diluted in seven further dilution phases (dilution step 1:3). Controls were pure DMSO and etoposide, diluted in DMSO at a concentration of 0.32 mg/l (see Section 5.7.4). The human bladder cancer cells were then incubated and cytotoxicity was measured using a special method incorporating the neutral red test according to Wende (method is patented, no further information available).

Results from the investigation of *B. inquinans* ether extract cytotoxicity are shown in Table 8. The second and third column contain figures showing the activity of the pure medium (control) and the medium mixed with DMSO (solvent control). Extract dilutions with an intact cell count of less than 75% are to be classified as toxic. Only average values should be considered for the definition of cytotoxicity.

The cytotoxic studies classify the *B. inquinans* ether extract as toxic. At a dilution equal to etoposide (0.3 mg/l), the ether extract shows stronger cytotoxic activity than etoposide itself. The IC₉₀ is approximately 10 µg/ml while the IC₅₀ is approximately 0.8 µg/ml: the strong cytotoxicity is probably due to the presence of azaphilones.

	Medium	Medium/ DMSO 1.125%	Etoposide 0.32 mg/l	Ether extract dilution						
				200 mg/l	64 mg/l	22 mg/l	7.4 mg/l	2.5 mg/l	0.8 mg/l	0.3 mg/l
Intact cells, %	100.88	53.78	83.13	0.00	0.00	0.00	not given	not given	not given	70.83
	97.01	48.15	77.15	0.00	0.00	0.00	8.79	24.96	50.44	75.75
	104.39	50.97	77.70	0.00	0.00	0.00	not given	28.82	59.58	76.45
	99.82	58.70	85.59	0.00	0.00	0.00	not given	34.45	61.69	77.86
	104.39	56.94	81.72	0.00	0.00	0.00	10.19	not given	65.20	78.91
	93.50	54.13	77.15	0.00	0.00	0.00	not given	28.82	56.06	75.75
Average	100.00	53.78	82.07	0.00	0.00	0.00	9.49	29.26	58.59	75.92
Average 2	76.89		82.07	24.75						
Standard deviation		3.51	3.95	0.00	0.00	0.00	0.70	3.38	5.04	2.55

Table 8: Determination of cytotoxicity of *B. inquinans* ether extract

Cytotoxicity was tested with human bladder cancer cells

A count of intact cells was used as a measure of toxicity. Extract dilutions with an intact cell count of less than 75% are classified as toxic. No intact cells were found at a dilution higher than 22 mg/l.

Note: dilution levels of 200 mg/l, 67 mg/l and 22 mg/l are not relevant for classifying an extract as toxic, nor do they exclude its subsequent use as an antibiotic. For details, see text.

As indirect proof of the cytotoxicity of the *Bulgaria* ether extract due to its azaphilone content, a methanol extract was also tested: this extract contains only traces of azaphilones (no yellow fluorescence in UV 366 nm or characteristic red colour in ammonia vapour and agar media were detected on TLC plates) (Figure 49).

The cytotoxicity test classifies the methanol extract as only slightly toxic (Table 9).

Since this experiment only revealed a weak toxic effect, it was therefore possible to conclude that azaphilones are the cytotoxic agents within the *Bulgaria* ether extract.

While the methanol extract showed strong antibacterial activity against *S. aureus*, as also seen in the ether extract, the mechanism of this activity clearly depends on substances belonging to compound classes other than azaphilones.

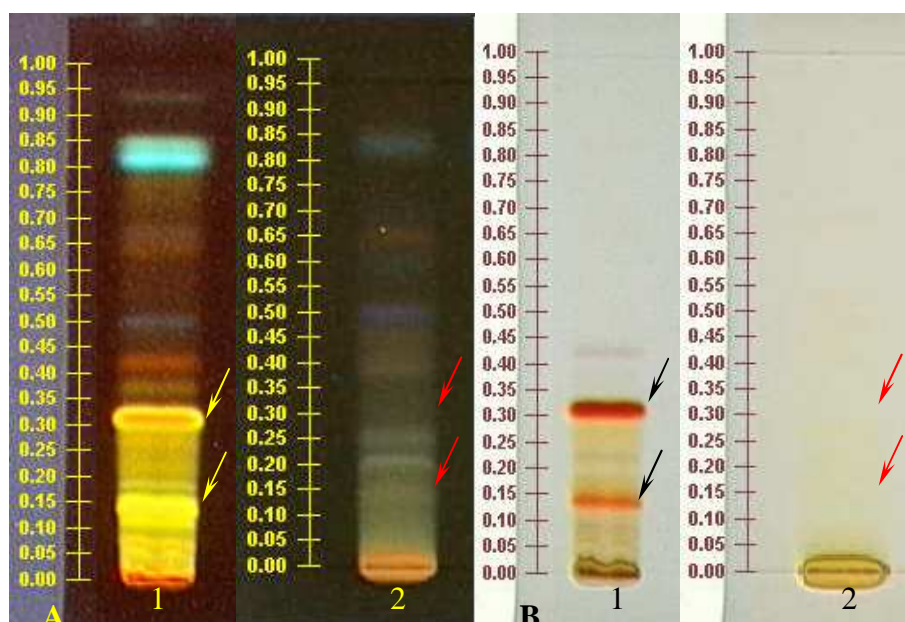


Figure 49: Comparison of azaphilone content in *B. inquinans* ether and methanol extracts
 Solvent system: toluene/acetone (7:3)
 Detection mode: (A) UV light 366 nm; (B) visible light after reaction with ammonia vapour
 (1) Ether extract; (2) methanol extract.

	Medium	DMSO 1.125%	Etoposide 0.32 mg/l	Methanol extract dilution						
				200 mg/l	64 mg/l	22 mg/l	7.4 mg/l	2.5 mg/l	0.8 mg/l	0.3 mg/l
Intact cells, %	97.99	50.41	76.51	0.00	19.70	87.87	101.01	94.62	98.52	99.23
	96.57	45.44	86.09	0.00	26.45	85.74	97.10	101.36	95.33	94.62
	104.73	50.77	88.22	0.00	24.67	87.87	101.72	100.30	99.59	95.33
	103.31	50.06	84.32	0.00	22.54	83.25	102.43	102.43	96.75	93.55
	105.80	51.12	82.90	0.00	25.38	87.87	98.17	102.07	102.43	94.62
	91.60	46.15	74.38	0.00	not given	85.74	96.04	89.29	89.29	93.55
Average	100.00	48.99	82.07	0.00	23.75	86.39	99.41	98.34	96.98	95.15
Average 2	74.50		82.07	71.43						
Standard deviation		2.29	5.00	0.00	2.39	1.70	2.42	4.82	4.10	1.93

Table 9: Determination of cytotoxicity of *B. inquinans* methanol extract

This table illustrates the low cytotoxicity of the *Bulgaria* methanol extract, presumably due to the very low azaphilone level. For further explanations, see Table 8

The results of bioactivity studies on *B. inquinans* can be outlined as follows:

- *B. inquinans* exhibits the strongest antimicrobial activity among the thirty species of fungi tested
- Both extracts examined (ether and methanol) exhibited very strong antibacterial activity in tests with *S. aureus*, as was also the case with the hydrodistillate. Strong cytotoxic and haemolytic activity was shown by the ether extract, with the methanol extract displaying weak cytotoxicity. Such antibacterial, haemolytic and cytotoxic biological activities as shown in the *Bulgaria* ether extract are likely to be dependent on the presence of azaphilones (bulgariolactones B and D).
- The present research represents the first occasion on which the antibacterial activity of a *B. inquinans* hydrodistillate was determined by the agar overlay technique on TLC. This activity was ascribed to two specific compounds: bulgariafuran and linoleic acid.

3.3 Investigations of *Meripilus giganteus*

3.3.1 Taxonomy of *Meripilus*

While the foundational fungi database lists 8 different *Meripilus* species, only *M. giganteus* occurs naturally within Europe [131]. Note that the “Dictionary of fungi” accepts only five separate *Meripilus* species [24]. A number of synonyms have been coined for *M. giganteus* (teleomorph name, anamorph connections unknown): MycoBank offers a compilation [131]. The better-known synonyms of *Meripilus giganteus* (Pers.) P. Karst. include *Boletus giganteus* Pers. (Basionym), *Grifola gigantea* (Pers.) Pilát and *Polyporus giganteus* (Pers.) Fr. Trivial names include Riesenporling (German), Polypore géant (French) and Giant Polypore or "Rooster of the Woods" [106, 107, 108, 109].

Phylum: Basidiomycota

Order: Polyporales

Family: Meripilaceae

3.3.2 Biological characteristics of *M. giganteus*

Fruit body: Cluster 50–80 cm broad or more; individual caps 5–20 cm across, fan-shaped, smooth, whitish becoming brownish with age, often radially streaked and concentrically zoned; the margin thin; pore surface whitish, rapidly becoming dirty tan and then bruising black when bruised or cut; pores small (3–5 per mm); tubes to 1 cm deep; stem whitish, tough, short, usually lateral; flesh white, soft and fibrous (Figure 50). Aggregates of caps can be up to 1 m in diameter and 70 kg fresh weight. Hyphal structure monomitic; generative hyphae lacking clamps.

Taste/odour: Mild, slightly sour. Edible. Like many polypores, it is one of those species for which allergies in some individuals are reported. Mild odour [110, 111].



Figure 50: Fruit bodies of *M. giganteus* growing in a habitat near Pinneberg (Germany)

Microscopy and spore print: Microscopic investigations of *M. giganteus* fruit bodies harvested for the present work showed nonamyloid, smooth, thin-walled and broadly elliptical spores (4.5–6 μm) (Figure 51, A). Subhymenium hyphae are thin-walled, 3–4 μm wide (Figure 51, B). In trama, hyphae are unbranched or sparingly branched, strongly thick-walled (skeletal hyphae), up to 9 μm wide (Figure 51, C). These major microscopic features accorded well with the literature [110, 111].

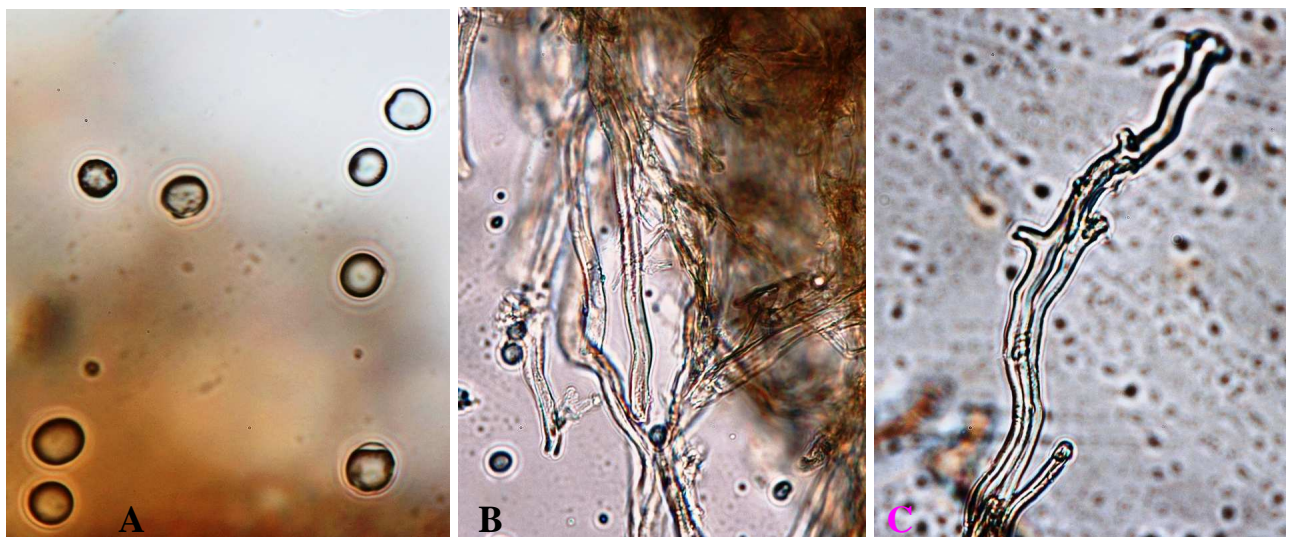


Figure 51: Microscopic preparation of *M. giganteus* (A) spores; (B) subhymenium hyphae; (C) skeletal hyphae in trama. For details, see text.

Ecology and habitat: Parasitic on living hardwoods and saprobic on the dead wood of hardwoods; causing a white rot. This fungus grows in large clusters of rosettes near the bases of trees; often reappearing in the same place in subsequent years. Can

be found at the base of deciduous trees or stumps or some distance from them arising from the roots, usually on beech but sometimes also on oak.

Season: autumn, annual.

Occurrence: Frequent.

Distribution: as a circumboreal distribution in the northern hemisphere.

3.3.3 Chemical composition and bioactivity – an overview

Articles about the bioactivity and chemical constituents of *M. giganteus* were scarce in the literature.

Seeger and Beckert discovered that the quantity of magnesium in dried fungus ranges from 1470 to 2240 mg/kg. Fresh fruit bodies contain 160–270 mg/kg of magnesium [112].

Results obtained by Slovenian scientists show that *M. giganteus* tends to accumulate K, P, N, Ca, Mg and Na independently from both its ecologic group affiliation and its habitat. *M. giganteus* was also found to be a superaccumulator of iron [113].

A homologous series of odd-numbered n-alkanes has been identified in fruit bodies of *Meripilus*. The presence of an unusually high content of even-carbon n-alkanes was also confirmed by column chromatography on silicic acid, preparative TLC on silica gel, IR-spectroscopy and gas-liquid chromatography [114].

A mixture of saturated and unsaturated fatty acids is found in methanol extracts of *M. giganteus* (Figure 52), as was ergosterol-5,8-peroxide; both the latter and the fatty acids were identified as immunosuppressive principles [45, 115]. However, when tested for immunosuppressive activity in a different assay system, various extracts of *Meripilus* were not active, in contrary to the pure substances (Figure 52) [116]. In these experiments, the assay was based on the ability of the extract to inhibit the binding of endotoxin to CD14⁺ cells and to influence LPS-induced release of proinflammatory cytokines (IL-1 β , IL-6, TNF- α), regulatory cytokines (IL-2, IL-4, IL-10, IFN- γ) and the release of reactive oxygen species; these are physiological responses consistent with hypersensitivity reactions, such as asthma.

Other authors reported on a homologous series of straight-chained saturated hydrocarbons with 22–26 and 29–32 C-atoms occurring in *Meripilus*: docosane ($C_{22}H_{46}$), tricosane ($C_{23}H_{48}$), tetracosane ($C_{24}H_{50}$), pentacosane ($C_{25}H_{52}$), hexacosane ($C_{26}H_{54}$), nonacosane ($C_{29}H_{60}$), triacontane ($C_{30}H_{62}$), hentriacontane ($C_{31}H_{64}$), dotriacontane ($C_{32}H_{66}$) [45, 115].

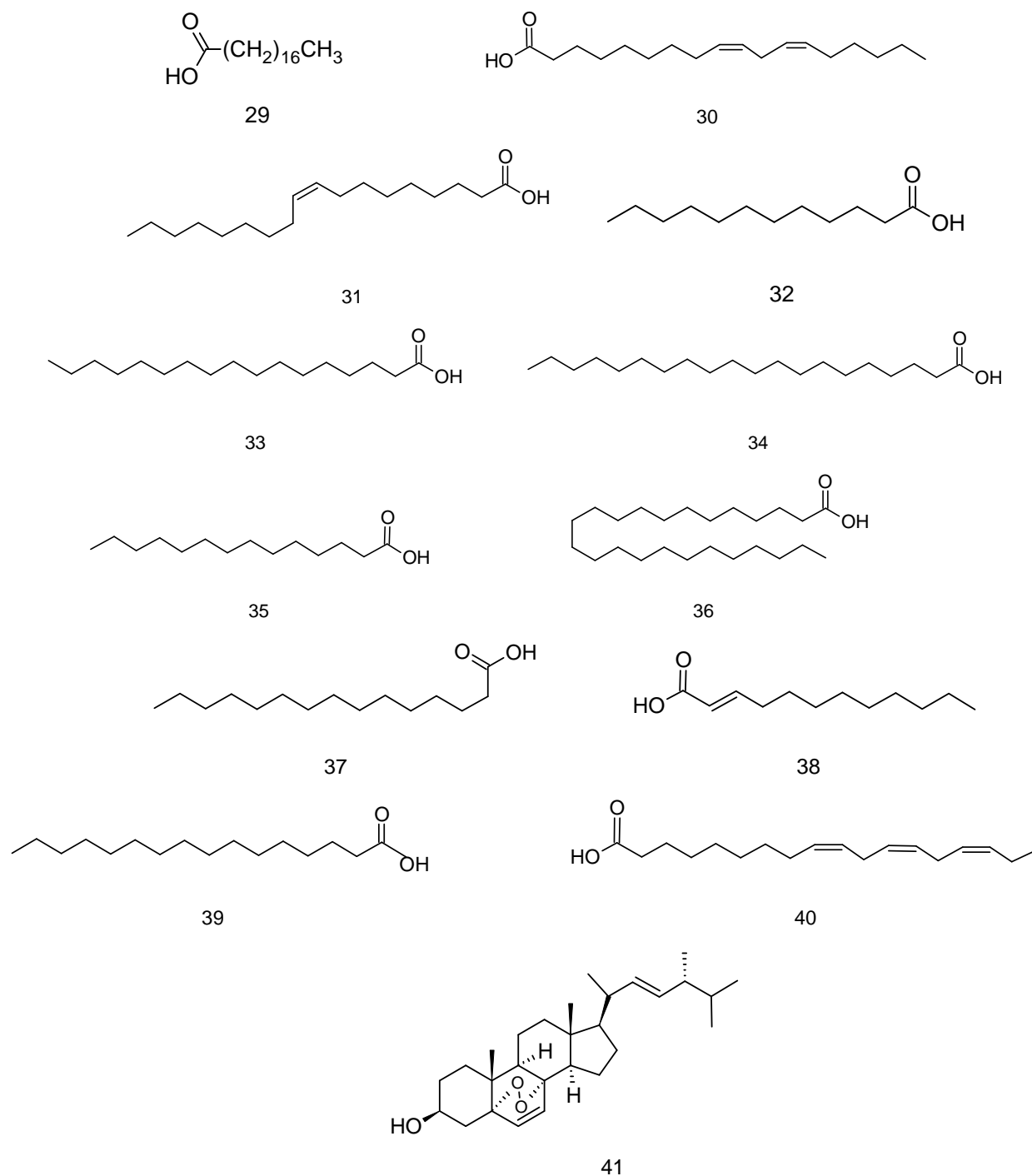


Figure 52: Compounds identified in *M. giganteus* methanol extract
 Stearic acid (29), linoleic acid (30), oleic acid (31), lauric acid (32), margaric acid (33), arachnic acid (34), myristic acid (35), lignoceric acid (36), pentadecanoic acid (37), lauroleic acid (38), palmitic acid (39), α -linolenic acid (40) and ergosterol-5,8-peroxide (41).

The enzyme with galactanase activity and its cDNA sequence from *M. giganteus* can be used in components for the digestion of material derived from plant cell walls in a number of industrial applications, such as detergents, food and feed additives, and the production of wine or juices [117].

A dichloromethane extract of *M. giganteus* displayed activity against *B. subtilis*, *E. coli* and *C. albicans* [40].

A crude methanol extract from *Meripilus* was shown to have significant cytotoxic activity against a murine cancer cell line 3LL (Lewis lung carcinoma), with an IC_{50} of $19.8 \pm 2.6 \mu\text{g/ml}$ [38].

3.3.4 Detection of bioactive compounds in *Meripilus* extracts

3.3.4.1 Determination of haemolytic TLC zones in ether extract

A literature review revealed no studies concerning the haemolytic activity of *M. giganteus*; and appropriate experiment was therefore conducted. Details of this haemolytic activity test (blood gelatine) have already been discussed in Section 3.2.4.1. For technical details, see Section 5.7.3.

Three clear haemolytic zones were observed on the TLC plate: their R_f values were found to be 0.24, 0.33 and 0.45 (Figure 53, mode 1). When comparing results of this blood gelatine test plate with the parallel TLC plate sprayed with anisaldehyde reagent and acquired in visible light, it was possible to establish the exact position of two bands: active band with $R_f = 0.45$ and band with $R_f = 0.31$. It was not possible to assign the third haemolytic zone ($R_f = 0.24$) to a distinct zone on the parallel TLC plate. No isolation was therefore attempted.

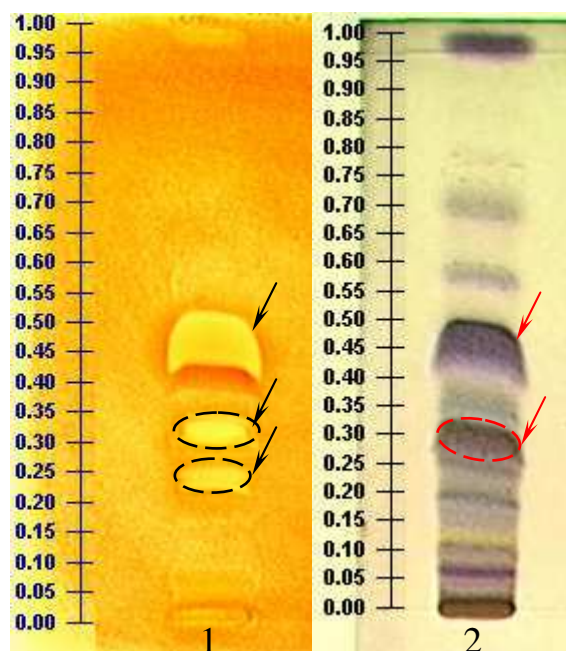


Figure 53: Haemolytic activity of *M. giganteus* ether extract (blood gelatine test)
 Solvent system: trichloromethane/toluene/methanol (8:1:1)
 Detection mode: (1) visible light (blood gelatine plate); (2) visible light (spraying with anisaldehyde reagent); arrows indicate the position of the haemolytic bands (for details, see text). The third haemolytic zone could not be clearly assigned to a distinct zone on (2).

3.3.4.2 TLC zones with antibacterial activity

The agar overlay method was applied to establish zones with antibacterial properties for further isolation in the *Meripilus* ether extract (Section 5.7.2). A TLC plate with an applied extract was developed in the solvent system trichloromethane/toluene/methanol (8:1:1), then dried and covered with a thin layer of warm agar containing an inoculum of *S. aureus*.

On evaluation, the results showed the presence of only one clear zone of bacterial growth inhibition, corresponding to the band with $R_f = 0.31$ (Figure 54) on the plate sprayed with anisaldehyde.

While collecting the fungus and conducting the extraction procedure, it was noticed that fruit bodies of *Meripilus* blacken fairly rapidly. To determine whether this phenomenon is associated with the formation of any antibacterial compounds – which may serve as defence mechanisms – a series of microbiological experiments with *Meripilus* ether extracts were carried out.

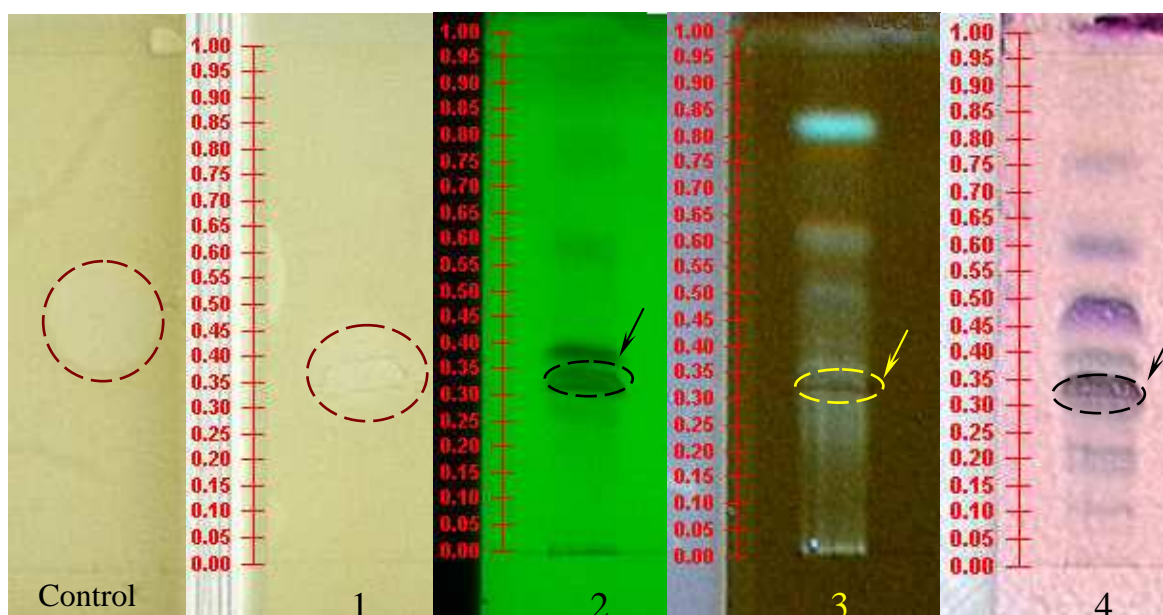


Figure 54: Detection of bacterial growth inhibition zones on TLC plates (agar overlay technique) in *M. giganteus* ether extract (for details, see text).

Solvent system: trichloromethane/toluene/methanol (8:1:1); control: ciprofloxacin 3.5 μg .
 Detection mode: (1) visible light (agar overlaid extract); (2) UV light 254 nm; (3) UV light 366 nm; (4) visible light (spraying with anisaldehyde reagent).

Two different kinds of ether extracts were therefore prepared. The first extract was obtained from freshly collected fungi, while the second was prepared from fungal material that had been mechanically damaged and left exposed to air at room temperature until the fruit bodies blackened. Both extracts were then tested for activity against *S. aureus*. As can be seen from Figure 55, there is an obvious difference between the activities in each extract: only the extract from blackened fungus exhibits any antibacterial activity. As described above, the zone of bacterial growth inhibition matched the band with $R_f = 0.31$: however, this bioactive band was not found in an ether extract prepared from fresh fruit bodies. Clearly, the compound responsible for antibacterial activity is formed after the fungus suffers mechanical damage.

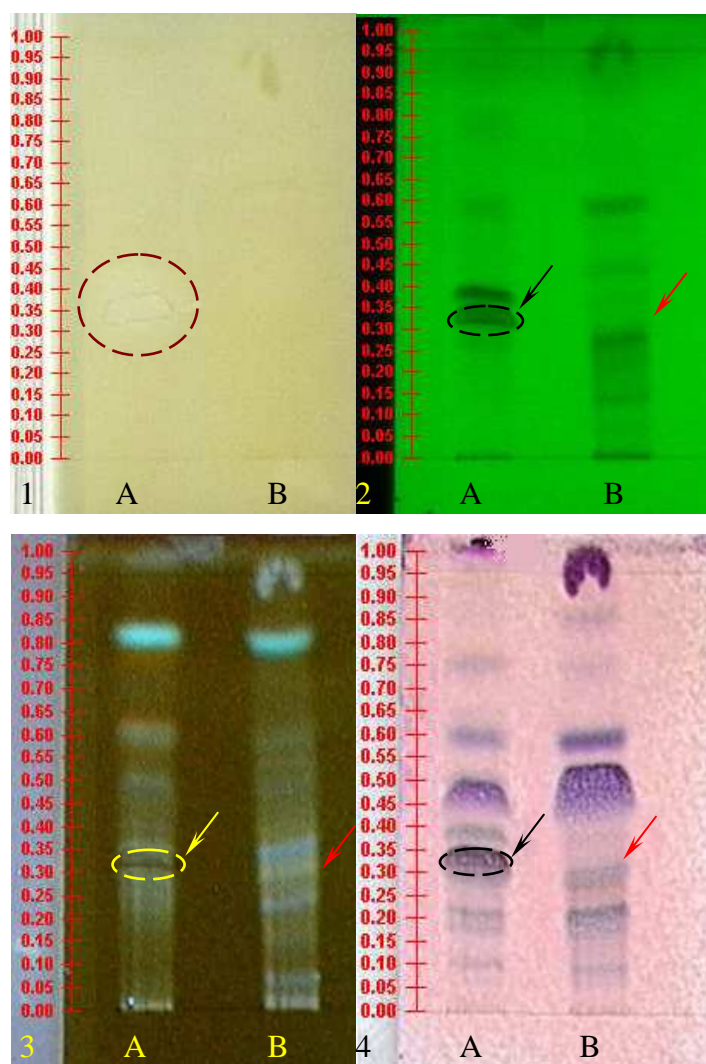


Figure 55: Detection of bacterial growth inhibition zones on TLC plates (agar overlay technique) in *M. giganteus* ether extracts (for details, see text).

(A) Ether extract from blackened fruit bodies, (B) ether extract from fresh fruit bodies

Solvent system: trichloromethane/toluene/methanol (8:1:1)

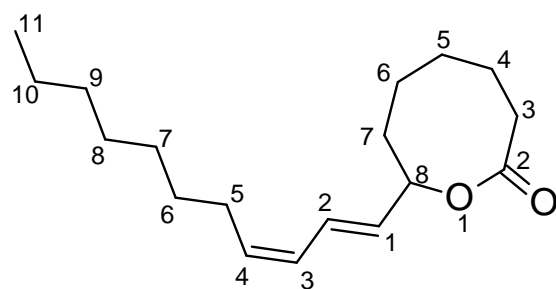
Detection mode: (1) visible light (agar overlay extract); (2) UV light 254 nm; (3) UV light 366 nm;

(4) visible light (spraying with anisaldehyde reagent). Yellow and black arrows mark the antibacterial band; red arrows indicate the absence of the antibacterial band.

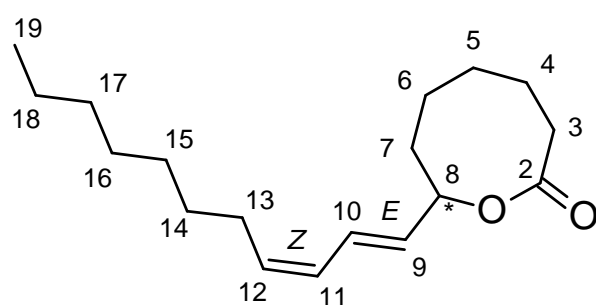
3.3.5 Isolation of antibacterial substances from *Meripilus* extract

The isolation of the antibacterial zone from the *Meripilus* ether extract was carried out on preparative TLC plates developed in the solvent system trichloromethane/toluene/methanol (8:1:1). The band with $R_f = 0.31$ in Figure 55 (detection mode: 4) was eluted from the plates with pure ether. Due to losses incurred during the purification process, only approximately 1 mg of this compound was obtained from the *Meripilus* ether extract (prepared from 2 kg of fungus). In order to increase the yield for structure elucidation, three further extractions were carried out. Each isolated portion of the antibacterial compound was first tested separately (MS and ^1H NMR) in order to prove the identity and antibacterial character of the isolated substances. Overall, the extractions yielded a total of 2.5 mg of isolated antibacterial compound.

3.3.5.1 Structure elucidation of meripiluslactone



IUPAC: 8-[(1E,3Z)-undeca-1,3-dien-1-yl]oxocan-2-one



Note: the numbering shown here follows the same system as used for bulgarialactones; this system will also be used in the subsequent discussion

Once isolated from TLC, as described above, the elemental composition of this compound was determined by fast atom bombardment MS (FAB) (MNBA matrix) analysis and TOF. The normal EI mass spectrum is depicted in Figure 56. The molecular peak m/z 278 fits with the supposed elemental composition: $\text{C}_{18}\text{H}_{30}\text{O}_2$.

From the chemical formula suggested for the molecular ion, it was possible to estimate that double-bond/ring equivalent is equal to 4. The results of ^1H and ^{13}C NMR spectroscopy are given in the Table 10.

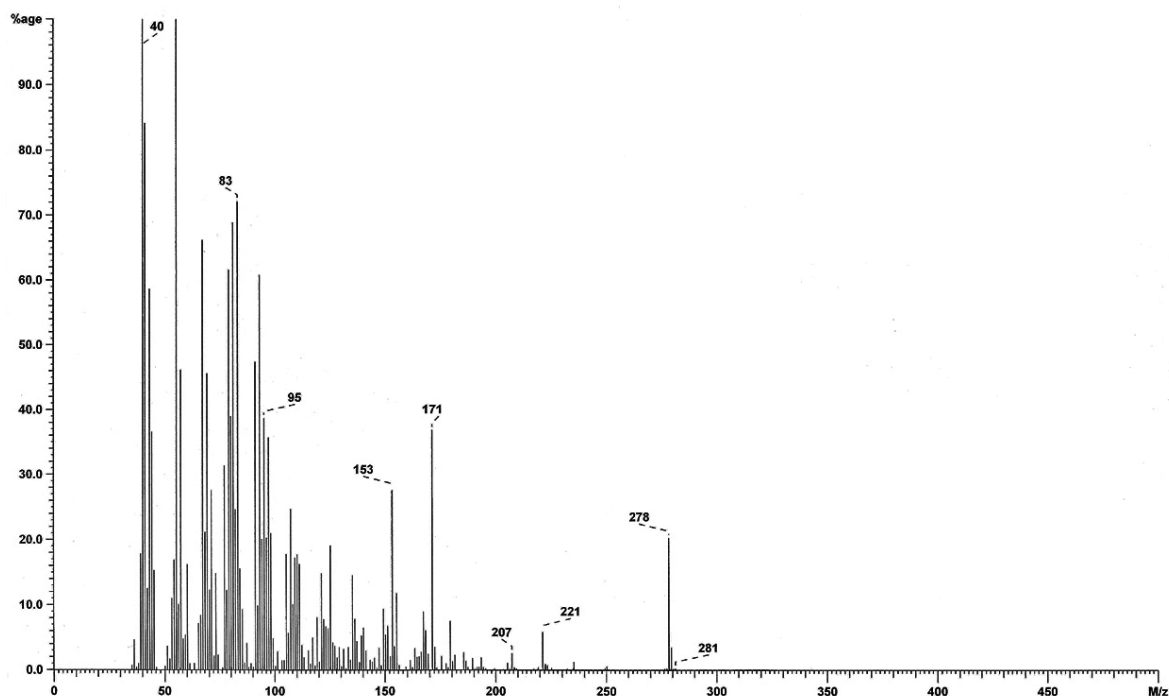


Figure 56: EI MS spectrum of meripiluslactone isolated from *M. giganteus* ether extract ($R_f = 0.31$, Figure 55, 4)

The ^{13}C spectrum (Appendix I, Figure 72) reveals 18 C-atoms, which is in accordance with the molecular formula. The spectrum also shows three double bonds, one of which is a carbonyl function ($\text{C}=\text{O}$). Consequently, this molecule possesses one ring.

From the HSQC spectrum obtained (Figure 58), it was possible to assign associated protons to all 18 C-atoms and thus discover their multiplicity. NMR data analysis revealed the presence of two double bonds ($\text{C}=\text{C}$) between $\delta = 127.7$ and 135.7 ppm, one $>\text{C}=\text{O}$ group at $\delta = 177.6$ ppm and a tertiary carbon ($>\text{CH}-$) at $\delta = 72.9$ ppm. The chemical shift of the latter suggests an adjacent heteroatom, i.e. oxygen.

The overall ^1H spectrum (Figure 57) reveals the presence of 4 protons (H-9 to H-12) in the olefinic region ($\delta = 4.5\text{--}6.5$ ppm), while 25 protons were located in the

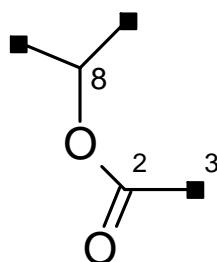
aliphatic region ($\delta = 0\text{--}2.5$ ppm). The range from $\delta = 0.5$ to 2.5 ppm encompasses a well-separated methyl group (H-19 at 0.89 ppm) and a broad, intense signal comprising seven $\text{CH}_2\text{--}$ groups (H-5, H-6, H-14, H-15, H-16, H-17 and H-18), as can be gathered from the expansion in Figure 57. One isolated proton signal was found at $\delta = 4.16$ ppm (CH–O region), which was split to a quadruplet.

Nr	$^{13}\text{C-NMR}$ (CD_3CN) by 100.13 MHz, ppm	C- atom	Structural element	$^1\text{H-NMR}$ (CD_3CN) by 400.13 MHz, ppm	H,H-coupling constants, Hz
1	14.0 <i>q</i>	19	–CH ₃	3H, 0.89 <i>t</i>	$^3J_{\text{H-19, H-18}} = 6.9$
2	22.5 <i>s</i>	17	–CH ₂ –	2H, 1.24-1.43 <i>br m</i>	
3	24.6 <i>t</i>	4	–CH ₂ –	2H, 1.63 <i>m</i>	
4	25,3 <i>t</i>	6	–CH ₂ –	2H, 1.24-1.43 <i>br m</i>	
5	27.7 <i>t</i>	13	–CH ₂ –	2H, 2.17 <i>m</i>	
6	28.9 <i>t</i>	5	–CH ₂ –	2H, 1.24-1.43 <i>br m</i>	
7	29.1 <i>t</i>	15-16*	–CH ₂ –	2H, 1.24-1.43 <i>br m</i>	
8	29.3 <i>t</i>	15-16*	–CH ₂ –	2H, 1.24-1.43 <i>br m</i>	
9	29.3 <i>t</i>	14	–CH ₂ –	2H, 1.24-1.43 <i>br m</i>	
10	31.4 <i>t</i>	18	–CH ₂ –	2H, 1.24-1.43 <i>br m</i>	
11	33.6 <i>t</i>	3	–CH ₂ –	2H, 2.35 <i>t</i>	$^3J_{\text{H-3, H-4}} = 7.5$
12	37.3 <i>t</i>	7	–CH ₂ –	2H _{a,b} , 1.53 <i>m</i>	
13	72.9 <i>d</i>	8	>CH–	1H, 4.16 <i>dd</i>	$^3J_{\text{H-8, H-9}} = 6.9$ $^3J_{\text{H-8, H-7a}} = 13.1$
14	125.9 <i>d</i>	10	=CH–	1H, 6.49 <i>dd</i>	$^3J_{\text{H-10, H-11}} = 11.0$ $^3J_{\text{H-10, H-9}} = 15.2$
15	127.7 <i>d</i>	11	=CH–	1H, 5.97 <i>t</i> or <i>dd</i>	$^3J_{\text{H-11, H-10}} = 11.0$ $^3J_{\text{H-11, H-12}} = 11.0$
16	133.1 <i>d</i>	12	=CH–	1H, 5.45 <i>m</i>	$^3J_{\text{H-12, H-11}} = 11.0$ $^3J_{\text{H-12, H-13}} = 7.75$ $^3J_{\text{H-12, H-10}} = 7.75$
17	135.7 <i>d</i>	9	=CH–	1H, 5.66 <i>dd</i>	$^3J_{\text{H-9, H-8}} = 6.9$ $^3J_{\text{H-9, H-10}} = 15.2$
18	177.6 <i>s</i>	2	>C=O	1, 6.69 <i>m</i>	

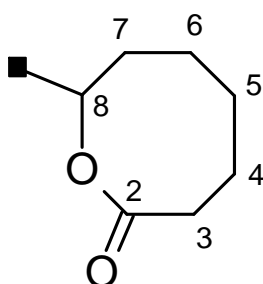
Table 10: NMR characteristics of meripiluslactone isolated from *Meripilus* ether extract

* Differentiation of these two carbon atoms proved impossible due to strong overlapping of the signals.

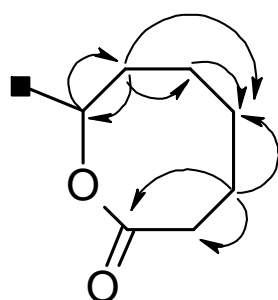
The carbonyl function (C-2) was chosen as a starting point for the structure elucidation: its characteristic chemical shift of $\delta = 177.6$ ppm suggests an adjacent heteroatom (oxygen). Indeed, an analysis of HMBC and COSY spectra, taken together with chemical shift values, strongly suggests that the heteroatom should be positioned between the carbonyl group and tertiary carbon. The following partial structure may therefore be postulated:



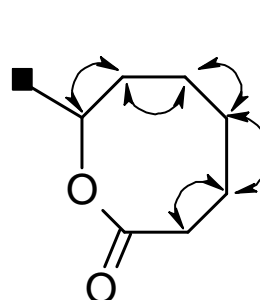
As regards chemical shift values, this structure also accords with the proton NMR data: for H-8, the shift value is 4.16 ppm, suggesting an adjacent oxygen; for H-3, a δ -value of 2.35 ppm can be observed, perfectly in accordance with an adjacent carbonyl function (Figure 57). Following analysis of the HMBC (Figure 73) and COSY spectra, it was possible to prove that this structure is a part of an eight-membered ring system. These results can be summarised in the following diagrams, which include the structural elements C-2–C-8 (for clarity, the number of couplings is reduced to the minimum count necessary):



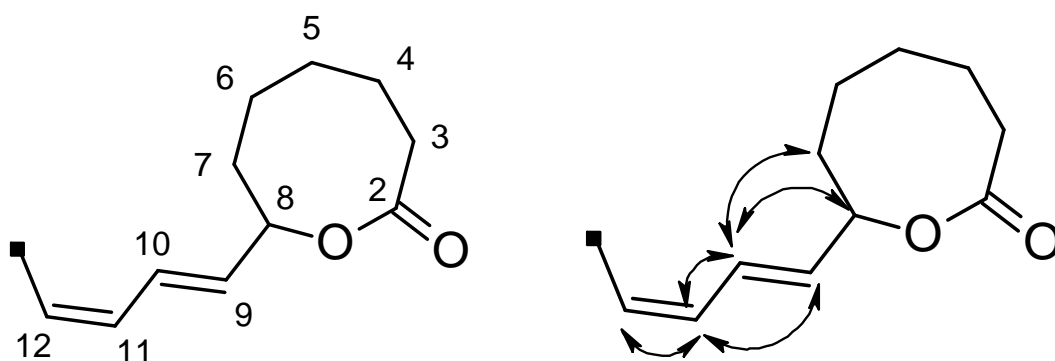
HMBC:



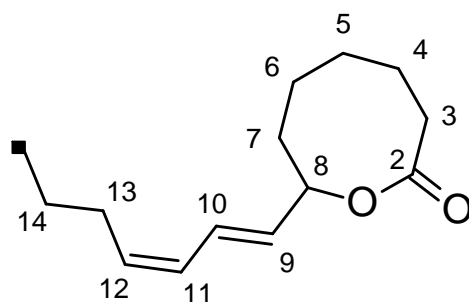
COSY:



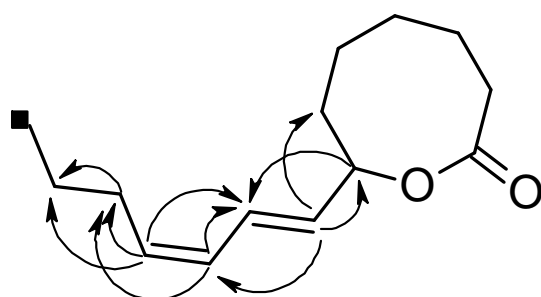
The proton belonging to the >CH— group at C-8 appears as a quadruplet that can be interpreted as a double doublet (Figure 57), showing a vicinal coupling to proton H-9 (${}^3J_{\text{H-8, H-9}} = 6.9$ Hz) and another vicinal coupling with one of the protons of H-7a,b (${}^3J_{\text{H-8, H-7a}} = 13.1$ Hz). As was determined from molecular modelling, the second proton H-7b should have an angle of about 90 degrees to H-8, thus explaining why no coupling constant could be registered (Karplus equation). A double doublet is therefore formed as a result of such a coupling. This is also confirmed by the proton spectrum, since H-9 clearly represents a double doublet (Figure 57), due to coupling with H-8 (${}^3J_{\text{H-9, H-8}} = 6.9$ Hz) and the olefinic H-10 (${}^3J_{\text{H-9, H-10}} = 15.2$ Hz). The same is essentially true for the adjacent olefinic proton H-10 at 6.49 ppm (Figure 57), whose the signal is also split into a double doublet (${}^3J_{\text{H-10, H-11}} = 11.0$ Hz and ${}^3J_{\text{H-10, H-9}} = 15.2$ Hz). The same situation also applies to the proton H-11 at 5.97 ppm, since it also represents a double doublet (${}^3J_{\text{H-11, H-10}} = 11.0$ Hz and ${}^3J_{\text{H-11, H-12}} = 11.0$ Hz); here, however, the two inner signals overlap, resulting in a triplet (Figure 57). Further detailed analysis showed that this proton was a part of a conjugated system consisting of two double bonds and comprising C-atoms from 9 to 12 (Figure 73). The coupling of protons at C-9 and C-10 (${}^3J = 15.2$ Hz) indicates a trans-configuration, whereas the two protons of the double bond between C-11 and C-12 couple with 10.9 Hz, which is the typical value of a cis-configuration. The couplings between protons detected in NOESY spectrum data also favour a configuration of 9*E*,11*Z*, as had been assumed from the coupling constant values.



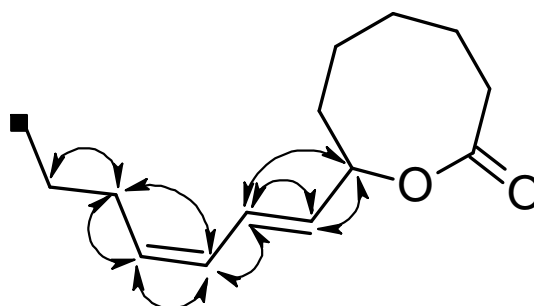
From an analysis of the HMBC spectrum (Figure 73), it was also possible to determine the next two $-\text{CH}_2-$ groups (C-13 and C-14), yielding the following structure:



HMBC:

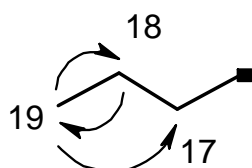


COSY:

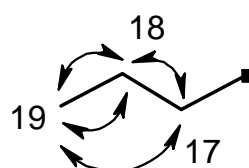


Further elucidation proved difficult, since it faced the obstacle of overlapping signals of the methylene groups C-15 and C-16. Accordingly, another approach was made, starting from the terminal $-\text{CH}_3$ group. It is important to note that the proton spectrum revealed the absence of further methyl groups; further branching in this chain could therefore be excluded. An analysis of the HMBC spectrum (Figure 73) established strong coupling between the carbon atoms at $\delta = 14.0$ ppm (C-19) and 31.4 ppm (C-18), and also between the carbon atoms at $\delta = 31.4$ ppm (C-18) and 22.5 ppm (C-17). As expected, the proton spectrum shows a characteristic triplet of the terminal $-\text{CH}_3$ group at 0.89 ppm, which derives from coupling with H-18 ($^3J_{\text{H-19, H-18}} = 6.9$ Hz). COSY spectrum data confirmed couplings for matching protons:

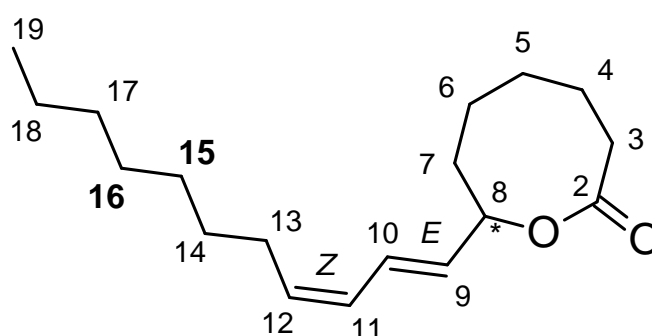
HMBC:



COSY:



However, the structure elucidation from this site on the molecule also became difficult, since H-15 and H-16 present as a broad multiplet and their signals overlap strongly. The proton spectrum (Figure 57) also shows a wide multiplet between 1.23 and 1.42 ppm, which indicates the presence of methylene groups that should form an alkyl chain [82, 118]. As a result of strong overlap between proton signals and very close carbon shift values, it was impossible to establish the exact positions of C-15 and C-16; nonetheless, construction of the complete structure was still possible (atoms shown in bold type remain undifferentiated):



The chirality of the C-8 atom could not be established from the measurements obtained.

NMR prediction software was employed to provide an additional check on the accuracy of the new structure, namely the applications UpSol and ACD Labs. Table 11 presents relative shift values predicted by each package, together with results obtained experimentally. As can be seen from the table, the suggested structure accords well with the data obtained from the prediction software. Major deviations were registered in only three instances: however, these deviations were not confirmed by both prediction applications. NMR prediction software was also used in order to confirm proton spectra. There were no deviations found between signal clusters and their assignment to carbon atoms in the predicted spectra and the spectra obtained experimentally.

No.	¹³ C NMR (CD ₃ CN) by 100.13 MHz, ppm	C- atom	¹³ C NMR prediction UpSol, ppm	¹³ C NMR prediction ACD/ Labs, ppm
1	14.0	19	14.01	14.1
2	22.5	17	23.1	31.7
3	24.6	4	25.1	23.9
4	25.3	6	24.1	24.7
5	27.7	13	30.4	27.6
6	28.9	5	29.8	26.6
7	29.1	15-16	30.4	29.3
8	29.3	15-16	30.4	29.3
9	29.3	14	30.4	30.4
10	31.4	18	32.5	22.8
11	33.6	3	33.7	33.9
12	37.3	7	34.4	33.0
13	72.9	8	78.4	72.6
14	125.9	10	128.0	132.5
15	127.7	11	128.7	127.2
16	133.1	12	130.3	136.6
17	135.7	9	133.6	133.4
18	177.6	2	172.0	172.9

Table 11: Comparison of meripiluslactone NMR data with data generated by NMR prediction software. Major prediction differences are shown in bold type.

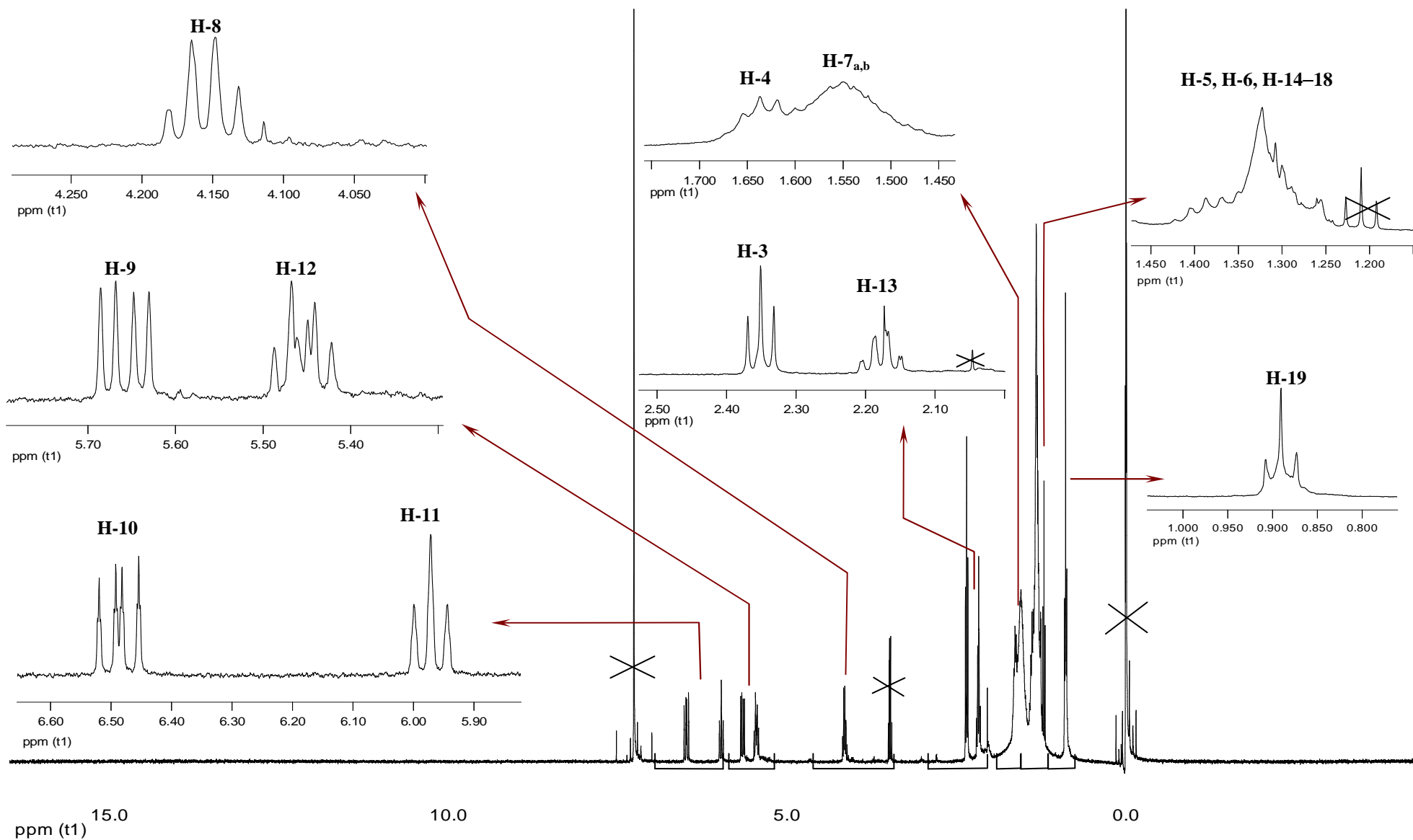


Figure 57: ^1H NMR spectrum of meripiluslactone isolated from *Meripilus* ether extract. Impurities are struck through, as are solvent and TMC signals.

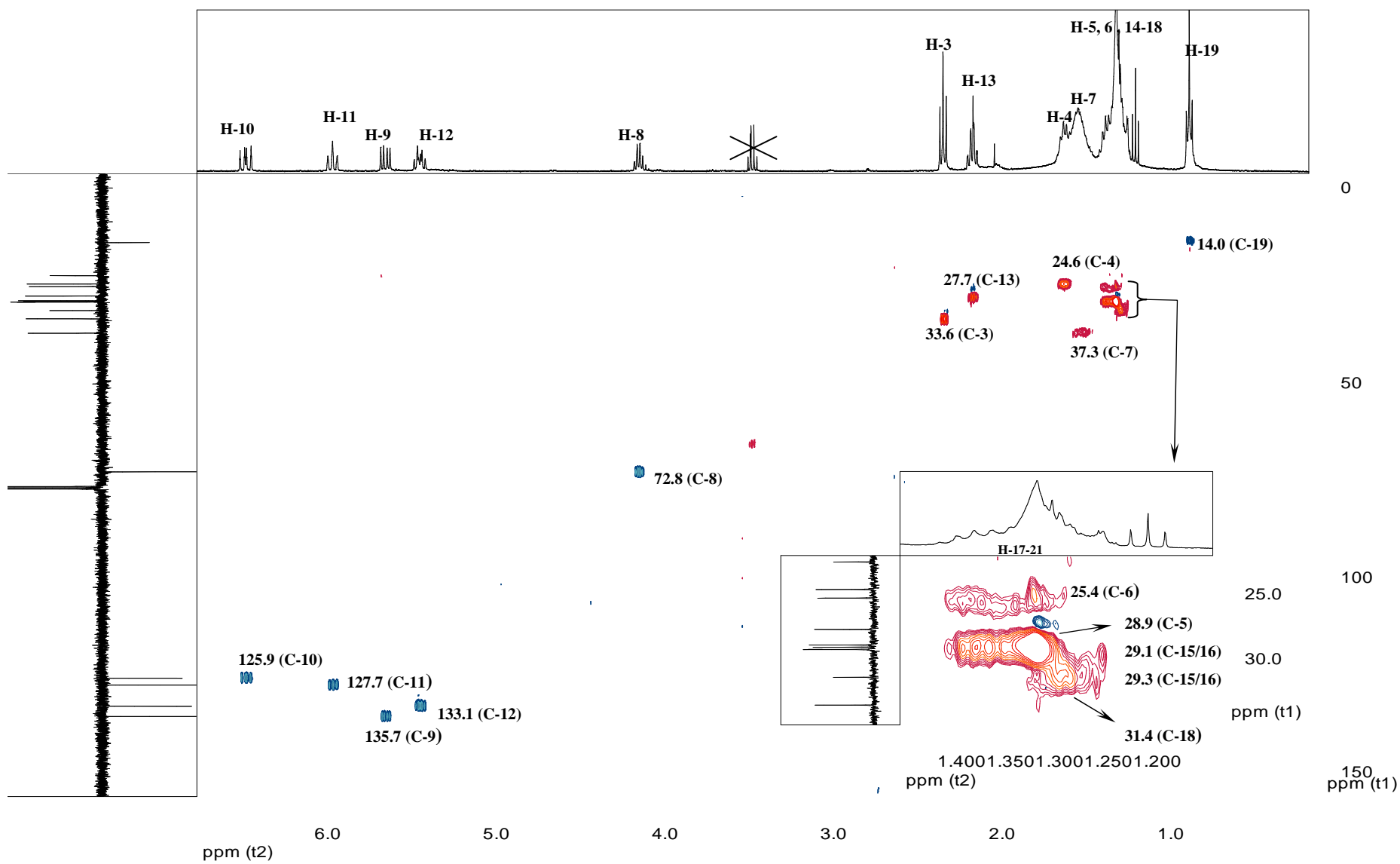
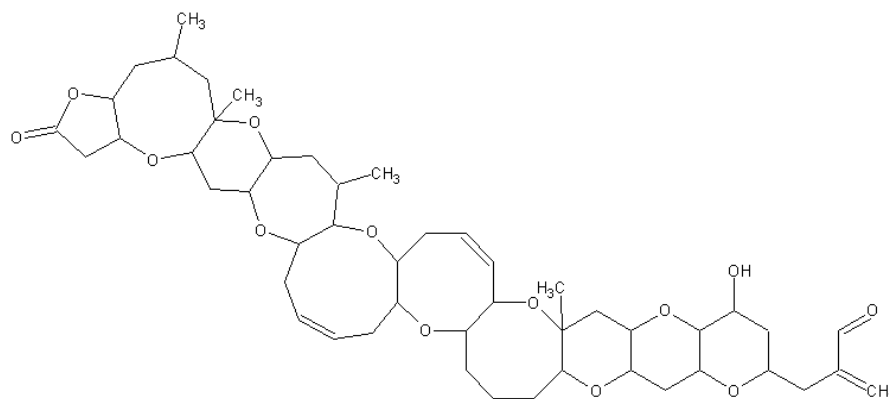


Figure 58: HSQC NMR spectrum of meripiluslactone isolated from *Meripilus* ether extract

The trivial name meripiluslactone is proposed for the substance 8-[(1*E*,3*Z*)-undeca-1,3-dien-1-yl]oxocan-2-one as isolated from *Meripilus*. This substance is a member of the oxocanes, i.e. a saturated eight-membered heterocycle with seven carbon atoms and an oxygen. More precisely, the substance is an oxocanelactone and thus a new compound, i.e. not only a new *Meripilus* constituent, but also a new naturally-occurring substance. Indeed, even the basic oxocanelactone skeleton has not been discovered in nature: the only natural compound group that contains oxocane (as a substructure element) is the brevetoxin group, but this group does not contain oxocanelactone. The brevetoxins are a group of polyether ladder toxins with a linear series of transfused ether rings of varying sizes from 5 to 9 members with assorted appended methyl and hydroxyl substituents:

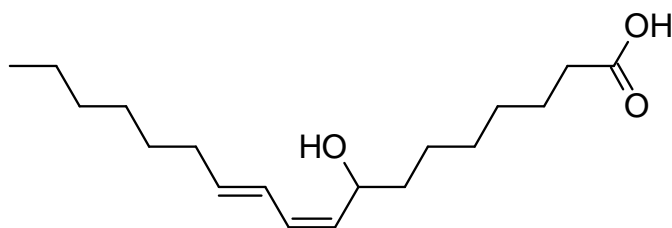


Brevetoxins are highly toxic metabolites of *Karenia brevis* – a marine dinoflagellate commonly found in the Gulf of Mexico: this microscopic, single-celled, photosynthetic organism is known to cause the infamous ‘red tide’ phenomenon responsible for massive fish kills, and is also an agent of neurotoxic shellfish poisoning and bronchial irritation or asthma-like symptoms in humans [119].

The new oxocanelactone meripiluslactone shows strong bioactivity, namely haemolytic and antibacterial effects. It is also clear that meripiluslactone is formed by the fungus following mechanical damage; this fact may be interpreted as a defence mechanism.

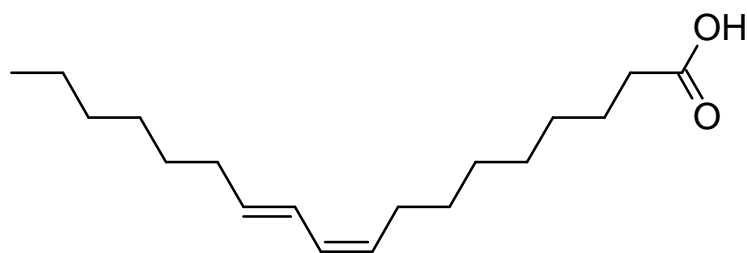
Analogous to the formation of cyclic lactones in flavourings and other chemicals as described in food chemistry, utilising hydroxy fatty acid as a precursor,

one may propose the linoleic acid derivative 8-hydroxy-(9*E*,11*Z*)-octadecadienoic acid as a precursor to meripiluslactone:



To date, this particular unsaturated hydroxy acid has been described for only a single species of fungus: it has been isolated from the fruit body and mycelium of the parasitic macro fungus *Sparassis crispa* (Sparassidaceae); experimentation indicates it may inhibit diabetes mellitus in mice [120].

Less specifically, one may also propose (9*E*,11*Z*)-octadecadienoic acid (conjugated linoleic acid, CLA) as a precursor to meripiluslactone. However, while CLA has indeed been isolated from fungi in rare cases (*Agaricus bisporus* and *A. blazei* only [122, 123]), its presence in fungi (or plants) is remarkable, since fatty acids with conjugated diene systems have previously been described only as constituents of ruminant animal tissue. Here, it is formed as an intermediate or by-product in the biohydrogenation of linoleic acid by microorganisms in the rumen; 9-*cis*,11-*trans*-octadecadienoic (rumenic) acid is the predominant conjugated linoleic acid (CLA) isomer in milk and beef:



In addition, CLA also has a number of beneficial medical properties, and has been proven to exhibit anti-cancer properties [121 122, 123].

To provide experimental support for the above proposal, an attempt was made to isolate the possible precursor of meripiluslactone from the ether extract. It was observed that the ether extract prepared from intact *Meripilus* fruit bodies contained a greater amount of a constituent with $R_f = 0.47$ (Figure 59, B). In contrast, the extract from blackened (damaged) fruit bodies contained less of this compound, but a new band (meripiluslactone) with $R_f = 0.31$ emerged (Figure 59, A). The band located at $R_f = 0.47$ may therefore be a precursor of meripiluslactone (8-hydroxy-(9*E*,11*Z*)-octadecadienoic acid or CLA). The band with $R_f = 0.47$ was isolated from preparative TLC plates, but its severe instability precluded further successful analysis.

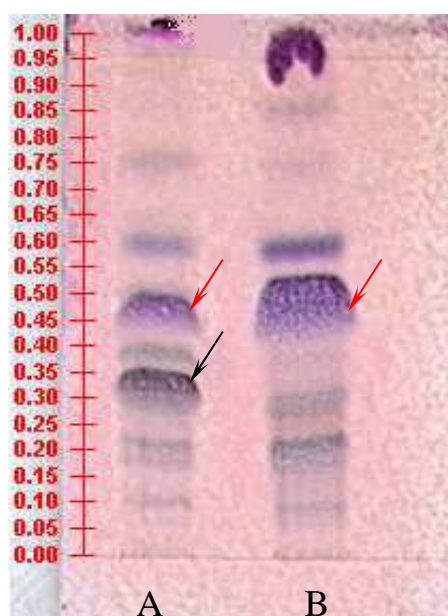


Figure 59: Detection of the proposed precursor of meripiluslactone on TLC plates in ether extracts (for details, see text).

(A) Ether extract from blackened fruit bodies; (B) ether extract from fresh fruit bodies

Solvent system: trichloromethane/toluene/methanol (8:1:1)

Detection mode: visible light (spraying with anisaldehyde reagent). Red arrows indicate the possible precursor zone; the black arrow indicates meripiluslactone.

Investigations of bioactive compounds from *M. giganteus* ether extracts can be summarised as follows:

- It was established that only the extracts from blackened *Meripilus* fruit bodies (old, damaged, heated, etc.) are biologically active. The ether extract contained a single antibacterial substance.
- The compound responsible for this antibacterial effect was isolated and identified as 8-[(1*E*,3*Z*)-undeca-1,3-dien-1-yl]oxocan-2-one. It is not only a new natural constituent, but even represents a new compound class – the oxocanelactones. The trivial name meripiluslactone is proposed for this new substance.
- The fact that meripiluslactone was detected only in blackened fungi suggests that it may be formed as a defensive response to the fungus suffering mechanical damage; it was shown that intact fruit bodies of *Meripilus* do not contain meripiluslactone.
- 8-hydroxy-(9*E*,11*Z*)-octadecadienoic acid is proposed as a precursor to meripiluslactone

3.3.6 Volatiles of *Meripilus* fruit bodies

Since antibacterial properties had been discovered in volatiles from *B. inquinans*, the decision was therefore made to focus on *Meripilus* volatiles, particularly since their composition has not been studied to date.

Since results from preliminary screening had shown antibacterial activity for a *Meripilus* hydrodistillate, the chemical composition of its hydrodistillate was investigated using GC and GC-MS methods. Identification of compounds was performed by comparing the mass spectra with those given by several electronic libraries. Additionally, retention indices of reference compounds were used, and co-injection of commercially-available standards was also performed.

The results of these analyses are summarised in Figure 60 (TIC) and Table 12. Overall, a total of 12 constituents were identified, representing 45.09% of all volatiles. As can be seen from Table 12, the major components of the *M. giganteus* hydrodistillate are linoleic acid (~14%), n-hexadecanoic acid (~8%), linoleic acid ethyl ester (~7%), n-hexadecanoic acid ethyl ester (~2%) and *E*-nerolidol (~2%; all figures are proportions of the total hydrodistillate). The occurrence of 18 unusual and unidentified N-containing compounds also deserves mention: these represent 21.15% of the total volatiles, thus forming the second-largest group after volatiles derived from fatty acid metabolism (~42%). It is remarkable that *E*-nerolidol (~2%) was the only typical volatile constituent from the sesquiterpene group found in the *M. giganteus* hydrodistillate.

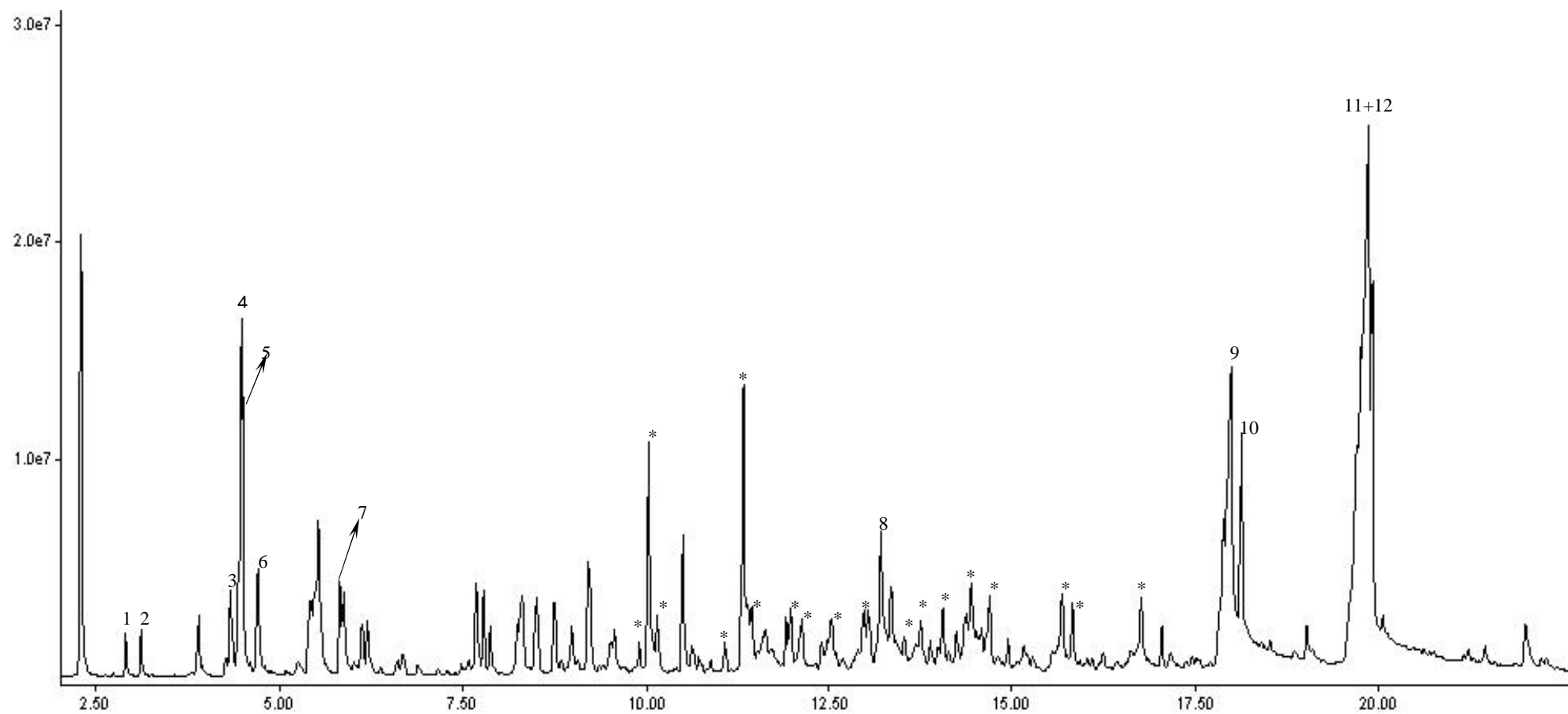


Figure 60: GC-MS chromatogram (TIC) of *M. giganteus* hydrodistillate
N-containing substances are starred; peak numbering refers to Table 12

Peak No.	Substance	GC-MS				Identified by
		Retention Time	Kováts retention index	TIC, %	[M+]	
1	1-Hexanol	2.89	847	0.43	102	EI-MS/RI
2	2-Heptanone	3.12	867	0.48	114	EI-MS/RI
3	1-Hepten-3-one	4.33	956	1.07	112	EI-MS/RI
4	1-Octen-3-ol	4.48	967	3.92	128	EI-MS/RI
5	3-Octanon	4.51	968	1.68	128	EI-MS/RI
6	3-Octanol	4.71	982	1.77	130	EI-MS/RI
7	2-Octen-1-ol	5.82	1052	1.26	128	EI-MS
8	<i>E</i> -Nerolidol	13.21	1552	2.39	222	EI-MS/RI Co-injection
9	<i>n</i> -Hexadecanoic acid	17.98	1966	7.85	256	EI-MS/RI
10	<i>n</i> -Hexadecanoic acid ethyl ester	18.12	1978	2.37	284	EI-MS/RI
11	Linoleic acid	19.85	2154	14.45	280	EI-MS/RI Co-injection
12	Linoleic acid ethyl ester	19.92	2160	7.42	308	EI-MS/RI

Table 12: Chemical composition of *M. giganteus* hydrodistillate

3.3.7 Antibacterial activity of *Meripilus* hydrodistillate

As mentioned, previously, preliminary agar diffusion tests showed *M. giganteus* volatiles to be active against *S. aureus* (see Section 3.1.1). A decision was therefore made to apply the agar overlay technique to the hydrodistillate (HD) in order to identify the substances responsible for this effect. TLC plates with applied HD were developed in a toluene/ethyl acetate (95:5) solvent system.

Two zones of bacterial growth inhibition were discovered: one matched a band with $R_f = 0.40$, while the second growth inhibition zone was more widespread (from $R_f = 0$ to $R_f = 0.25$) and included several very faint bands visible in UV light (Figure 1, modes 2 and 3). Only spraying with anisaldehyde reagent clearly revealed the band (not visible in UV light) which was responsible for antibacterial activity (Figure 61, mode 4). The activity of this band was comparable to the control (ciprofloxacin) (Figure 61, 1a).

Since both active bands were well-separated on the TLC plate and easily detected in visible light after spraying with anisaldehyde reagent, the decision was therefore

made to isolate these bands from the preparative TLC plates. As far as is known, this research constitutes the first occasion on which the agar overlay technique was applied to *M. giganteus* hydrodistillate.

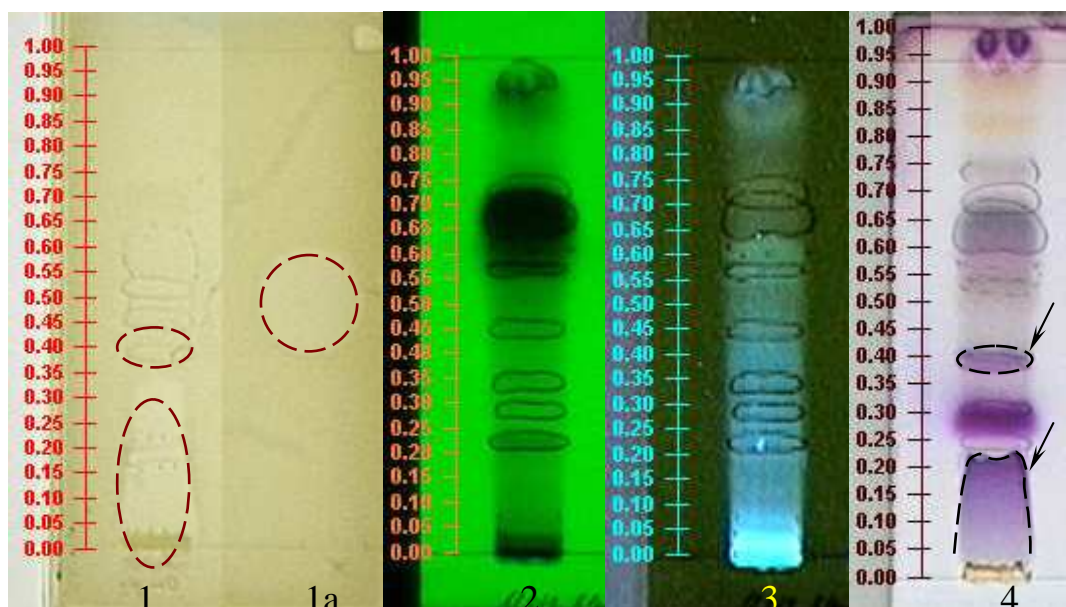


Figure 61: Antibacterial activity of *M. giganteus* hydrodistillate against *S. aureus*

Solvent system: toluene/ethyl acetate (95:5)

(1) Agar overlaid plate with HD; (1a) control: ciprofloxacin 3.5 µg

Detection modes: (2) UV light 254 nm; (3) UV light 366 nm; (4) visible light (anisaldehyde reagent). Bioactive bands are indicated with arrows. For details, see text.

Both bioactive bands were isolated from preparative TLC plates and analysed by GC-MS, yielding *E*-nerolidol ($R_f = 0.40$) and linoleic acid ($R_f \sim 0.15$). Commercially available standards were analysed to corroborate the results: these standards were injected into the GC-MS system both separately and together with the isolated compounds (co-injection). No differences in either retention time or MS spectra were observed; further isolation for NMR structure elucidation was therefore deemed unnecessary (Figure 60 and Table 12). Both *E*-nerolidol and linoleic acid are substances known for their antimicrobial activity [84, 85, 124, 125].

Since the literature reports that cis-trans isomers differ with the respect to their bioactivity, both isomers of nerolidol (*E* and *Z*) were analysed [126]. Experiments showed that only *E*-nerolidol is active against *S. aureus*, whereas *Z*-nerolidol does not exhibit any activity. (Note: in this case only, commercially-available standards were used for experimentation.)

During the microbiological tests, it had been noticed that the hydrodistillate of *Meripilus* is not always active against *S. aureus*. Both bioactive and inactive hydrodistillates were analysed using TLC (Figure 62), with *E*-nerolidol and linoleic acid being used as reference substances. The results convincingly demonstrate that *E*-nerolidol and linoleic acid are absent from the inactive hydrodistillate (Figure 62, mode 3).

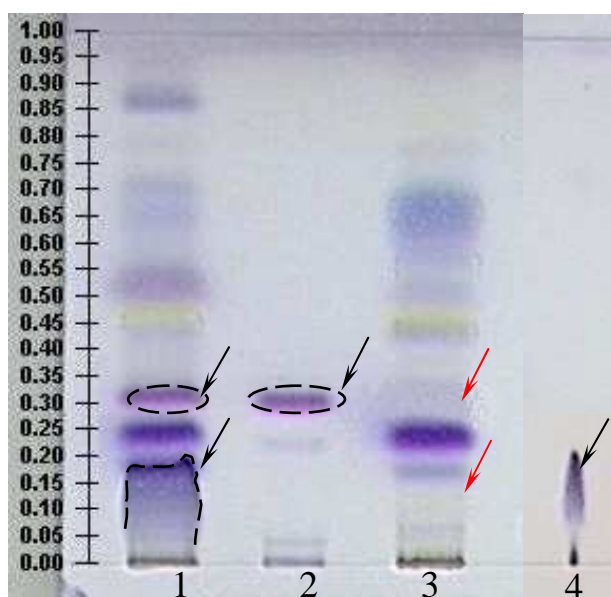


Figure 62: Hydrodistillates of *M. giganteus* compared with *E*-nerolidol and linoleic acid as reference substances. Solvent system: toluene/ethyl acetate (95:5). Detection mode: visible light (anisaldehyde reagent).

(1) Bioactive HD; (2) *E*-nerolidol; (3) inactive HD; (4) linoleic acid.

Red arrows indicate the absence of bioactive compounds. For details, see text.

To sum up:

- The present research represents the first occasion on which a hydrodistillate of *M. giganteus* was tested against *S. aureus*; the hydrodistillate was found to be active
- The chemical composition of the *Meripilus* hydrodistillate was analyzed by GC and GC-MS, resulting in the identification of 12 constituents that represented about 45% of the total volatiles
- The major components were established as linoleic acid (~14%), n-hexadecanoic acid (~8%), linoleic acid ethyl ester (~7%), n-hexadecanoic acid ethyl ester (~2%) and *E*-nerolidol (~2%)
- The application of the agar overlay technique on TLC plates to a *Meripilus* hydrodistillate established both *E*-nerolidol and linoleic acid as antibacterial principles. Hydrodistillates of *Meripilus* fruit bodies lacking *E*-nerolidol and linoleic acid showed no antibacterial activity.
- The *E*-isomer of nerolidol is solely responsible for the antibacterial properties.

3.3.8 Cytotoxicity of *Meripilus* extracts

As already mentioned (Section 3.3.3), previous studies had demonstrated significant cytotoxic activity against a murine cancer cell line 3LL (Lewis lung carcinoma; IC₅₀ of 19.8±2.6 µg/ml) for a crude *Meripilus* methanol extract [38]. Based on these data and results obtained from the haemolytic tests, a decision was made to test dried methanol and ether extracts of *Meripilus* against human bladder cancer cells (cell line 5637). Both types of extracts were diluted in DMSO. The first dilution was 200 mg/l and this solution was then successively diluted in seven further dilution phases (dilution step 1:3). Controls were pure DMSO and etoposide, diluted in DMSO at a concentration of 0.32 mg/l (see Section 5.7.4). The human bladder cancer cells were then incubated and the cytotoxicity was measured using a special method incorporating the neutral red test according to Wende (method is patented, no further information available).

Results from the cytotoxicity investigations of methanol and ether extracts are shown in Table 13 and Table 14. The second and third column contain figures showing activity of the pure medium (control) and the medium mixed with DMSO (solvent control). Extract dilutions with an intact cell count of less than 75% are to be classified as toxic. Only average values should be considered for the definition of cytotoxicity. As can be seen from the tables, both extracts may be classified as non-toxic. These results make *Meripilus* a promising subject of study for further investigation as a potential source of antibiotics.

	Medium	Medium/ DMSO 1.125%	Etoposide 0.32 mg/l	Methanol extract dilution						
				200 mg/l	67 mg/l	22 mg/l	7.4 mg/l	2.5 mg/l	0.8 mg/l	0.3 mg/l
Intact cells, %	97.92	45.64	82.04	61.93	89.48	95.71	100.34	97.92	98.73	97.12
	97.52	43.23	78.02	55.90	89.48	98.93	106.77	96.31	95.51	99.53
	104.39	50.97	77.70	0.00	0.00	0.00	not given	28.82	59.58	76.45
	99.82	58.70	85.59	0.00	0.00	0.00	not given	34.45	61.69	77.86
	105.56	50.47	80.83	66.76	88.67	100.56	97.12	107.98	101.94	103.95
	91.49	48.86	78.42	54.69	86.26	92.49	85.86	91.89	84.25	98.73
Average	100.00	47.65	82.04	61.46	90.35	98.46	99.46	100.27	97.25	101.61
Average 2	73.83		82.04	92.69						
Standard deviation		2.91	4.26	4.62	3.48	4.13	6.85	5.40	6.24	3.38

Table 13: Determination of cytotoxicity of *M. giganteus* methanol extract

Cytotoxicity was tested with human bladder cancer cells

A count of intact cells was used as a measure of toxicity. Extract dilutions with an intact cell count of less than 75% are classified as toxic. No intact cells were found at a dilution higher than 22 mg/l.

Note: dilution levels of 200 mg/l, 67 mg/l and 22 mg/l are not relevant for classifying an extract as toxic, nor do they exclude its subsequent use as an antibiotic. For details, see text.

	Medium	Medium/ DMSO 1.125%	Etoposide 0.32 mg/l	Ether extract dilution						
				200 mg/l	67 mg/l	22 mg/l	7.4 mg/l	2.5 mg/l	0.8 mg/l	0.3 mg/l
Intact cells, %	101.54	52.63	81.53	0.00	78.57	96.54	100.99	101.17	107.29	103.40
	100.06	48.55	78.20	0.00	73.01	88.39	98.02	90.43	101.73	101.91
	106.73	57.81	84.87	0.00	77.08	92.84	103.95	97.10	96.91	105.99
	100.80	53.00	85.98	0.00	77.08	95.06	105.81	95.61	102.10	102.29
	98.21	55.22	83.76	0.00	84.13	95.06	93.95	103.77	106.92	104.88
	92.65	46.70	70.04	0.00	75.97	85.79	94.32	89.68	98.39	94.87
Average	100	52.32	80.73	0.00	77.64	92.28	99.51	96.29	102.22	102.22
Average 2	76.16			95.03						
Standard deviation		3.76	5.40	0.00	3.36	3.90	4.50	5.15	3.89	3.58

Table 14: Determination of cytotoxicity of *M. giganteus* ether extract

Cytotoxicity was tested with human bladder cancer cells

A count of intact cells was used as a measure of toxicity. Extract dilutions with an intact cell count of less than 75% are classified as toxic. No intact cells were found at a dilution higher than 22 mg/l.

Note: dilution levels of 200 mg/l, 67 mg/l and 22 mg/l are not relevant for classifying an extract as toxic, nor do they exclude its subsequent use as an antibiotic. For details, see text.

The results of bioactivity studies on *M. giganteus* can be summarised as follows:

- Together with *B. inquinans*, *M. giganteus* exhibits the strongest antibacterial activity from all thirty species of fungi tested
- Both ether and methanol extracts exhibited very strong antibacterial effects against *S. aureus*, as was also the case with the hydrodistillate. In addition, the ether extract also possesses strong haemolytic properties.
- The bioactive constituents were determined by the agar overlay technique as meripiluslactone (ether extract), *E*-nerolidol and linoleic acid (hydrodistillate)
- While the literature describes cytotoxic properties for a *Meripilus* methanol extract, data provided by the present research classifies both the methanol and ether extract as non-toxic (note, however, that there are disparities in the test systems used)

4. Summary and outlook

The objective of this doctoral thesis was to research macrofungi native to Germany for their antimicrobial potential. A two-stage approach was taken to achieve this objective. The first stage involved the screening of extracts (mainly ether and methanol) of a selected group of fungi (about 30 species) with respect to their antibacterial potency (against *Staphylococcus aureus* and *Escherichia coli*). These investigations of antibiotic activity were carried out using agar diffusion and agar overlay techniques. The agar overlay technique was modified for rapid, highly-accurate microbiological tests on TLC plates and permits the determination of antimicrobial activity of the extracts while simultaneously localising bioactive compounds on TLC plates. The second stage focused on the isolation and structure elucidation of the active principles of the two fungi exhibiting the strongest bioactivity: *Bulgaria inquinans* (Pers.) Fr. (ascomycetidae) and *Meripilus giganteus* (Pers.) P. Karst. (basidiomycetidae). In this stage, a number of chromatographic techniques (TLC, HPLC, also in preparative mode) were used to isolate the antimicrobial constituents from acetonitrile and ether extracts, as well as from hydrodistillates. Structure elucidation was achieved by applying various MS (EI in low and high resolution, FAB, ESI, GC-MS) and NMR techniques (¹H NMR, ¹³C NMR, HMBC, HSQC, H,H-COSY, NOESY).

The remainder of this section summarises the results of these investigations for each species.

Bulgaria inquinans

The agar overlay technique on TLC plates revealed the presence of two antibacterial substances in the ether extract of *Bulgaria* fruit bodies. Both compounds displayed a strong antibacterial activity against *S. aureus*, comparable with the activity of the reference antibiotic ciprofloxacin (3.5-5 µg). Owing to their instability, isolation of these compounds in sufficient amounts was possible only by using cold extracts (ether or acetonitrile), freshly prepared at sub-zero temperatures (−18 °C). Structure elucidation led to the identification of two compounds with an azaphilone

structure. Additional evidence for azaphilone properties was provided by the compounds' fluorescence in UV light (366 nm) and reaction with agar (staining red = reaction with nitrogen-containing substances). This evidence led to the identification of bulgarialactone B and a new azaphilone, termed bulgarialactone D, which proved to be an entirely new natural compound.⁴ Bulgarialactone D is relatively unstable and tends to decompose partially to bulgarialactone B. Further, HPLC experiments also suggest that bulgarialactone D is likely to be the only original azaphilone in fruit bodies of *B. inquinans*. Bulgarialactone B, previously found by Stadler *et al* [58], is probably formed from bulgarialactone D during extraction, concentration or storage of the ready extract, i.e. it is an artefact; the same holds true for the other bulgarialactones identified, A and C [58].

The ether extract exhibited strong cytotoxicity in tests with human bladder cancer cells: this is probably due to the presence of azaphilones, which are also responsible for the strong haemolytic effect (blood gelatine test). This theory is supported by running the above tests using a methanol extract of *Bulgaria* fruit bodies: since this extract has been shown to contain no azaphilones, it is therefore only slightly toxic in this test system. This cytotoxic test data, combined with the fact that microscopy revealed the presence of azaphilones in the black fungi spores (indicated by red staining of structural elements), suggests that direct contact with this fungus should be avoided.

It was further established that *Bulgaria* fruit bodies produce traces of volatiles, the composition of which was investigated for the first time. A total of 16 substances, representing approximately 66% of the hydrodistillate, were identified by GC/MS analysis, combined with the co-injection of standards and the comparison of retention indices. No typical volatiles of either the terpene or the phenylpropanoid group were encountered in this hydrodistillate. Instead, the majority of volatiles derived from fatty acid metabolism (~60%), primarily n-hexadecanoic acid (~16%), linoleic acid

⁴ Note that the literature now refers to two different substances as "bulgarialactone D"; in the present work, the bulgarialactone isolated by Musso *et al* [83] is referred to as bulgarialactone D_(Musso). See also Chapter 3.2.3.

(~19%), linoleic acid ethyl ester and oleic acid ethyl ester (10%; all figures are proportions of the total hydrodistillate). No hydrocarbons were present. Another main constituent of the volatiles (~4%) was 1-Octene-3-ol: it was isolated by preparative TLC and the determination of its enantiomeric ratio ($R(-)/S(+)$ = 99:1) was achieved after derivatisation by means of enantioselective GC. The occurrence of 1,3-diphenyl-2-propanone (4.3%) among the volatile constituents is also noteworthy. While commonly used as flavouring and fragrance agent in the food industry, it was previously unknown as a naturally-occurring substance. Since contamination of the hydrodistillate by the introduction of this substance can be excluded, the present work is the first research to demonstrate that 1,3-diphenyl-2-propanone is a natural compound.

Testing of the *Bulgaria* hydrodistillate for antibacterial potential (agar overlaying technique on TLC) revealed two major zones of bacterial growth inhibition. On analysing with GC/MS, the larger zone was shown to contain three common acids, namely pentadecanoic, hexadecanoic and linoleic acid. This zone's antibacterial activity could therefore be explained by the presence of linoleic acid, which has known antimicrobial properties. The second bioactive TLC zone consisted of only a single compound, which amounted to about 3% in the hydrodistillate. Structure elucidation established a new natural compound, 2-[(1*E*,3*E*,5*E*)-7-methylnona-1,3,5-trienyl]furan, for which the trivial name bulgariafuran is suggested. Structurally, the substance is similar to dendrolasin, dehydrodendrolasin, perillene and rosefuran: these substances are pheromones that belong to the class of furano-sesquiterpenes and have been isolated from insects, marine animals and plant species [90, 91, 92, 93]. Since bulgariafuran is detectable only in the hydrodistillate (and is not present in the pentane extract) and possesses strong antibacterial qualities, this leads one to suspect that the substance is not a genuine constituent, but is possibly formed as a defensive response to damage or calefaction (probably from bulgarialactone D).

Meripilus giganteus

This fungus is a member of the basidiomycetidae and is able to form huge fruit bodies (on hard woods), which are blackened by damage, age or heating. It was discovered that only such blackened fruit bodies exhibit antibiotic properties.

In determining the antibacterial activity of a *Meripilus* ether extract on TLC plates (agar overlay technique), a single spacious zone of bacterial growth inhibition was revealed. This zone consists of a single compound, the structure of which was elucidated as 8-[(1*E*,3*Z*)-undeca-1,3-dien-1-yl]oxocan-2-one. This substance is a new natural constituent that has not previously been isolated. Furthermore, the substance also introduces a new compound class, that of the oxocane-lactones. The trivial name meripiluslactone is suggested for this new compound. The biosynthetic pathway of this new compound could involve 8-hydroxy-(9*E*,11*Z*)-octadecadienoic acid: the formation of a lactone ring could be analogous to other lactones described in food chemistry. Interestingly, this acid has been recently discovered in fruit bodies of *Sparassis crispa* – another macrofungus that belongs to the basidiomycetes class.

Meripiluslactone shows strong antibacterial activity against *S. aureus*, comparable with the activity of the reference antibiotic ciprofloxacin (3.5–5 µg). The lactone was also responsible for the haemolytic activity of a *Meripilus* ether extract (*in situ* blood gelatine test). The fact that this lactone was only detected in blackened fungi leads to the assumption that it may be formed as a defence response against mechanical damage to the fungus. It was demonstrated that intact fruit bodies of *Meripilus* do not contain meripiluslactone.

Experimentation also showed that fruit bodies of *M. giganteus* biosynthesise traces of volatiles. A total of 12 substances, representing approximately 45% of the hydrodistillate, were identified by GC/MS analysis, combined with the co-injection of standards and the comparison of retention indices. As was found with *Bulgaria*, the predominant volatiles are derived from fatty acid metabolism and represent approximately 42% of total volatiles. The major compounds of this group are linoleic acid (~14%), n-hexadecanoic acid (~8%), linoleic acid ethyl ester (~7%) and n-hexadecanoic acid ethyl ester (~2%; all figures are proportions of the total

hydrodistillate). The occurrence of 18 unusual and unidentified N-containing compounds also deserves mention: these represent about 21% of the total volatiles, thus forming the second-largest group. It is remarkable that the only typical volatile constituent from the sesquiterpene group found in this hydrodistillate was *E*-nerolidol (~2%).

On application of the agar overlay technique to a *Meripilus* hydrodistillate on TLC for determination of antibiotic activity (test against *S. aureus*), two zones of bacterial growth inhibition were observed. GC/MS analysis revealed the presence of linoleic acid in the first zone and the sesquiterpene *E*-nerolidol in the second zone. The presence of *E*-nerolidol is especially striking, since it occurs very rarely in fungi [127]. Microbiological experiments conducted on both nerolidol isomers (*E*, *Z*) discovered antibacterial properties only for the *E*-isomer.

For hydrodistillates gained from blackened *Meripilus* fruit bodies, however, no antibacterial activity was found. One possible explanation for this phenomenon is as follows. The hydrodistillate from intact (non-blackened) fruit bodies contains *E*-nerolidol and linoleic acid, and therefore exhibits antibacterial activity. However, the hydrodistillate from blackened fruit bodies lacks *E*-nerolidol and linoleic acid. The presence of non-volatile meripiluslactone in the ether extract of damaged (blackened) fruit bodies (but not intact bodies) suggests that damage to fruit bodies may trigger the formation of this compound, possibly involving both *E*-nerolidol and linoleic acid in the biosynthesis pathway. This process would result in the hydrodistillate exhibiting no antibacterial activity. However, further experimentation is required to determine the extent to which *E*-nerolidol and linoleic acid are involved in the biosynthesis of meripiluslactone.

Concerning cytotoxicity, methanol and ether extracts of *Meripilus* fruit bodies showed no toxic effects in tests conducted on human bladder cancer cells; however, a methanol extract was defined as toxic by other authors when applying a different test system (murine cancer cells) [38].

In conclusion, research conducted for this thesis has confirmed the theoretical standpoint outlined at the beginning of this work, namely that fungi represent a promising and insufficiently investigated group of organisms that possess considerable antimicrobial potency. Experimentation has shown that even such common fungi as *Bulgaria inquinans* and *Meripilus giganteus* represent a highly interesting potential source of new antibiotics. Whereas bulgariolactones cannot be applied directly for medical use as antibiotics because of their cytotoxicity, meripiluslactone certainly merits further investigation in terms of its practical use as an antibiotic.

4. Zusammenfassung und Ausblick

Thema dieser Doktorarbeit war es, zunächst die Extrakte (Lösungsmittel: Äther und Methanol) von 30 ausgewählten Pilzarten in Hinblick auf ihr antimikrobielles Potenzial (gegen *Staphylococcus aureus* und *Escherichia coli*) zu testen.

Zur Bestimmung der antibiotischen Aktivität wurden der Agardiffusionstest und die Agarüberschichtungstechnik angewendet. Letztere wurde für einen schnellen mikrobiologische Test auf Dünnschichtplatten modifiziert. Dieser erlaubt gleichzeitig mit hoher Genauigkeit die Bestimmung antibakterieller Aktivität und ihre Zuordnung zu spezifischen Substanzonen des Extraktes auf der DC.

In einem zweiten Arbeitsprozess konzentrierten wir uns auf die Isolierung and Strukturaufklärung der aktiven Substanzonen von den zwei Pilzen, deren Extrakte die stärksten antimikrobiellen Effekte aufgewiesen hatten: *Bulgaria inquinans* (Pers.) Fr. (Ascomycetidae) und *Meripilus giganteus* (Pers.) P. Karst. (Basidiomycetidae).

Wir isolierten die antimikrobiellen Inhaltstoffe von Acetonitril- und Ätherextrakten sowie von Wasserdampfdestillaten durch Einsatz verschiedener chromatographischer Techniken (DC und HPLC, auch im präparativen Modus). Die Strukturaufklärung geschah durch verschiedener MS-Messungen wie EI in Nieder- und Hochauflösung, FAB, ESI, GC/MS und NMR-Techniken (¹H-NMR, ¹³C-NMR, HMBC-, HSQC-, HH-COSY, NOESY).

Die Ergebnisse dieser Untersuchungen werden für jeden Pilz getrennt zusammengefaßt.

Bulgaria inquinans

Mittels der Agarüberschichtungstechnik konnte auf der Dünnschichtplatte die Anwesenheit von zwei antibakteriellen Substanzonen in einem Ätherextrakt von *Bulgaria*fruchtkörpern nachgewiesen werden. Beide wiesen eine starke Hemmwirkung gegenüber *S. aureus* auf, vergleichbar der des Referenzantibiotikums Ciprofloxacin (3,5-5µg). Wegen ihrer Instabilität konnten diese Verbindung in ausreichenden Mengen nur aus kaltem (-18 °C), frisch hergestellten, Äther- bzw. Acetonitrilextrakten gewonnen werden. Die Strukturaufklärung ergab das Vorliegen

von zwei Substanzen mit einem Azaphilongrundgerüst. Dies Ergebnis wurde auch durch ihre charakteristische Fluoreszenz im UV-Licht (366 nm) gestützt, sowie durch ihre Reaktion mit Agar (Rotfärbung durch Reaktion mit stickstoffhaltigen Verbindungen). Wir identifizierten Bulgarialacton B und ein neues Azaphilone, das wir „Bulgarialacton D“ nannten und welches einen neuen Naturstoff darstellt. Es erwies sich als relativ instabil und neigte dazu, sich teilweise zu Bulgarialacton B umzulagern. HPLC-Experimente ließen vermuten, dass dieses Bulgarialacton D vielleicht die einzige genuine Komponente dieser Substanzklasse in den Fruchtkörpern von *B. inquinans* darstellt. Bulgarialacton B, welches zuvor von Stadler et al. [58] nachgewiesen wurde, entsteht wahrscheinlich aus Bulgarialacton D während der Prozesse der Extraktion und Einengung bzw. der Lagerung des Extraktes. Bulgarialacton B ist deshalb wahrscheinlich ein Artefakt, was vermutlich auch für die anderen von Stadler isolierten Bulgarialacton (A und C) [58] gilt.

In einem Testsystem mit Zellkulturen von menschlichen Blasenkrebszellen konnte eine starke Zytotoxizität bei einem Etherextraktes dieses Pilzes nachgewiesen werden, die vermutlich auf die Anwesenheit von Azaphilonen zurückzuführen ist. Diese sind vermutlich auch verantwortlich für die starke hämolytische Wirkung dieses Extraktes im Blutgelatine-Test. Diese Annahme wird unterstützt durch die Tatsache, dass ein Methanolextrakt von *Bulgaria*fruchtkörpern, der frei von Azaphilonen ist, in dem benutzten Testsystem nur eine geringe Toxizität aufweist. Die durch den zytotoxischen Test erhaltenen Daten zusammen mit der Tatsache, dass wir das Vorkommen von Azaphilonen in den schwarzen Pilzsporen mikroskopisch nachweisen konnten (Rotfärbung von bestimmten Strukturen) geben Anlass zu der Vermutung, dass der direkte Kontakt mit diesem Pilz vermieden werden sollte.

Fruchtkörper von *Bulgaria inquinans* bilden Spuren einer Mischung flüchtiger Verbindungen, deren Zusammensetzung hier erstmalig untersucht wurde. 16 Substanzen, deren Gehalt zusammen etwa 66% der gesamten Mischung flüchtiger Verbindungen ausmacht, wurden mittels GC/MS, Coinjektion von Referenzsubstanzen und dem Vergleich von Retentionindices identifiziert. Es konnten keine typischen flüchtigen Verbindungen aus der Terpen- oder

Phenylpropannaturstoffgruppe im Wasserdampfdestillat aufgefunden werden. Stattdessen entstammte die überwiegende Anzahl der flüchtigen Verbindungen dem Fettsäurestoffwechsel (über 60%), wobei Palmitinsäure (~ 16%), Linolsäure (~ 19%), Linolsäureethylester und Ölsäureethylester (~ 10%) die Hauptkomponenten darstellten. Kohlenwasserstoffe fehlten. 1-Octen-3-ol ist eine andere mengenmäßig bedeutsame (~4%) flüchtige Komponente. Sie wurde mittels präparativer Dünnschichtchromatographie isoliert; die Bestimmung des Verhältnisses ihrer Enantiomeren ($R(-):S(+) = 99 : 1$) geschah durch enantioselektive GC nach vorheriger Derivatisierung. Das Vorkommen von 1,3-Diphenyl-2-Propanon (4,3%) unter den flüchtigen Verbindungen ist bemerkenswert, da diese Substanz gewöhnlich als Geschmacks- und Duftstoff in der Lebensmittelindustrie eingesetzt wird, doch bisher noch nicht als Naturstoff aufgefunden worden ist. Da wir ausschließen können, dass diese Substanz bei der Wasserdampfdestillation als Verunreinigung eingeschleppt wurde, ist 1,3-Diphenyl-2-Propanon hier erstmals als Naturstoff nachgewiesen worden.

Im antimikrobiellen Test des Wasserdampfdestillats von Bulgariafruchtkörpern mittels der Agar-Überschichtungs Technik auf der DC beobachteten wir zwei starke Zonen mit antibakterieller Wachstumshemmung. Die größte Zone bestand nach der GC/MS-Analyse aus den drei trivialen Substanzen Pentadecan-, Hexadecan- und Linolsäure. Entsprechend ist die antibakterielle Wirkung dieser Zone auf die Anwesenheit von Linolsäure zurückzuführen, dessen antimikrobielle Eigenschaften bekannt sind.

Die zweite bioaktive DC-Zone besteht demgegenüber aus einer einzigen Verbindung, die mit etwa 3% im Wasserdampfdestillat auftritt. Ihre Strukturaufklärung führte zu einem neuen Naturstoff ((2-[(1*E*,3*E*,5*E*)-7-methylnona-1,3,5-trienyl]furan), dem wir den Trivialnamen „Bulgariafuran“ gaben. Seine Struktur weist Verwandtschaft zu Dendrolasin, Dehydrodendrolasin, Perillen und Rosenfuran auf, Substanzen, die zur Gruppe der Furano-Sesquiterpene gehören. Diese Furano-Sesquiterpene sind als Pheromone bekannt und wurden von Insekten, marinen Tieren und Pflanzenarten isoliert [90, 91, 92, 93]. Aus der Tatsache, dass Bulgariafuran nur im

Wasserdampfdestillat aber nicht im Pentanextrakt auftrat, könnte man schlussfolgern, dass es eventuell ein Artefakt ist; zwar konnten wir für diese Vermutung keinen Beweis (z.B. eine entsprechende Ausgangsverbindung) finden, jedoch liegt ein Entstehen aus Bulgarialacton D nahe.

Meripilus giganteus

Dieser Pilz gehört zu Unterklasse der Basidiomycetidae und kann große Fruchtkörper (an Harthölzern) bilden, die bei Verletzung, Alterung oder Erhitzen schwarz werden. Wir fanden heraus, dass nur solche schwarzverfärbten Fruchtkörper antibiotische Eigenschaften aufweisen.

Die Bestimmung der antibakteriellen Aktivität eines Ätherextraktes dieses Pilzes auf der DC mittels der Agarüberlagerungstechnik ergab nur eine starke Zone bakterieller Wachstumshemmung. Sie besteht aus einer einzigen reinen Komponente, deren Struktur als 8-[(1*E*,3*Z*)-undeca-1,3-dien-1-yl]oxocan-2-on, identifiziert wurde. Offensichtlich handelt es sich dabei nicht nur um einen neuen Naturstoff sondern sogar um den Repräsentanten einer neuen Verbindungsklasse (Oxocan-Lacton). Dieser neuen Komponente gaben wir den Trivialnamen „Meripiluslactone“. Vermutlich wird dieses analog anderen Lactonen aus dem Lebensmittelbereich biosynthetisiert, d.h. ausgehend von 8-Hydroxy-(9*E*, 11*Z*)-Octadecadiensäure. Diese postulierte Säure ist bereits in Fruchtkörpern von *Sparassis crispa* nachgewiesen worden – einem anderen Makromyzenten, der ebenfalls in den Basidiomyceten gehört.

Meripiluslactone zeigt eine starke antibakterielle Aktivität gegenüber *S. aureus*, vergleichbar etwa mit der des Referenzantibiotikums Ciprofloxacin (3,5-5 µg). Dieses Lacton ist auch verantwortlich für die hämolytische Wirkung eines Meripilusextrakts (Blut-Gelatine-Test *in situ*). Die Tatsache, dass diese aktive Komponente nur in schwarzgefärbten Pilzen nachweisbar war, führt zu der Vermutung, dass sie als Verteidigungsreaktion gebildet wird gegen mechanische Verletzungen, z.B. durch Tiere. Es konnte nachgewiesen werden, dass intakte *Meripilus*-Fruchtkörper kein Meripiluslacton enthalten.

Unsere Untersuchungen ergaben auch, dass Fruchtkörper von *M. giganteus* in der Lage sind, Spuren flüchtiger Verbindungen zu bilden, die eine antibakterielle Wirkung gegenüber *S. aureus* aufwiesen. Insgesamt gelang es uns, 12 dieser Verbindungen, die etwa 45% des Wasserdampfdestillates repräsentieren, mittels GC/MS zu identifizieren. Wie im Falle von *Bulgaria*, so leiten sich auch hier die vorherrschenden flüchtigen Komponenten mit einem prozentualen Gesamtanteil von etwa 42% vom Fettsäurestoffwechsel ab. Die Hauptkomponenten dieser Gruppe sind Linolsäure (~ 14%), Palmitinsäure (~ 8%), Linolsäureethylester (~ 7%) und Palmitinsäure-ethylester (~ 2%). Das Vorkommen von 18 ungewöhnlichen und unbekanntem stickstoffhaltigen Verbindungen verdient besondere Erwähnung. Insgesamt verkörpern sie mit etwa 21% die zweitstärkste Fraktion flüchtiger Komponenten im Chromatogramm. Es ist bemerkenswert, dass wir als einziges Sesquiterpen *E*-Nerolidol (mit etwa 2%) in diesem Wasserdampfdestillat nachweisen konnten.

Bei der Untersuchung eines Wasserdampfdestillates von *M. giganteus* auf antibakterielle Aktivität mittels der Agarüberschichtungstechnik konnten auf der DC-Platte zwei wachstumsinhibierende Zonen beobachtet werden. Die GC/MS-Analyse ergab, dass es sich bei der ersten Zone um Linolsäure handelte und die zweite Zone durch das Sesquiterpen *E*-Nerolidol gebildet wurde, das in Pilzen bisher nur selten aufgefunden wurde [127].

Es konnte auch nachgewiesen werden, dass einige Wasserdampfdestillate, die von *Meripilus* Fruchtkörpern gewonnen wurden, keine antibakterielle Wirkungen aufwiesen. Dieser Sachverhalt kann folgendermaßen erklärt werden: das Wasserdampfdestillat von intakten (nicht verfärbten) Pilzkörpern enthält *E*-Nerolidol und Linolsäure und zeigt deshalb antibakterielle Aktivität. In beschädigten (schwarz verfärbten) Fruchtkörpern findet zum einen die Bildung des nicht flüchtigen *Meripilus*lactons statt, und andererseits lassen sich im Wasserdampfdestillat solcher Fruchtkörper *E*-Nerolidol und Linolsäure nicht nachweisen, so dass dieses auch keine antibakterielle Wirkung erkennen lässt. Diese Beobachtung wirft die Frage auf, inwieweit diese antibakteriellen Substanzen an der Biosynthese von *Meripilus*laktone

beteiligt sein können. Mikrobiologische Experimente mit beiden Nerolidolisomeren (*E*, *Z*) ergaben, dass nur das *E*-Isomer antibakterielle Eigenschaften besitzt.

Was die Zytotoxizität angeht, so ließen Methanol- und Ätherextrakte der *Meripilus*fruchtkörper keine toxischen Effekte im Testsystem mit menschlichen Blasenkrebszellen erkennen. Andere Autoren, die ein unterschiedliches Testsystem (Krebszellen der Maus) benutzten, definieren dagegen einen solchen Methanolextrakt als toxisch [38].

Aus den Ergebnissen dieser Arbeit wird deutlich, dass selbst so ubiquitäre Pilze wie *Bulgaria inquinans* und *Meripilus giganteus* interessant erscheinen als potenzielle Quelle für neue antibiotische Substanzen.

Diese Daten belegen einmal mehr die Tatsache, dass Pilze eine viel versprechende und ungenügend untersuchte Organismengruppe mit einem beträchtlichen antimikrobiellen Potenzial darstellen.

Während Bulgarialactone wegen ihrer Zytotoxizität nicht direkt medizinisch als Antibiotika angewendet werden könnten, wäre *Meripilus*lacton in Bezug auf einen praktischen Einsatz hin zu überprüfen.

5. Materials and Methods

5.1 Fungi material

Thirty different species of fungi were tested for microbiological bioactivity (Table 15).

Species	Family
<i>Amanita phalloides</i> (Vaill. ex Fr.) Link	Amanitaceae
<i>Armillaria mellea</i> (Vahl) P. Kumm.	Physalacriaceae
<i>Armillaria ostoyae</i> (Romagn.) Herink	Physalacriaceae
<i>Ascocoryne sarcoides</i> (Jacq.) J.W. Groves & D.E. Wilson	Helotiaceae
<i>Bulgaria inquinans</i> (Pers.) Fr.	Helotiaceae
<i>Chondrostereum purpureum</i> (Pers.) Pouzar	Cyphellaceae
<i>Rhodocollybia maculata</i> (Alb. & Schwein.) Singer = <i>Collybia maculata</i> (Alb. & Schwein.) P. Kumm.	Marasmiaceae
<i>Coprinus atramentarius</i> (Bull.) Fr.	Psathyrellaceae
<i>Fistulina hepatica</i> (Schaeff.) With.	Fistulinaceae
<i>Ganoderma applanatum</i> (Pers.) Pat. = <i>G. lipsiense</i> (Batsch) G.F. Atk.	Ganodermataceae
<i>Geastrum triplex</i> Jungh.	Geastraceae
<i>Gyromitra esculenta</i> (Pers.) Fr.	Discinaceae
<i>Hypholoma capnoides</i> (Fr.) P. Kumm.	Strophariaceae
<i>Hypholoma fasciculare</i> (Huds.) P. Kumm.	Strophariaceae
<i>Inonotus obliquus</i> (Ach. ex Pers.) Pilát	Hymenochaetaceae
<i>Ischnoderma benzoinum</i> (Wahlenb.) P. Karst.	Fomitopsidaceae
<i>Laetiporus sulphureus</i> (Bull.) Murrill	Fomitopsidaceae
<i>Langermannia gigantea</i> (Batsch) Rostk.	Agaricaceae
<i>Lycoperdon perlatum</i> Pers.	Agaricaceae
<i>Lyophyllum connatum</i> (Schumach.) Singer	Lyophyllaceae
<i>Meripilus giganteus</i> (Pers.) P. Karst.	Meripilaceae
<i>Paxillus atrotomentosus</i> (Batsch.) Fr.	Tapinellaceae
<i>Paxillus involutus</i> (Batsch.) Fr	Paxillaceae
<i>Phaeolus spadiceus</i> (Pers.) Rauschert = <i>P. schweinitzii</i> (Fr.) Pat.	Fomitopsidaceae
<i>Scleroderma citrinum</i> Pers.	Sclerodermataceae
<i>Stereum hirsutum</i> (Willd.) Pers.	Stereaceae
<i>Stropharia aeruginosa</i> (Curtis) Quéf.	Strophariaceae
<i>Stropharia rugosoannulata</i> Farl. ex Murrill	Strophariaceae
<i>Trametes gibbosa</i> (Pers.) Fr.	Polyporaceae

Table 15: Fungi species investigated. Species names are given according to the Dictionary of the Fungi [24] and Index Fungorum [53].

5.2 Origin of fungi

All fungi material was collected in the vicinity of Hamburg, Northern Germany (at a maximum distance of 70 km). Material collected was used for immediate extraction and hydrodistillation or deep-frozen for storage at $-18\text{ }^{\circ}\text{C}$.

With the exception of hydrodistillation, no temperature treatment was applied to fungal material during extraction.

5.3 Microscopy

Microscopic investigations were performed using an Olympus microscope (model BX-51) equipped with DIC (differential interference contrast). A digital camera (Canon EOS 500 D) was connected via an adapter. Preparations were made using distilled water. Melzer's reagent (preparation: 20 ml water, 1.5 g potassium iodide and 0.5 g iodine; 20 g of chloral hydrate was added after mixing [110, 111]) was used for the dyeing of amyloid ascus pores.

5.4 Methods of extraction

Pentane, methanol, ether extracts and hydrodistillates were used for both chromatographic and bioactivity tests.

5.4.1 Preparation of extracts

Approximately 50.0 g of fresh or frozen fungi material was taken and 100–150 ml of pentane, methanol or ether was added. Flasks with extracts were agitated for 4 h (50 agitations/min) in an HLB GFL DARGAT2 shaker.

The extracts were filtrated when ready. Ether extracts were filtered through filters to which waterless sodium sulphate Na_2SO_4 had been applied. All extracts were concentrated at $40\text{ }^{\circ}\text{C}$ with a vacuum evaporator (Büchi Rotavapor R-200) using a V-800 vacuum controller, Vac V-500 pump and B-490 heating bath.

Pentane and ether extracts were concentrated to a volume of about 10 ml.

Methanol extracts were dried under deep vacuum and the dry residue was then treated with 10 ml methanol. The undissolved residue, consisting mostly of polysaccharides, was discarded. Further analysis was conducted exclusively on the methanol solution.

5.4.2 Hydrodistillation

Volatiles were gained from fungi material by circulation steam distillation, using an apparatus according to Sprecher [128].

Approximately 150 g of fungi material was placed into a 2-litre round flask, to which approximately 1 litre of distilled water was added.

The hydrodistillate (HD) was collected in 1–2 ml of pentane; the process duration was 4 h. The pentane solution (HD) of volatile compounds was concentrated to about 0.5 ml. This solution was then used for gas chromatography (GC), gas chromatography coupled with mass spectrometry (GC-MS), thin layer chromatography (TLC) and microbiological tests.

5.5 Chromatography

5.5.1 Thin layer chromatography (TLC)

Chromatographic tests were carried out using TLC plates with normal phase (silica gel 60 F₂₅₄; Merck), reversed phase (HPTLC-Ready Plates RP-18 F₂₅₄ for nano-TLC and TLC plates silica gel 60 RP-18 F₂₅₄) and aluminium sheets coated with cellulose (Merck).

Plate sizes used: 10 × 5 cm, 10 × 10 cm, 10 × 20 cm, 20 × 20 cm. Layer thickness: 0.25 mm.

5.5.2 Preparative and semi-preparative chromatography

Preliminary fractionation processes and substance isolation were carried out on semi-preparative plates 10 × 20 cm and 20 × 20 cm (PSC plates silica gel 60 F₂₅₄, 0.5 mm, Merck) and preparative plates 20 × 20 cm (PSC plates silica gel 60 F₂₅₄, 1 mm, Merck).

5.5.3 Biological *in situ* tests on TLC

Determination of biological activity was completed using silica gel pre-coated TLC plates (Adamant UV₂₅₄, Macherey-Nagel, Germany). This type of plate was chosen since silica gel plates from Merck proved sub-optimal: the application of hot agar caused exfoliation of the plate surface.

Plate sizes: 10 × 5 cm, 10 × 10 cm, 10 × 20 cm. Layer thickness was 0.25 mm.

This technique was used for the determination of antibacterial constituents by the agar overlay method (Section 5.7.1) and haemolytic activity in the blood-gelatine test (Section 5.7.3).

5.5.4 Solvent systems for thin layer chromatography

To perform the phytochemical investigations and bioassays of the methanol, ether and pentane extracts, plus hydrodistillates, TLC analysis was applied. The analysis utilised the following solvent systems: trichloromethane/toluene/methanol (8:1:1) and dichloromethane/toluene/methanol (8:2:2) for methanol and ether extracts; toluene/ethyl acetate (95:5), toluene/acetone (7:3) and pure pentane for hydrodistillates.

5.5.5 Detection on TLC plates

The detection of the extract zones commenced with UV light irradiation (wavelengths 254 and 366 nm) using a Desaga system (Desaga HP-UVIS). Photodocumentation was completed using a Cab UVIS UV unit and Hitachi HV-C20 camera. Data acquisition and processing was carried out using ProViDoc VD 40 software, version 3.01.510 (Desaga GmbH, Germany).

For additional TLC detection, an anisaldehyde/sulphuric acid spray reagent was chosen. This reagent was prepared from 0.5 ml anisaldehyde, 10 ml anhydrous acetic acid, 85 ml methanol and 5 ml concentrated sulphuric acid. Once prepared, the reagent was then stored at a temperature of about 4 °C. TLC plates were sprayed with reagent and subsequently heated under observation on a Camag III TLC plate heater for about 5 minutes at 110 °C. The plates were evaluated in visual light.

Azaphilone detection involved the application of 25% ammonia; evaluation was performed in visual light.

5.5.6 Analytical High Performance Liquid Chromatography (HPLC)

All HPLC measurements were run on a Merck Hitachi LaChrom instrument (software version 4.1, P/N: 810-8652-01, interface D-7000, DAD L-7455, autosampler L-7200, pump L-7100).

Extract analyses were performed on a column of type LiChroCART® 125-4 HPLC cartridge, filled with LiChrospher® 100 RP-18e (particle size 5 µm). The column was protected with a suitable guard column.

For azaphilone determination, the following method was applied:

Solvent A: acetonitrile – 70%

Solvent B: water – 30%

Acquisition time: 35 min

Flow: 0.25 ml/min

Injection volume: 5–50 µl

Wavelength range: 220–550 nm

Monitoring wavelength: 450 nm

5.5.7 Preparative High Performance Liquid Chromatography (Preparative HPLC)

Azaphilone separation and isolation was conducted using Merck Hitachi LaChrom equipment, consisting of a pump (L-600), autosampler (AS 2000 A), UV monitor (655 A) and interface (D-7000). The system was controlled by a computer running software version 4.1 (P/N: 810-8662-01).

A LiChroCART® 250-10 HPLC cartridge filled with LiChrospher® 100 RP-18 (particle size 10 µm) was used as a main column and was protected by a pre-column guard to trap any impurities.

The standard procedure for azaphilone isolation was as follows:

Solvent mixture: acetonitrile/water (70:30)

Acquisition time: 35 min

Flow: 3 ml/min

Injection volume: 200 µl

Monitoring wavelength: 450 nm

5.5.8 Gas chromatography (GC)

The GC conditions for the analysis of fungi volatiles are summarised in Table 16.

Equipment	HP 6890 Series	HP 5890 Series II
Column	J&W DB Wax 30 m × 0.25 mm Film thickness 0.25 µm	CP-Sil 5 CB (Varian) 30 m × 0.25 mm Film thickness 0.26 µm
Carrier gas	Nitrogen	Nitrogen
Flow	0.7 ml/min	0.7 ml/min
Injector	Split; split ratio: 1:16	Split; split ratio: 1:16
Temperature program	45–240 °C (40 min hold) heating rate 3 °C/min	a) 80 °C (2 min isotherm) → 270 °C (20 min hold) heating rate 10 °C/min b) 45–240 °C (40 min hold) heating rate 3 °C/min
Injector temperature	200 °C	200 °C
Detector	FID; temperature: 250 °C	FID; temperature: 280 °C
Injection volume	1 µl	1 µl

Table 16: GC parameters

5.5.8.1 Determination of the absolute configuration of 1-octen-3-ol

1-octen-3-ol was isolated from a pentane extract of *B. inquinans* on preparative TLC plates developed in the solvent system toluene/ethyl acetate (95:5); the isolated substance was then analysed by enantioselective gas chromatography.

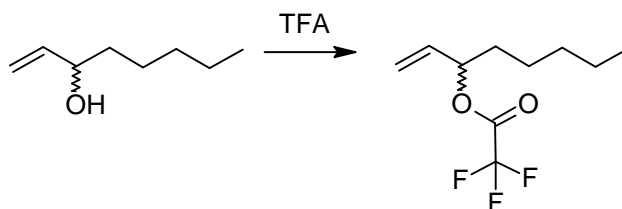
GC parameters of the enantioselective analysis are given in Table 17.

S-(+)-1-octen-3-ol (Fluka, Germany) and *R*-(-)-1-octen-3-ol (kindly donated by Prof. W. Francke of the Institute of Organic Chemistry, University of Hamburg) were used as reference substances.

Gas chromatograph	HP 5890 Series II (Hewlett Packard)
Column	LIPODEX® E octakis-(2,6-di-O-pentyl-3-O-butyryl)- γ -cyclodextrin 25 m \times 0.25 mm (kindly loaned by the Institute of Organic Chemistry, University of Hamburg)
Carrier gas	Nitrogen
Flow	0.7 ml/min
Injector	Split; split ratio 1:16
Temperature program	45 °C (10 min isotherm) – 60 °C, heating rate 1 °C/min
Injection temperature	200 °C
Detector	FID; temperature: 210 °C
Injection volume	1 μ l

Table 17: Enantioselective GC parameters

The enantioselective analysis of 1-octen-3-ol was performed after derivatisation with trifluoroacetic anhydride (TFA):



Although there is a standard method for derivatisation of 1-octen-3-ol (König [98, 99]) it was decided to simplify the process and to proceed as described below.

TFA derivatisation was performed by heating the isolated substance with 10 μ l of trifluoroacetic anhydride and 100 μ l of ethyl acetate at 60 °C for 30 min. The reaction mixture was carefully dried under a gentle nitrogen stream. The residue was dissolved in 100 μ l of ethyl acetate and a 1 μ l aliquot was then injected into the GC system.

5.6 Spectroscopic methods

5.6.1 Mass spectrometry in ESI mode

For ESI spectra, a Varian MAT 95 XL Trap apparatus was used (Table 18).

Mass spectrometer	MAT 95 XL Trap Accelerating voltage 5 kV Resolution 1500 Scan range 100–1000 m/z with 3 s/mass decade
Electrospray	API III ESI apparatus Negative ions Heated capillary at 230 °C ESI voltage 3.2 kV
Sample inlet	Harvard syringe pump 1–20 $\mu\text{l}/\text{min}$ Solvent: <i>i</i> -propanol

Table 19: MS parameters

5.6.2 GC-MS coupling

GC/MS measurements were conducted on a HP GC system (HP5890, Agilent Technologies) coupled with a sector field MS (VG-70-250 S) from VG Analytics. For details, see Table 20. The following electronic libraries were used to identify GC/MS spectra:

- MassLib (v. 9.3-106) (Max-Planck-Institut für Kohlenforschung, Mülheim (Germany), incorporating MassLib software 1996–2008 distributed by MPS Kofel (Zollikofen, Switzerland). Including the following libraries (from “Chemical Concepts”, Wiley):
 - Wiley / NBS Registry of Mass Spectral Data (4th Ed.)
 - NIST / EPA / NIH Mass Spectral Data Base (2005)
 - Library MPI (Mühlheim, 2006)
 - CC (4th Ed.)
 - Geochemicals (1st Edition)

- MRC Collection (1st Edition)
- MassFinder 3.53c (2004), including a terpene library from D. Hochmuth, Prof. W. A. König [129]
- Compilation of mass spectra of volatile compounds in food, TNO Institute, Zeist, Netherlands, Chemical Concepts (Weinheim, 1985)
- Identification of essential oil compounds by gas chromatography/quadrupole mass spectroscopy (Prof. R. P. Adams), Allured Publishing Company, Carol Stream (Illinois, 2001)
- Internal MS library of essential oil compounds (Priv-Doz. Dr. W. Schultze, Institute of Pharmacy, University of Hamburg)

Mass Frontier (v. 2.0) spectral interpretation software (Thermo Scientific, Germany) was applied for the interpretation of EI-MS data.

Gas chromatograph	HP5890 Series II
Mass spectrometer	VG-70-250 S
Column	CP-Sil 5 CB 25 m × 0.25 mm Film thickness 0.4 µm
Carrier gas	Helium
Flow	2 ml/min
Injector	Split 1:17
Temperature program	a) 45–270 °C (40 min hold), heating rate 5 °C/min
	b) 80 °C (2 min isotherm) – 270 °C (20 min hold), heating rate 10 °C/min
Injector temperature	200 °C
Injection volume	1 µl
Ionisation	Electron impact (EI), 70 eV
Mass range	35–300 <i>m/z</i> and 600 <i>m/z</i> , respectively

Table 20: GC-MS parameters

5.6.3 Nuclear magnetic resonance spectroscopy (NMR)

NMR measurements such as ^1H , ^{13}C , H,H-COSY (Proton-Proton Correlation Spectroscopy), HMBC (Heteronuclear Multiple Bond Correlation), HSQC (Heteronuclear Single Quantum Coherence) and NOESY spectroscopy (Nuclear Overhauser Effect Spectroscopy) were run on AMX 400, AV 400 and DRX 500 spectrometers (all from Bruker, Germany).

Deuterated solvents used were trichloromethane (CDCl_3), methanol (CD_3OD), acetonitrile (CD_3CN) and acetone ($(\text{CD}_3)_2\text{CO}$), all supplied by Deutero (Kastellaun, Germany). Tetramethylsilane (TMS) was added as an internal standard.

MestRec software (version 4.4.1.0, Mestrelab Research, Santiago de Compostela, Spain) was utilised for spectra processing and analysis.

5.7 Bioassays

5.7.1 Determination of antimicrobial activity (agar diffusion test)

Gamma-sterile Petri dishes (100 mm in diameter) were used for this test.

Culture medium

Standard I agar (Merck[®]), 37 g/l in Millipore-filtered water.

Test microorganisms

Staphylococcus aureus ATCC 25923, *Escherichia coli* ATCC 25922 and *Candida albicans* ATCC 10231 were used for biological assays.

Bacteria suspension

Colonies of *S. aureus*, *E. coli* and *C. albicans* were mixed with 4.5 ml of sterile isotonic sodium chloride solution for moderate opalescence. Microbial suspension turbidity was adjusted to a density equivalent to a 0.5 McFarland standard (approximate cell density 10^8 CFU/ml), absorbance 0.125 ± 0.02 at 550 nm. A 0.5 McFarland standard is prepared by mixing 0.05 ml of 1.175% barium chloride dihydrate ($\text{BaCl}_2 \times 2\text{H}_2\text{O}$), with 9.95 ml of 1% sulphuric acid (H_2SO_4).

Test technique

Sterile cotton-tip sticks were used for bacteria sowing. The bacterial suspension was distributed on agar in Petri dishes in three different directions. Extracts to be tested

for antimicrobial activity were spotted on four filter paper discs with a diameter of 6-7 mm and a thickness of 0.7 mm; the amounts applied were 25 µl, 50 µl, 100 µl and 200 µl, respectively. Solvents were removed by drying the discs above a hot plate. Discs with pure solvents were employed as a control for solvent activity. Standard gemifloxacin (5 µg) discs were used as a reference for antibacterial activity. Antifungal effects were measured using discs treated with clotrimazole (10 µg) as a reference standard.

Following application, all discs were placed on the surface of inoculated agar. Petri dishes were placed in an incubator at a temperature of 37 ± 1 °C for approximately 18 ± 2 hours. Activity was determined by visual inspection and measurement of the diameter of clear inhibition zones around the discs. To determine the quantity of dry substance in applied extracts, test discs were weighed before and after the application of the extract.

5.7.2 *In-situ* bioassays on thin layer plates (agar overlay method)

Two types of gamma-sterile Petri dishes were selected: square (100 mm) and round (140 mm diameter).

Test plates

For details, see Section 5.5.3, “Biological in situ tests on TLC”.

Culture media

Medium 1: Standard I agar (Merck®), 37 g/l in Millipore-filtered water, autoclaved (15 min at 121 °C).

Medium 2: China blue lactose agar (CM0209), 35.5 g/litre in Millipore-filtered water, autoclaved (15 min at 121 °C).

Test microorganisms

Agar overlay tests were performed with *S. aureus* ATCC 25923.

Bacteria suspension

Colonies of *S. aureus* were mixed with 4.5 ml of sterile isotonic sodium chloride solution for moderate opalescence. Microbial suspension turbidity was adjusted to a

density equivalent to a 0.5 McFarland standard (approximate cell density 10^8 CFU/ml), absorbance 0.125 ± 0.02 at 550 nm.

Test technique

50 ml hot agar was cooled to a temperature of approximately 37-38 °C and mixed with 500 µl of inoculum (ratio 1:100) before being distributed evenly over a TLC plate placed inside a Petri dish. An aqueous solution of ciprofloxacin (3.5-5 µg) was employed as a reference for antibacterial activity and spotted on the TLC plate before agar application. Following solidification of the agar, the Petri dishes with TLC plates were placed in an incubator at 37 ± 1 °C for about 18 ± 2 hours.

On removal from the incubator, activity was estimated by visual inspection and measurement of the clear inhibition zones around active bands. Photo documentation was completed using a Hitachi HV-C20 video camera connected to a CAB UVIS UV-unit and controlled by a computer running ProViDoc VD 40 software (v. 3.01.510, Desaga GmbH/Sarstedt Group, Germany).

5.7.3 Haemolytic activity assay (blood gelatine test)

Test plates

For details, see Section 5.5.3, “Biological in situ tests on TLC”.

Reagents

For this test, the following reagents were used: ethanol 70% (v/v), gelatine, isotonic phosphate buffer solution and a single unit of stored blood (from University Clinic Hamburg-Eppendorf, blood transfusion station).

Phosphate buffer composition

Composition: 40.08 g $\text{Na}_2\text{HPO}_4 \times 12 \text{H}_2\text{O}$; 4.36 g $\text{NaH}_2\text{PO}_4 \times 2\text{H}_2\text{O}$; 0.74 g NaCl.

The dry chemicals were measured accurately and dissolved in 160 ml of slightly heated water. After cooling, this mixture was diluted with 1000 ml of water. The pH of the prepared solution must be 7.4.

Blood gelatine

4.6 g of gelatine powder were mixed with 100 ml of phosphate buffer solution. The mixture was left to soak for approximately 30 minutes and was then heated gently to

ensure the gelatine was completely dissolved. Once prepared, the gelatine solution was cooled to approximately 38 °C and 20 ml of blood were then added by slow stirring.

Test technique

The extracts were applied to two TLC plates (10 × 10 cm); both plates were then developed in a suitable solvent system under the same conditions. The solvent was then evaporated from the plate by drying and substance (band) detection was then performed in UV light (245 and 366 nm).

One TLC plate was then placed centrally in a large Petri dish (19 cm in diameter) and its surface was carefully covered with a thin layer of 25 ml of warm (37 °C) blood gelatine. To prevent rapid drying at the blood gelatine surface, strips of wet filter paper were placed in the Petri dish near the TLC plate (all contact with the blood gelatine covering the plate was avoided). The Petri dish was then covered, placed in a refrigerator (at 4 °C) and investigated 12 hours later.

On investigation, positive haemolytic zones were identifiable as clear zones (colourless to slightly red) around the bands. Photodocumentation was completed using the abovementioned still image system.

A second identical TLC plate was sprayed with anisaldehyde/sulphuric acid reagent and heated for 5 min at 110 °C under observation. This plate was used as a reference to establish a correlation between the coloured bands and the bioactive zones on the TLC plate used for the blood gelatine test.

5.7.4 Cytotoxicity test

These investigations were carried out at the Institute of Pharmacy of the Ernst-Moritz-Arndt University of Greifswald, by the diploma student Bente Will (supervision: Prof. U. Lindequist, Dr. Schultze and N. Osmanova) under the guidance of Dr. Kristian Wende.

Dried methanol and ether extracts of *B. inquinans* and *M. giganteus* were prepared and then diluted in DMSO to a concentration of 200 mg/l. This solution was then successively diluted in seven further dilution phases (dilution step 1:3). For this

test, human bladder cancer cells (cell line 5637) were used. The bladder cancer cells were cultivated under standard conditions (37 °C, 5% CO₂, humid atmosphere) and passaged multiple times before being employed. Cell density was estimated by measuring a cell suspension with a haemocytometer. This permitted the determination of the exact cell number per millilitre.

The cell suspension was mixed with a culture medium and then applied to a 96-well microtitre plate (12 rows with 8 wells per row). Quantity used was 100 µl/well. The outside rows were not filled, since this area is subjected to an excessive risk of evaporation and was therefore unlikely to yield precise measurements during evaluation in a UV/Visible detector. Diluted etoposide and pure DMSO were used as controls and placed in the second and eleventh rows, respectively. Rows from three to ten were filled with the seven extract dilutions described above, in order of increasing dilution. The cells were then incubated and cytotoxicity was measured using a special method incorporating the neutral red test according to Wende (method is patented, no further information available).

6. Hazardous chemicals

		Risk-phrases	Safety-phrases
Acetic acid	C	10-35	23.2-26-45
Acetone	F	11	9-16-23.2-33
Acetonitrile	F, T	11-23/24/25	16-27-45
Acetonitrile- <i>d</i> ₆	F, T	11-23/24/25	16-27-37-45
Anisaldehyde	Xn	22-36/37/38	26-36
Dichloromethane	Xn	40	23.2-24/25-36/37
Diethyl ether	F	12-19	9-16-29-33
Ethanol	F	11	7-16
Ethyl acetate	F, Xi	11	16-23.2-29-33
Etoposide	T	22-45	26-36/37/39-45-53
Hydrogen (gas)	F ⁺	12	2-9-16-33
Massoia lactone	Xi	38-43	24-37
Methanol	F, T	11-23/25	7-16-24-45
1-Octen-3-ol	Xn, T	20-36/38	26-36
Pentane	F	11	9-16-29-33
Propan-2-ol	F	11	7-16
Guaiazulene	Xn	22	22-26-36/37/39
Sulphuric acid	C	35	26-30-45
Tetramethylsilane (TMS)	F	12	9-16-29-43.3
Toluene	F, Xn	11-20	16-25-29-33
Trichloromethane	Xn	22-38-40-48/20/22	36/37
Trichloromethane- <i>d</i> ₁	Xn	22-38-40-48/20/22	36/37
Trifluoroacetic anhydride (TFA)	C, Xn	14-20-35-52/53	26-43-36/37/39-45-61

7. Appendix I

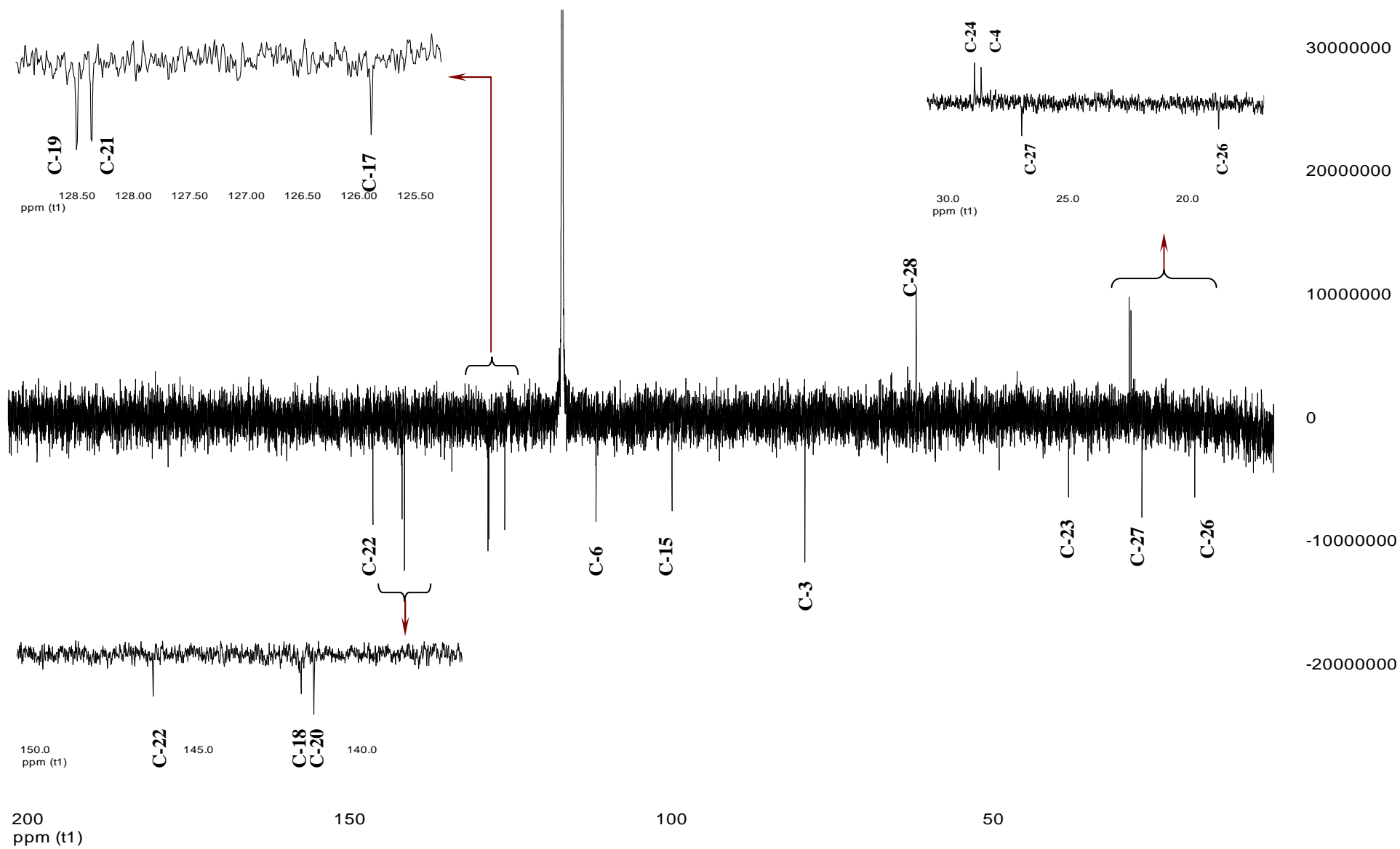


Figure 63: ^{13}C NMR spectrum of bulgarialactone B (HPLC Peak 2)

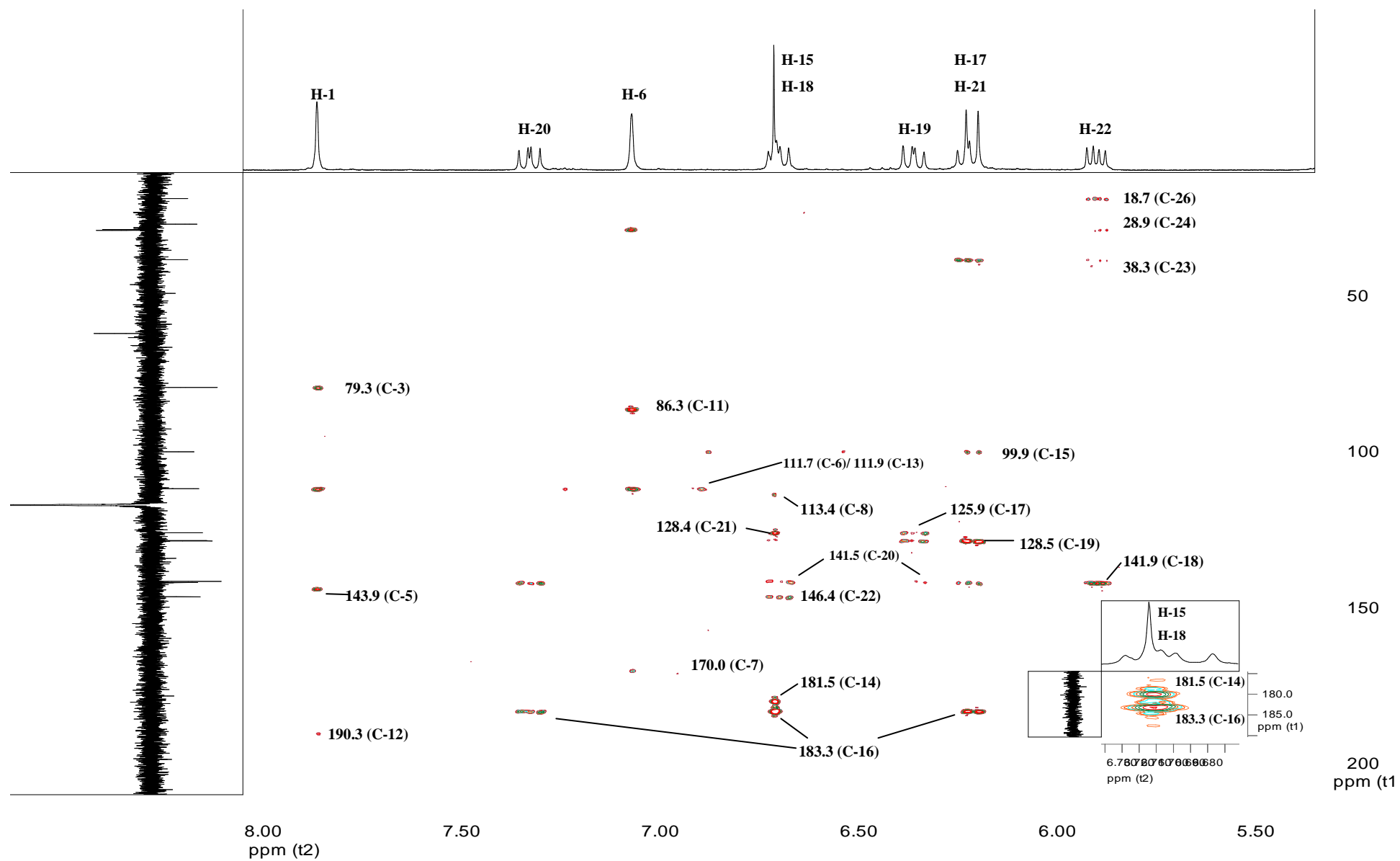


Figure 64: HMBC NMR spectrum (part 1) of bulgarialactone B (HPLC Peak 2)

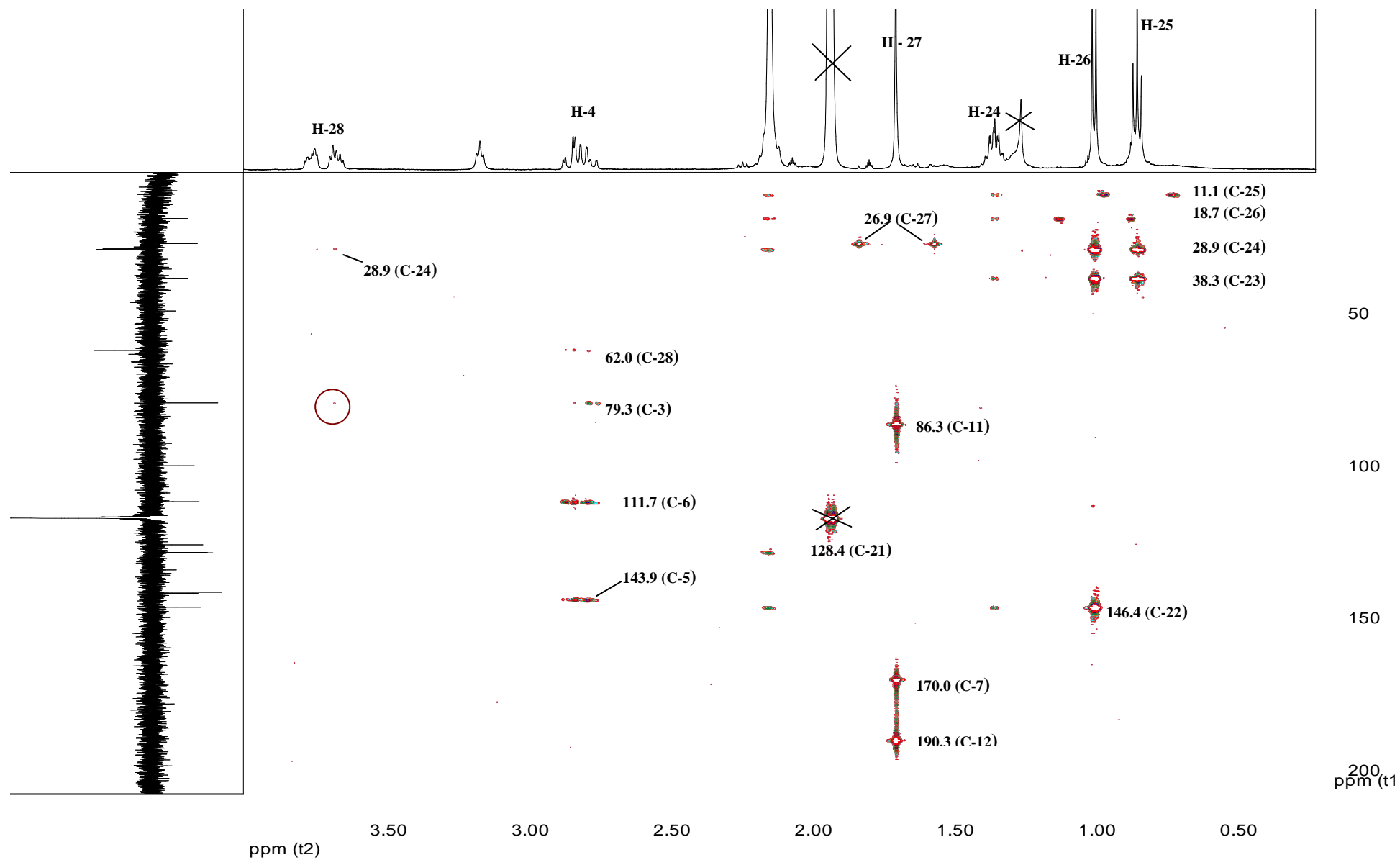


Figure 65: HMBC NMR spectrum (part 2) of bulgarialactone B (HPLC Peak 2)

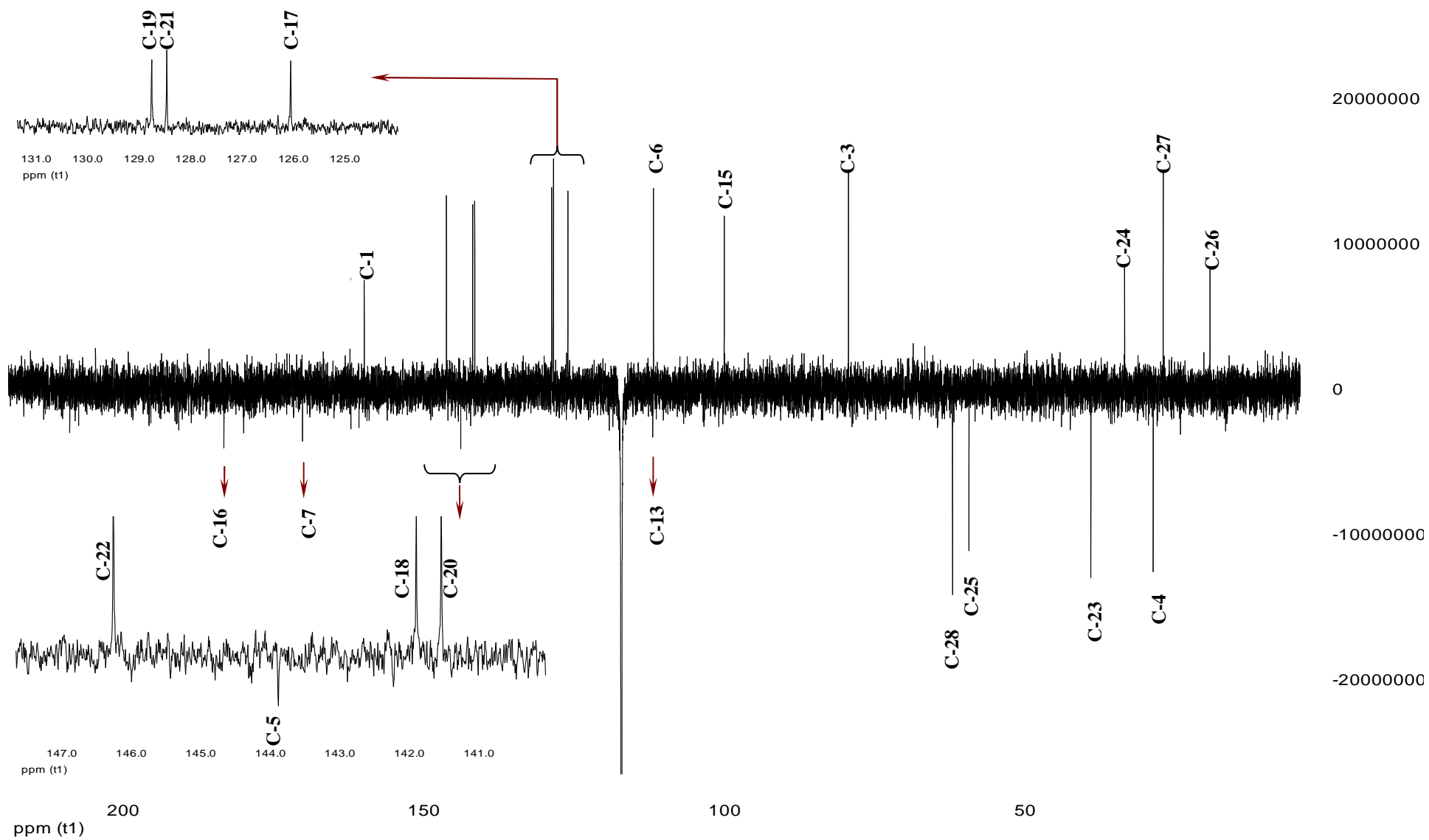


Figure 66: ^{13}C NMR spectrum of bulgarialactone D (HPLC Peak 1)

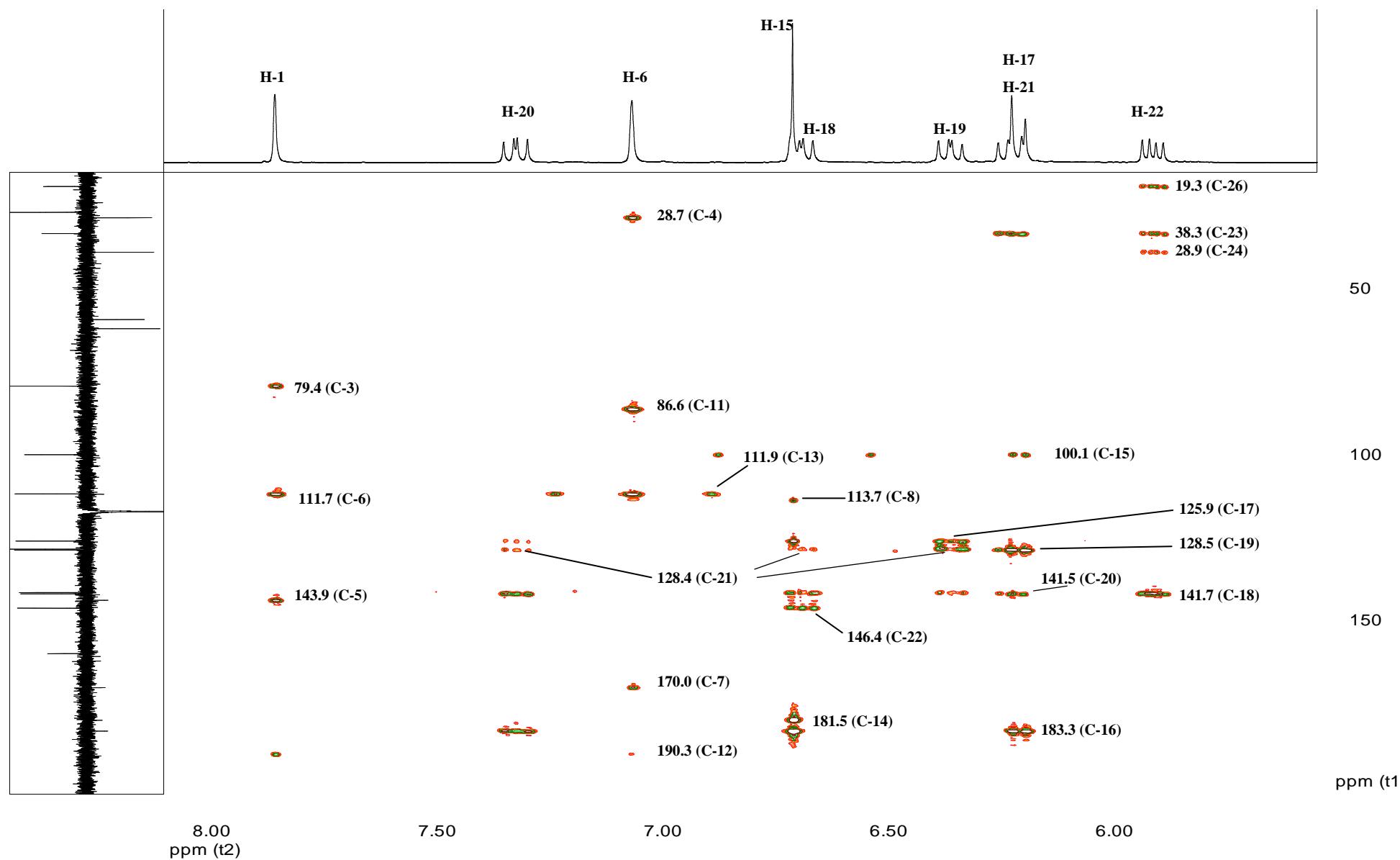


Figure 67: HMBC NMR spectrum (part 1) of bulgarialactone D (HPLC Peak 1)
165

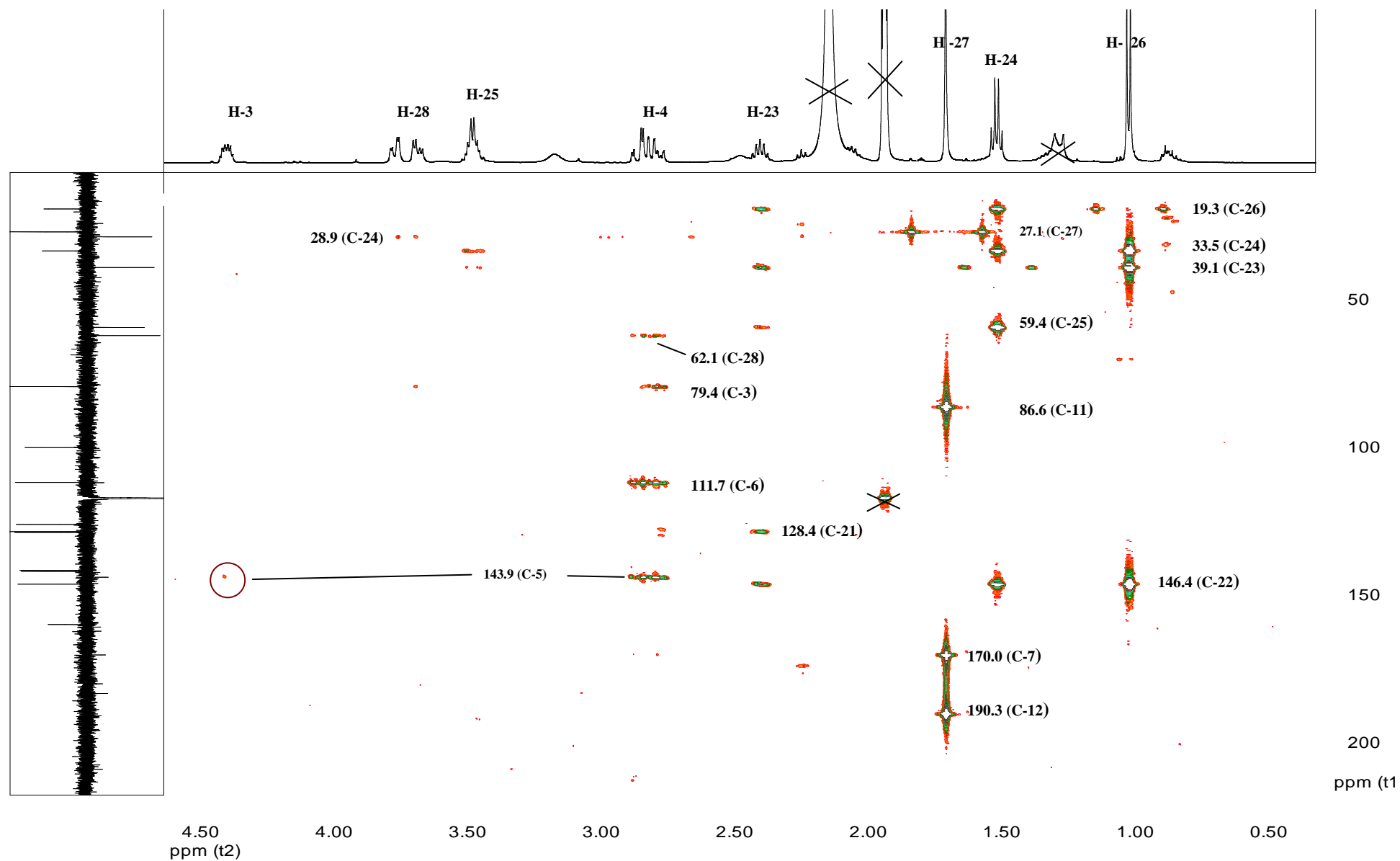


Figure 68: HMBC NMR spectrum (part 2) of bulgarialactone D (HPLC Peak 1)

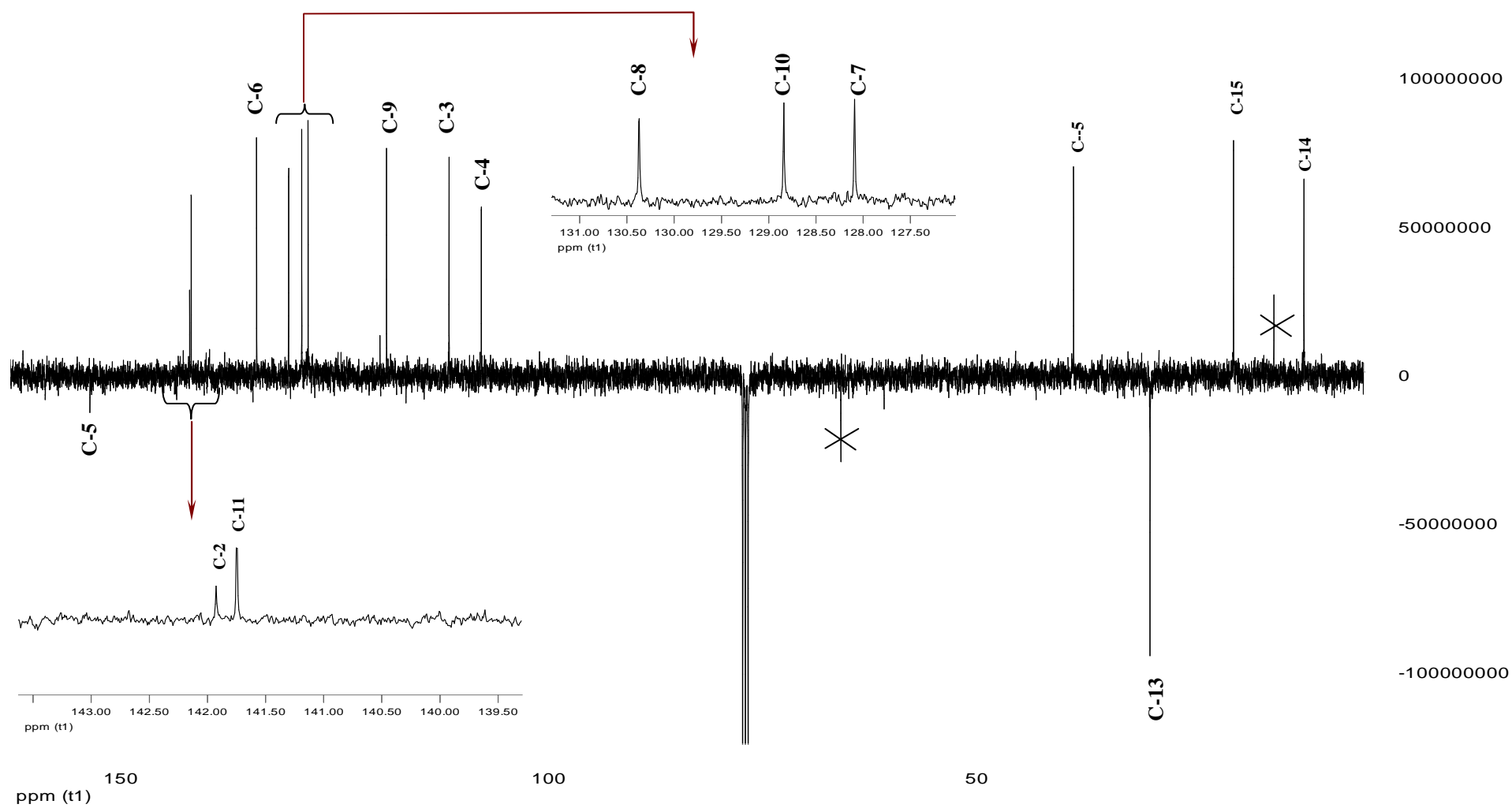


Figure 69: ^{13}C NMR spectrum of bulgariafuran from *B. inquinans* hydrodistillate

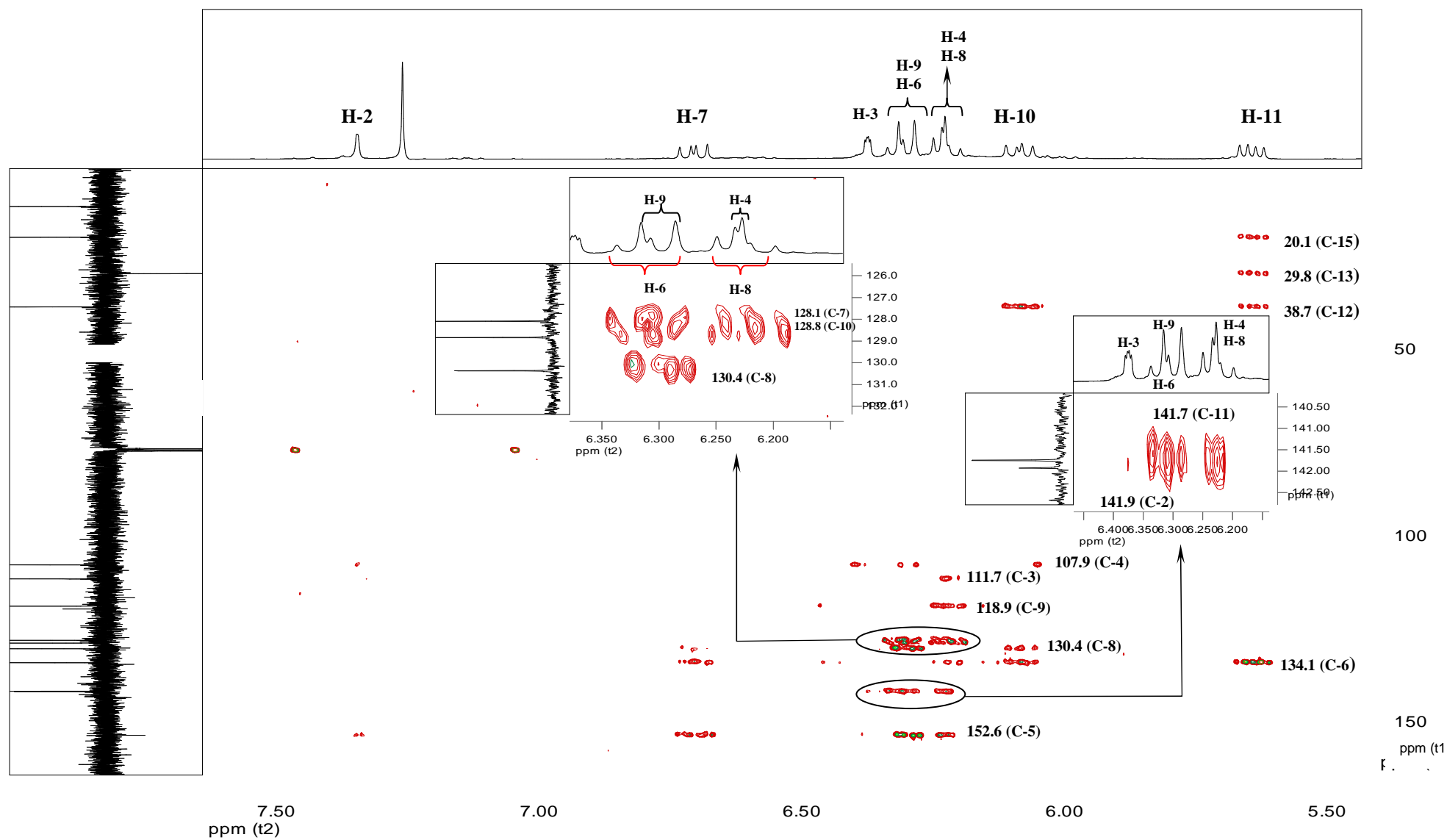


Figure 70: HMBC NMR spectrum (part 1) of bulgariafuran from *B. inquinans* hydrodistillate

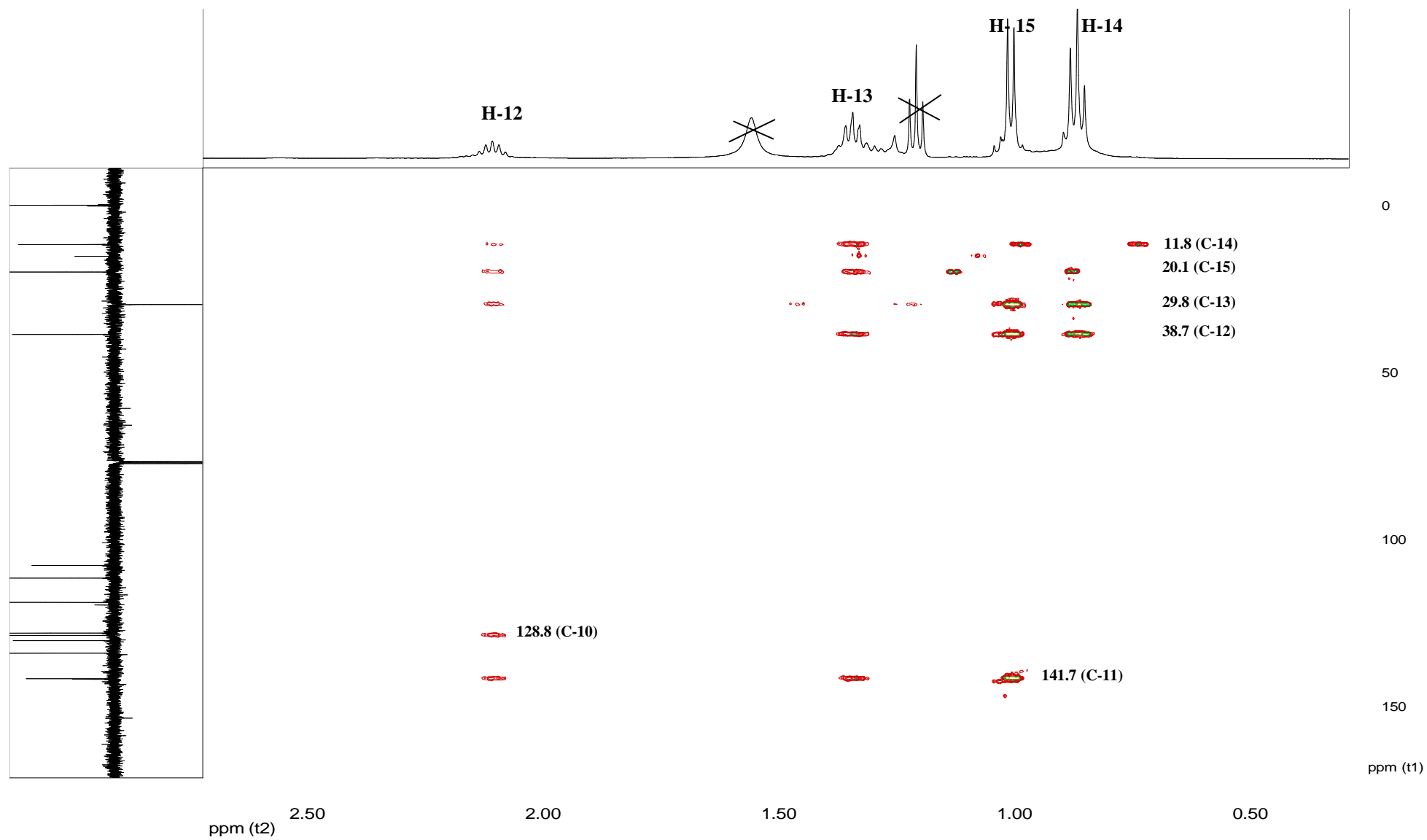


Figure 71: HMBC NMR spectrum (part 2) of bulgariafuran from *B. inquinans* hydrodistillate

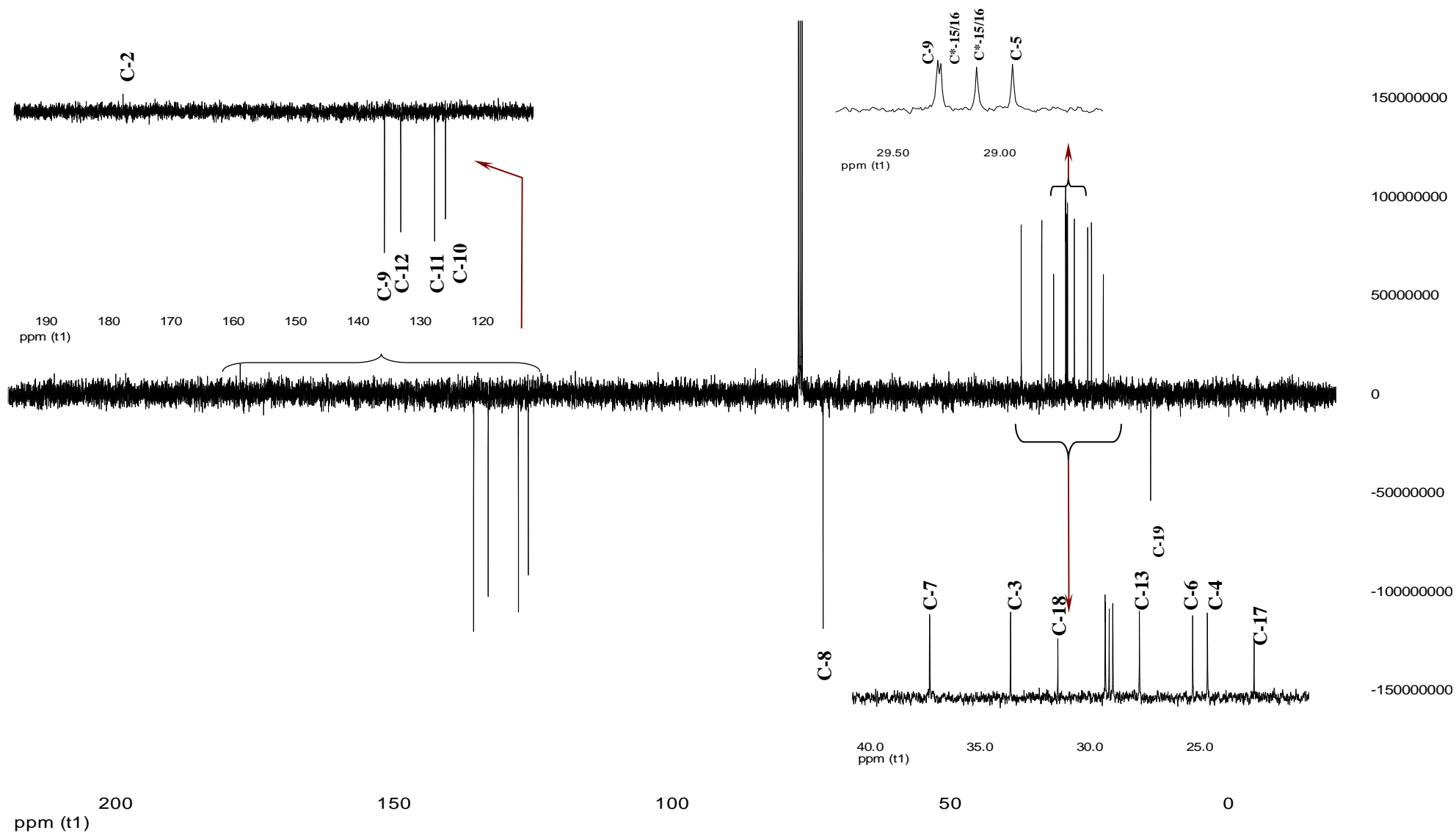


Figure 72: ^{13}C NMR spectrum of meripiluslactone isolated from *Meripilus* ether extract. Starred carbon signals could not be differentiated.

8. Appendix II

Review (Phytochem Rev 9: 315–342)

Azaphilones: a class of fungal metabolites with diverse biological activities.

Natalia Osmanova, Wulf Schultze, Nahla Ayoub

^a – Institute of Pharmacy, Department of Pharmaceutical Biology and Microbiology, University of Hamburg, Hamburg, Germany.

^b – Department of Pharmacognosy, Ain Shams University, Cairo, Egypt

Abstract

This review presents an overview of azaphilones isolated from different fungal species, detailing their chemical structures and biological activities as covered in the recent literature. Over 170 different azaphilone compounds occur in fungi belonging to 23 genera from 13 families: these azaphilones can be classified into ten different structural groups. Numerous azaphilone structures have been described, particularly from members of the *Trichocomaceae* and *Xylariaceae* families. Azaphilones exhibit a wide range of interesting biological activities, such as antimicrobial, antifungal, antiviral, antioxidant, cytotoxic, nematocidal and anti-inflammatory activities. Many of these effects may be explained by the reactions of azaphilones with amino groups, such as those found in amino acids, proteins and nucleic acids, resulting in the formation of vinylogous γ -pyridones.

Keywords: azaphilones, bioactivity, lactones, *Trichocomaceae*, *Xylariaceae*

Introduction

Fungi have long been known to produce a wide variety of biologically active compounds and have been used for medicinal purposes in Africa and Asia from ancient times (e.g. Ying *et al.* 1987, Molitoris, 2002, Hobbs, 2003). Fungi continue to provide active ingredients for important modern drugs, including statins and antifungal agents such as cyclosporine and echinocandin. It is therefore unsurprising that several publications have focused on the discovery of new active principles from fungi (Steglich, 1981, Lorenzen and Anke, 1998, Wasser, 2002, Lindequist, *et al.* 2005). Many different chemical groups have been identified in fungi, including organic acids, polyynes, polyketides (such as quinones, anthraquinones, xanthenes, etc.), mono- to triterpenes (volatiles and steroids), polysaccharides, lipopolysaccharides, and N- and S-containing compounds (Turner, 1971; Turner and Aldridge, 1983; Gill and Steglich, 1987; Steglich *et al.* 2001; Quang *et al.* 2005b).

Azaphilones are another interesting set of secondary fungal metabolites. Considered together, their group is generally held to be a relatively small subset of the polyketide class – indeed, some authors group azaphilones into polyketides without giving any further definition (Turner, 1971; Gill and Steglich, 1987; Gill, 1996; Gill, 1999). However, a more precise definition of this term is required since polyketides represent an array of often structurally complex natural products produced by diverse organisms and include such classes as anthraquinones, flavonoid pigments, macrolide antibiotics, naphthalenes and naphthaquinones, polyenes antibiotics, tetracyclines and tropolones (Turner, 1971; Gill and Steglich, 1987). Polyketides are usually categorised by their chemical structures (Hutchinson, 1999). In this respect, azaphilones can be defined as a structurally-diverse class of fungal secondary metabolites (polyketide derivatives), namely pigments with pyrone-quinone structures containing a highly oxygenated bicyclic core and a chiral quaternary centre (Sturdikova *et al.* 2000; Zhu *et al.* 2005; Dong *et al.* 2006). Note that both a pyrone-quinone structure and a chiral quaternary centre are essential for structures to be classified as azaphilones.

The name azaphilone arose as a result of their affinity for ammonia: the pigments react with amines – such as proteins, amino acids and nucleic acids – to form red or purple vinylogous γ -pyridones due to the exchange of pyrane oxygen for nitrogen (Stadler *et al.* 1995; Sturdikova *et al.* 2000; Way and Yao, 2005). This appears to be a characteristic reaction. It can take place both with ammonia alone as found in the case of monascorubramine and rubropunctamine (Akihisa *et al.* 2005; Akihisa *et al.* 2005a) and the side chain of a macrocyclic polypeptide as discovered for chlorofusin (Duncan *et al.* 2001, 2003).

It is necessary, however, to note that azaphilones are not the only structural class reacting with primary amines. Thus, fluorones isolated from *Echinodontum tinctorium* and *Pyroformes albomarginatus* also change their colour on exposure to ammonia (Gill, 1996). However, they are not azaphilones and should not be mistakenly included in the azaphilone class.

This review does not address the detailed aspects of azaphilone biosynthesis. However, this article will present some general information about possible biosynthetic pathways.

Biosynthetically, most pigments produced by fungi are polyketide-based (some may involve polyketide-amino acid mixed biosynthesis) and involve complex pathways catalysed by iterative type I polyketide synthases.

The biosynthesis of azaphilones uses both the polyketide pathway and the fatty acid synthesis pathway. The polyketide pathway assembles the main polyketide chain of the azaphilone pigments from acetic acid (the starter unit) and five malonic acid molecules (the chain extender unit) in a conventional way to generate the chromophore structure. The fatty acid synthesis pathway produces a medium-chain fatty acid (octanoic or hexanoic acid) that is then bound to the chromophore by a transesterification reaction (Hajjaj, *et al.* 1999; Velíšek, *et al.* 2008).

Biosynthetic pathways are suggested for the following azaphilones: monascorubrin and monascoflavin (Kurono *et al.* 1963); mitorubrin and rubropunctatin (Turner, 1971); ascochitine (Turner and Aldridge, 1983); ochrephilone (Turner and Aldridge, 1983); citrinin (Turner and Aldridge, 1983; Hajjaj *et al.* 1999); monascusones A and

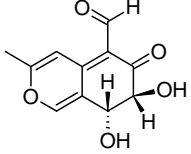
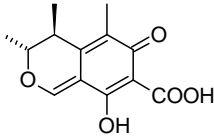
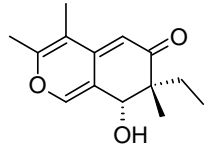
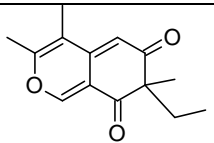
B, monascin (Jongrungruangchok, *et al.* 2004) and sassafrin D (Quand, *et al.* 2005). However, some researchers are of the opinion that comprehensive knowledge about the biosynthetic pathway of polyketide pigments (including the extensively studied *Monascus* pigments) is not yet available (Mapari *et al.* 2009).

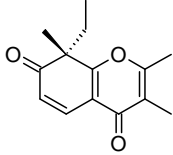
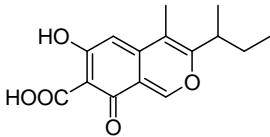
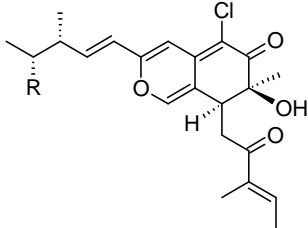
Azaphilones exhibit a wide range of interesting biological activities, such as antimicrobial, antifungal, antiviral, antioxidant, cytotoxic, nematocidal and anti-inflammatory activities. The potent non-selective biological activities of azaphilones may be related to their production of vinylogous γ -pyridones (Park *et al.* 2005).

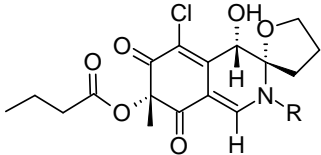
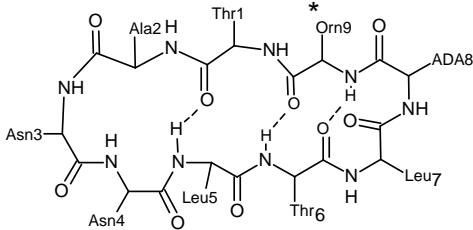
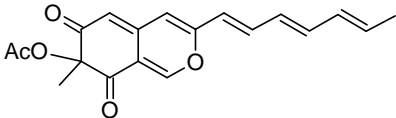
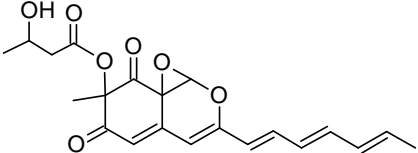
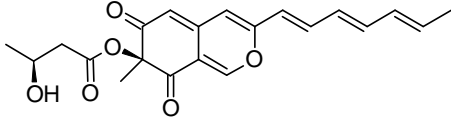
Some azaphilone structures have already been presented in reviews of secondary metabolites such as fungal pigments. However, since these reviews of fungal metabolites are general and deal with numerous substance classes (Turner, 1971; Turner and Steglich, 1983; Gill and Steglich, 1987; Quang *et al.* 2006), this necessarily means that azaphilones are presented only as a marginal group.

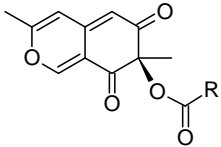
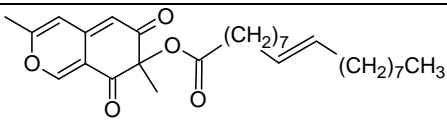
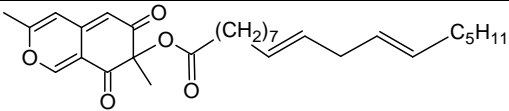
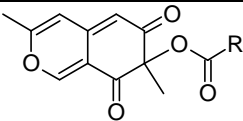
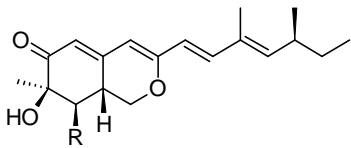
Azaphilones are also mentioned in a number of systematic reviews of certain families or genera of fungi (Frisvad *et al.* 1990; Stadler *et al.* 2005; Stadler and Fournier, 2006; Pelaez *et al.* 2008). However, these authors cover only a fraction of all known azaphilones, since their articles naturally omit the azaphilones produced by fungi not included in their reviews.

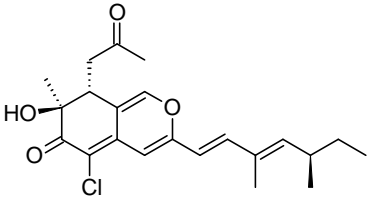
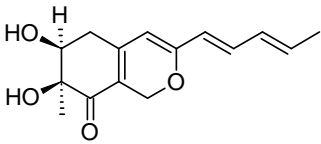
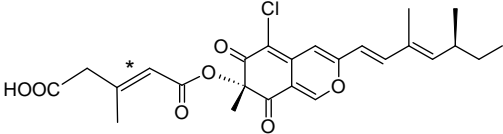
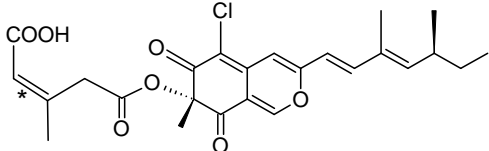
Our review therefore aims to provide readers with essential, clearly summarised data on azaphilones as presented in the literature to date. Presenting this data in a concise, tabular format, the article offers information about chemical structures, producing species and identified biological activities.

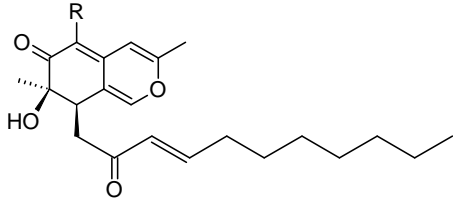
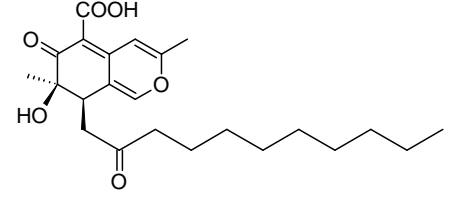
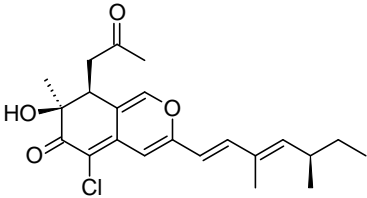
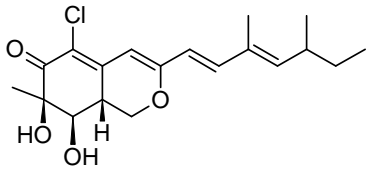
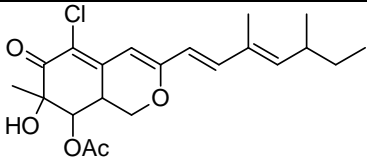
Azaphilone	Structure	Species	Activity
Bicyclic azaphilones			
Austdiol (Vleggaar et al., 1974; Sturdikova <i>et al.</i> , 2000)		<i>Aspergillus ustus</i>	
Citrinin (Endo and Kuroda, 1976; Natsume <i>et al.</i> , 1988; Blanc <i>et al.</i> , 1995; Pisareva <i>et al.</i> , 2005)		<i>Monascus sp.</i> <i>P. ultimum</i> <i>P. odoratum</i> <i>P. viridicatum</i>	Phytotoxin; inhibitor of cholesterol synthesis; nephrotoxic agent; chlamyospore-like cell-inducing agent
Pseudohalonectrin A (Dong <i>et al.</i> , 2006)		<i>Pseudohalonectria adversaria</i>	Nematicidal activity against the pine wood nematode <i>Bursaphelenchus xylophilus</i>
Spiciferinone (Nakajima <i>et al.</i> , 1992)		<i>Cochliobolus spicifer</i>	Phytotoxin

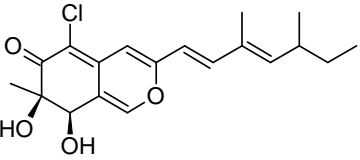
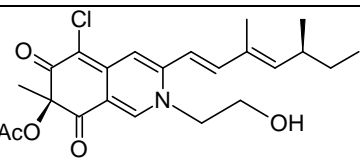
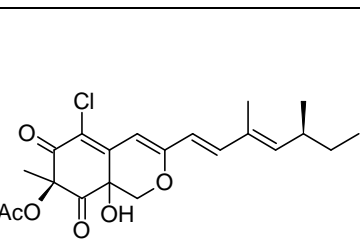
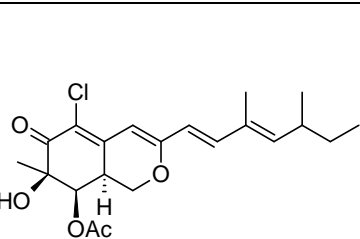
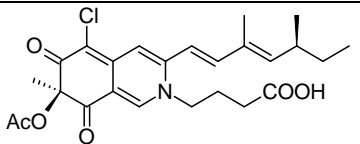
<p>Spiciferone A (Nakajima <i>et al.</i>, 1992)</p>		<p><i>C. spicifer</i></p>	<p>Phytotoxin</p>
<p>Bicyclic azaphilones with aliphatic side chain</p>			
<p>Ascochitine (Turner and Aldridge, 1983; Beed <i>et al.</i>, 1994; Kusnick <i>et al.</i>, 2002; Seibert <i>et al.</i>, 2006)</p>		<p><i>Ascochyta obiones</i> <i>A. salicorniae</i> <i>A. fabae</i> <i>Kirschsteiniothelia maritima</i></p>	<p>Potential inhibitor of protein phosphatases; enzymatic activity Of MPtpB (mycobacterial protein tyrosine phosphatases B) inhibitor; causes necrosis and wilting of plant cuttings</p>
<p>Chaetomugilin I, J (Muroga <i>et al.</i>, 2009)</p>	 <p>Chaetomugilin I R = OH; Chaetomugilin J R = H</p>	<p><i>C. globosum</i></p>	<p>Growth inhibition of P388, HL-60, L1210, and KB cell lines; selective cytotoxic activity against 39 human cancer cell lines</p>

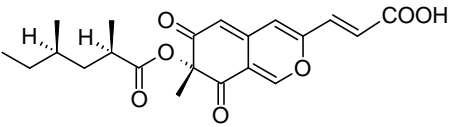
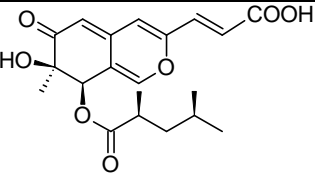
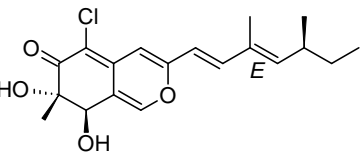
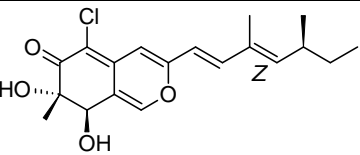
<p>Chlorofusin (Duncan <i>et al.</i>, 2001; Duncan <i>et al.</i>, 2003)</p>	 <p style="text-align: center;">R =</p>  <p style="text-align: center;">asterisk shows the linkage with azaphilone core</p>	<p><i>Fusarium</i> sp.</p>	<p>Anticancer agent: antagonist of p53/MDM2 interaction</p>
<p>Chrysodin (Closse, and Hauser, 1973; Haraguchi <i>et al.</i>, 1990)</p>		<p><i>Sepedonium chrysospermum</i></p>	<p>Antifungal antimetabolite inhibits growth of yeasts</p>
<p>CT 2108A (Laakso <i>et al.</i>, 2003)</p>		<p><i>Penicillium solitum</i> (Westling) strain CT2108</p>	<p>Antifungal agent: inhibitor of fungal fatty acid synthase</p>
<p>CT 2108B (Laakso <i>et al.</i>, 2003)</p>		<p><i>P. solitum</i> (Westling) strain CT2108</p>	<p>Antifungal agent: inhibitor of fungal fatty acid synthase</p>

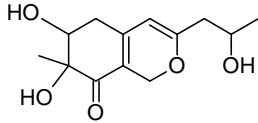
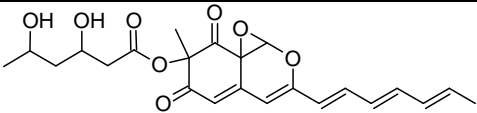
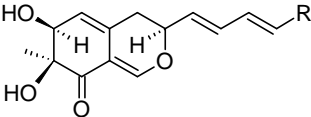
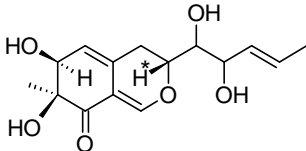
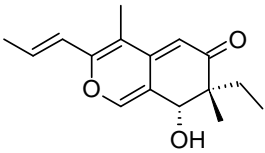
<p>Daldinins A1 and A2 (Hashimoto <i>et al.</i>, 1994)</p>	 <p>Daldinin A1 R = (CH₂)₁₄CH₃ Daldinin A2 R = (CH₂)₁₆CH₃</p>	<p><i>Daldinia concentrica</i></p>	
<p>Daldinin A3, B3 (Hashimoto <i>et al.</i>, 1994)</p>		<p><i>D. concentrica</i></p>	
<p>Daldinin A4, B4 (Hashimoto <i>et al.</i>, 1994)</p>		<p><i>D. concentrica</i></p>	
<p>Daldinins B1 and B2 (Hashimoto <i>et al.</i>, 1994)</p>	 <p>Daldinin B1 R = (CH₂)₁₄CH₃ Daldinin B2 R = (CH₂)₁₆CH₃</p>	<p><i>D. concentrica</i></p>	
<p>Dechloroisochromophilones III and IV (Matsuzaki <i>et al.</i>, 1998)</p>	 <p>Dechloroisochromophilone III R = OH Dechloroisochromophilone IV R = OAc</p>	<p><i>P. multicolor</i></p>	

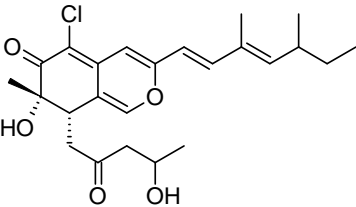
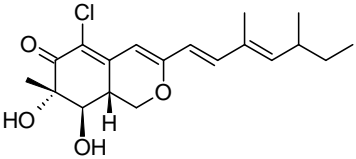
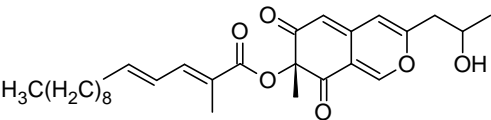
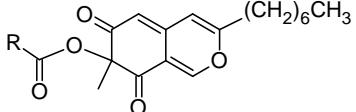
<p>epi-Isochromophilone II (Kanokmedhakul <i>et al.</i>, 2006)</p>		<p><i>Chaetomium cupreum</i> CC3003</p>	
<p>Harziphilone (Qian-Cutrone <i>et al.</i>, 1996)</p>		<p><i>Trichoderma harzianum</i></p>	<p>Cytotoxic activity against the murine tumour cell line M- 109; inhibitor of REV- protein to RRE RNA binding</p>
<p>Helicusins A and B (Yoshida <i>et al.</i>, 1995)</p>	 <p>Helicusin A (E)* Helicusin B (Z)*</p>	<p><i>Talaromyces helicus</i></p>	<p>Monoamine oxidase (MAO) inhibitor</p>
<p>Helicusins C and D (Yoshida <i>et al.</i>, 1995)</p>	 <p>Helicusin C (E)* Helicusin D (Z)*</p>	<p><i>T. helicus</i></p>	<p>MAO inhibitor</p>

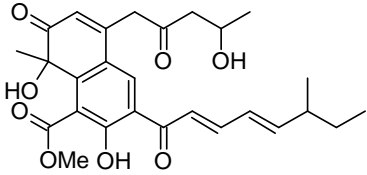
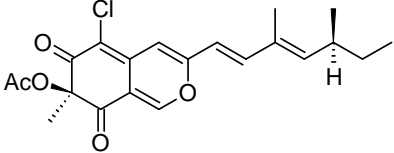
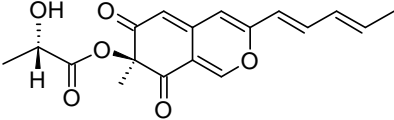
<p>Helotialins A and B (Zou <i>et al.</i>, 2009)</p>	 <p>Helotialin A R = COOH Helotialin B R = H</p>	<p>unidentified species of <i>Helotiales</i>.</p>	<p>inhibitory effects on HIV-1 replication in C8166 cells</p>
<p>Helotialin C (Zou <i>et al.</i>, 2009)</p>		<p>unidentified species of <i>Helotiales</i></p>	
<p>Isochromophilone II (Matsuzaki <i>et al.</i>, 1995; Matsuzaki <i>et al.</i>, 1998)</p>		<p><i>P. multicolor</i> FO-2338</p>	<p>gp120-CD4 binding inhibitor</p>
<p>Isochromophilone III (Arai <i>et al.</i>, 1995; Matsuzaki <i>et al.</i>, 1998; Tomoda <i>et al.</i>, 1999)</p>		<p><i>P. multicolor</i> FO-2338</p>	<p>gp120-CD4 binding inhibitor</p>
<p>Isochromophilone IV (Arai <i>et al.</i>, 1995; Matsuzaki <i>et al.</i>, 1998; Nam <i>et al.</i>, 2000)</p>		<p><i>P. multicolor</i> FO-2338 <i>P. multicolor</i> F1753</p>	<p>gp120-CD4 binding inhibitor; Acyl-CoA inhibitor</p>

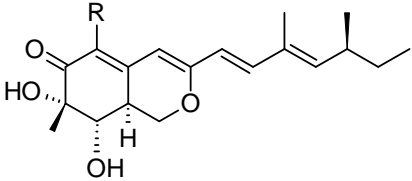
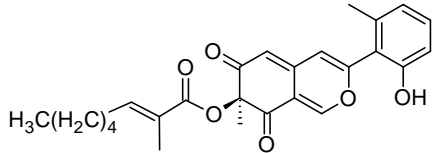
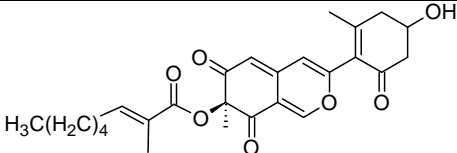
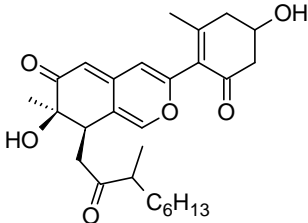
<p>Isochromophilone V (Arai <i>et al.</i>, 1995; Matsuzaki <i>et al.</i>, 1998)</p>		<p><i>P. multicolor</i> FO-2338</p>	<p>gp120-CD4 binding inhibitor; Acyl-CoA inhibitor</p>
<p>Isochromophilone VI (Arai <i>et al.</i>, 1995)</p>		<p><i>P. multicolor</i> FO-2338 <i>P. multicolor</i> F1753</p>	<p>gp120-CD4 binding inhibitor; Acyl-CoA inhibitor</p>
<p>Isochromophilone VII (Yang <i>et al.</i>, 1996)</p>		<p><i>Penicillium sp.</i></p>	<p>Inhibitor of diacylglycerol acyltransferase activity; cholesterol acyltransferase activity inhibitor</p>
<p>Isochromophilone VIII (Yang <i>et al.</i>, 1996; Michael <i>et al.</i>, 2003)</p>		<p><i>Penicillium sp.</i></p>	<p>Inhibitor of diacylglycerol acyltransferase activity; cholesterol acyltransferase activity inhibitor</p>
<p>Isochromophilone IX (Michael <i>et al.</i>, 2003)</p>		<p><i>Penicillium sp.</i></p>	<p>Antibiotic against Methicillin-resistant <i>S. aureus</i> (MRSA)</p>

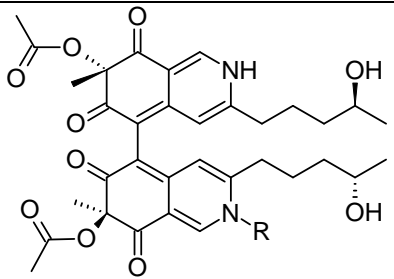
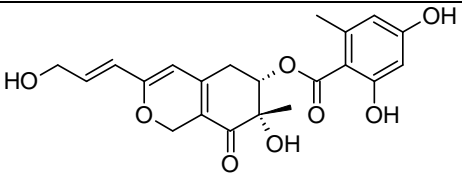
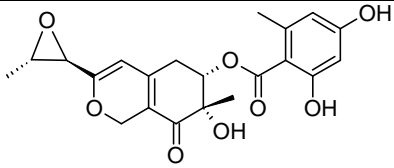
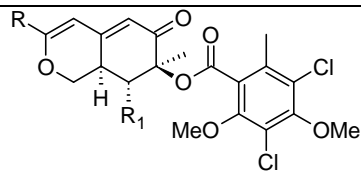
<p>Lunatoic acid A (Marumo <i>et al.</i>, 1982; Natsume <i>et al.</i>, 1988; Matsuzaki <i>et al.</i>, 1998)</p>		<p><i>C. lunatus</i> IFO 5997 <i>P. multicolor</i> FO-2338</p>	<p>Aversion factor; antifungal activity against <i>Curvularia trifolii</i>; chlamyospore-like cell-inducing agent</p>
<p>Lunatoic acid B (Natsume <i>et al.</i>, 1988; Nukina and Marumo, 1977)</p>		<p><i>C. lunatus</i> IFO 5997 <i>P. multicolor</i> FO-2338</p>	<p>Aversion factor</p>
<p>Luteusin A (Antibiotic RP 1551-7, Luteusin, TL-1) (Fujimoto <i>et al.</i>, 1990; Pairet <i>et al.</i>, 1995; Yoshida <i>et al.</i>, 1996; Matsuzaki <i>et al.</i>, 1998; Sturdikova <i>et al.</i>, 2000)</p>		<p><i>P. multicolor</i> FO-2338 <i>P. sclerotiorum</i> X11853 <i>P. vonarxii</i> <i>T. luteus</i></p>	<p>gp120-CD4 binding inhibitor; MAO inhibitor <i>in vitro</i>; Endothelin receptors binding agent</p>
<p>Luteusin B (TL-2) (Fujimoto <i>et al.</i>, 1990; Pairet <i>et al.</i>, 1995)</p>		<p><i>T. luteus</i> <i>P. sclerotiorum</i> X11853</p>	

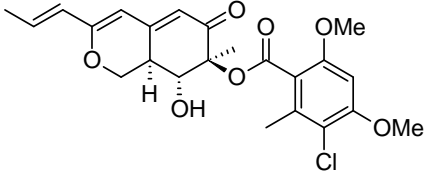
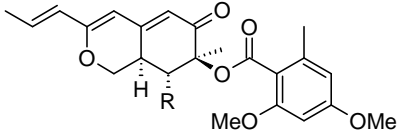
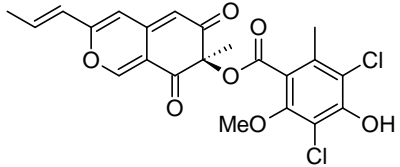
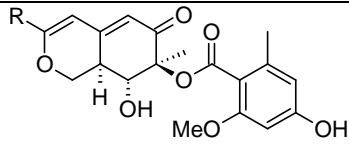
<p>Monascusone A (Jongrungruangchok <i>et al.</i>, 2004)</p>		<p><i>Monascus kaoliang</i></p>	
<p>Patulodin (Sakuda <i>et al.</i>, 1995)</p>		<p><i>P. urticae</i></p>	<p>Antifungal agent</p>
<p>Phomoeuphorbins A and B (Yu <i>et al.</i>, 2008)</p>	 <p>Phomoeuphorbin A R= COOH Phomoeuphorbin B R= H</p>	<p><i>Phomopsis euphorbiae</i></p>	<p>Phomoeuphorbin A: Inhibitor of HIV replication in C8166 cells <i>in vitro</i>; Phomoeuphorbin B is not active</p>
<p>Phomoeuphorbins C and D (Yu <i>et al.</i>, 2008)</p>	 <p>Phomoeuphorbin D (S)*</p>	<p><i>P. euphorbiae</i></p>	<p>Phomoeuphorbin C: Inhibitor of HIV replication in C8166 cells <i>in vitro</i>; Phomoeuphorbin D is not active</p>
<p>Pseudohalonectrin B (Dong <i>et al.</i>, 2006)</p>		<p><i>P. adversaria</i> YMF1.01019</p>	<p>Nematicidal activity against the pine wood nematode <i>B.</i> <i>xylophilus</i></p>

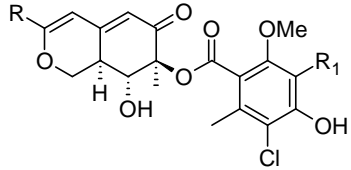
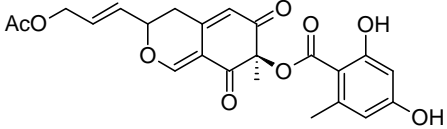
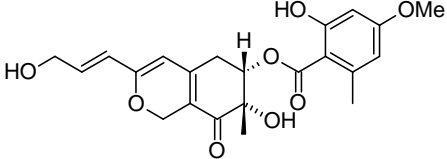
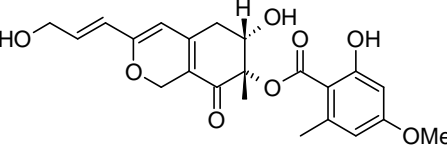
<p>RP 1551-2 (Toki <i>et al.</i>, 1999)</p>		<p><i>Penicillium sp.</i> SPC-21609</p>	<p>Inhibitor of platelet-derived growth factor (PDGF) binding to its receptor; antibacterial activity against <i>Bacillus subtilis</i>, <i>Enterococcus faecium</i>, <i>Staphylococcus aureus</i></p>
<p>RP 1551-M2 (Toki <i>et al.</i>, 1999)</p>		<p><i>Penicillium sp.</i> SPC-21609</p>	<p>Inhibitor of (PDGF) binding to its receptor; antibacterial against <i>B. subtilis</i>, <i>E. faecium</i>, <i>S. aureus</i></p>
<p>Rubiginosin C (Quang <i>et al.</i>, 2004; Quang <i>et al.</i>, 2006a)</p>		<p><i>Hypoxylon rubiginosum</i>.</p>	<p>Antioxidant; inhibits nitric oxide (NO) production in RAW 264.7 cells</p>
<p>S 15183a and S 15183b (Kono <i>et al.</i>, 2001)</p>	 <p>S 15183a R = (CH₂)₆CH₃ S 15183b R = (CH₂)₈CH₃</p>	<p><i>Zopfiella inermis</i> SANK 15183</p>	<p>Inhibits sphingosine kinase from rat liver and endogenous SPH kinase activity in intact platelets</p>

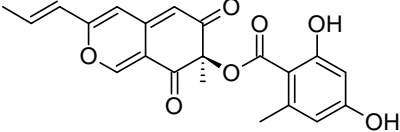
<p>Sassafrin D (Quang <i>et al.</i>, 2005)</p>		<p><i>Creosphaeria sassafras</i></p>	<p>Broad-spectrum antimicrobial activity</p>
<p>Sclerotiorin (Natsume <i>et al.</i>, 1988; Pairet <i>et al.</i>, 1995; Tomoda <i>et al.</i>, 1999; Nam <i>et al.</i>, 2000; Chidananda <i>et al.</i>, 2006)</p>		<p><i>P. multicolor</i> F1753 <i>P. sclerotiorum</i> X11853 <i>P. frequentans</i> <i>P. hirayamae</i> Udagawa</p>	<p>Inhibits binding between Grb2-SH2 domain and phosphopeptide derived from the Shc protein; aldose reductase inhibitor; antibacterial activity against <i>Bacillus spp.</i>; chlamyospore-like cell-inducing agent; Endothelin receptors binding agent</p>
<p>T22 azaphilone (Vinale <i>et al.</i>, 2006)</p>		<p><i>T. harzianum</i> strains T22</p>	<p><i>In vitro</i> inhibitor of <i>Rhizoctonia solani</i>, <i>Pythium ultimum</i> and <i>Gaeumannomyces graminis</i> var. <i>tritici</i>.</p>

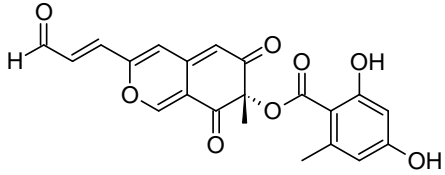
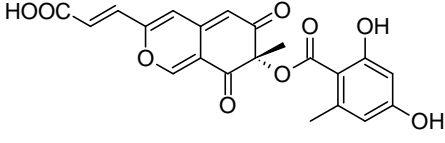
<p>(8S,8a-R)-7-deacetyl-1,08,8,8a-tetrahydro-7-epi-sclerotiorin and 5-dechloro analog (Pairet <i>et al.</i>, 1995)</p>	 <p>(8S,8a-R)-7-deacetyl-1,08,8,8a-tetrahydro-7-epi-sclerotiorin R = Cl 5-dechloro analog R = H</p>	<p><i>P. sclerotiorum</i> X11853</p>	<p>Endothelin receptors binding agent</p>
<p>Bicyclic azaphilones with aliphatic side chain and aromatic ring</p>			
<p>Cohaerin A (Quang <i>et al.</i>, 2005a; Quang <i>et al.</i>, 2006a,b)</p>		<p><i>H. cohaerens</i></p>	<p>Antioxidant; inhibits NO production in RAW 264.7 cells</p>
<p>Cohaerin B (Quang <i>et al.</i>, 2005a; Quang <i>et al.</i>, 2006a,b)</p>		<p><i>H. cohaerens</i></p>	<p>Antioxidant; inhibits NO production in RAW 264.7 cells</p>
<p>Cohaerin F (Quang <i>et al.</i>, 2006b)</p>		<p><i>A. cohaerens</i></p>	<p>Inhibits NO production in RAW cells; strong nonselective antimicrobial agent</p>

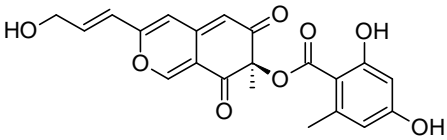
Dimeric azaphilones			
Chaetoglobins A and B (Ming <i>et al.</i> , 2008)	 <p>Chaetoglobin A R = H; Chaetoglobin B R = (CH₂)₂OH</p>	<i>C. globosum</i>	Antitumor activity in cell line MCF-7 and colon cancer cell line SW1116
Bicyclic azaphilones with o-orsellinic acid or o-orsellinic acid derivatives			
Entonaemin A (Buchanan <i>et al.</i> , 1995; Quang <i>et al.</i> , 2004; Quang <i>et al.</i> , 2006a)		<i>H. rubiginosum</i> <i>Entonaema splendens</i>	Antioxidant; inhibits NO production in RAW 264.7 cells
Entonaemin B (Buchanan <i>et al.</i> , 1995)		<i>E. splendens</i>	
Falconensins A, B, C and D (Itabashi <i>et al.</i> , 1996; Yasukawa <i>et al.</i> , 2008)	 <p>Falconensin A R = propenyl; R₁ = OH Falconensin B; R = n-propyl; R₁ = OH Falconensin C R = propenyl; R₁ = OAc Falconensin D R = n-propyl; R₁ = OAc</p>	<i>Emericella falconensis</i>	Anti-inflammatory activity induced by TPA (12-O-tetradecanoylphorbol-13-acetate)

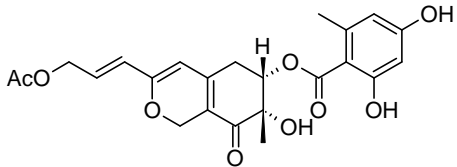
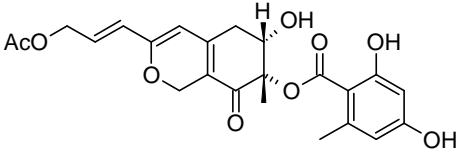
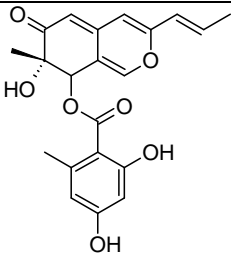
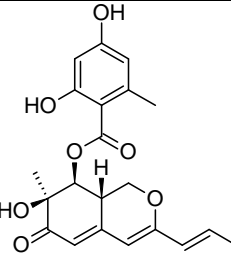
Falconensin E (Itabashi <i>et al.</i> , 1996; Yasukawa <i>et al.</i> , 2008)		<i>E. falconensis</i>	Anti-inflammatory activity induced by TPA
Falconensins F and G (Itabashi <i>et al.</i> , 1996; Yasukawa <i>et al.</i> , 2008)	 <p data-bbox="551 555 864 643">Falconensin F R = OH Falconensin G R = OAc</p>	<i>E. falconensis</i>	Anti-inflammatory activity induced by TPA
Falconensin H (Itabashi <i>et al.</i> , 1993; Itabashi <i>et al.</i> , 1996; Yasukawa <i>et al.</i> , 2008)		<i>E. falconensis</i>	Anti-inflammatory activity induced by TPA
Falconensins I and J (Ogasawara and Kawai, 1998; Yasukawa <i>et al.</i> , 2008)	 <p data-bbox="551 1066 902 1153">Falconensin I R = propenyl Falconensin J R = n-propyl</p>	<i>E. falconensis</i> <i>E. fruticulosa</i>	Anti-inflammatory activity induced by TPA

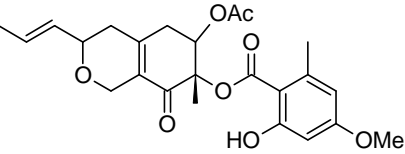
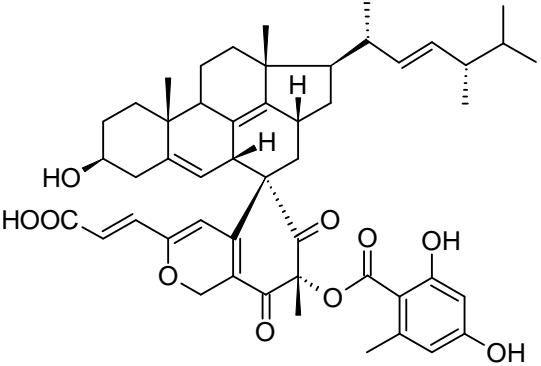
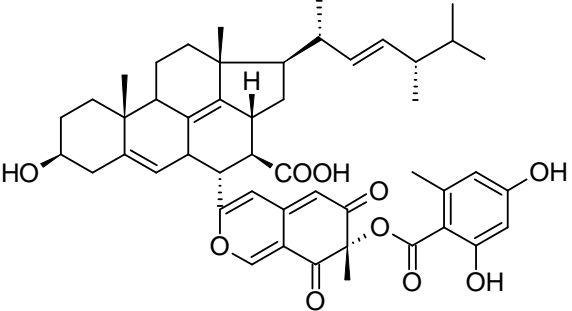
<p>Falconensins K, L, M and N (Ogasawara and Kawai, 1998; Yasukawa <i>et al.</i>, 2008)</p>	 <p>Falconensin K R = propeyl; R₁ = H Falconensin L R = n-propyl; R₁ = H Falconensin M R = propenyl; R₁ = Cl Falconensin N R = n-propyl; R₁ = Cl</p>	<p><i>E. falconensis</i> <i>E. fruticulosa</i></p>	<p>Anti-inflammatory activity induced by TPA</p>
<p>Hypomiltin (Hellwig <i>et al.</i>, 2005; Stadler <i>et al.</i>, 2005)</p>		<p><i>H. hypomiltum</i> <i>H. intermedium</i> <i>H. perforatum</i> <i>H. trugodes</i> <i>H. piceum</i> (= <i>Pyrenomyxa</i> <i>picea</i>) <i>Pulveria porrecta</i></p>	
<p>Kasanosin A (Kimura <i>et al.</i>, 2008)</p>		<p><i>Talaromyces sp.</i></p>	<p>Specific inhibitor of eukaryotic DNA polymerases β and λ</p>
<p>Kasanosin B (Kimura <i>et al.</i>, 2008)</p>		<p><i>Talaromyces sp.</i></p>	<p>Specific inhibitor of eukaryotic DNA polymerases β and λ</p>

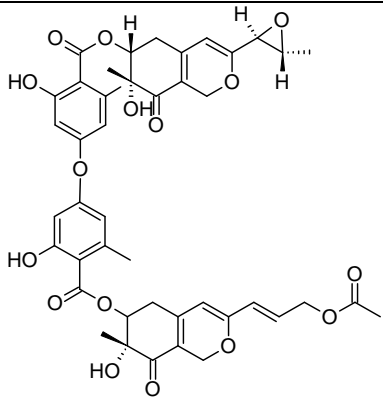
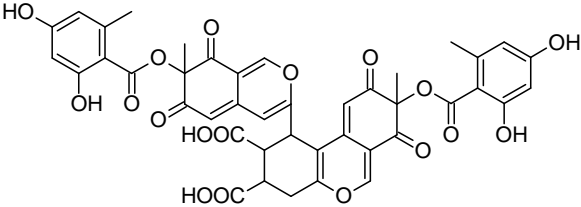
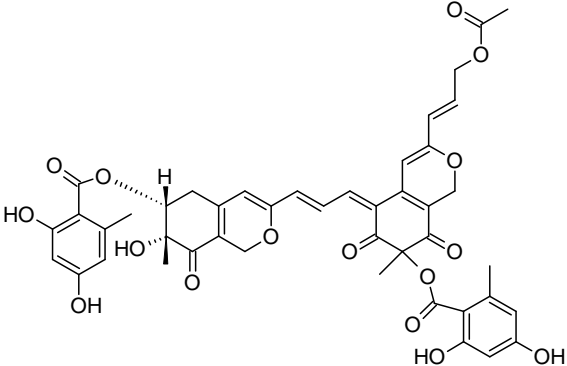
<p>(-)-Mitorubrin (Buechi <i>et al.</i>, 1965; Frisvad <i>et al.</i>, 1990; Mühlbauer <i>et al.</i>, 2002; Hellwig <i>et al.</i>, 2005; Stadler <i>et al.</i>, 2006)</p>		<p><i>E. cinnabarina</i> <i>H. aucklandiae</i> <i>H. crocopeplum</i> <i>H. dingleyae</i> <i>H. fendleri</i> <i>H. fragiforme</i> <i>H. fuscum</i> <i>H. haematostroma</i> <i>H. howeianum</i> <i>H. pilgerianum</i> <i>H. rubiginosum</i> <i>H. subcrocopeplum</i> <i>H. subgilvum</i> <i>H. subrutiloides</i> <i>H. subticiense</i> <i>H. ticinense</i> <i>P. rubrum</i> <i>T. flavus</i> <i>T. macrosporus</i> <i>T. mimosinus</i> <i>T. udagawae</i> <i>T. wortmannii</i></p>	<p>Nematicidal activity against <i>Caenorhabditis elegans</i>; antimicrobial activity against <i>B. subtilis</i>, <i>Yarrowia lipolytica</i>; antifungal agent</p>
--	--	---	--

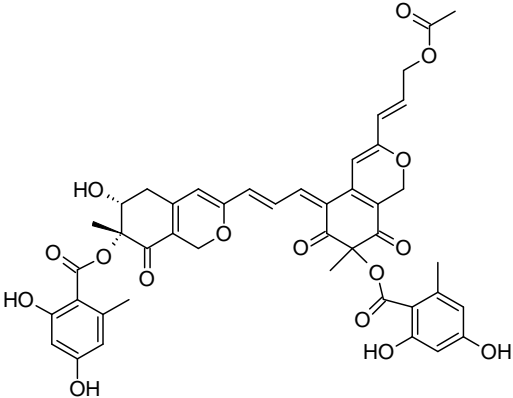
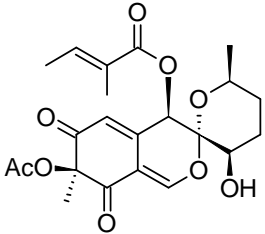
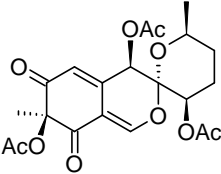
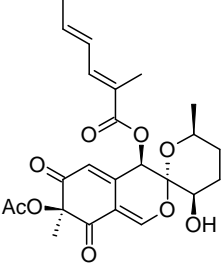
<p>(-)-Mitorubrinol (Suzuki <i>et al.</i>, 1999)</p>	 <p>The structure shows a central chromone ring system. At the 2-position, there is a propenal side chain (-CH=CH-CHO). At the 3-position, there is a methoxy group (-OCH₃). At the 4-position, there is a methyl group (-CH₃). At the 7-position, there is a propionate ester group (-COO-CH₂-CH₂-COO-), which is further esterified to a 3,4-dihydroxyphenyl group.</p>	<p><i>T. austrocalifornicus</i> <i>T. convolutus</i></p>	<p>Nematicidal activity against <i>C. elegans</i>; antimicrobial activity against <i>B. subtilis</i>, <i>Y. lipolytica</i>; antifungal agent</p>
<p>Mitorubrinic acid (Locci <i>et al.</i>, 1967; Steglich <i>et al.</i>, 1974; Natsume <i>et al.</i>, 1988; Frisvad <i>et al.</i>, 1990; Suzuki <i>et al.</i>, 1999; Lesova <i>et al.</i>, 2000; Lesova <i>et al.</i>, 2000a; Quang <i>et al.</i>, 2006a; Stadler <i>et al.</i>, 2006,)</p>	 <p>The structure is similar to (-)-Mitorubrinol, but the propenal side chain at the 2-position is replaced by a propionic acid side chain (-CH=CH-COOH).</p>	<p><i>H. fragiforme</i> <i>P. rubrum</i> <i>P. funiculosum</i> <i>P. porrecta</i> <i>Pyrenomyxa invocans</i> <i>T. austrocalifornicus</i> <i>T. convolutes</i> <i>T. flavus</i> <i>T. macrosporus</i> <i>T. mimosinus</i> <i>T. udagawae</i> <i>T. wortmannii</i></p>	<p>Trypsin inhibitor; nematicidal activity against <i>C. elegans</i>; antimicrobial activity against <i>B. subtilis</i>, <i>Y. lipolytica</i>; antifungal agent; inhibits NO production in RAW 264.7 cells; chlamydospore-like cell-inducing agent</p>

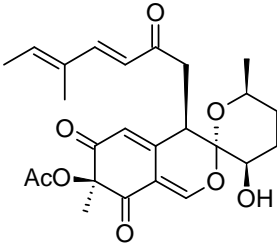
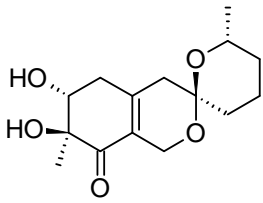
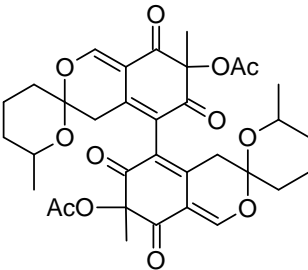
<p>Mitorubrinol (Buechi <i>et al.</i>, 1965; Steglich <i>et al.</i>, 1974; Frisvad <i>et al.</i>, 1990; Proksa <i>et al.</i>, 1992; Sturdikova <i>et al.</i>, 2000; Mühlbauer <i>et al.</i>, 2002; Hellwig <i>et al.</i>, 2005; Stadler <i>et al.</i>, 2005; Quang <i>et al.</i>, 2006a; Stadler <i>et al.</i>, 2006)</p>		<p><i>E. cinnabarina</i> <i>H. aucklandiae</i> <i>H. crocopeplum</i> <i>H. dihgleyae</i> <i>H. fedleri</i> <i>H. fragiforme</i> <i>H. haematostroma</i> <i>H. howeianum</i> <i>H. julianii</i> <i>H. laschii</i> <i>H. rutilum</i> <i>H. subcrocopeplum</i> <i>H. subgilvum</i> <i>H. subticiense</i> <i>H. ticiense</i> <i>P. funiculosum</i> <i>P. rubrum</i> <i>P. vermiculatum</i> <i>P. wortmannii</i> <i>P. invocans</i> <i>T. wortmannii</i></p>	<p>Nematicidal activity against <i>C. elegans</i>; antimicrobial activity against <i>B. subtilis</i>, <i>Y. lipolytica</i>; antifungal agent; inhibits NO production in RAW 264.7 cells</p>
---	--	---	---

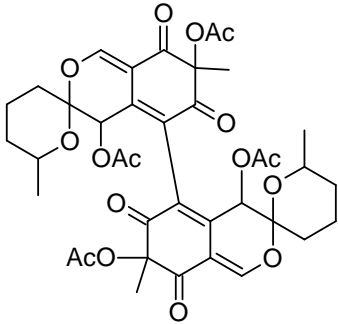
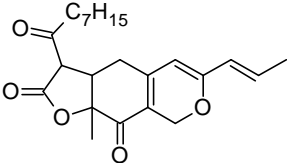
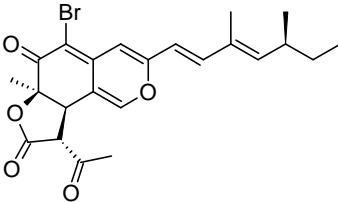
<p>Rubiginosin A (Mühlbauer <i>et al.</i>, 2002; Quang <i>et al.</i>, 2004; Hellwig <i>et al.</i>, 2005; Stadler <i>et al.</i>, 2005; Quang <i>et al.</i>, 2006a)</p>		<p><i>E. cinnabarina</i> <i>H. dingleyae</i> <i>H. julianii</i> <i>H. laschii</i> <i>H. rubiginosum</i> <i>H. rutilum</i> <i>H. subticinense</i> <i>P. invocans</i></p>	<p>Antioxidant; inhibits NO production in RAW 264.7 cells</p>
<p>Rubiginosin B (Quang <i>et al.</i>, 2004; Quang <i>et al.</i>, 2006a)</p>		<p><i>H. rubiginosum</i></p>	<p>Antioxidant; inhibits NO production in RAW 264.7 cells</p>
<p>Sch 1385568 (Yang <i>et al.</i>, 2009)</p>		<p><i>Aspergillus sp.</i> culture (SPRI-0814)</p>	<p>antifungal activity against <i>Saccharomyces cerevisiae</i> (PM503)</p>
<p>Sch 725680 (Yang <i>et al.</i>, 2006)</p>		<p><i>Aspergillus sp.</i></p>	<p>Inhibitor of <i>S. cerevisiae</i> (PM503) and <i>Candida albicans</i> (C43) growth</p>

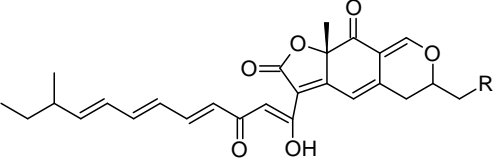
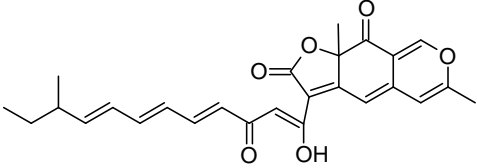
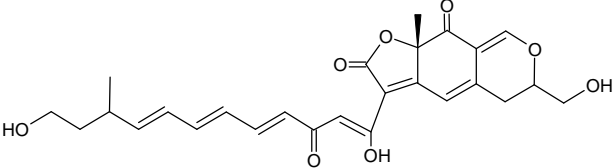
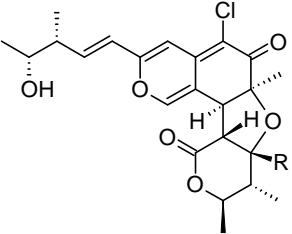
<p>Wortmin (Merlini, <i>et al.</i>, 1973; Turner and Aldridge 1983; Sturdikova <i>et al.</i>, 2000)</p>		<p><i>P. wortmannii</i> <i>T. wortmannii</i></p>	
<p>Bicyclic azaphilones with ergostane skeleton and o-orsellinic acid</p>			
<p>Ergophilone A (Hyodo <i>et al.</i>, 1994)</p>		<p><i>Penicillium sp.</i> BM-99</p>	<p>Inhibitor of the rat platelet Phospholipase A2 (PLA2)</p>
<p>Ergophilone B (Hyodo <i>et al.</i>, 1994)</p>		<p><i>Penicillium sp.</i> BM-99</p>	<p>Inhibitor of the rat platelet PLA2</p>

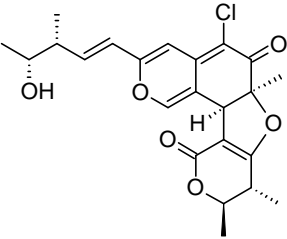
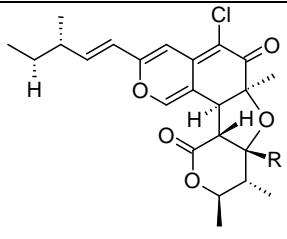
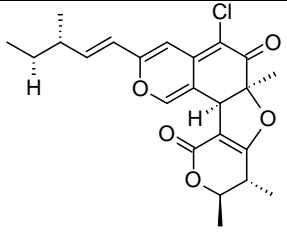
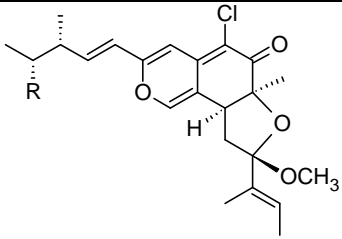
Dimeric azaphilones with o-orsellinic acid moiety			
<p>Entonaemin C (Hashimoto and Asakawa, 1998)</p>		<p><i>E. splendens</i></p>	
<p>Diazaphilonic acid (Tabata <i>et al.</i>, 1999)</p>		<p><i>T. flavus</i></p>	<p>Inhibitor of DNA amplification by polymerase chain reaction (PCR) and inhibitor of telomerase activity</p>
<p>Rutilin A (Quang <i>et al.</i>, 2005b; Quang <i>et al.</i>, 2006a)</p>		<p><i>H. rutilum</i></p>	<p>Antioxidant; inhibits NO production in RAW 264.7 cells</p>

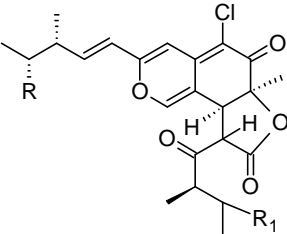
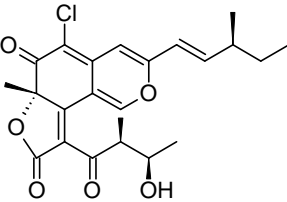
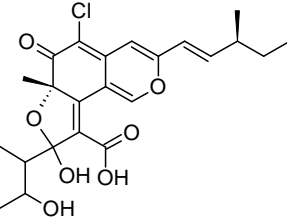
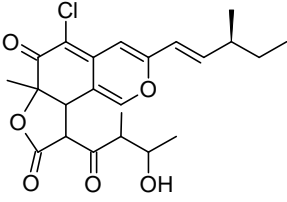
<p>Rutilin B (Quang <i>et al.</i>, 2005b; Quang <i>et al.</i>, 2006a)</p>		<p><i>H. rutilum</i></p>	<p>Antioxidant; inhibits NO production in RAW 264.7 cells</p>
<p>Bicyclic spiro-azaphilones</p>			
<p>Daldinin C (Hashimoto and Asakawa, 1998; Quang <i>et al.</i>, 2004; Quang <i>et al.</i>, 2004a; Quang <i>et al.</i>, 2006a)</p>		<p><i>H. rubiginosum</i> <i>H. fuscum</i> <i>D. concentrica</i></p>	<p>Antioxidant; inhibits NO production in RAW 264.7 cells</p>
<p>Daldinin D (Ariza <i>et al.</i>, 2001)</p>		<p><i>P. thymicola</i></p>	
<p>Daldinin E (Quang <i>et al.</i>, 2004; Quang <i>et al.</i>, 2006a,b)</p>		<p><i>H. fuscum</i></p>	<p>Antioxidant; inhibits NO production in RAW 264.7 cells</p>

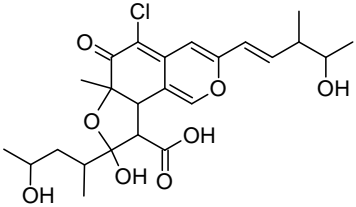
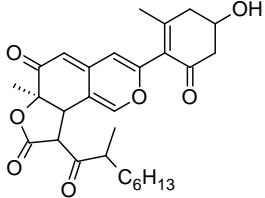
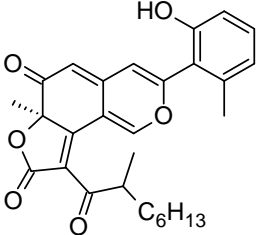
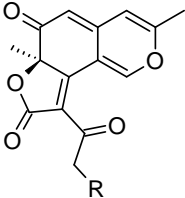
<p>Daldinin F (Quang <i>et al.</i>, 2004a; Quang <i>et al.</i>, 2006a,b)</p>		<p><i>H. fuscum</i></p>	<p>Antioxidant; inhibits NO production in RAW 264.7 cells</p>
<p>Pestafolide A (Ariza <i>et al.</i>, 2001; Ding <i>et al.</i>, 2008)</p>		<p><i>Pestalotiopsis foedans</i></p>	<p>Antifungal agent</p>
<p>Dimeric spiro-azaphilones</p>			
<p>Cochliodone A, B (Phonkerd <i>et al.</i>, 2008)</p>		<p><i>C. cochlioides</i></p>	<p>Antimalarial activity against <i>Plasmodium falciparum</i>; antimycobacterial activity against <i>Mycobacterium tuberculosis</i>; cytotoxic activity against KB, BC1, and NCI-H187 cell lines</p>

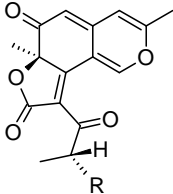
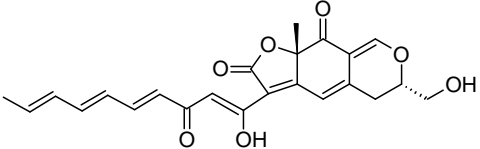
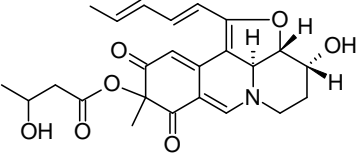
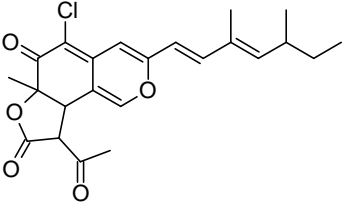
<p>Cochliodone C, D (Phonkerd <i>et al.</i>, 2008)</p>		<p><i>C. cochlioides</i></p>	<p>Antimycobacterial activity against <i>M. tuberculosis</i></p>
<p>Azaphilones with lactone ring</p>			
<p>Ankaflavin (Manchand <i>et al.</i>, 1973; Turner and Aldridge, 1983; Akihisa <i>et al.</i>, 2005)</p>		<p><i>M. anka</i> <i>M. pilosus</i></p>	<p>Food dye; anti-inflammatory activity (TPA-induced); inhibitory effects on neuron-derived orphan receptor-1 (NOR-1) activation; Epstein-Barr virus early antigen activator</p>
<p>(+)-5-Bromochrephilone (Matsuzaki <i>et al.</i>, 1998)</p>		<p><i>P. multicolor</i> FO-2338</p>	<p>gp120-CD4 binding inhibitor</p>

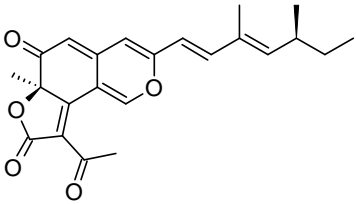
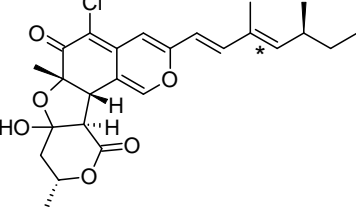
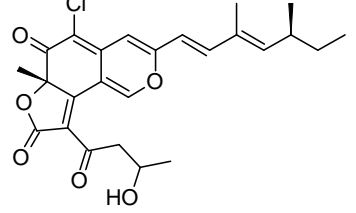
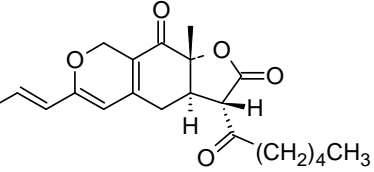
<p>Bulgarialactones A and B (Stadler <i>et al.</i>, 1995)</p>	 <p>Bulgarialactone A R = H Bulgarialactone B R = OH</p>	<p><i>Bulgaria inquinans</i></p>	<p>Antimicrobial activity against <i>B. brevis</i>, <i>B. subtilis</i> and <i>Micrococcus luteus</i>; cytotoxic agent; nematocidal agent; inhibitor of 3H-SCH 23390 binding to the dopamine D1 receptor</p>
<p>Bulgarialactone C (Stadler <i>et al.</i>, 1995)</p>		<p><i>B. inquinans</i></p>	
<p>Bulgarialactone D (Osmanova, unpublished results)</p>		<p><i>B. inquinans</i></p>	<p>Strong antimicrobial activity against <i>St. aureus</i></p>
<p>Chaetomugilins A and B (Park <i>et al.</i>, 2005; Muroga <i>et al.</i>, 2008; Yamada <i>et al.</i>, 2008)</p>	 <p>Chaetomugilin A R = OH; Chaetomugilin B R = OMe</p>	<p><i>C. globosum</i></p>	<p>Antifungal agent; cytotoxic activity against cultured P388 leukemia cells and HL-60 cells; selective cytotoxicity activity against 39 human cancer cell lines</p>

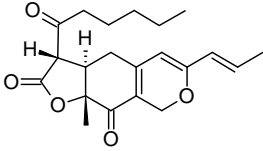
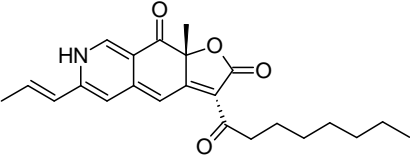
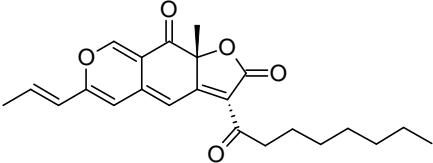
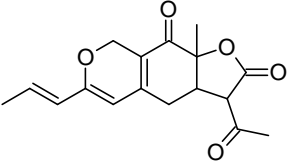
<p>Chaetomugilin C (Park <i>et al.</i>, 2005; Muroga <i>et al.</i>, 2008; Yamada <i>et al.</i>, 2008)</p>	 <p>The structure shows a complex polycyclic core with a chlorine atom at the top, a hydroxyl group on the left, and a methyl group at the bottom. It features a fused ring system with multiple oxygen atoms and a side chain with a double bond and a hydroxyl group.</p>	<p><i>C. globosum</i></p>	<p>Cytotoxic activity against cultured P388 cells and HL-60 cells</p>
<p>Chaetomugilins D and E (Park <i>et al.</i>, 2005; Muroga <i>et al.</i>, 2008; Yamada <i>et al.</i>, 2008)</p>	 <p>The structure is similar to Chaetomugilin C but includes a hydroxyl group and an 'R' group on the right side of the core.</p> <p>Chaetomugilin D R = OH; Chaetomugilin E R = OMe</p>	<p><i>C. globosum</i></p>	
<p>Chaetomugilin F (Muroga <i>et al.</i>, 2008; Yamada <i>et al.</i>, 2009)</p>	 <p>The structure is similar to Chaetomugilin C but includes a hydroxyl group and an 'R' group on the left side of the core.</p>	<p><i>C. globosum</i></p>	<p>Selective cytotoxicity activity against 39 human cancer cell lines</p>
<p>Chaetomugilins K and L (Muroga <i>et al.</i>, 2009)</p>	 <p>The structure is similar to Chaetomugilin C but includes a hydroxyl group, a methoxy group (OCH₃), and a methyl group on the right side of the core.</p> <p>Chaetomugilin K R = OH; Chaetomugilin L R = H</p>	<p><i>C. globosum</i></p>	<p>Growth inhibition of P388, HL-60, L1210, and KB cell lines</p>

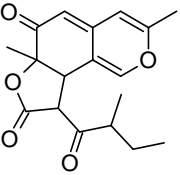
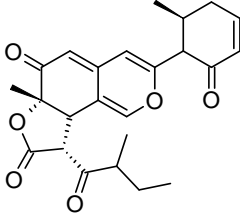
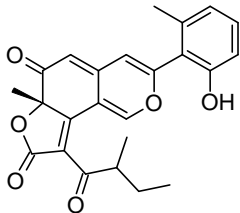
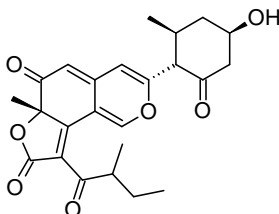
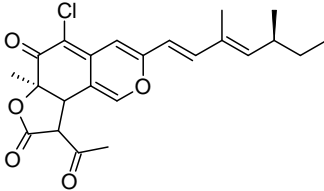
<p>Chaetomugilins M, N and O (Muroga <i>et al.</i>, 2009)</p>	 <p>Chaetomugilin M R = OH; R₁ = OH (S) Chaetomugilin N R = OH; R₁ = H Chaetomugilin O R = H; R₁ = H</p>	<p><i>C. globosum</i></p>	<p>Growth inhibition of P388, HL-60, L1210, and KB cell lines</p>
<p>Chaetoviridin A (Takahashi <i>et al.</i>, 1990; Yasukawa <i>et al.</i>, 1994; Tomoda <i>et al.</i>, 1999; Park <i>et al.</i>, 2005,)</p>		<p><i>C. globosum</i> var. <i>flavoviridae</i> <i>P. multicolor</i> FO-2338</p>	<p>Antifungal agent; inhibitor of cholesteryl ester transfer protein (CETP) <i>in vitro</i>; anti-inflammatory activity</p>
<p>Chaetoviridin B (Takahashi <i>et al.</i>, 1990; Matsuzaki <i>et al.</i>, 1998; Tomoda <i>et al.</i>, 1999; Park <i>et al.</i>, 2005)</p>		<p><i>C. globosum</i> var. <i>flavoviridae</i> <i>P. multicolor</i> FO-2338</p>	<p>Antifungal agent; inhibitor of cholesteryl ester transfer protein (CETP) <i>in vitro</i></p>
<p>Chaetoviridin C (Takahashi <i>et al.</i>, 1990)</p>		<p><i>C. globosum</i> var. <i>flavoviridae</i></p>	

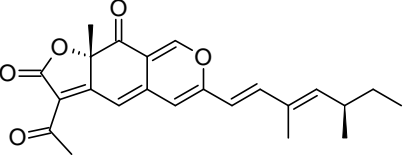
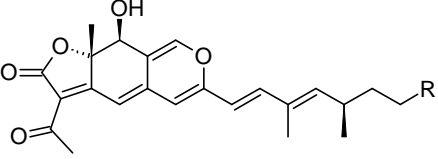
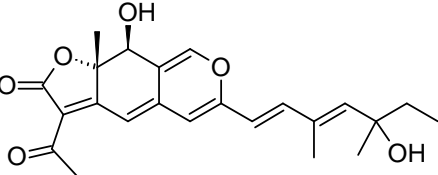
<p>Chaetoviridin D (Takahashi <i>et al.</i>, 1990)</p>		<p><i>C globosum</i> var. <i>flavoviridae</i></p>	
<p>Cohaerins C and D (Quang <i>et al.</i>, 2006b)</p>	 <p>Cohaerin D: double bond in lactone ring</p>	<p><i>Annulohypoxyton cohaerens</i></p>	<p>Inhibits NO production in RAW cells; strong nonselective antimicrobial agent</p>
<p>Cohaerin E (Quang <i>et al.</i>, 2006a,b)</p>		<p><i>A. cohaerens</i></p>	<p>Inhibits NO production in RAW cells; strong nonselective antimicrobial agent</p>
<p>Deflectins 1a, 1c and A (1b) (Anke <i>et al.</i>, 1981)</p>	 <p>Deflectin 1a R = C₆H₁₃ Deflectin 1c R = C₁₀H₂₁ Deflectin A (1b) R = C₈H₁₇</p>	<p><i>A. deflectus</i></p>	<p>Deflectins 1a and 1c are not active; Deflectin A 1(b): Antibacterial and weak antifungal agent; cytotoxic activity against Ehrlich carcinoma cells of mice; lytic activity towards bacteria and erythrocytes</p>

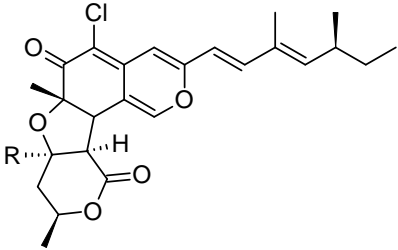
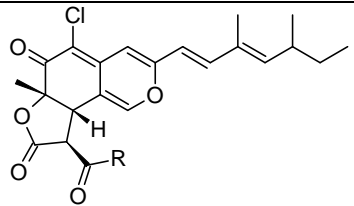
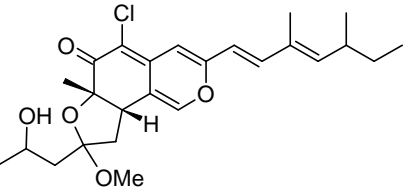
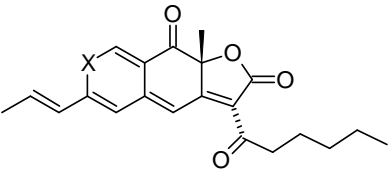
<p>Deflectins B (2a) and 2b (Anke <i>et al.</i>, 1981)</p>	 <p>Deflectin B (2a) R = n-C₁₈H₁₇ Deflectin 2b R = n-C₁₀H₂₁</p>	<p><i>A. deflectus</i></p>	<p>Antibacterial and weak antifungal agent; cytotoxic activity against Ehrlich carcinoma cells of mice; lytic activity towards bacteria and erythrocytes; Deflectin 2b is not active</p>
<p>Epicocconone (Bell and Karuso, 2003)</p>		<p><i>Epicoccum nigrum</i></p>	
<p>Fleophilone (Qian-Cutrone <i>et al.</i>, 1996)</p>		<p><i>T. harzianum</i></p>	<p>HIV REV/RRE binding inhibitor</p>
<p>Isochromophilone I (Matsuzaki <i>et al.</i>, 1995; Matsuzaki <i>et al.</i>, 1998; Tomoda <i>et al.</i>, 1999)</p>		<p><i>P. multicolor</i> FO-2338</p>	<p>gp120-CD4 binding inhibitor</p>

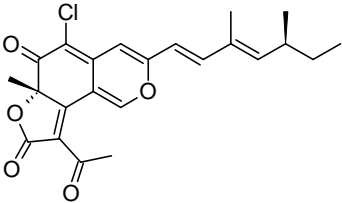
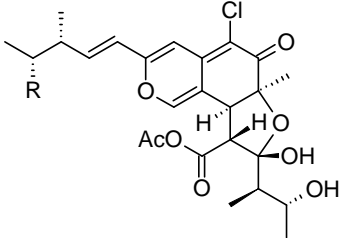
<p>(+)-Isorotiorin (5-chloroisorotiorin) (Pairet <i>et al.</i>, 1995; Matsuzaki <i>et al.</i>, 1998)</p>		<p><i>P. multicolor</i> <i>P. sclerotiorum</i> X11853</p>	<p>gp120-CD4 binding inhibitor; Endothelin receptors binding agent</p>
<p>Luteusins C and D (Yoshida <i>et al.</i>, 1996a,b)</p>	 <p>Luteusin C (E)* Luteusin D (Z)*</p>	<p><i>T. luteus</i></p>	
<p>Luteusin E (Yoshida <i>et al.</i>, 1996b)</p>		<p><i>T. luteus</i></p>	
<p>Monascin (Akihisa <i>et al.</i>, 2005; Akihisa <i>et al.</i>, 2005a)</p>		<p><i>M. pilosus</i></p>	<p>Food dye; anti-inflammatory activity (TPA-induced); inhibitory effects on NOR 1 activation; Epstein-Barr virus early antigen activator</p>

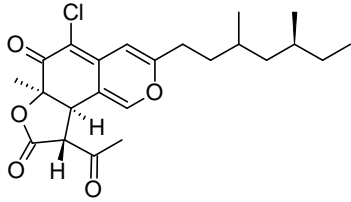
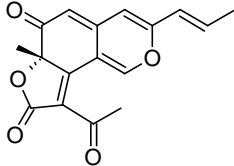
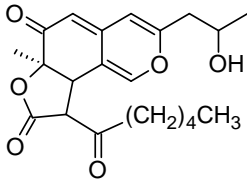
<p>Monascoflavin (Kurono <i>et al.</i>, 1963; Takahashi <i>et al.</i>, 1990)</p>		<p><i>M. purpureus</i></p>	
<p>Monascorubramine (Akihisa <i>et al.</i>, 2005; Akihisa <i>et al.</i>, 2005a)</p>		<p><i>M. pilosus</i></p>	<p>Anti-inflammatory activity (TPA-induced); inhibitory effects on NOR 1 activation; Epstein-Barr virus early antigen activator</p>
<p>Monascorubrin (Yasukawa <i>et al.</i>, 1994; Akihisa <i>et al.</i>, 2005; Akihisa <i>et al.</i>, 2005a; Miyake <i>et al.</i>, 2008)</p>		<p><i>Monascus sp.</i></p>	<p>Food dye; anti-inflammatory activity (TPA-induced); inhibitory effects on NOR 1 activation; Epstein-Barr virus early antigen activator</p>
<p>Monascusone B (Jongrungruangchok <i>et al.</i>, 2004)</p>		<p><i>Monascus sp</i></p>	

<p>Monochaetin (Steyn and Vlegaar, 1986)</p>		<p><i>Monochaetia compta</i></p>	
<p>Multiformins A and B (Quang <i>et al.</i>, 2005c)</p>	 <p>Multiformin B: double bond in lactone ring</p>	<p><i>H. multiforme</i></p>	<p>Non-selective antimicrobial activity</p>
<p>Multiformin C (Quang <i>et al.</i>, 2005c)</p>		<p><i>H. multiforme</i></p>	<p>Non-selective antimicrobial activity</p>
<p>Multiformin D (Quang <i>et al.</i>, 2005c; Quang <i>et al.</i>, 2006b)</p>		<p><i>H. multiforme</i></p>	<p>Non-selective antimicrobial activity; antioxidant; inhibits NO production in RAW 264.7 cells</p>
<p>Ochrephilone (Seto and Tanabe, 1974; Pairet <i>et al.</i>, 1995; Matsuzaki <i>et al.</i>, 1998; Tomoda <i>et al.</i>, 1999)</p>		<p><i>P. multicolor</i> FO-2338 <i>P. sclerotiorum</i> X11853</p>	<p>gp120-CD4 binding inhibitor; Endothelin receptors binding agent</p>

<p>(-)-Rotiorin (Matsuzaki <i>et al.</i>, 1998; Tomoda <i>et al.</i>, 1999; Kanokmedhakul <i>et al.</i>, 2006)</p> <p>(+)-Rotiorin (Kanokmedhakul <i>et al.</i>, 2006)</p>		<p><i>C. cupreum</i> CC3003</p>	<p>Antifungal activity against <i>C. albicans</i>; CETP inhibitor <i>in vitro</i>; gp120-CD4 binding inhibitor; (+)-Rotiorin is not active</p>
<p>Rotiorinols A and C (Kanokmedhakul <i>et al.</i>, 2006)</p>	 <p>Rotiorinol A R = H Rotiorinol C R = OH</p>	<p><i>C. cupreum</i> CC3003</p>	<p>Antifungal activity against <i>C. albicans</i></p>
<p>Rotiorinol B (Kanokmedhakul <i>et al.</i>, 2006)</p>		<p><i>C. cupreum</i> CC3003</p>	

<p>RP 1551-1, RP 1551-M1 and RP 1551-6 (Toki <i>et al.</i>, 1999)</p>	 <p>RP 1551-1 R = OH; RP 1551-M1 R = OMe RP 1551-6 diastereomer of RP 1551-1;</p>	<p><i>Penicillium sp.</i> SPC-21609</p>	<p>Antibacterial activity against <i>B. subtilis</i>, <i>E. faecium</i>, <i>S. aureus</i></p>
<p>RP 1551-3 and RP 1551-4 (Toki <i>et al.</i>, 1999)</p>	 <p>RP 1551-3 R = propenyl; RP 1551-4 R = 2-hydroxypropyl</p>	<p><i>Penicillium sp.</i> SPC-21609</p>	<p>Antibacterial activity against <i>B. subtilis</i>, <i>E. faecium</i>, <i>S. aureus</i></p>
<p>RP 1551-5 (Toki <i>et al.</i>, 1999)</p>		<p><i>Penicillium sp.</i> SPC-21609</p>	<p>Antibacterial activity against <i>B. subtilis</i>, <i>E. faecium</i>, <i>S. aureus</i></p>
<p>Rubropunctamine and Rubropunctatin (Akihisa <i>et al.</i>, 2005a)</p>	 <p>Rubropunctamine X = NH; Rubropunctatin X = O</p>	<p><i>M. pilosus</i></p>	<p>Anti-inflammatory activity (TPA-induced); inhibitory effects on NOR 1 activation; Epstein-Barr virus early antigen activator</p>

<p>Rubrorotiorin (Gray and Whalley, 1971; Matsuzaki <i>et al.</i>, 1998; Tomoda <i>et al.</i>, 1999; Kanokmedhakul <i>et al.</i>, 2006)</p>		<p><i>C. cupreum</i> CC3003 <i>P. hirayamae</i> Udagawa <i>P. multicolor</i> FO-2338</p>	<p>Antifungal activity against <i>C. albicans</i>; CETP inhibitor <i>in vitro</i>; gp120-CD4 binding inhibitor</p>
<p>Sassafrins A, B and C (Quang <i>et al.</i>, 2005; Quang <i>et al.</i>, 2006a)</p>	 <p>Sassafrin A R = CH₃; Sassafrin B R = H Sassafrin C R = CH₃ and double bond in lactone ring</p>	<p><i>C. sassafras</i></p>	<p>Broad-spectrum antimicrobial activity; antioxidant; inhibits NO production in RAW 264.7 cells</p>
<p>Seco-chaetomugilins A and D (Yamada <i>et al.</i>, 2009)</p>	 <p>Seco-chaetomugilin A R = OH Seco-chaetomugilin D R = H</p>	<p><i>C. globosum</i></p>	<p>Seco-chaetomugilin A is not active; Seco-chaetomugilin D: growth inhibitory activity against cultured murine P388 leukemia cell lines P388 and L1210; the human leukemia cell line HL-60 and KB epidermoid carcinoma</p>

<p>Tetrahydroisochromophilon e (Matsuzaki, <i>et al.</i>, 1998)</p>	 <p>The structure shows a complex polycyclic system with a benzopyran core. It features a chlorine atom at the 6-position, a methyl group at the 9-position, and a long branched side chain at the 3-position. The pyran ring is fused to a benzene ring, which is further fused to a five-membered ring containing two carbonyl groups and a hydroxyl group.</p>	<p><i>P. multicolor</i> FO-2338</p>	<p>gp120-CD4 binding inhibitor</p>
<p>Trichoflectin (Thines, <i>et al.</i>, 1998)</p>	 <p>The structure is a benzopyran derivative with a methyl group at the 9-position and a propenyl side chain at the 3-position. It has a similar fused ring system with carbonyl and hydroxyl groups.</p>	<p><i>Trichopezizella nidulus</i></p>	<p>Antimicrobial agent; inhibitor of dihydroxynaphthalene melanin biosynthesis in fungi</p>
<p>6H-Furo[2,3-h]-2-benzopyran-6,8(6aH)-dione, 9,9a-dihydro-3-(2-hydroxypropyl)-6a-methyl-9-(1-oxohexyl) (Campoy, <i>et al.</i>, 2006)</p>	 <p>The structure is a benzopyran with a methyl group at the 6a-position, a 2-hydroxypropyl side chain at the 3-position, and a 1-oxohexyl side chain at the 9-position. It features a fused ring system with carbonyl and hydroxyl groups.</p>	<p><i>Monascus sp</i></p>	<p>Food dye</p>

Summary and Outlook

The review presents an overview of the structural diversity of azaphilones so far found in different species of fungi. In addition, it summarises the broad spectrum of biological activities detected and indicates the promising potential of azaphilones as a prolific base for new drugs. However, this potential should be contrasted with the lack of selectivity exhibited by azaphilones in their reactions with various amines: this characteristic presents considerable difficulties and may be the primary reason why azaphilones have yet to be pursued intensively for drug development.

The table includes 177 azaphilone structures. These can be classified into ten different structural groups (see headings in the table), occurring in fungi belonging to 23 genera from 13 families. Numerous azaphilone structures have been described, particularly from members of the *Trichocomaceae* and *Xylariaceae* families.

Most of the species producing azaphilones are what are termed moulds: microscopic fungi such as *Penicillium*, *Monascus*, *Chaetomium* and *Talaromyces*. Fungi not exhibiting mould appearance include such genera as *Hypoxylon*, *Daldinia*, *Creosphaeria* (members of the *Xylariaceae* family) and *Bulgaria* (*Bulgariaceae*).

The presence of some azaphilones is very specific for certain fungi species and is appropriate for use as an accurate determinant of taxonomy. Thus, sassafrins A-D, initially found in *Creosphaeria sassafras*, are not found in any other species of the family *Xylariaceae*. Conversely, various azaphilones identified from genera *Hypoxylon* and *Daldinia* have been shown to be absent in *C. sassafras*. These results show that, in this respect, the genus *Creosphaeria* is not closely allied to *Hypoxylon* or *Daldinia* and is instead an isolated genus within the family *Xylariaceae*. These results have been confirmed by molecular data (Quang *et al.* 2005).

As far as the taxonomic situation is concerned, one should note that considerable changes have occurred in fungal systematics during the last decade. *Daldinia childiae*, for example, was previously confused with *D. concentrica* and was still referred to by this name as late as 1994 – for example, in an evaluation of its secondary metabolites conducted by Hashimoto *et al.* However *D. childiae* has now been re-classified as a separate species based on metabolite and rDNA patterns

(Rogers *et al.* 1999; Stadler *et al.* 2001; Stadler *et al.* 2001a). Based on the morphological characteristics and the analyses of β -tubulin and α -actin gene sequences, the taxa assigned to *Hypoxylon* sect. *Annulata* have been placed in a new genus, *Annulohypoxylon* (Ju *et al.* 2005). The presence of specific azaphilones in this genus such as Cohaerin A, Multiformin A and Sassafrin D also supports the status of *Annulohypoxylon* as a separate genus, since none of these azaphilones have been detected in *Hypoxylon* or other *Xylariaceae* (Stadler and Fournier, 2006). Recent molecular data clearly supports the re-classification of *Hypoxylon cohaerens* to *Annulohypoxylon cohaerens* (Pelaez *et al.* 2008). Based on morphological traits, Stadler *et al.* (2005) now regards *Hypoxylon piceum* and *Pulveria porrecta* as synonymous and has transferred them to *Pyrenomyxa*. Further investigation of metabolite patterns also suggests a close relationship between *Pyrenomyxa* and *Hypoxylon*: the name *Pyrenomyxa picea* has been accepted *ad interim* as a synonym for *Hypoxylon piceum* until the phylogenetic relationships among *Hypoxylon* have been further evaluated using chemotaxonomic, morphological and molecular methods (Stadler *et al.* 2005).

As a result of these and other similar developments, our article is careful to cite only the species names used by the authors of the respective original publications. In this context, the reader is also advised that nomenclature and classification for the fungi reviewed has been confirmed using the standard academic reference: Dictionary of the Fungi (10th edition) (Kirk *et al.* 2008).

Considering the variety of azaphilones that occurs, one finds that some organisms are able to produce a huge variety of diverse types, whereas others are able to produce only one or two different types. An example of the first kind is *Penicillium* spp. of the *Trichocomaceae* family, which produces over 40 azaphilones from five types: azaphilones with an aliphatic side chain; azaphilones with o-orsellinic acid; azaphilones with an ergostane skeleton and o-orsellinic acid; bicyclic spiro-azaphilones; and azaphilones with a lactone ring. In contrast, *Phomopsis euphorbiae* contains only one type of azaphilone, namely an azaphilone with an aliphatic side chain. The largest group of azaphilones (azaphilones with a lactone ring) includes 68

substances; the smallest subsets of azaphilones are dimeric and dimeric spiroazaphilones, whereby each group comprises only two substances.

Structure-activity relationships have been established for several azaphilones. For example, a halogen atom at C-5, a proton at C-8 and a diene structure in the C-3 side chain of the 6-oxoisochromane ring are necessary for gp120-CD4 binding (isochromophilones and known derivatives) (Matsuzaki *et al.* 1998). Furthermore, the presence of (an) electrophilic ketone(s) and/or enone(s) at both C-6 and C-8 in the 6-oxoisochromane ring is essential for cholesteryl ester transfer protein (CETP) inhibitory activity (chaetoviridin B, sclerotiorin, rotiorin, etc.) (Tomoda *et al.* 1999). Research has also shown that the inhibition of NO production in RAW 264.7 cells also depends on the structure of azaphilones. For example, daldinins C, E and F (spiro-derivatives) only weakly suppress NO production. Azaphilones with a lactone ring in their molecule, such as multiformin D and sassafrins A – C, possess stronger inhibitory activity when compared to daldinins. Entonaemin A and rubiginosins A and B are all azaphilones with an orsellinic acid moiety attached to the bicyclic azaphilone backbone through an ester linkage. However, since only rubiginosin A exhibits strong activity in this group, the location of the orsellinic acid moiety cannot therefore affect the activity of the compounds. Nonetheless, the presence of an acetyl group (as is the case with rubiginosin A) is essential for an increase in activity. Azaphilones with a fatty acid side chain linked to a bicyclic azaphilone by an ester bond (rubiginosin C, cohaerins A and B) exhibited only weak activity. The greatest inhibitors of NO production are dimeric azaphilones, namely rutilins A and B. One may infer that the inhibitory activities of azaphilones are considerably strengthened by the number of orsellinic acid moieties in the molecule and the presence of conjugated double bonds in dimeric compounds. In conclusion, the acetyl group is necessary for inhibition, whereas the location of orsellinic acid does not change their activities (Quang *et al.* 2006a).

Research conducted by the authors has identified a new azaphilone present in the fruit bodies of *B. inquinans*. This azaphilone has been named bulgarialactone D

(molecular formula: C₂₇H₃₀O₇). In microbiological tests, bulgarialactone D exhibits strong antimicrobial activity against *S. aureus* (Osmanova, thesis in preparation).

References

Akihisa T, Tokuda H, Ukiya M, Kiyota A, Yasukawa K, Sakamoto N, Kimura Y, Suzuki T, Takayasu J, Nishino H (2005) Anti-tumor-initiating effects of monascin, an azaphilone pigment from the extract of *Monascus pilosus* fermented rice (red-mold rice). *Chem Biodiversity* 2:1305-1309

Akihisa T, Tokuda H, Yasukawa K, Ukiya M, Kiyota A, Sakamoto N, Suzuki T, Tanabe N, Nishino H (2005)a Azaphilones, furanoisophthalides, and amino acids from the extracts of *Monascus pilosus* - fermented rice (Red-Mold Rice) and their chemopreventive effects. *J Agric Food Chem* 53:562-565

Anke H, Kemmer T, Höfle G (1981) Deflectins, new antimicrobial azaphilones from *Aspergillus deflectus*. *J Antibiot* 34:923-928

Arai N, Shiomi K, Tomoda H, Tabata N, Yang DJ, Masuma R, Kawakubo T, Omura S (1995) Isochromophilones III-VI, inhibitors of acyl-CoA:cholesterol acyltransferase produced by *Penicillium multicolor* FO-3216. *J Antibiot* 48:696-702

Ariza MR, Larsen TO, Petersen BO, Duus JO, Christophersen C, Barrero A.F (2001) A Novel Alkaloid Serantrypinone and the Spiro Azaphilone Daldinin D from *Penicillium thymicola*. *J Nat Prod* 64:1590-1592

Beed FD, Strange RN, Onfroy C, Tivoli B (1994) Virulence for faba bean and production of ascochitine by *Ascochyta fabae*. *Plant Pathol* 43:987-997

Bell PJJ, Karuso P (2003) Epicocconone, a novel fluorescent compound from the fungus *Epicoccum nigrum*. *J Am Chem Soc* 125:9304-9305

Blanc PJ, Laussac JP, Le Bars J, Le Bars P, Loret MO, Pareilleux A, Prome D, Prome JC, Santerre AL, Goma G (1995) Characterization of monascidin A from *Monascus* as citrinin. *Int J Food Microbiol* 27: 201-13

- Buchanan MS, Hashimoto T, Yasuda A, Takaoka S, Kan Y, Asakawa Y (1995) The structures of novel cytochalasins, azaphilones, and aromatic compounds isolated from five ascomycetous fungi. *Tennen Yuki Kagobutsu Toronkai Koen Yoshishu* 37:409-414
- Buechi G, White JD, Wogan GN (1965) The structures of mitorubrin and mitorubrinol. *J Am Chem Soc* 87:3484-3489
- Campoy S, Rumbero A, Martin JF, Liras P (2006) Characterization of a hyperpigmenting mutant of *Monascus purpureus* IB1: Identification of two novel pigment chemical structures. *Appl Microbiol Biotechnol* 70:488-496
- Chidananda C, Rao L, Sattur A (2006) Sclerotiorin, from *Penicillium frequentans*, a potent inhibitor of aldose reductase. *Biotechnol Lett* 28:1633-1636
- Closse A, Hauser D (1973) Isolation and constitution of chrysodin. *Helv Chim Acta* 56:2694-2698. Journal written in German
- Ding G, Liu S, Guo L, Zhou Y, Che Y (2008) Antifungal Metabolites from the Plant Endophytic Fungus *Pestalotiopsis foedan*. *J Nat Prod* 71:615-618
- Dong J, Zhou Y, Li R, Zhou W, Li L, Zhu Y, Huang R, Zhang K (2006) New nematicidal azaphilones from the aquatic fungus *Pseudohalonestria adversaria* YMF1.01019. *FEMS Microbiol Lett* 264:65-69
- Duncan SJ, Grueschow S, Williams DH, McNicholas C, Purewal R, Hajek M, Gerlitz M, Martin S, Wrigley SK, Moore M (2001) Isolation and structure elucidation of chlorofusin, a novel p53-MDM2 antagonist from a *Fusarium* sp. *J Am Chem Soc* 123: 554-560
- Duncan SJ, Cooper MA, Williams DH (2003) Binding of an inhibitor of the p53/MDM2 Interaction to MDM2. *Chem Commun* 3: 316-317
- Endo A, Kuroda M (1976) Citrinin, an inhibitor of cholesterol synthesis. *J Antibiot* 29:841-843

- Frisvad JC, Filtenborg O, Samson RA, Stolk AC (1990) Chemotaxonomy of the genus *Talaromyces*. *Antonie van Leeuwenhoek*. 57:179-189
- Fujimoto H, Matsudo T, Yamaguchi A, Yamazaki M (1990) Two new fungal azaphilones from *Talaromyces luteus*, with monoamine oxidase inhibitory effect. *Heterocycles* 30:607-616
- Gray RW, Whalley WB (1971) The chemistry of fungi. Part LXIII. Rubrorotiorin, a metabolite of *Penicillium hirayamae* Udagawa. *J Chem Soc* 21:3575 – 3577
- Hajjaj H, Kläbe A, Loret MO, Goma G, Blanc PJ, Francois J (1999) Biosynthetic pathway of citrinin in the filamentous fungus *Monascus ruber* as revealed by ¹³C nuclear magnetic resonance. *Appl Environ Microbiol* 65:311-314
- Haraguchi H, Taniguchi M, Motoba K, Shibata K, Oi S, Hashimoto K (1990) Chrysodin, an antifungal antimetabolite. *Agric Biol Chem* 54:2167-2168
- Hashimoto T, Asakawa Y (1998) Biologically active substances of Japanese inedible mushrooms. *Heterocycles* 47:1067-1110
- Hashimoto T, Tahara S, Takaoka S, Tori M, Asakawa Y (1994) Structures of daldinins A, B, C, three novel azaphilone derivatives from ascomycetous fungus *Daldinia concentrica*. *Chem Pharm Bull* 42:2397-2379
- Hellwig V, Ju YM, Rogers JD, Fournier J, Stadler M (2005) Hypomiltin, a novel azaphilone from *Hypoxylon hypomiltum*, and chemotypes in *Hypoxylon* sect. *Hypoxylon* as inferred from analytical HPLC profiling. *Mycol Progress* 4:39-54
- Hobbs C (2003) Medicinal mushrooms: an exploration of tradition, health and culture. Botanica press, Canada
- Hutchinson C R (1999) Microbial polyketide synthases: More and more prolific. *Proc Natl Acad Sci USA* 96:3336–3338
- Hyodo S, Fujita K, Kasuya O, Takahashi I, Uzawa J, Koshino H (1994) Structures of phospholipase A2 inhibitors, ergophilone A and B. *Tennen Yuki Kagobutsu Toronkai Koen Yoshishu* 36:760-767

- Itabashi T, Nozawa K, Nakajima S, Kawai KI (1993) A new azaphilone, falconensin H, from *Emericella falconensis*. Chem Pharm Bull 41:2040-2041
- Itabashi T, Ogasawara N, Nozawa K, Kawai KI (1996) Isolation and structures of new azaphilone derivatives, falconensins E-G, from *Emericella falconensis* and absolute configurations of falconensins A-G. Chem Pharm Bull 44:2213-2217
- Jongrungruangchok S, Kittakoop P, Yongsmith B, Bavovada R, Tanasupawat S, Lartpornmatulee N, Thebtaranonth Y (2004) Azaphilone pigments from a yellow mutant of the fungus *Monascus kaoliang*. Phytochemistry 65:2569-2575
- Ju HM, Hsieh HM, Rogers JD (2005) Molecular phylogeny of Hypoxylon and closely related genera. Mycologia 97:844–865
- Kanokmedhakul S, Kanokmedhakul K, Nasomjai P, Louangsysouphanh S, Soytong K, Isobe M, Kongsaree P, Prabpai S, Suksamrarn A (2006) Antifungal Azaphilones from the Fungus *Chaetomium cupreum* CC3003. J Nat Prod 69:891-895
- Kimura T, Nishida M, Kuramochi K, Sugawara F, Yoshida H, Mizushina Y (2008) Novel azaphilones, kasanosins A and B, which are specific inhibitors of eukaryotic DNA polymerases beta and lambda from *Talaromyces* sp. Bioorg Med Chem 16:4594-4599
- Kirk PM, Cannon PE, Minter DW, Stalpers JA (2008) Dictionary of fungi, 10th edition, CABI Europe – UK
- Kono K, Tanaka M, Ono Y, Hosoya T, Ogita T, Kohama T (2001) S-15183a and b, new sphingosine kinase inhibitors, produced by a fungus. J Antibiot 54:415-420
- Kusnick C, Jansen R, Liberra K, Lindequist U (2002) Ascochital, a new metabolite from the marine ascomycete *Kirschsteiniothelia maritima*. Pharmazie 57:510-512
- Kurono M, Nakanishi K, Shindo K, Tada M (1963) Biosyntheses of Monascorubrin and Monascoflavin. Chem Pharm Bull 11:359-362

- Laakso JA, Rauili R, McElhaney-Feser GE, Actor P, Underiner TL, Hotovec BJ, Mocek U, Cihlar RL, Broedel SE Jr (2003) CT2108A and B: new fatty acid synthase inhibitors as antifungal agents. *J Nat Prod* 66:1041-1046
- Lesova K, Sturdikova M, Rosenberg M (2000) Factors affecting the production of (-)- mitorubrinic acid by *Penicillium funiculosum*. *J Basic Microbiol* 40:369-375
- Lesova K, Sturdikova M, Tybitanclova K (2000)a. Selection of mutant strain of *Penicillium funiculosum* for (-)- mitorubrinic acid production. *Biologia (Bratislava)* 55:633-636
- Lindequist U, Niedermeyer THJ, Jülich WD (2005) The Pharmacological Potential of Mushrooms. *eCAM* 2:285-299
- Locci R, Merlini L, Nasini G, Locci JR (1967) Mitorubrinic acid and related compounds from a strain of *Penicillium funiculosum*. *Gioron Microbiol* 15:92-102
- Lorenzen K, Anke T (1998) Basidiomycetes as a source for new bioactive natural products. *Curr Org Chem* 2:329-364
- Manchand PS, Whalley WB, Chen FC (1973) Isolation and structure of ankaflavine. New pigment from *Monascus anka*. *Phytochemistry* 12:2531-2532
- Mapari S, Meyer AS, Thrane U, Frisvad JC (2009) Identification of potentially safe promising fungal cell factories for the production of polyketide natural food colorants using chemotaxonomic rationale. *Microb Cell Fact* 8:24.
- Marumo S, Nukina M, Kondo S, Tomiyama K (1982) Lunatoic acid A, a morphogenic substance inducing chlamydospore-like cells in some fungi. *Agric Biological Chem* 46:2399-2401
- Matsuzaki K, Tahara H, Inokoshi J, Tanaka H, Masuma R, Omura S (1998) New brominated and halogen-less derivatives and structure-activity relationship of azaphilones inhibiting gp120-CD4 binding. *J Antibiot* 51:1004-1011

- Matsuzaki K, Tanaka H, Omura S (1995) Isochromophilones I and II, novel inhibitors against gp120-CD4 binding produced by *Penicillium multicolor* FO-2338. II. Structure elucidation. *J Antibiot* 48:708-713
- Merlini L, Mondelli R, Nasini G, Hesse M (1973) Structure of wortmin, a new metabolite from *Penicillium wortmannii*. *Helv Chim Acta* 56:232-239
- Michael AP, Grace EJ, Kotiw M, Barrow RA (2003) Isochromophilone IX, a novel GABA-containing metabolite isolated from a cultured fungus, *Penicillium sp.* *Aust J Chem* 56:13-15
- Ming GH, Yun ZW, Ding G, Saparpakorn P, Chun SY, Hannongbua S, Tan RX (2008) Chaetoglobins A and B, two unusual alkaloids from endophytic *Chaetomium globosum* culture. *Chem Commun (Cambridge, UK)* 45:5978-5980
- Miyake T, Kono I, Nozaki N, Sammoto H (2008) Analysis of pigment compositions in various *Monascus* cultures. *Food Sci Technol Res* 14:194-197
- Molitoris HP (2002) Mushrooms in medicine, folklore and religion. *Feddes Repertorium* 113:165-182
- Muroga Y, Yamada T, Numata A, Tanaka R (2008) Chaetomugilins, new selectively cytotoxic metabolites, produced by a marine fish-derived *Chaetomium* species. *J Antibiotics* 61:615-622
- Muroga Y, Yamada T, Numata A, Tanaka R (2009) Chaetomugilins I–O, new potent cytotoxic metabolites from a marine-fish-derived *Chaetomium* species. Stereochemistry and biological activities. *Tetrahedron* 65:7580-7586
- Mühlbauer A, Triebel D, Persoh D, Wollweber H, Seip S, Stadler M (2002) Macrocarpones, novel metabolites from stromata of *Hypoxylon macrocarpum* and new evidence on the chemotaxonomy of *Hypoxylon*. *Mycological Progress* 1:235-248
- Nakajima H, Kimura Y, Hamasaki T (1992) Spiciferinone, an azaphilone phytotoxin produced by the fungus *Cochiliobolus spicifer*. *Phytochemistry* 31:105-107

- Nam JY, Son KH, Kim HK, Han MY, Kim SU, Choi JD, Kwon BM (2000) Sclerotiorin and isochromophilone IV: Inhibitors of Grb2-Shc interaction, isolated from *Penicillium multicolor* F1753. *J Microbiol Biotechnol* 10:544-546
- Nukina M, Marumo S (1977) Lunatoic acid A and B, aversion factor and its related metabolite of *Cochliobolus lunata*. *Tetrahedron Lett* 30:2603-2606
- Natsume M, Takahashi Y, Marumo S (1988) Chlamydospore-like cell-inducing substances of fungi: close correlation between chemical reactivity with methylamine and biological activity. *Agric Biol Chem* 52:307-31
- Ogasawara N, Kawai KI (1998) Hydrogenated azaphilones from *Emericella falconensis* and *E. fruticulosa*. *Phytochemistry* 47:1131-1135
- Osmanova N Studies on constituents and antimicrobial effects of selected fungi in particular consideration of *Bulgaria inquinans* (Pers.) Fr. (Bulgariaceae). (Ph.D. dissertation) University of Hamburg, Unpublished results
- Pairat L, Wrigley SK, Chetland I, Reynolds EE, Hayes M A, Holloway J, Ainsworth AM, Katzer W, Cheng XM (1995) Azaphilones with endothelin receptor binding activity produced by *Penicillium sclerotiorum*: taxonomy, fermentation, isolation, structure elucidation and biological activity. *J Antibiot* 48: 913-23.
- Park JH, Choi GJ, Jang KS, Lim HK, Kim HT, Cho KY, Kim JC (2005) Antifungal activity against plant pathogenic fungi of chaetoviridins isolated from *Chaetomium globosum*. *FEMS Microbiol Lett* 252:309-313
- Pelaez F, Gonzalez V, Platas G, Sanchez-Ballesteros J, Rubio V (2008) Molecular phylogenetic studies within the Xylariaceae based on ribosomal DNA sequences. *Fungal Diversity* 31:111-134
- Phonkerd N, Kanokmedhakul S, Kanokmedhakul K, Soyong K, Prabpai S, Kongsearee P (2008) Bis-spiro-azaphilones and azaphilones from the fungi *Chaetomium cochliodes* VTh01 and *C. cochliodes* CTh05. *Tetrahedron* 64:9636-9645

- Pisareva E, Savov V, Kujumdzieva A (2005) Pigments and citrinin biosynthesis by fungi belonging to genus *Monascus*. *Z. Naturforsch* 60:116-120
- Proksa B, Uhrin D, Fуска J, Michalkova E (1992) (-)- Mitorubrinol and phthaldehydic acids, new metabolites of *Penicillium vermiculatum* DANG. *Collect Czech Chem Commun* 57:408-414
- Qian-Cutrone J, Huang S, Chang LP, Pirnik DM, Klohr SE, Dalterio RA, Hugill R, Lowe S, Alam M, Kadow KF (1996) Harziphilone and fleophilone, two new HIV REV/RRE binding inhibitors produced by *Trichoderma harzianum*. *J Antibiot* 49:990-997
- Quang DN, Hashimoto T, Asakawa Y (2006) Inedible Mushrooms: A Good Source of Biologically Active Substances. *Chem Rec* 6:79–99
- Quang DN, Hashimoto T, Stadler M, Asakawa Y (2004) New azaphilones from the inedible mushroom *Hypoxylon rubiginosum*. *J Nat Prod* 67:1152-1155
- Quang DN, Harinantenaina L, Nishizawa T, Hashimoto T, Kohchi C, Soma GI, Asakawa Y (2006)a Inhibition of nitric oxide production in RAW 264.7 cells by azaphilones from xylariaceous fungi. *Biol Pharm Bull* 29:34-37
- Quang DN, Hashimoto T, Fournier J, Stadler M, Radulovic N, Asakawa Y (2005) Sassafrins A-D, new antimicrobial azaphilones from the fungus *Creosphaeria sassafras*. *Tetrahedron* 61:1743-1748
- Quang DN, Hashimoto T, Nomura Y, Wollweber H, Hellwig V, Fournier J, Stadler M, Asakawa Y (2005)a Cohaerins A and B, azaphilones from the fungus *Hypoxylon cohaerens*, and comparison of HPLC-based metabolite profiles in *Hypoxylon* sect. *Annulata*. *Phytochemistry* 66:797-809
- Quang DN, Hashimoto T, Stadler M, Asakawa Y (2005)b Dimeric azaphilones from the xylariaceous ascomycete *Hypoxylon rutilum*. *Tetrahedron* 61:8451-8455

- Quang DN, Hashimoto T, Stadler M, Radulovic N, Asakawa Y (2005)c Antimicrobial azaphilones from the fungus *Hypoxylon multiforme*. *Planta Med* 71:1058-1062
- Quang DN, Hashimoto T, Tanaka M, Stadler M, Asakawa Y (2004)a Cyclic azaphilones daldinins E and F from the ascomycete fungus *Hypoxylon fuscum* (Xylariaceae). *Phytochemistry* 65:469-473
- Quang DN, Stadler M, Fournier J, Tomita A, Hashimoto T (2006)b Cohaerins C- F, four azaphilones from the xylariaceous fungus *Annulohypoxylon cohaerens*. *Tetrahedron* 62:6349-6354
- Rogers JD, Ju YM, Watling R, Whalley AJS (1999) A reinterpretation of *Daldinia concentrica* based upon a recently discovered specimen. *Mycotaxon* 72:507–520
- Sakuda S, Otsubo Y, Yamada Y (1995) Structure of patulodin, a new azaphilone epoxide, produced by *Penicillium urticae*. *J Antibiot* 48:85-86
- Seibert SF, Eguereva E, Krick A, Kehraus S, Voloshina E, Raabe G, Fleischhauer J, Leistner E, Wiese M, Prinz H, Alexandrov K, Janning P, Waldmann H, Koenig G. M (2006) Polyketides from the marine-derived fungus *Ascochyta salicorniae* and their potential to inhibit protein phosphatases. *Org Biomol Chem* 4:2233-2240
- Seto H, Tanabe M (1974) Utilization of ¹³C-¹³C coupling in structural and biosynthetic studies. III. Ochrephilone - a new fungal metabolite. *Tetrahedron Lett* 15:651-654
- Stadler M, Akne H, Dekermendjian K, Reiss R, Sterner O, Witt R (1995) Novel bioactive azaphilones from fruit bodies and mycelial cultures of the Ascomycete *Bulgaria inquinans* (FR.). *Nat Prod Lett* 7:7-14
- Stadler M, Baumgartner M, Grothe T, Muehlbauer A, Seip S, Wollweber H (2001) Concentricol, a taxonomically significant triterpenoid from *Daldinia concentrica*. *Phytochemistry* 56:787–793

Stadler M, Fournier J (2006) Pigment chemistry, taxonomy and phylogeny of the Hypoxyloideae (Xylariaceae). *Rev Iberoam Micol* 23:160-170

Stadler M, Laessle T, Vasilyeva L (2005) The genus *Pyrenomyxa* and its affinities to other cleistocarpous *Hypoxyloideae* as inferred from morphological and chemical traits. *Mycologia* 97:1129-1139

Stadler M, Quang DN, Tomita A, Hashimoto T, Asakawa Y (2006) Changes in secondary metabolism during stomatal ontogeny of *Hypoxylon fragiforme*. *Mycol res* 110:811-820

Stadler M, Wollweber H, Mühlbauer A, Asakawa Y, Hashimoto T, Rogers JD, Ju Y-M, Wetzstein HG, Tichy HV (2001)a. Molecular chemotaxonomy of *Daldinia* and other Xylariaceae. *Mycol Res* 105:1191-1205

Steglich W, Klaar M, Furtner W (1974) (+)-Mitorubrin derivatives from *Hypoxylon fragiforme*. *Phytochemistry* 13:2874-2875

Steglich W (1981) Biologically active compounds from higher fungi. *Pure Appl Chem* 53:1233-1240

Steglich W, Fugmann B, Lang-Fugmann S (2001) RÖMPP Encyclopedia Natural Products. Georg Thieme Verlag

Steyn PS, Vlegaar R (1986) A reinvestigation of the structure of monochaetin, a metabolite of *Monochaetia compta*. *J Chem Soc* 11:1975-1976

Sturdikova M, Slugen D, Lesova K, Rosenberg M (2000) Mikrobiálna produkcia farbnych azaphilonovych metabolitov. *Chem Listy* 94:105-110

Suzuki S, Hosoe T, Nozawa K, Yaguchi T, Udagawa SI, Kawai KI (1999) Mitorubrin derivatives on ascomata of some *Talaromyces* species of ascomycetous fungi. *J Nat Prod* 62:1328-1329

Tabata Y, Ikegami S, Yaguchi T, Sasaki T, Hoshiko S, Sakuma S, Shin-Ya K, Seto H (1999) Diazaphilonic acid, a new azaphilone with telomerase inhibitory activity. *J Antibiot* 52:412-414

- Takahashi M, Koyama K, Natori S (1990) Four new azaphilones from *Chaetomium globosum* var. *flavo-viridae*. Chem Pharm Bull 38:625-628
- Thines E, Anke H, Sterner O (1998) Trichoflectin, a bioactive azaphilone from the ascomycete *Trichopezizella nidulus*. J Nat Prod 61:306-308
- Toki S, Tanaka T, Uosaki Y, Yoshida M, Suzuki Y, Kita K, Mihara A, Ando K, Lokker NA, Giese NA, Matsuda Y (1999) RP-1551s, a family of azaphilones produced by *Penicillium* sp., inhibit the binding of PDGF to the extracellular domain of its receptor. J Antibiot 52:235-244
- Tomoda H, Matsushima C, Tabata N, Namatame I, Tanaka H, Bamberger MJ; Arai H, Fukazawa M, Inoue K, Omura S (1999) Structure-specific inhibition of cholesteryl ester transfer protein by azaphilones. J Antibiot 52:160-170
- Turner WB (1971) Fungal metabolites. Academic press, London
- Turner WB, Aldridge DC (1983) Fungal metabolites II. Academic press, London
- Velisek J, Davidek J, Cejpek K (2008) Biosynthesis of food constituents: Natural pigments. Part 2 – a review. Czech J Food Sci 26:73–98
- Vinale F, Marra R, Scala F, Ghisalberti EL, Lorito M, Sivasithamparam K (2006) Major secondary metabolites produced by two commercial *Trichoderma* strains active against different phytopathogens. Lett Appl Microbiol 43:143-148
- Vlegaar R, Steyn PS; Nagel DW (1974) Constitution and absolute configuration of austdiol, the main toxic metabolite from *Aspergillus ustus*. J Chem Soc 1:45-49
- Wasser SP (2002) Medicinal mushrooms as a source of antitumor and immunomodulating polysaccharides. Appl Microbiol Biotechnol 60:258-274
- Wei WG, Yao ZJ (2005) Synthesis studies toward chloroazaphilone and vinylogous γ -pyridones: two common natural product core structures. J Org Chem 70:4585-4590

- Yamada T, Doi M, Shigeta H, Muroga Y, Hosoe S, Numata A, Tanaka R (2008) Absolute stereostructures of cytotoxic metabolites, chaetomugilins A-C, produced by a *Chaetomium* species separated from a marine fish. *Tetrahedron Lett* 49:4192-4195
- Yamada T, Muroga Y, Tanaka R (2009) New Azaphilones, Seco-Chaetomugilins A and D, Produced by a Marine-Fish-Derived *Chaetomium globosum*. *Mar. Drugs* 7:249-257
- Yang DJ, Tomoda H, Tabata N, Masuma R, Omura S (1996) New isochromophilones VII and VIII produced by *Penicillium* sp. FO-4164. *J Antibiot* 49:223-229
- Yang SW, Chan TM, Terracciano J, Patel R, Patel M, Gullo V, Chu M (2006) A new hydrogenated azaphilone Sch 725680 from *Aspergillus* sp. *J Antibiot* 59:720-723
- Yang SW, Chan TM, Terracciano J, Loebenberg D, Patel M, Gullo V, Chu M (2009) Sch 1385568, a new azaphilone from *Aspergillus* sp. *J Antibiot* 62:401-403
- Yasukawa K, Itabashi T, Kawai KI, Takido M (2008) Inhibitory effects of falconensins on 12-O-tetradecanoylphorbol-13-acetate-induced inflammatory ear edema in mice. *J Natural Medicines* 62:384-386
- Yasukawa K, Takahashi M, Natori S, Kawai KI, Yamazaki M, Takeuchi M, Takido M (1994) Azaphilones inhibit tumor promotion by 12-O-tetradecanoylphorbol-13-acetate in two-stage carcinogenesis in mice. *Oncology* 51:108-112
- Ying J, Mao X, Ma Q, Zong Y, Wen H (1987) *Icons of medicinal fungi from China*. Science press, Beijing, China
- Yoshida E, Fujimoto H, Baba M, Yamazaki M (1995) Four new chlorinated azaphilones, helicusins A-D, closely related to 7-epi-sclerotiorin, from an ascomycetous fungus, *Talaromyces helicus*. *Chem.Pharm Bull* 43:1307-1310
- Yoshida E, Fujimoto H, Yamazaki M (1996) Ex vivo study on MAO inhibitory activity of luteusin A, from an ascomycete *Talaromyces luteus*, and Ro16-6491, a reversible MAO-B inhibitor. *J. Natural Medicines* 50:54-57

Yoshida E, Fujimoto H, Yamazaki M (1996)a Revised stereostructures of luteusins C and D. *Chem Pharm Bull* 44:1775

Yoshida E, Fujimoto H, Yamazaki M (1996)b Isolation of three new azaphilones, luteusins C, D, and E, from an ascomycete, *Talaromyces luteus*. *Chem Pharm Bull* 44:284-287

Yu BZ, Zhang GH, Du ZZ, Zheng YT, Xu JC, Luo XD (2008) Phomoeuphorbins A-D, azaphilones from the fungus *Phomopsis euphorbiae*. *Phytochemistry* 69:2523-2526

Zhu J, Grigoriadis NP, Lee JP, Porco JAJr (2005) Synthesis of the Azaphilones Using Copper-Mediated Enantioselective Oxidative Dearomatization. *J Am Chem Soc* 127:9342-9343

Zou XW, Sun BD, Chen XL, Liu XZ, Che YS (2009) Helotialins A–C, Anti-HIV Metabolites from a Helotialean Ascomycete. *Chinese Journal of Natural Medicines*, 7:140–144

9. References

1. The global burden of disease, update WHO, 2004, http://www.who.int/healthinfo/global_burden_disease/2004_report_update/en/index.html
2. Waksman, S. A. 1947. What is an antibiotic or an antibiotic substance? *Mycologia* 39: 565–569
3. von Nussbaum, F., Brands, M., Hinzen, B., Weigand, S., Häbich, D. 2006. Medicinal chemistry of antibacterial natural products – exodus or revival? *Angew Chem Int Ed* 45 (31): 5072–5129, McGraw-Hill Concise Encyclopedia 5th edition
4. Davey, P. G. 2000. Antimicrobial chemotherapy. in Ledingham JGG, Warrell, D. A. *Concise Oxford Textbook of Medicine*. Oxford: Oxford University Press. 1475p
5. <http://www.cdc.gov>
6. http://www.medicinenet.com/vancomycin-resistant_enterococci_vre/article.htm
7. Alper, J. 1998. Effort to combat microbial resistance lags. *ASM News* 64: 440–441
8. Marjorie, M. C. 1999. Plant products as antimicrobial agents. *Clin Microbiol Rev* 12 (4): 564–582
9. Clark, A. M. 1996. Natural products as a resource for new drugs. *Pharm Res* 13 (8): 1133–44
10. Lindequist, U., Niedermeyer, T. H. J, Jülich, W. D. 2005. The pharmacological potential of mushrooms. *eCAM* 2: 285–299.
11. Hobbs, C., Beinfield, H. 1995. *Medicinal mushrooms - an exploration of tradition, healing & culture*. Botanica Press. 251p

12. Kirk, P. M., Cannon, P. E., Minter D. W., Stalpers, J. A. 2008. Dictionary of fungi, 10th edition, CABI Europe – UK, 784p
13. Feher, M., Schmidt, J. M. 2003. Property distributions: differences between drugs, natural products, and molecules from combinatorial chemistry *J. Chem Inf Comput Sci* 43 (1): 218–227
14. Ying, J., Mao, X., Ma, Q., Zong, Y., Wen, H., 1987. Icons of medicinal fungi from China. Science press, Beijing, China. 575p
15. Zaika L. L., 1986. Spices and herbs: their antimicrobial activity and ist determination. *J Food Saf* 9 (2): 97–118
16. Geissman, T. A., 1963. Flavonoid compounds, tannins, lignins and related compounds, p.265. In Florkin, M. and Stotz, E. H. (ed.) *Pyrrolepigments, isoprenoid compounds and phenolic plant constituents*, vol. 9. Elsevier
17. Newman, D. J., Cragg, G. M. 2007. Natural products as a source of new drugs over the past 25 years. *J Nat Prod* 70 (3): 461–477
18. Richard A. Dixon, 2001. Natural products and plant disease resistance. *Nature* 411: 843-847
19. Rietz, S. Parker, J. E. 2007. Plant disease and defence. *Encyclopedia of life sciences*, John Wiley & Sons, Ltd. *Handbook of plant science Vol.1*: 1460-1467
20. Purves, W. K., Sadava, D., Orians, G. H., Heller, H.G. from “The science of biology”, Seventh Edition, by Chapter 28. Protists and the Dawn of the Eukarya
21. Hawksworth, D. L. 1991. The fungal dimension of biodiversity: magnitude, significance, and conservation. *Mycol Res* 95: 641–655
22. Carlile, M. J., Watkinson, S. C., Gooday, G. W. 2001. *The fungi*. 2nd edition, Academic Press, San Diego, 603p

23. Shoji, J. Y, Arioka, M., Kitamoto, K. 2006. Possible involvement of pleomorphic vacuolar networks in nutrient recycling in filamentous fungi. *Autophagy* 2 (3): 226–27
24. Kirk, P. M., Cannon, P. E., Minter D. W., Stalpers, J. A. 2008. Dictionary of fungi, 10th edition, CABI Europe – UK, 784p
25. Turner, W. B. 1971. Fungal metabolites. Academic press, London
26. Turner, W. B., Aldridge, D. C. 1983. Fungal metabolites II. Academic press, London
27. Steglich, W., Fugmann, B., Lang-Fugmann, S. 2001. RÖMPP Encyclopedia Natural Products, Thieme, 748p
28. Steglich, W. 1981. Biologically active compounds from higher fungi. *Pure Appl Chem* 53: 1233–1240
29. Lorenzen, K., Anke, T. 1998. Basidiomycetes as a source for new bioactive natural products. *Curr Org Chem* 2: 329–364
30. Wasser, S. P. 2002. Medicinal mushrooms as a source of antitumor and immunomodulating polysaccharides. *Appl Microbiol Biotechnol* 60: 258–274
31. Gadd, G. M. 2007. Geomycology: biogeochemical transformations of rocks, minerals, metals and radionuclides by fungi, bioweathering and bioremediation. *Mycol Res* 111: 3–49
32. Lindahl, B. D., Ihrmark, K., Boberg, J., Trumbore, S. E., Högberg, P., Stenlid, J., Finlay, R. D. 2007. Spatial separation of litter decomposition and mycorrhizal nitrogen uptake in a boreal forest. *New Phytol* 173: 611–20
33. Barea, J. M., Pozo, M. J., Azcón, R., Azcón-Aguilar, C. 2005. Microbial co-operation in the rhizosphere. *J Exp Bot* 56: 1761–78
34. Weber, H. 1993, Allgemeine Mykologie. Gustav Fischer Verlag Jena, Stuttgart

35. Strasburger, E., Noll, F., Schenck, H., Schimper, A. F. W. 2008. Strasburger Lehrbuch der Botanik, Spektrum Akademischer Verlag Heidelberg
36. Molitoris, H.P. 2002. Mushrooms in medicine, folklore and religion. Feddes Repertiorum 113: 165–182
37. Hobbs, C. 2003. Medicinal mushrooms: an exploration of tradition, health and culture. Botanica press, Canada
38. Tomassi, S., Lohezic-Le Devehat, F., Sauleau, P., Bezivin, C., Boustie, J. 2004. Cytotoxic activity of methanol extracts from Basidiomycete mushrooms on murine cancer cell lines. Pharmazie 59 (4): 290–293
39. Zhang, P., Li, X., Li, N., Xu, J., Li, Z. L., Wang, Y., Wang, J. H. 2005. Antibacterial constituents from fruit bodies of ascomyces *Bulgaria inquinans*. Arch Pharm Res 28 (8): 889–891
40. Keller C., Maillard M., Keller J., Hostettmann, K. 2002. Screening of european fungi for antibacterial, antifungal, larvicidal, molluscicidal, antioxidant and free-radical scavenging activities and subsequent isolation of bioactive compounds. Pharm Biol 40 (7): 518–525
41. Stamets, P. 2002. Novel antimicrobials from mushrooms. HerbalGram 54: 28–33
42. Hsiao, W. L., Li, Y.Q., Lee, T.L., Li, N., You, M. M., Chang, S. T. 2004. Medicinal mushroom extracts inhibit *ras*-induced cell transformation and the inhibitory effect requires the presence of normal cells. Carcinogenesis 25 (7): 1177–1183
43. Lübken, T., Schmidt, J., Porzel, A., Arnold, N., Wessjohann, L. 2004. Hygrophorones A–G: fungicidal cyclopentenones from *Hygrophorus* species (Basidiomycetes). Phytochemistry 65: 1061–1071

44. Terekhova, L., Galatenko, O., Laiko, A., Sumarukova, I., Golova, T., Tolstykh, I., Kozlova, J. 1999. *Actinoplanes brasiliensis* INA 3802 – producent peptidnykh antibiotikov. *Antibiot Khimioterap* 4: 5–8
45. Narbe, G., Lindequist, U., Teuscher, E., Franke, P., Vainiotalo, P., Basner, R. 1991. Studies of the chemistry of immunosuppressively active fractions from *Meripilus giganteus* (Pers. ex. Fr.) Karst. *Pharmazie* 46: 738–740
46. Gu, Y. H., Sivam, G. 2006. Cytotoxic effect of oyster mushroom *Pleurotus ostreatus* on human androgen-independent prostate cancer PC-3 Cells. *J Med Food* 9: 196–204
47. Sone, Y., Misaki, A., Torii, M. 1991. Immunochemical studies of exocellular polysaccharides of *Tremella* and *Cryptococcus*. *Agr Biol Chem Tokyo* 55: 2683–2686
48. Sievers, A. 2004. Screening einheimischer Pflanzen und Pilze mittels dünnschichtchromatografischer Bioassays und Hochdurchsatz-Screening auf pharmakologisch wirksame Inhaltsstoffe unter besondere Berücksichtigung des Wurzelschwammes *Heterobasidion annosum* (Fr.) Bref. Doctor dissertation. Hamburg, Germany. 198p
49. Rahalison, L., Hamburger, M., Hostettmann, F., Monod, M., Frenk, E. 1991. A bioautographic agar overlay method for the detection of antifungal compounds from higher plants. *Phytochem Analysis* 2 (5): 199–203
50. Eriksson, O. E. 2006. Outline of ascomycota. *Myconet* 12: 1–88
51. Dennis, R. W. G. B. 1981. British ascomycetes. Gantner Verlag, Germany. 122p
52. Hanse, L., Knudsen, H. 2000. Nordic Macromycetes. Ascomycetes. Nordsvamp, Copenhagen. vol. 1: 309p
53. <http://www.indexfungorum.org>

54. Identification Guide to British and European Fungi: http://www.first-nature.com/fungi/id_guide/ascomycetes/bulgaria_inquinans.htm
55. <http://bc biodiversity.homestead.com/cupshaped.html>
56. <http://www.rogersmushrooms.com/gallery/DisplayBlock~bid~5672.asp>
57. Edwards, R. L., Lockett, H. J. 1976. Constituents of the higher fungi. Part XVI. Bulgarhodin and bulgarein, novel benzofluoranthenequinones from the fungus *Bulgaria inquinans* (Fries). J Chem Soc 20: 2149–2155
58. Stadler, M., Akne, H., Dekermendjian, K., Reiss, R., Sterner, O., Witt, R. 1995. Novel bioactive azaphilones from fruit bodies and mycelial cultures of the Ascomycete *Bulgaria inquinans* (Fr.). Nat Prod Lett 7: 7–14
59. Cui, D., Wang, S., Ding, X. 1997. Studies on chemical constituents of *Bulgaria inquinans*. Zhongguo Zhongyao Zazhi 22: 485–487 (Journal written in Chinese)
60. Bao, H. Y, Li, Y. 2003. Studies on the chemical composition of *Bulgaria inquinans*. Junwu Xitong 22: 303–307 (Journal written in Chinese)
61. Shuyuan, X., Jingxiu, C., Xiaokun, D. 2003. A method for preparing medicine containing *Bulgaria inquinans* (Pers.) Fr. or its mycelium extract for the treatment of psoriasis, vitiligo and scytitis, and its preparation method. Faming Zhuanli Shenqing Gongkai Shuomingshu, Patent
62. Ling, X. 2004. *Bulgaria inquinans* polysaccharide, method for preparing the same and pharmaceutical composition using the compound as active component. Faming Zhuanli Shenqing Gongkai Shuomingshu, Patent
63. Zhang. P., Li, X., Li, N., Xu, J., Li, Z. L., Wang, Y., Wang, J. H. 2005. Antibacterial constituents from fruit bodies of ascomyces *Bulgaria inquinans*. Arch Pharm Res 28 (8): 889–891

64. Jiang, S., Tsumuro, T., Takubo, M., Fujii, Y., Kamei, C. 2005. Antipruritic and antierythema effects of Ascomycete *Bulgaria inquinans* extract in ICR mice. *Biol Pharm Bull* 28 (12): 2197–2200
65. Xian Li, P. Z., Jing Xu, N. L., Meng, D. L., Sha, Y. 2006. A new perylenequinone from the fruit bodies of *Bulgaria inquinans*. *J Asian Nat Prod Res* 8 (8): 743–746
66. Zhang, P., Li, X., Zhang, Y., Li, N., Meng, D.-L. 2007. Chemical constituents of organic acid part from *Bulgaria inquinans*. *Shenyang Yaoke Daxue Xuebao* 24 (8): 482–483
67. Sturdikova, M., Slugen, D., Lesova, K., Rosenberg, M. 2000. Mikrobiálna produkcia farbnych azaphilonovych metabolitov. *Chem Listy* 94: 105–110
68. Wei W. G., Yao Z. J. 2005. Synthesis studies toward chloroazaphilone and vinylogous γ -pyridones: two common natural product core structures. *J Org Chem* 70: 4585–4590
69. Akihisa, T., Tokuda, H., Ukiya, M., Kiyota, A., Yasukawa, K., Sakamoto, N., Kimura, Y., Suzuki, T., Takayasu, J., Nishino, H. 2005. Anti-tumor-initiating effects of monascin, an azaphilonoid pigment from the extract of *Monascus pilosus* fermented rice (red-mold rice). *Chem Biodivers* 2: 1305–1309
70. Akihisa, T., Tokuda, H., Yasukawa, K., Ukiya, M., Kiyota, A., Sakamoto, N., Suzuki, T., Tanabe, N., Nishino, H. 2005. Azaphilones, furanoisophthalides, and amino acids from the extracts of *Monascus pilosus* - fermented rice (red-mold rice) and their chemopreventive effects. *J Agric Food Chem* 53: 562–565
71. Duncan, S. J., Grueschow, S., Williams, D. H., McNicholas, C., Purewal, R., Hajek, M., Gerlitz, M., Martin, S., Wrigley, S. K., Moore, M. 2001. Isolation and structure elucidation of chlorofusin, a novel p53-MDM2 antagonist from a *Fusarium* sp. *J Am Chem Soc* 123: 554–560

72. Duncan, S. J., Cooper, M. A., Williams, D. H. 2003. Binding of an inhibitor of the p53/MDM2 Interaction to MDM2. *Chem Commun* 3: 316–317
73. Park, J. H., Choi, G. J., Jang, K. S., Lim, H. K., Kim, H. T., Cho, K. Y., Kim, J. C. 2005. Antifungal activity against plant pathogenic fungi of chaetoviridins isolated from *Chaetomium globosum*. *FEMS Microbial Lett* 252: 309-313
74. Flammer, R., Gallen, S. 1983. Hemolysis in mushroom poisoning: facts and hypotheses. *Schweiz Med Wochenschr* 113: 1555–1561
75. Winterstein, D., 2000. Hämolyse in Pilzen. Attacken auf die roten Blutkörperchen. *Der Tintling* 4: 10–25
76. Tateno, H., Goldstein, I. J. 2003. Molecular cloning, expression, and characterization of novel hemolytic lectins from the mushroom *Laetiporus sulphureus*, which show homology to bacterial toxins. *J Biol Chem* 278: 40455–40463
77. Tomita, T., Noguchi, K., Mimuro, H., Ukaji, F., Ito, K., Sugawara-Tomita, N., Hashimoto, Y. 2004. Pleurotolysin, a novel sphingomyelin-specific two-component cytolysin from the edible mushroom *Pleurotus ostreatus*, assembles into a transmembrane pore complex. *J Biol Chem* 279(26): 26975–26982
78. Bernheimer, A. W., Avigada, L. S. 1979. A cytolytic protein from the edible mushroom, *Pleurotus ostreatus*. *Biochim Biophys Acta* 585: 451–461
79. Lin, J-Y., Wua, H-L., Shia, G-Y. 1975. Toxicity of the cardiotoxic protein, flammutoxin, isolated from the edible mushroom *Flammunlina velutipes*. *Toxicon* 13: 323–326
80. Itabashi, T., Nozawa, K., Nakajima, S., Kawai, K. I., 1993. A new azaphilone, falconensin H, from *Emericella falconensis*. *Chem Pharm Bull* 41: 2040–2041

81. Ogasawara, N., Kawai, K. I., 1998. Hydrogenated azaphilones from *Emericella falconensis* and *E. fruticulosa*. *Phytochemistry* 47: 1131–1135
82. Silverstein, R. M., Bassler, G. C., Morrill, T. C., 1981. Spectrometric identification of organic compounds. 4th edition. Wiley&Sons. 442p
83. Musso, L., Dallavalle, S., Merlini, L., Bava, A., Nasini, G., Penco, S., Giannini, G., Giommarelli, C., De Cesare, A., Zuco, V., Vescei, L., Pisano, C., Dal Piaz, F., De Tommasi, N., Zunino, F. 2010. Natural and semisynthetic azaphilones as a new scaffold for Hsp90 inhibitors. *Bioorg Med Chem* 18: 6031–6043
84. Dellar, J. E., Cole, M. D., Waterman, P. G. 1996. Unusual antimicrobial compounds from *Aeollanthus buchnerianus*, *Experientia* 52: 157–179.
85. Zheng, C., Yoo, J., Lee, T., Cho, H., Kim, Y., Kim, W., 2005. Fatty acids synthesis is a target for antibacterial activity of unsaturated fatty acids. *FEBS Lett* 579: 5157–5162
86. Stahl, E., 1964. Gradient and Low-temperature thin layer chromatography. *Angew Chem internat* 3(12): 784–791
87. Sonwa, M. M., König, W. A. 2001. Chemical study of the essential oil of *Cyperus rotundus*. *Phytochemistry* 58: 799–810
88. Asaka, Y., Kamikawa, T., Kubota, T. 1973. Constituents of *Vitex Rotundifolia* L. fil. *Chem Lett* 9: 37-940
89. Smith, R. M. 2004. Understanding Mass spectra: a basic approach, 2nd Edition, Wiley. 392 p
90. Tada, M., Chiba, K., Hashizume, T. 1982. Formation of dendrolasin, sesquirosefuran, perillene and rosefuran by biomimetic autooxidation. *Agric Biol Chem* 46 (3): 819–820

91. Ksebati, M., B., M., Schmit, F., J. 1988. Sesquiterpene furans and thiosesquiterpenes from the nudibranch *Ceratosoma brevicaudatum*. *J Nat Prod* 51: 857–861
92. Clark, R., Garson, M., J., Brereton, J., M., John A. Kennedy, J., A. 1999. Vinylfurans revisited: a new sesquiterpene from *Euryspongia deliculata*. *J Nat Prod* 62: 915–916
93. Chowdhury, J., U., Nandi, N., C., Uddina, M., Rahmanb, M. 2007. Chemical constituents of essential oils from two types of spearmint (*Mentha spicata* L. and *M. cardiaca* L.) introduced in Bangladesh. *Bangladesh J Sci Ind Res* 42 (1): 79–82
94. Dick, R., Quirin, K. W., Cresp, P. 1992. Massoia lactone, extraction and concentration by supercritical carbon dioxide. *Parfums, cosmétiques, arômes*, 103: 91–93
95. Simonsen, H. T., Riedel, C., Gade, L. B., Jebjerg, C, P., Guzman, A., Moelgaard, P. 2009. Chemical composition and antibacterial activity of the leaf essential oil of *Baccharis magellanica* (Lam.) Pers. and *Baccharis elaeoides* Remy from Chile. *J Essent Oil Res* 21: 377–380
96. Benoni, H., Hardebeck, K. 1964. The isolation and pharmacological study of a natural levorotatory massoia lactone. *Arzneimittel-Forschung* 14: 40–42
97. <http://www.thegoodscentcompany.com/data/rw1005501.html>
98. König, W. A., Krebber, R., Evers, P., Bruhn, G. 1990. Stereochemical analysis of constituents of essential oils and flavor compounds by enantioselective capillary gas chromatography. *J High Res Chromatog* 13: 328–332
99. Campos-Ziegenbein, F., Hanssen, H-P., König, W.A. 2006. Chemical constituents of the essential oils of three wood-rotting fungi. *Flavour Fragr J* 21: 813–816

100. Tsutsumi, H., Katagi, M., Miki, A., Shima, N., Kamata, T., Nishikawa, M., Nakajima, K., Tsuchihashi, H. 2005. Development of simultaneous gas chromatography–mass spectrometric and liquid chromatography–electrospray ionization mass spectrometric determination method for the new designer drugs, N-benzylpiperazine (BZP), 1-(3-trifluoromethylphenyl) piperazine (TFMPP) and their main metabolites in urine. *J Chromatogr* 819: 315–322
101. Campos-Ziegenbein, F. 2006. Isolierung und Identifizierung von Naturstoffen aus Baumpilzen (Basidiomycetes) Dissertation, Univ. Hamburg, Dep. Chemistry
102. Fäldt, J., Jonsell, M., Nordlander, G., Borg-Karlson, A. K. 1999. Volatiles of bracket fungi *Fomitopsis pinicola* and *Fomes fomentarius* and their functions as insect attractants. *J Chem Ecol* 25: 567–590
103. Pierce, A. M., Pierce, H. D. Jr., Oehlschlager, A. C., Borden, J. H. 1991. 1-octen-3-ol, attractive semiochemical for foreign grain beetle, *Ahasverus advena* (Waltle) (Coleoptera: Cucujidae). *J Chem Ecol* 17: 567–580
104. Kline, D. L., Allan, S. A., Bernier, U. R., Welch, C. H. 2007. Evaluation of the enantiomers of 1-octen-3-ol and 1-octyn-3-ol as attractants for mosquitoes associated with a freshwater swamp in Florida, U.S.A. *Med Vet Entomol* 21: 323–331
105. Sawahata, T., Shimano, S., Suzuki, M. 2008. *Tricholoma matsutake* 1-Ocen-3-ol and methyl cinnamate repel mycophagous *Proisotoma minuta* (Collembola: Insecta). *Mycorrhiza* 18: 111–114
106. Overholts, L. O. 1953. The Polyporaceae of the United States, Alaska, and Canada. Univ. Michigan Press 466p
107. Ryvarden, L. 1985. Type studies in the Polyporaceae 17. Species described by W. A. Murrill. *Mycotaxon* 23: 169–198

108. Phillips, R. 2005. Mushrooms and other fungi of North America. Firefly books. Buffalo, NY. 319p
109. Lincoff, G. H. 1981. National audubon society field guide to North American mushrooms. Knopf/Chanticleer Press, NY. 928p
110. Larsen, M, J, Lombard, F, F. 1988. The status of *Meripilus giganteus* (Aphyllorphorales, Polyporaceae) in North America. *Mycologia* 80(5): 612–621
111. Ryvarden L., Gilbertson R. L. 1994. European Polypores. Part 2: *Meripilus-Tyromyces*. *Synopsis Fungorum* 7. Oslo: 395–397
112. Seeger, R., Beckert, M. 1979. Magnesium in höheren Pilzen. *Z Lebensm Unters For* 168(4): 264–281
113. Karaman, M. A.; Matavulj, M. N. 2005. Macroelements and heavy metals in some lignicolous and tericolous fungi. *Zbornik Matice Srpske za Prirodne Nauke* 108: 255–267
114. Jandric, Z., Prostenik, M. 1986. Lipids of higher fungi. X. Hydrocarbons in fruit bodies of mushrooms. *Jugoslavenske Akademije Znanosti i Umjetnosti* 425: 41–46
115. Narbe, G., Lindequist, U., Teuscher, E. 1990. Immunosuppressive actions of *Meripilus giganteus* (Pers.: Fr.) Karst. *Die Pharmazie*, 45, 637–638
116. Koch, J., Witt, S., Lindequist, U. 2002. The influence of selected higher Basidiomycetes on the binding of lipopolysaccharide to CD14+ cells and on the release of cytokines. *Int J Med Mush* 4: 229–235
117. Kofod, L. V, Kauppinen, M. S, Andersen, L. N, Clausen, I. G. 1997. An enzyme with galactanase activity and its cDNA sequence from *Meripilus giganteus*. *PCT Int Appl* 48 p (patent)
118. Friebolin, H. 2006. Ein- und zweidimensionale NMR-Spektroskopie. Wiley-VCH. 399p

119. Michelliza, S., Abraham, W. M., Jacocks, H. M., Schuster, T., Baden, D. G. 2007. Synthesis, modeling, and biological evaluation of analogues of the semisynthetic brevetoxin antagonist β -naphthoyl-brevetoxin. *Chembiochem* 8: 2233–2239
120. Yoshikawa, K., Hashimoto, T., Hirasawa, A., Tsujimoto, G., Yamamoto, K., Inose, T., Kimura, T. 2010. Unsaturated fatty acids derived from *Sparassis crispa* fruiting body and/or mycelium for inhibiting diabetes mellitus. Patent 11p (patent written in Japanese)
121. Sébédio, J.-L., Christie, W. W., Adlof, R. (Editors). 2003. Advances in conjugated linoleic acid research. Vol. 2 (AOCS Press, Champaign, IL): 341p (153)
122. Jang, W. J., Hyung, S. W., Park, C. W., Kim, S. J., Kim, Y. S., Kim, M. S., Cerbo, R. M., Kim, J. O., HA, Y. L. 2004. Production of natural *c9,t11* conjugated linoleic acid (*c9,t11* CLA) by submerged liquid culture of mushrooms. Session 33G, Nutraceuticals & Functional Foods: Lipid and probiotic functional foods IFT Annual Meeting, July 12-16 - Las Vegas, NV
123. Shiuan Chen, S., Oh¹, S. R., Phung¹, S., Hur, G., Ye¹, J. J., Kwok¹, S. K., Shrode, G. E., Belury, M., Adams, L. S., Dudley Williams, D. 2006. Anti-aromatase activity of phytochemicals in white button mushrooms (*Agaricus bisporus*). *Cancer Res* 66: 12026–12034
124. Park, M. J., Gwak, K. S., Yang, I., Kim, K. W., Jeung, E. B., Chang, J. W., Choi, I. G. 2009. Effect of citral, eugenol, nerolidol and α -terpineol on the ultrastructural changes of *Trichophyton mentagrophytes*. *Fitoterapia* 80: 290–296
125. Brehm-Stecher, B. F., Eric A. Johnson, E. A. 2003. Sensitization of *Staphylococcus aureus* and *Escherichia coli* to antibiotics by the sesquiterpenoids nerolidol, farnesol, bisabolol, and apritone. *Antimicrob Agents Chemother* 47: 3357–3360

126. Leffingwell, J. C. 2003. Chirality & Bioactivity. I.: Pharmacology. Leffingwell Reports 3: 1–27
127. Liu, H., Jia, W., Zhang, J., Pan, Y. 2008. GC-MS and GC-olfactometry analysis of aroma compounds extracted from culture fluids of *Antrodia camphorate*. World J Microbiol Biotechnol 24: 1599–1602
128. Sprecher, E. 1963. Rücklaufdestillation zur erschöpfenden Wasserdampfdestillation ätherischer Öle. Dtsch Apoth Ztg 103: 213
129. König, W. A., Julian, D., Hochmuth, D. H., Terpenoids and related constituents of essential oils, Hochmuth scientific software, Hamburg, Germany
130. Osmanova, N., Schultze, W., Ayoub, N. 2010. Azaphilones: a class of fungal metabolites with diverse biological activities. Phytochem Rev 9: 315–342
131. www.mycobank.org

Publications

Handoussa, H., Osmanova, N., Ayoub, N., Mahran, L. 2009. Spicatic acid: A 4-carboxygentisic acid from *Gentiana spicata* extract with potential hepatoprotective activity Drug Discov Ther 3 (6): 278–286.

Osmanova, N., Schultze, W., Ayoub, N. 2010. Azaphilones: a class of fungal metabolites with diverse biological activities. Phytochem Rev 9: 315–342

Bogma, M., Osmanova, N., Eruzin, A., Potehina, T., Manoylova, L. 2010. Evaluation of the low temperature plasma effects on the chemical composition and microbiological contamination of plant materials. Chemistry of plant raw material ISSN (1029-5151 Print, 1029-5143 On-Line). Accepted for publication.

**Eidesstattliche Versicherung über die selbständige Anfertigung der Arbeit und
Erklärung über frühere Promtionsversuche**

Hiermit erkläre ich, die vorliegende Arbeit selbständig angefertigt und nur die
angegeben Hilfsmittel benutzt zu haben.

Natalia Osmanova

Hamburg, den 08.11.2010

Erklärung über Promotionsversuche

Hiermit erkläre ich, dass es sich um meinen ersten Promotionsversuch handelt.

Natalia Osmanova

Hamburg, den 08.11.2010